Titre: Title:	Self-Healing, Stretchable and Recyclable Conductors Based on PEDOT:PSS and Polyurethane Blends for Bioelectronics Applications
Auteur: Author:	Jinsil Kim
Date:	2026
Type:	Mémoire ou thèse / Dissertation or Thesis
Référence: Citation:	Kim, J. (2026). Self-Healing, Stretchable and Recyclable Conductors Based on PEDOT:PSS and Polyurethane Blends for Bioelectronics Applications [Thèse de doctorat, Polytechnique Montréal]. PolyPublie. https://publications.polymtl.ca/76195/

URL de PolyPublie: PolyPublie URL:	https://publications.polymtl.ca/76195/
Directeurs de recherche: Advisors:	Fabio Cicoira
Programme: Program:	Génie chimique

POLYTECHNIQUE MONTRÉAL

affiliée à l'Université de Montréal

Self-Healing, Stretchable and Recyclable Conductors Based on PEDOT:PSS and Polyurethane Blends for Bioelectronics Applications

JINSIL KIM

Département de génie chimique

Thèse présentée en vue de l'obtention du diplôme de *Philosophiæ Doctor*

Génie chimique

Mars 2026

POLYTECHNIQUE MONTRÉAL

affiliée à l'Université de Montréal

Cette thèse intitulée :

Self-Healing, Stretchable and Recyclable Conductors Based on PEDOT:PSS and Polyurethane Blends for Bioelectronics Applications

présentée par **Jinsil KIM**

en vue de l'obtention du diplôme de *Philosophiæ Doctor*
a été dûment acceptée par le jury d'examen constitué de :

Jean-Marie RAQUEZ, président

Fabio CICOIRA, membre et directeur de recherche

David MELANÇON, membre

Guglielmo LANZANI, membre externe

ACKNOWLEDGEMENTS

I would like to express my deepest gratitude to my research supervisor, Prof. Fabio Cicoira, for his continuous guidance, encouragement, and support throughout my doctoral studies. His scientific insight, constructive feedback, and patience were essential to the completion of this work. I am particularly grateful for the intellectual freedom he provided, which allowed me to develop this research with independence and confidence.

I sincerely thank the members of my thesis committee, Prof. Jean-Marie Raquez, Prof. David Melançon, and Prof. Guglielmo Lanzani, for accepting to evaluate this thesis and for their valuable time, insightful comments, and constructive suggestions. Their expertise and perspectives greatly contributed to improving the quality and clarity of this dissertation.

I would also like to acknowledge my colleagues and collaborators for the stimulating discussions, technical assistance, and collaborative spirit that made this research both productive and enjoyable. The supportive environment of the research group played an important role in overcoming challenges encountered during this doctoral journey.

I gratefully acknowledge the institutional and technical support provided by Polytechnique Montréal and its research facilities, which enabled the successful completion of this work.

Finally, I would like to express my heartfelt gratitude to my family for their unwavering support, understanding, and encouragement throughout my doctoral studies. Their patience and trust were a constant source of motivation during both the rewarding and challenging moments of this journey.

RÉSUMÉ

Les dispositifs électroniques souples et portables exigent des matériaux capables de conserver leurs performances électriques malgré des déformations mécaniques répétées, des dommages accidentels et une utilisation prolongée. Toutefois, les polymères conducteurs conventionnels, notamment le poly(3,4-éthylènedioxythiophène):polystyrène sulfonate (PEDOT:PSS), demeurent limités par une faible robustesse mécanique, une capacité d'auto-cicatrisation incomplète et un manque de durabilité environnementale. Cette thèse vise à relever ces défis par la conception rationnelle de systèmes conducteurs à base de PEDOT:PSS, à la fois auto-cicatrisants, extensibles et recyclables, destinés aux applications électroniques souples. Deux générations de composites PEDOT:PSS/polyuréthane (PU) ont été développées afin d'améliorer progressivement la durabilité mécanique, l'auto-cicatrisation autonome et la circularité des matériaux. La première étude (Chapitre 4) repose sur le mélange de PEDOT:PSS avec une matrice de polyuréthane basée sur des interactions de liaisons hydrogène et des additifs plastifiants. Cette approche permet d'augmenter significativement l'extensibilité, la ténacité et l'auto-cicatrisation mécanique tout en conservant une conductivité électrique fonctionnelle. Ce travail met en évidence que l'auto-cicatrisation des dispositifs souples doit inclure non seulement la récupération électrique, mais aussi la restauration de l'intégrité mécanique afin d'assurer une fiabilité à long terme. La possibilité de reconfiguration mécanique démontre également le potentiel de réutilisation du matériau. La seconde étude (Chapitre 5) introduit un composite de nouvelle génération intégrant des liaisons disulfure dynamiques en complément des liaisons hydrogène, permettant une auto-cicatrisation autonome à température ambiante, sans stimulus externe. Ce système présente une récupération rapide des propriétés électriques et mécaniques après des rayures et des coupures, et démontre de manière notable la cicatrisation de perforations dans un polymère conducteur entièrement solide. L'auto-cicatrisation électrique est obtenue pour des films continus d'une épaisseur aussi faible que ~1,4 µm, tandis que l'imprimabilité, l'auto-adhésion et la stabilité électromécanique permettent des applications concrètes telles que des électrodes réutilisables et des tatouages électroniques. Une analyse prospective (Chapitre 6) situe ces résultats dans le contexte plus large de l'électronique souple, en identifiant les compromis persistants entre conductivité, conformité mécanique, capacité d'auto-cicatrisation et durabilité. Dans l'ensemble, cette thèse démontre que l'utilisation de réseaux polymériques à faible température de transition vitreuse et de liaisons dynamiques permet de transformer les conducteurs à base de PEDOT:PSS en plateformes robustes, multifonctionnelles et

durables. Les connaissances acquises fournissent des lignes directrices concrètes pour le développement futur de dispositifs bioélectroniques, portables et robotiques souples.

ABSTRACT

Soft and wearable electronic devices require materials that can maintain electrical functionality under repeated mechanical deformation, accidental damage, and long-term use. However, conventional conducting polymers, including poly(3,4-ethylenedioxythiophene):polystyrene sulfonate (PEDOT:PSS), remain limited by mechanical fragility, incomplete self-healing, and poor sustainability. This thesis addresses these challenges through the rational design of self-healing, stretchable, and recyclable PEDOT:PSS-based conducting polymer systems for soft electronic applications. Two generations of PEDOT:PSS/polyurethane (PU) composites were developed to progressively improve mechanical durability, autonomous self-healing, and circularity. A roadmap analysis (Chapter 4) contextualized these findings within the broader field of soft electronics, identifying persistent trade-offs between conductivity, mechanical compliance, healing capability, and sustainability. In the first study (Chapter 5), PEDOT:PSS was blended with a hydrogen-bonded polyurethane matrix and plasticizing additives to enhance stretchability, toughness, and mechanical self-healing while preserving electrical conductivity. This work established that reliable self-healing in soft electronics must involve not only electrical recovery but also restoration of mechanical integrity to prevent cumulative damage under cyclic deformation. Mechanical remolding demonstrated the feasibility of reuse, introducing sustainability as a core design consideration. Building on these results, the second study (Chapter 6) introduced a next-generation composite incorporating dynamic disulfide bonds alongside hydrogen bonding, enabling autonomous self-healing at room temperature without external stimuli. This system exhibited rapid electrical and mechanical recovery after scratches and cuts, and notably demonstrated solid-state puncture healing—one of the most severe and rarely addressed damage modes in conducting polymers. Electrical self-healing was achieved in continuous films as thin as ~1.4 μm, while printability, strong self-adhesion, and stable electromechanical performance enabled practical implementations such as reusable freestanding electrodes and electronic tattoos. Overall, this thesis demonstrates that dynamic bonding and low glass-transition polymer networks can transform PEDOT:PSS-based conductors into robust, multifunctional, and sustainable platforms. The insights provided here offer practical design guidelines for future bioelectronic, wearable, and soft robotic systems.

TABLE OF CONTENTS

LIST OF TABLES

LIST OF FIGURES

LISTE OF SYMBOLS AND ABBREVIATIONS

APDS	Aminophenyl disulfide
ASTM	American Society for Testing Materials
CE	Counter electrode
CNT	Carbon nanotubes
DMSO	Dimethyl sulfoxide
DA	Diels–Alder reaction
DEG	Diethylene glycol
DMF	Dimethylformamide
DBTDL	Dibutyltin dilaurate
DSC	Differential scanning calorimetry
EtOH	Ethanol
E-waste	Electronic waste
E-tattoo	Electronic tattoo
EG	Ethylene glycol
E-skin	Electronic skin
ECG	Electrocardiogram
EgaIn	Eutectic gallium–indium
FTIR	Fourier-transform infrared spectroscopy
GPTMS	Poly(glutamic acid)–trimethoxysilane
GPC	Gel permeation chromatography
^{1}H NMR	Proton nuclear magnetic resonance
IPDI	Isophorone diisocyanate
ITO	Indium tin oxide

IPA	Isopropanol
MDSC	Modulated DSC
NCO	Isocyanate groups
OH	Hydroxyl groups
PEDOT:PSS	Poly(3,4-ethylenedioxythiophene):poly(styrenesulfonate)
PUs	Polyurethanes
PEG	Poly(ethylene glycol)
PSS	Polystyrene sulfonate
PEDOT	Poly(3,4-ethylenedioxythiophene)
PANI	Polyaniline
PPy	Polypyrrole
PIL	Poly(ionic liquid)
PDMS	Poly(dimethylsiloxane)
PAA	Poly(acrylic acid)
PG	Propylene glycol
PDO	1,3-propanediol
PCL diol	Poly(ε-caprolactone) diol
PET	Polyethylene terephthalate
PTFE	Polytetrafluoroethylene
PUD	Polyurethane diols
PA	Polyacrylates
PDMS	Polydimethylsiloxane
R_s	Sheet resistance
S	Sensitivity

T_g	Glass transition temperatures
TPU	Thermoplastic polyurethane
TGA	Thermogravimetric analysis
THF	Tetrahydrofuran
TMP	Trimethylolpropane
UPy	Ureidopyrimidinone
ρ	Electrical resistivity
σ	Electrical conductivity
$I_{pristine}$	Pristine current
$d_{damaged}$	Damaged depth
d_{healed}	Healed depth
$U_{t,pristine}$	Pristine toughness
$U_{t,healed}$	Healed toughness

LIST OF APPENDICES

CHAPTER 1 INTRODUCTION

1.1 Recyclable Self-healing Conductive Polymers

The concept of self-healing materials was first proposed in the early 2000s, inspired by biological recovery mechanisms [5]. In natural systems, plants and animals possess inherent mechanisms that allow them to respond to external damage by repairing tissues, preserving essential functions, and limiting further deterioration. For example, in plants, damage to stems or leaves is rapidly sealed to prevent water loss and pathogen invasion, followed by tissue regeneration that restores mechanical strength and structural continuity. This biomimetic healing principle presented a new design paradigm for material systems that can maintain functionality after damage, and it has driven growing interest in self-healing polymers within material science [6].

Early self-healing polymer systems relied on extrinsic approaches, in which healing agents were embedded within microcapsules or microchannels [7]. Although these systems can autonomously release healing agents to repair cracks, their healing capability is inherently limited, leading to rapid performance degradation under repeated damage conditions [8]. In addition, the presence of capsule or channel architectures can compromise the mechanical stability of the polymer matrix, leading to limitations in structural reliability, particularly for practical device applications and long-term use. As a result, intrinsic self-healing systems, in which the healing mechanism is incorporated directly into the polymer molecular structure, have recently emerged as the dominant research direction [9].

Intrinsic self-healing systems are designed based on reversible molecular interactions such as hydrogen bonding, disulfide exchange, metal-ligand coordination, and ionic interactions. These dynamic bonds can be dissociated and reform in response to external stimuli (e.g., heat, moisture, or light), enabling the rearrangement of polymer chains and the recovery of functional properties after damage. Notably, this intrinsic approach allows repeated healing behavior, offering an advantage over extrinsic approaches under conditions involving recurrent damage [8, 9].

The development of next-generation electronic devices, such as wearable electronic devices, stretchable sensors, soft robotics, and flexible electronics, is closely associated with the growing interest in self-healing polymers [10, 11]. Conventional inorganic-based electronic materials provide high electrical performance, but they are vulnerable to repetitive mechanical deformation

and external impact, leading to inevitable performance degradation upon cracking or fracture [12]. In contrast, polymer-based electronic materials offer tunable mechanical flexibility, elongation, and compliance through molecular structure design, while also being well suited for low-cost, large-area fabrication techniques such as solution processing and printing [13]. Owing to these characteristics, self-healing conductive polymer materials have attracted increasing attention as key components for extending device lifetime and improving operational reliability [14]. Meanwhile, as the use of polymer-based electronic devices continues to expand, the demand for sustainability has also become increasingly prominent [15]. Many electronic devices incorporate plastic-based components that are difficult or even impossible to recycle at the end of their service life, thereby contributing significantly to the growing issue of electronic waste (E-waste). In particular, conductive polymers or composite materials pose additional challenges for recycling, as the complex integration of dissimilar materials hinders efficient separation and reuse [16]. To address these environmental concerns, increasing research efforts have focused on polymer electronic materials that combine self-healing functionality with recyclability or reprocessability [4]. However, the simultaneous implementation of self-healing and recyclability within a single material system remains a significant challenge [17]. Self-healing functionality relies on polymer chain mobility and the formation of reversible bonds, which can often compromise mechanical strength or thermal stability [14, 17]. As one promising approach, strategies that integrate conductive polymers with self-healing polymer matrices have attracted considerable attention. In particular, poly(3,4-ethylenedioxythiophene) polystyrene sulfonate (PEDOT:PSS) has been widely used in wearable and soft electronic applications due to its solution processability, high electrical conductivity, and biocompatibility. Polyurethanes (PUs) have been employed as soft polymer matrix owing to its excellent stretchability, toughness, self-healing, and recyclability [8]. Combining conductive polymers with self-healing and recyclable polymer matrices has therefore been proposed as a promising strategy to achieve sustainable material platforms while maintaining mechanical reliability and electrical performance.

This work aims to address these challenges through the development of a PU-based conductive polymer composite that integrates self-healing capability, recyclability, and mechanical stretchability and durability. These properties are systematically validated through mechanical, electrical, and functional characterization.

1.2 Motivations

Despite significant advances in self-healing conductive polymers, several critical challenges remain. In particular, the simultaneous integration of self-healing capability, recyclability, and mechanical durability within a single material system is still limited. Many existing systems exhibit inherent trade-offs, whereby improvements in one property often compromise others, ultimately hindering practical implementation in electronic devices.

Furthermore, maintaining stable electrical performance under repeated mechanical deformation, healing, and reprocessing cycles remains a major challenge. These limitations underscore the need for material design strategies that enable the balanced integration of multiple functional properties without mutual interference.

To address these challenges, this thesis focuses on the development of a PU-based conductive polymer composite, incorporating PEDOT:PSS as the conductive component within a dynamically crosslinked PU matrix. By introducing dynamic interactions such as disulfide exchange and hydrogen bonding, the system is designed to simultaneously achieve self-healing, recyclability, and mechanical robustness.

In addition, the incorporation of additives, such as glycerol and polyethylene glycol (PEG) is used to enhance electrical performance, mechanical flexibility, and healing behavior, while maintaining compatibility with scalable fabrication techniques, such as printing.

Ultimately, this work establishes a conductive polymer platform that enables the balanced integration of self-healing, recyclability, stretchability, and mechanical durability without compromising electrical performance, thereby providing a viable pathway toward sustainable and practical electronic materials.

Specifically, this thesis delivers:

- PEDOT:PSS/PU/PEG composite systems that integrate self-healing capability, recyclability, and mechanical durability.
- PEDOT:PSS/PU systems designed with simultaneous consideration of printing, room-temperature self-healing, and recyclability.
- A design framework for PEDOT:PSS-based conductive polymer systems that emphasizes both functional integration and compatibility with scalable manufacturing processes.

These strategies collectively provide a new direction for polymer electronic materials enabling the simultaneous realization of practicality, sustainability, and high performance.

1.3 Objectives

The primary objective of this research is to develop a conductive polymer composite system that enables the simultaneous integration of self-healing, recyclability, electrical conductivity, and mechanical stretchability.

To achieve this, this thesis adopts PEDOT:PSS as the conductive component and a dynamically crosslinked polyurethane (PU) matrix as the structural framework. The material system is designed by incorporating dynamic interactions, including disulfide bonding and hydrogen bonding, to enable autonomous healing and reprocessability while maintaining mechanical integrity.

In addition, the incorporation of polyethylene glycol (PEG) and glycerol is employed to enhance electrical performance, increase chain mobility, and improve process compatibility. Through these design strategies, this work aims to overcome the conventional trade-offs between healing capability, recyclability, and mechanical durability in conductive polymer systems.

The first research objective is to develop a PEDOT:PSS/PU composite system that integrates self-healing functionality with thermally induced remolding capability. In this system, the high stretchability and physical interaction characteristics of PU matrix are leveraged to enable network reconstruction in response to external stimuli, such as heat, thereby allowing structural recovery under repeated mechanical deformation. Through this design, self-healing behavior and physical reprocessability are simultaneously incorporated within a single composite platform.

The second research objective focuses on constructing a more refined polymer network by tailoring the molecular structure of PU system, including the incorporation of disulfide bonds and modulation of diol composition. This molecular design strategy enables the realization of a composite system that exhibits autonomous self-healing at room temperature while maintaining mechanical stability and recyclability. The proposed system is capable of reprocessing and reuse through both solvent treatment (e.g., ethanol) and thermal processing, without the need for external healing stimuli. Furthermore, optimization of the polymer composition ensures long-term reliability and physical durability. Based on these material characteristics, practical electronic tattoo (e-tattoo) devices are fabricated, and their performance is systematically evaluated.

Building upon the material design insights obtained from the first and second research objectives, the third objective of this thesis is to propose a design guideline for PEDOT:PSS-based conductive polymer systems. This guideline identifies key factors influencing self-healing behavior, recyclability, and mechanical performance, and highlights their interdependence. Rather than establishing a universal framework, this work provides practical design insights to support the development of multifunctional conductive polymer materials for electronic applications.

Through the organic integration of self-healing capability, recyclability, mechanical stability, and processability within conductive polymer systems, this research aims to propose a material design strategy that extends beyond incremental property enhancement toward the realization of sustainable next-generation electronic devices. Moreover, by quantitatively evaluating the performance of materials developed through distinct design approaches, this thesis seeks to identify molecular structures and interaction strategies that are most suitable for real-world applications, ultimately providing guidance for the future design of versatile polymer-based electrode systems.

1.4 Organization of the Work

This thesis is organized as follows. Chapter 2 provides a comprehensive review of self-healable and recyclable conductive polymer composites for soft electronic applications, with a particular focus on PEDOT:PSS-based systems. Chapter 3 describes the experimental methods and materials used throughout this work.

Chapter 4 introduces a roadmap of PEDOT:PSS-based self-healing conductive materials (under revision for Flexible and Printed Electronics), outlining the current state of the field, key challenges, and future research directions.

Chapter 5 presents a research article (published in Materials Horizons), which reports the development of a stretchable, self-healing, and recyclable PEDOT:PSS/PU-based conductive polymer system. The material exhibits high elongation at break (~350%), high toughness (~24.6 MJ m^{-3}), and moderate electrical conductivity (~10 S cm^{-1}), along with efficient mechanical and electrical self-healing. In addition, it demonstrates excellent recyclability, maintaining its mechanical and electrical properties over multiple cycles. The material is further applied to ECG electrodes and pressure sensors, serving as proof of concept for sustainable electronic devices.

Chapter 6 presents a research article (under revision for Materials Horizons), which advances this material platform by enabling autonomous room-temperature self-healing, including recovery from severe mechanical damage such as scratches, cuts, and punctures. The composite exhibits enhanced mechanical performance (stretchability >650%) and strong self-adhesion, while maintaining stable electromechanical behavior. Furthermore, the material offers expanded solution processability using green solvents and can be fabricated via spin coating and printing into films, as well as transferable freestanding and electronic tattoo electrodes. It also supports both mechanical reuse and chemical recycling over multiple cycles while maintaining high performance. Device-level demonstrations, including printed electronic tattoos and freestanding electrodes, exhibit low impedance and high-quality ECG signal acquisition, highlighting the practical applicability of the system.

Finally, Chapter 7 summarizes the main findings of this thesis and presents the overall conclusions.

CHAPTER 2 LITERATURE REVIEW

This chapter first outlines the general characteristics of conductive polymers and the performance requirements associated with soft electronic applications, followed by a summary of intrinsic and extrinsic healing mechanisms in self-healing polymer systems. Subsequently, composite design strategies involving polyurethane-based self-healing elastomers and conductive polymers are discussed, along with material design approaches that consider recyclability and reprocessability. In addition, previous studies on PEDOT:PSS-based systems are reviewed with an emphasis on additive utilization and compatibility with printing-based fabrication processes, highlighting their limitations in achieving the integration of self-healing, recyclability, and mechanical durability. Through this literature review, the current limitations of self-healing conductive polymer systems are identified, and the research gaps addressed in this thesis are clarified.

2.1 Conductive Polymers

Conductive polymers are polymeric materials that exhibit electrical conductivity and play important roles in a wide range of applications, including wearable electronic devices, smart textiles, and bioelectronic systems. As organic polymer materials, they combine intrinsic electrical conductivity with mechanical flexibility and chemical durability, distinguishing them from conventional inorganic conductors. At the molecular level, conductive polymers possess conjugated backbones composed of sp^2-hybridized carbon atoms, which form delocalized π-electron systems that enable charge transport along the polymer chains (Figure 1) [18].

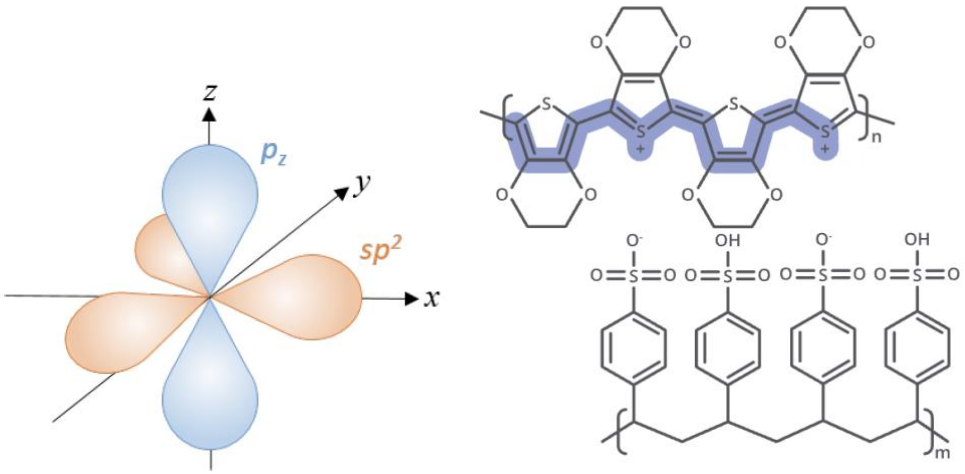

Figure 1. Schematic depiction of their sp²-hybridized conjugated orbitals and PEDOT and PSS molecular structures [18].

The electrical conductivity of conductive polymers is typically activated through doping processes involving oxidation–reduction (redox) reactions, which introduce mobile charge carriers into the conjugated backbone and facilitate electron transport. In most systems, including PEDOT-based materials, conductivity arises from oxidative (p-type) doping that removes electrons from the polymer chains, generating positively charged species such as polarons and bipolarons. Representative conductive polymers include poly(3,4-ethylenedioxythiophene):polystyrene sulfonate (PEDOT:PSS), polyaniline, and polypyrrole. These materials enable the simultaneous tuning of electrical conductivity and mechanical properties through compositional and structural control, such as adjusting the doping level, incorporating plasticizers or secondary additives, and modifying the polymer network. This versatility makes them particularly well suited for flexible electronic devices and smart display applications [19].

Beyond electrical performance, the mechanical properties of conductive polymers are critical for their practical use in deformable electronic systems. Mechanical flexibility and durability are essential characteristics for wearable and smart electronic devices, where materials are subjected to repeated mechanical deformation. These properties are typically quantified through tensile testing (e.g., elongation at break, Young's modulus), cyclic mechanical loading, and monitoring of electrical stability under repeated deformation [20]. For example, PEDOT:PSS offers a

favorable combination of electrical conductivity and mechanical flexibility, enabling its use in flexible displays and wearable devices. Similarly, polyaniline and polypyrrole enable precise control of electrical properties through electrochemical doping or conductivity modulation and have therefore been widely explored in applications such as smart sensors and bioelectronic devices [21]. In addition, conductive polymers exhibit chemical resistance and thermal stability, which has led to their use in various industrial applications, including electrodes, batteries, and capacitors.

Conductive polymers can further enhance device durability when integrated with self-healing polymer systems. Although certain conductive polymers, such as PEDOT:PSS, exhibit healing behavior under specific conditions (e.g., water-enabled recovery), their ability to restore severe mechanical damage remains constrained, as evidenced by limited recovery in mechanical properties (e.g., toughness or elongation at break) and incomplete restoration of electrical conductivity after damage. In such hybrid materials, conductive polymers provide electrical functionality, while self-healing polymers enable autonomous repair of mechanically damaged regions, thereby restoring both electrical and mechanical integrity after damage [21]. This synergistic integration can extend device lifetime, reduce maintenance and replacement costs, and improve overall operational efficiency. Moreover, self-healing conductive polymer systems contribute to enhanced long-term reliability and reduced material waste, offering advantages from an environmental sustainability perspective [7].

Their conductivity can be tuned through chemical doping, electrochemical reactions, or photochemical processes, enabling adaptation to diverse functional requirements. Continued advances in conductive polymer design and integration strategies are therefore expected to provide a critical materials foundation for next-generation smart and biointegrated electronic devices.

2.1.1 Poly (3,4-ethylenedioxythiophene) polystyrene sulfonate (PEDOT:PSS)

Poly(3,4-ethylenedioxythiophene) (PEDOT) is a representative π-conjugated conductive polymer that exhibits electrical conductivity typically ranging from 1 to 1000 $S \cdot cm^{-1}$ depending on doping conditions. It also shows high chemical and environmental stability, a relatively low oxidation potential, and a narrow HOMO–LUMO bandgap (~1.5–2.0 eV), which represents the energy difference between the highest occupied and lowest unoccupied molecular orbitals and governs charge excitation and transport. In addition, PEDOT-based systems have been widely explored in bioelectronic applications due to their reported biocompatibility.

PEDOT complexed with negatively charged polystyrene sulfonate (PSS), commonly referred to as PEDOT:PSS, is widely used owing to its water dispersibility, high stability, and ease of processing on various substrates. However, despite these advantages, PEDOT:PSS systems often exhibit limited mechanical robustness and recyclability, which restrict their applicability in deformable and sustainable electronic applications. These limitations highlight the need for material design strategies that enable the simultaneous integration of electrical conductivity with mechanical durability, self-healing capability, and recyclability [22].

Structurally, PEDOT:PSS is a polymer electrolyte complex formed through electrostatic interactions between positively charged PEDOT chains and negatively charged PSS chains (Figure 2a). While PEDOT is inherently insoluble in water in its oxidized state, PSS acts as a hydrophilic polyanion that stabilizes PEDOT in aqueous dispersions, thereby enabling solution processability. The complex typically adopts a micellar nanostructure, in which conductive PEDOT-rich domains form the core, surrounded by excess insulating PSS chains that constitute a shell (Figure 2b) [23].

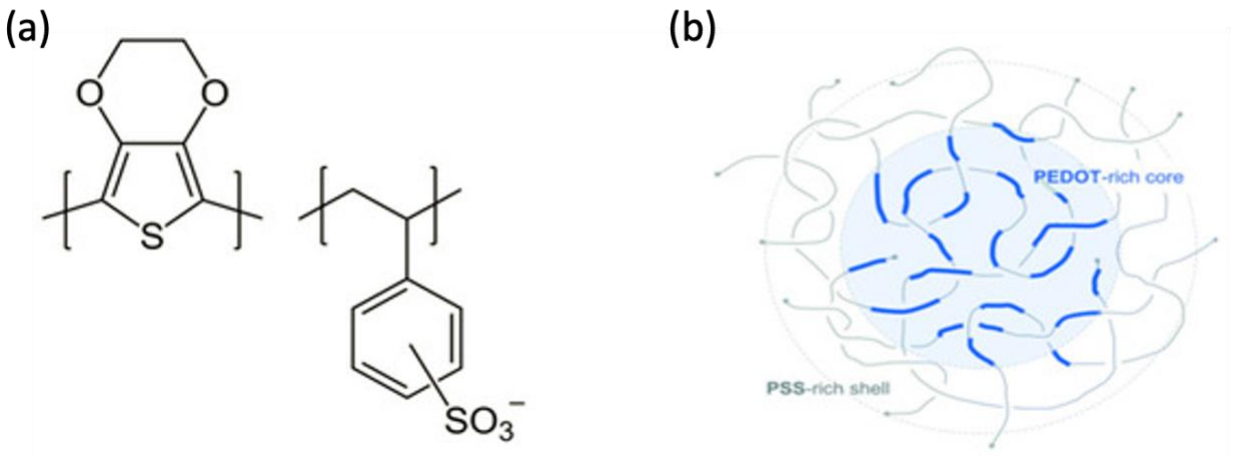

Figure 2. (a) Chemical structure of PEDOT:PSS and (b) Schematic core–shell morphology of the PEDOT:PSS complex in aqueous dispersion [23].

The electrical properties of PEDOT:PSS are intrinsically influenced by this structural configuration. In particular, excess PSS, which is electrically insulating, limits charge transport, making the incorporation of secondary dopants essential for enhancing conductivity [24]. Numerous studies have demonstrated that the addition of polar solvents such as dimethyl sulfoxide (DMSO), ethylene glycol (EG), D-sorbitol, and methanol to aqueous PEDOT:PSS dispersions can effectively increase electrical conductivity. These dopants strengthen interactions between PEDOT chains, induce phase rearrangement, or improve the planarity and alignment of PEDOT segments, thereby enhancing charge transport pathways. In addition, post-treatment processes applied to PEDOT:PSS films can remove excess PSS and reduce interparticle resistance, leading to conductivity enhancements of up to several orders of magnitude [24, 25]. Consequently, the electrical performance of PEDOT:PSS can be widely tuned through control of intermolecular interactions, microstructure, doping strategies, and post-treatment conditions, which is typically quantified by electrical conductivity ($S \cdot cm^{-1}$), sheet resistance (Ω/sq), and changes in resistance ($\Delta R/R_0$) under mechanical deformation.

Beyond its electrical properties, PEDOT:PSS exhibits high flexibility, mechanical stability, optical transparency, and biocompatibility, which have led to its widespread use in applications such as wearable devices, biosensors, electrochemical transistors, supercapacitors, and electronic skin (e-skin). As a water-processable polymer system, PEDOT:PSS is compatible with various fabrication

techniques, including inkjet printing, spray coating, and dry coating, making it particularly attractive for low-cost and flexible electronic devices, such as skin-attachable electronics and paper-based electrodes [26]. For these reasons, PEDOT:PSS remains one of the most actively investigated conductive polymers and serves as a key component in a wide range of functional composite material platforms.

2.2 Self-healing and Recyclable Polymers

Self-healing polymers are polymeric materials capable of autonomously repairing defects generated by external physical or chemical damage. These materials possess the ability to restore damaged regions through self-repair or re-bonding processes, thereby improving long-term durability and structural stability. Through their intrinsic healing mechanisms, self-healing polymers can recover mechanical, electrical, and chemical properties, contributing to extended service lifetimes and reduced maintenance costs in applications where durability is critical, including soft electronics, wearable devices, and flexible electronic systems [27].

Approaches to achieving self-healing polymers are generally classified into two categories (Figure 3): intrinsic and extrinsic self-healing, depending on the mechanisms employed to enable healing functionality. Intrinsic self-healing materials are activated through molecular diffusion, reversible or dynamic bonding, or supramolecular interactions that can be triggered by damage or external stimuli. Because these interactions and reactions are reversible, intrinsic self-healing materials are capable of repeated healing cycles [28]. In contrast, extrinsic self-healing materials typically rely on healing agents stored separately within microcapsules or vascular networks. When damage occurs and these reservoirs rupture, the released healing agents initiate repair reactions at the damaged site. Although extrinsic self-healing systems can provide rapid and effective healing, their healing capability is generally limited to a single event due to depletion of the stored healing agents [29].

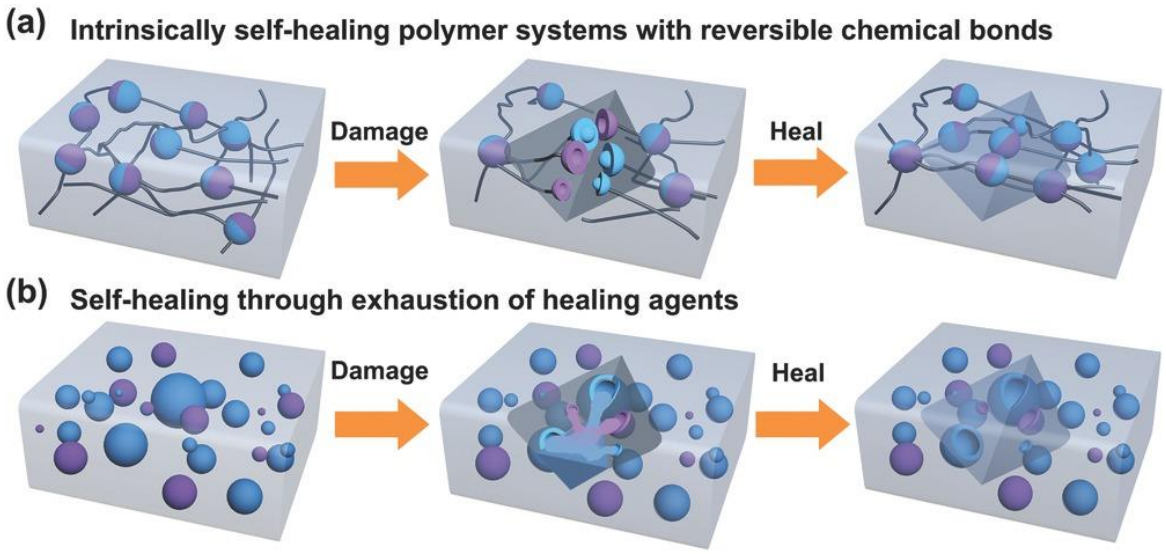

Figure 3. Two self-healing mechanisms in polymer systems: (a) bond reformation via reversible dynamic covalent interactions and (b) damage repair driven by the depletion of encapsulated healing agents [30].

2.2.1 Intrinsic Approaches

In intrinsic self-healing systems, polymers are designed to contain chemical bonds that can undergo fully reversible bond dissociation and reformation during the healing process (Figure 4). Key parameters governing the self-healing performance include bond dissociation and association kinetics, as well as polymer chain mobility. Reversible covalent bonds are particularly attractive for the design of self-healing polymers with enhanced mechanical properties due to their relatively high bond strength [31].

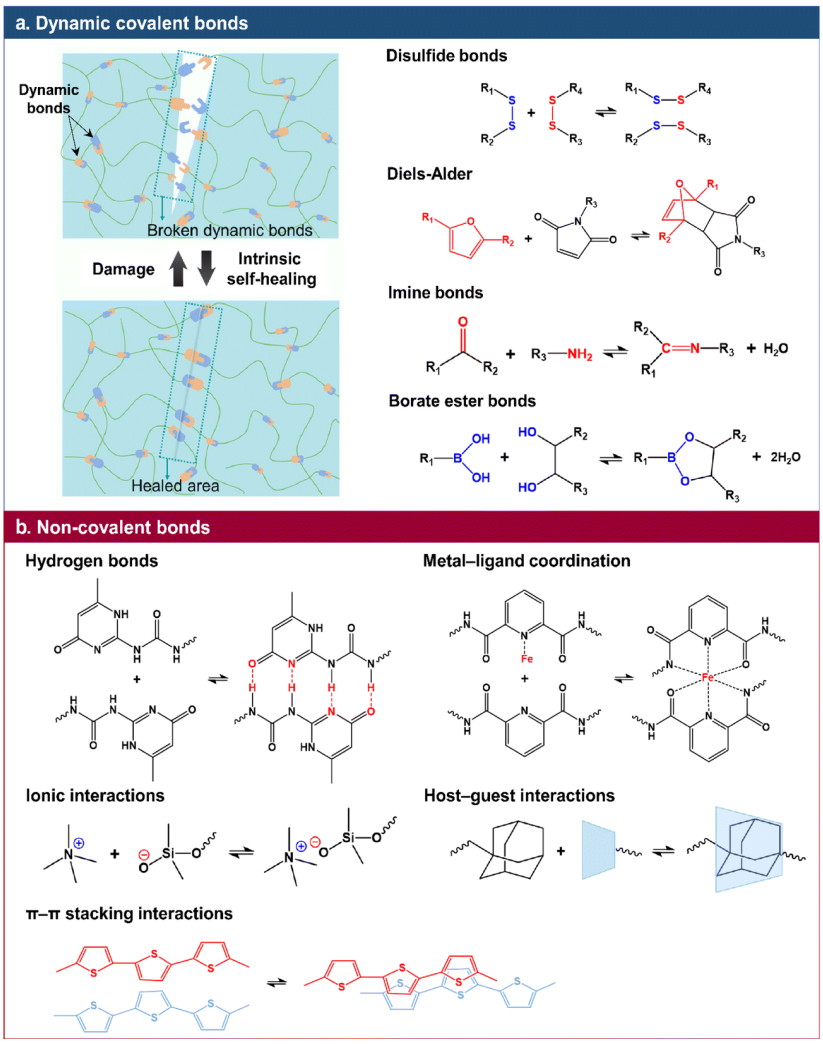

Figure 4. Schematic representation of self-healing materials categorized according to dynamic covalent bonding and non-covalent interaction mechanisms [31].

Among reversible covalent chemistries, the Diels–Alder reaction has been extensively investigated as a reliable self-healing mechanism in a variety of polymer systems [32]. This reaction enables the reconstruction of crosslinked polymer networks formed between diene and dienophile moieties. Under sufficient mechanical stress or elevated temperatures, the diene–dienophile adducts dissociate, whereas bond reformation occurs at lower temperatures, allowing damage to repair. Diels–Alder chemistry has been successfully applied to polymers such as polyimides, polyesters, and epoxies. However, because these systems typically exhibit high glass transition temperatures (T_g), efficient self-healing at room temperature is difficult to achieve.

To overcome the requirement for elevated temperatures, dynamic bond exchange reactions between reversible covalent bonds have also been explored as an alternative intrinsic self-healing strategy. These exchange reactions generally exhibit lower activation temperatures and can enable self-healing at or near room temperature. A representative example of such dynamic covalent chemistry is disulfide bonding [33]. Disulfide exchange reactions can be triggered by thermal stimuli, ultraviolet irradiation, light exposure, or redox conditions. During bond dissociation, free radicals are generated and subsequently participate in the repair of damaged regions. When sufficient chain mobility is present, fractured polymer chains can diffuse, react through radical-mediated processes, and reform covalent bonds, thereby realizing self-healing. Consequently, polymer chain mobility is a critical factor, and polymers with relatively low T_g are advantageous for efficient healing.

In addition to reversible covalent bonds, supramolecular interactions constitute an important class of intrinsic self-healing mechanisms. Supramolecular chemistry involves reversible noncovalent interactions, including hydrogen bonding, metal–ligand coordination, π–π interactions, ionic interactions, and host–guest interactions. Although these interactions are generally weaker than covalent bonds, they are highly dynamic and can form robust yet reversible polymer networks, making them particularly useful for self-healing material design [34]. Polymer networks connected through supramolecular interactions can reversibly reorganize into mechanically robust and elastic structures, and extensive research has been devoted to such systems. Upon mechanical deformation, weaker supramolecular bonds preferentially dissociate, dissipating energy, and subsequently reform through dynamic interactions, enabling self-healing.

Supramolecular polymers typically exhibit relatively low T_g values, resulting in enhanced chain mobility and ductility, which are advantageous for self-healing material development. Among noncovalent interactions, hydrogen bonding represents one of the strongest and most widely utilized mechanisms for tuning mechanical properties through dynamic bond formation and dissociation. For example, in polysiloxane elastomers, combinations of strong and weak hydrogen bonds have been employed to tailor stretchability, durability, and self-healing performance. Cooperative quadruple hydrogen bonding can be formed between phenyl urea units, whereas isophorone bisurea units form only double hydrogen bonds due to steric hindrance [8].

Metal–ligand coordination provides another versatile supramolecular approach for connecting polymer chains through coordination complexes. By introducing different metal ions and ligands, the strength of coordination bonds can be tuned to modulate mechanical properties. Under applied mechanical stress, coordination bonds dissociate, and upon removal of stress, they can be reformed, often triggered by temperature changes or electromagnetic radiation, resulting in self-healing behavior [35].

π–π interactions arise between π-electron donors and π-electron acceptors and can form thermally reversible polymer networks. In such systems, donor and acceptor polymer chains interact at defined distances to establish π–π stacking interactions. Self-healing can be achieved by tuning the glass transition temperature through control of intermolecular spacing or molecular configuration. π–π interactions are often incorporated alongside other supramolecular interactions, such as hydrogen bonding or metal coordination, to enhance overall healing performance [34].

Ionic interactions commonly appear in the form of ionomers, where polymer chains are interconnected through electrostatic interactions within the polymer network. Upon mechanical damage or impact, friction-generated heat can be transferred to the surrounding polymer matrix, inducing localized melting. The softened polymer surfaces can then diffuse across the damaged interface, enabling healing. Subsequent reformation of ionic interactions and long-term relaxation processes restore the mechanical properties of the polymer. The self-healing efficiency of ionically interacting systems can be tuned by environmental factors or additives. For instance, the introduction of water, highly polar salts, or solvents can adjust ionic bond strength, enhance chain mobility, and thereby improve healing efficiency [36].

Host–guest interactions provide spatially organized and size-selective binding between complementary polymer segments and are particularly attractive for hydrogel-based self-healing systems [37]. Common cyclic host molecules include cyclodextrins, cucurbiturils, crown ethers, calixarenes, and pillararenes. Host molecular structures can be designed to selectively interact with specific guest molecules, enabling flexible material design. By tailoring host and guest molecular structures, healing efficiency can be adjusted. For example, the incorporation of β-cyclodextrin and adamantane into the side chains of various water-soluble polymer backbones enables multivalent host–guest interactions, imparting hydrogels with high flexibility, durability, and self-healing capability. The mechanical properties of such systems can be tuned by varying the

concentration and ratio of host and guest components. Another representative host molecule is cucurbituril [8]. When in situ polymerization is carried out in the presence of cucurbituril, polymerizable guest molecules (1-benzyl-3-vinylimidazolium), and acrylamide, self-healing polymers can be formed. In this system, cucurbituril functions as a dynamic crosslinker and sacrificial bond, dissipating energy upon deformation and subsequently reforming to trigger self-healing.

2.2.2 Extrinsic Approaches

In extrinsic self-healing systems, liquid healing agents are typically pre-embedded within the polymer matrix using carriers such as microcapsules or microvascular networks. When mechanical damage occurs, these carriers rupture, allowing the healing agent to flow into the damaged region. Upon contact with catalysts that are pre-incorporated within the polymer matrix, polymerization reactions are initiated, leading to the repair of the damaged area [38].

Microcapsule-based self-healing systems have been successfully implemented in polymer matrices, such as epoxy resins. In these systems, the healing agent is encapsulated within microcapsules, and the distribution of catalysts is generally achieved through three representative strategies (Figure 5). In the first approach, the catalyst is directly dispersed within the polymer matrix. For example, when monomers released from ruptured microcapsules come into contact with catalysts dispersed in an epoxy matrix, ring-opening metathesis polymerization is triggered, enabling the recovery of mechanical damage [39]. In the second approach, both the healing agent and the catalyst are encapsulated separately. When both types of microcapsules rupture upon damage, the released healing agent and catalyst react with each other to initiate the healing process. This configuration is commonly referred to as a dual-capsule system. In the third strategy, residual reactive functional groups within the polymer matrix or external stimuli act as catalysts to trigger the healing reaction. A typical example involves the use of residual amine groups in epoxy matrices to initiate polymerization of the released healing agent.

Microvascular-based self-healing materials store healing agents within hollow channels or capillaries that can be interconnected to form three-dimensional microvascular networks. This architecture enhances healing efficiency and enables the repair of relatively large damage volumes. Unlike microcapsule-based systems, healing agents stored in microvascular networks can be introduced after the network has been integrated into the polymer matrix and can be replenished

after depletion, allowing multiple healing cycles. This capability represents a significant advantage over microcapsule-based systems, which are typically limited to a single healing event [40].

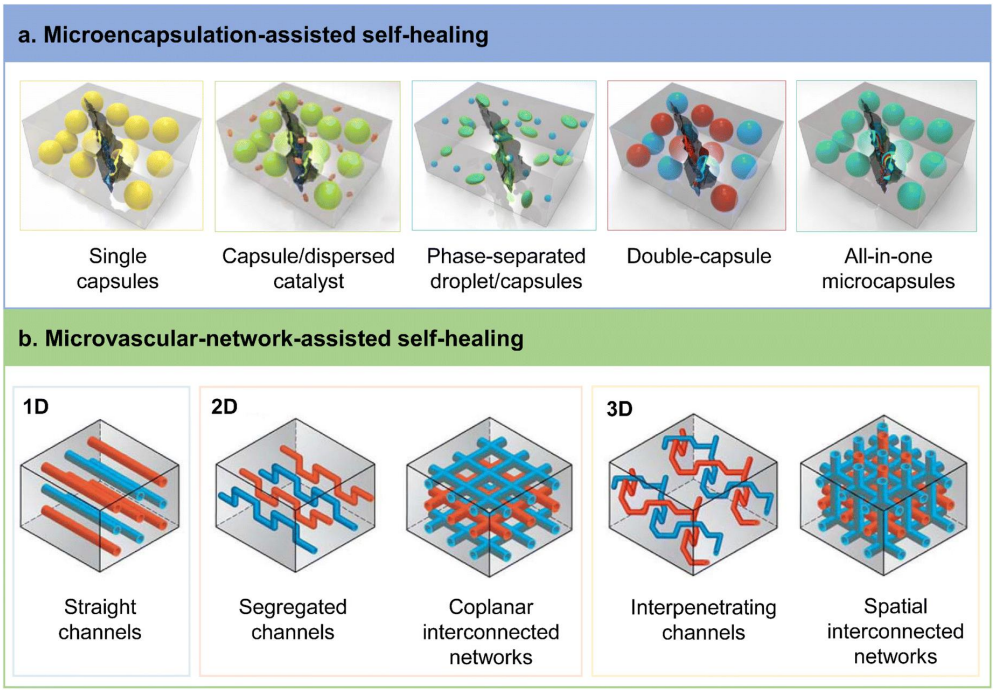

Figure 5. Schematic depiction of extrinsic self-healing approaches: (a) microcapsule-based healing and (b) vascular network-assisted repair systems [31].

2.2.3 Polyurethane-Based Elastomers in Self-Healing Systems

PU chemistry was first developed in 1937 by Otto Bayer via the polyaddition reaction between diisocyanates and polyols, leading to the formation of urethane linkages. This discovery laid the foundation foa a wide range of PU-based materials including foams, elastomers, adhesives, plastics, and fibers [41]. Approximately 15% of the global polyurethane market is utilized in elastomeric forms, which are widely employed across industrial sectors due to their excellent abrasion resistance, mechanical performance, and processability. As polymeric materials that combine high stretchability with elastic recovery, polyurethane elastomers have attracted considerable attention to applications in wearable electronics and flexible devices [42]. More recently, increasing research efforts have focused on exploiting these mechanical characteristics to develop

polyurethane-based functional polymers capable of autonomously restoring surface damage through self-healing behavior.

Polyurethanes (PUs) are synthesized through an addition polymerization reaction between alcohol-based compounds containing hydroxyl groups (–OH) and compounds containing isocyanate groups (–NCO), a process that is accompanied by heat release (Figure 6a). Isocyanates containing one or more NCO groups and alcohols containing one or more OH groups are classified as polyfunctional reactants, and their reaction leads to the formation of urethane linkages with a repeating $–[NHCOO]_n–$ structure. The polymer chains formed through repeated urethane bond formation constitute polyurethane (Figure 6b) [41].

PU elastomers are commonly synthesized using two representative approaches [43]. In the one-pot method, all reactive components are mixed simultaneously, enabling a simple and rapid synthesis; however, this approach often results in limited control over polymer chain length uniformity. In contrast, the two-stage, or prepolymer, method involves the initial reaction of a macrodiol (e.g., polyester- or polyether-based diols) with a diisocyanate to form a prepolymer, followed by chain extension using short-chain diols or diamines. This method provides superior structural uniformity and is therefore more suitable for the development of high-performance polyurethane materials.

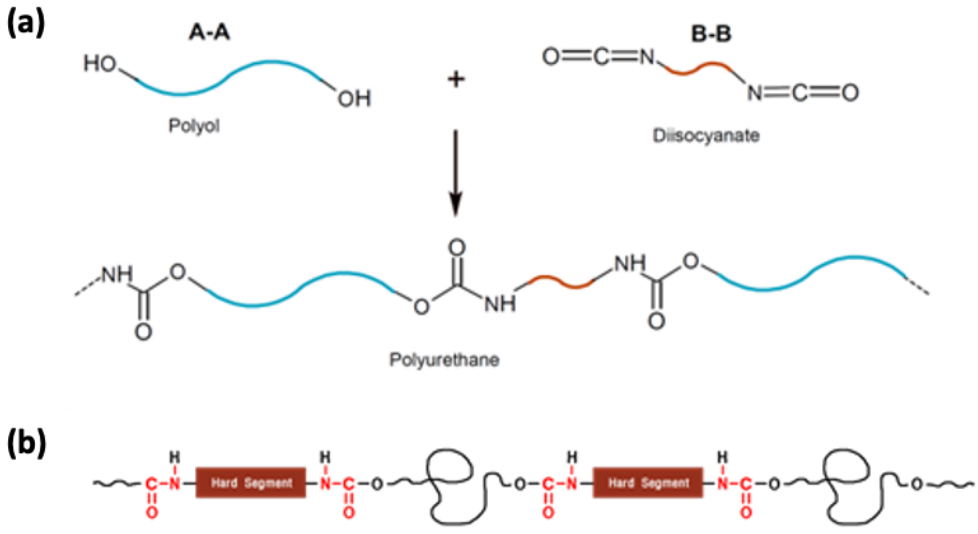

Figure 6. (a) Synthetic route of the polyurethane. (b) Schematic illustration of dynamic interactions between soft and hard segments [43].

The physical properties of PU elastomers are strongly governed by the composition and arrangement of soft and hard segments within the polymer structure (Figure 6b). Soft segments are typically composed of polyols, polyethers, polyesters, or polyethylene-based polymers and possess low glass transition temperatures (T_g), resulting in high chain mobility and flexibility [43]. In contrast, isocyanate-derived hard segments exhibit rigid structures and play a dominant role in determining the overall stiffness and elastic recovery of the material. By controlling parameters such as the molecular weight of the macrodiol, the compositional ratio of diols and diisocyanates, and block sequence arrangement, the mechanical strength, stretchability, and abrasion resistance of polyurethane elastomers can be precisely tuned, enabling the design of materials with diverse mechanical properties [44].

The design of polyurethane systems with self-healing functionality has primarily focused on the incorporation of reversible bonding motifs into the polymer network. Among these, disulfide bonds have been widely employed due to their relatively low activation energy for bond dissociation and reformation, enabling repeated self-healing under thermal or photochemical stimuli. For example, Li et al.[45] developed a polyurethane elastomer using a polyether diol as the soft segment and a disulfide-containing diisocyanate as the crosslinking unit, achieving more than 90% recovery of mechanical strength within several hours at room temperature. Notably, this system maintained stable elastic properties and tensile strength even after repeated healing cycles.

Another effective strategy involves constructing hydrogen-bonding networks within the polyurethane matrix. The incorporation of hydrogen-bonding motifs such as ureidopyrimidinone (UPy), barbituric acid, or catechol into functional urethane monomers enables the design of polyurethane films capable of autonomous self-healing without external stimuli. Xu et al.[46] reported polyurethane systems containing dual or quadruple hydrogen-bonding networks that recovered more than 80% of their original mechanical toughness within 24 hours. These materials exhibited relatively low T_g values and high chain mobility, facilitating effective molecular rearrangement and resulting in efficient self-healing behavior.

In addition, reversible covalent networks based on Diels–Alder (DA) reactions have been widely applied to thermally reversible self-healing polyurethane systems. In these materials, bond dissociation and reformation can be induced by thermal or ultraviolet stimuli, allowing damage repair at elevated temperatures. Polyurethane networks constructed using DA chemistry typically

exhibit healing behavior in the temperature range of 80–120 °C and maintain their mechanical properties after repeated thermal healing cycles [47].

Beyond these approaches, various self-healing polyurethane systems based on reversible physical or chemical interactions have been reported, including pH-responsive ionic interactions, metal–ligand coordination, and dynamic urea or urethane exchange reactions. These systems are designed according to specific performance metrics such as stimulus responsiveness, repeatability of healing, film stability, and curing kinetics. Owing to its structural versatility and compatibility with a wide range of functional bonding motifs, polyurethane represents an important and adaptable platform for the development of self-healing polymer materials.

2.2.4 Recyclable PUs System

PUs are a versatile polymeric material that can exhibit both thermoplastic and thermosetting characteristics, depending on its molecular architecture. Traditionally, PUs have been regarded as difficult to recycle due to its highly crosslinked network structures and irreversible curing behavior. Recently, however, recyclable PU systems have been increasingly reported through the introduction of reversible covalent bonds or dynamic physical interactions, enabling repeated reprocessing and reshaping [48]. These systems respond to external stimuli, such as heat or solvents, by temporarily reorganizing their network structures or increasing chain mobility, thereby allowing remolding while maintaining functional performance.

One representative chemical approach involves the incorporation of dynamic polysulfide bonds into the PU network (Figure 7a) [49]. Polysulfide (–S–S–) linkages were introduced into polymer chains to enable reversible sulfur–sulfur exchange reactions at relatively low temperatures (~140 °C). Owing to the low bond dissociation energy and high reactivity of polysulfide bonds, the polymer network could undergo dynamic rearrangement during thermal processing. As a result, the material retained a high level of mechanical performance, including tensile strength and elongation at break, even after multiple hot-press reprocessing cycles. This study demonstrated that chemically dynamic networks can simultaneously achieve recyclability and mechanical stability in PU systems.

Another chemically driven strategy was reported in polyurethane networks. In this work, reversible transcarbamoylation reactions within urethane linkages were utilized to allow dynamic bond exchange at elevated temperatures [50]. Through this mechanism, partial network dissociation and

reformation occurred during thermal treatment, enabling reprocessability and shape recovery behavior. Notably, the resulting PU networks maintained tensile strengths exceeding 35 MPa after reprocessing, highlighting the effectiveness of dynamic urethane chemistry in achieving both high elasticity and structural resilience (Figure 7b).

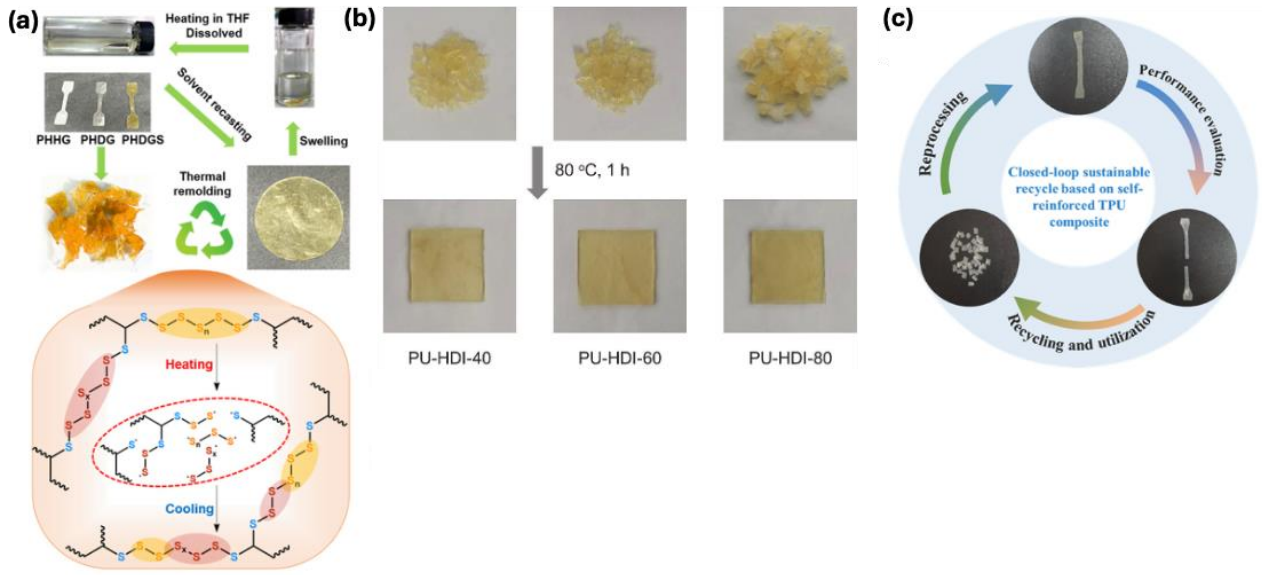

Figure 7. Recyclable polyurethane strategies: (a) polysulfide bond exchange [71], (b) transcarbamoylation-enabled dynamic urethane networks [72], and (c) physically crosslinked thermoplastic PU based on crystalline hard segments [73].

In addition to chemically dynamic approaches, recyclability in PU systems has also been realized through physical network design without relying on covalent bond exchange [51]. A thermoplastic PU system incorporating highly crystalline self-reinforcing domains was developed (Figure 7c). Strong phase separation and enhanced crystallinity of hard segments created physical crosslinking points, while the soft segments retained thermally induced mobility. This design enabled repeated reprocessing through conventional thermoplastic techniques such as extrusion and hot pressing, while preserving mechanical strength and thermal resistance after multiple cycles. Physical-network-based strategies are particularly attractive for industrial applications, as they avoid complex chemical modifications while offering long-term durability and processing flexibility.

Overall, recent recyclable PU systems can be broadly categorized into two main strategies. The first involves the use of dynamic covalent bonds to chemically reorganize polymer networks, enabling repeated reprocessing and, in some cases, self-healing behavior. The second relies on controlled phase separation and crystallinity to achieve reversible physical crosslinking while maintaining thermoplastic processability and mechanical integrity. These developments demonstrate that PUs are no longer limited to single-use or permanently crosslinked materials but is evolving into a sustainable functional polymer platform. Such advances are directly aligned with the design philosophy of this study, which aims to integrate self-healing capability and recyclability within conductive polymer composite systems.

2.3 Conductive Self-Healing Polymers

Conductive polymers are widely utilized as essential functional materials in diverse application fields, including flexible electronic devices, biointerfaces, and energy storage systems [52-54]. In Particularly in these applications, ensuring long-term electrical stability under repeated mechanical deformation or damage has emerged as a critical challenge [52, 55]. In response, recent research has increasingly focused on integrating self-healing functionality into conductive polymer systems, enabling the simultaneous recovery of electrical conductivity and mechanical integrity after damage [52, 55, 56]. Such self-healing capability can significantly enhance material reliability and device lifetime and is therefore of particular importance for applications subjected to prolonged use and repetitive mechanical stress, including wearable devices, electronic skin, and skin-mounted sensors [57, 58].

Conductive polymer systems incorporating self-healing functionality are generally classified into two main design strategies [55, 59, 60].

The first strategy involves introducing reversible covalent bonds or supramolecular interactions directly into the molecular structure of the conductive polymer itself, thereby enabling both electrical conductivity and self-healing behavior within a single polymer framework. Representative examples include conductive polymers such as polyaniline (PANI) and polypyrrole (PPy), which have been modified with disulfide bonds, Diels–Alder moieties, or multiple hydrogen-bonding motifs to allow molecular reconnection and functional recovery after damage [59, 60].

The second strategy, as widely reported in the literature, relies on compositing conductive polymers or conductive materials (e.g., PEDOT:PSS, carbon nanotubes, graphene) with soft polymer matrices that inherently possess self-healing capability, such as polyurethane, poly(dimethylsiloxane), or poly(vinyl alcohol) [61, 62]. In these systems, the self-healing polymer matrix provides mechanical recovery through its dynamic network, while the conductive component establishes electrical pathways. This dual-function design offers flexibility in material selection and processing and allows compatibility with a wide range of conductive fillers [55]. However, a common limitation of this approach is that disruption of the conductive network during damage and healing can lead to incomplete recovery of electrical performance [62].

In such composite systems, trade-offs among electrical conductivity, stretchability, self-healing efficiency, and mechanical stability are often application-dependent as different applications prioritize specific performance metrics, and therefore represent critical design considerations [4, 55, 63]. For instance, increasing the content of PEDOT:PSS can enhance electrical conductivity but may deteriorate the flexibility and healing capability of the polyurethane matrix [64]. Conversely, excessive incorporation of the self-healing polymer can compromise the continuity of the conductive network, resulting in a sharp decrease in electrical conductivity. Therefore, precise control over composition, phase-separated morphology, and dopant selection is essential to achieve a balanced integration of self-healing functionality and electrical performance [65].

To date, a variety of self-healing conductive polymer systems based on PANI, PPy, and PEDOT:PSS have been reported, with each material exhibiting distinct characteristics in terms of processability, mechanical properties, and healing mechanisms [66]. PANI-based systems demonstrate high redox activity and electrical conductivity but often suffer from limited processability and mechanical flexibility (Figure 8a); thus, they are frequently combined with hydrogel matrices or polyurethane-based polymers to improve healing efficiency and mechanical compliance [67]. PPy-based self-healing conductors are most commonly realized by integrating PPy into dynamic polymer matrices (e.g., elastomers or hydrogels) (Figure 8b), where reversible noncovalent interactions and/or coordination interactions enable healing, while the elastomeric matrix provides stretchability [68, 69]. Among these materials, PEDOT:PSS-based composites exhibit particularly favorable properties, including water processability, mechanical flexibility, and biocompatibility. Consequently, extensive efforts have been devoted to combining PEDOT:PSS with various dopants and polymer matrices to simultaneously enhance self-healing

behavior, electrical conductivity, and mechanical durability. Based on this background, the following section focuses on recent research trends in PEDOT:PSS-based self-healing platforms (Figure 8c), with particular emphasis on structural design, interaction mechanisms, healing efficiency, and electrical performance. [20, 70].

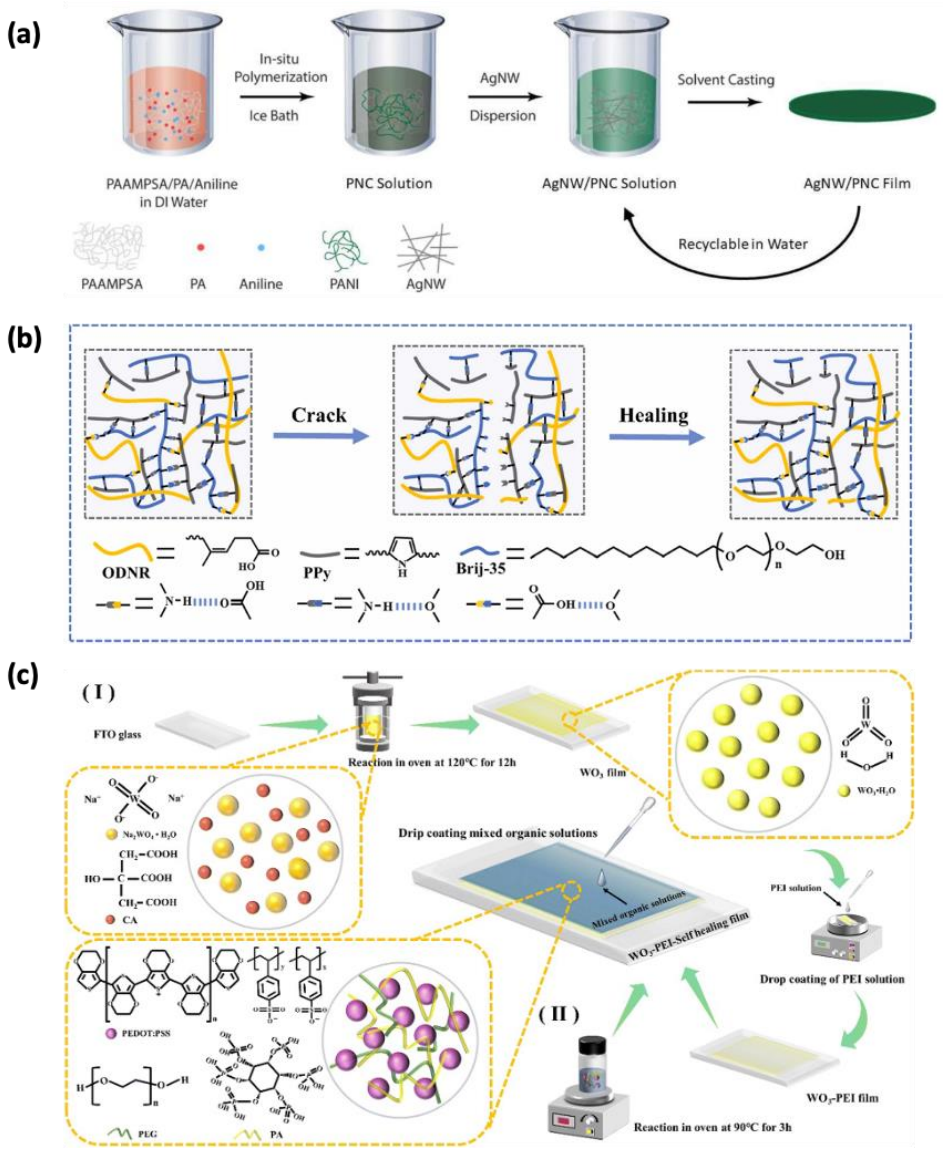

Figure 8. Comparison of representative self-healing conductive polymer systems based on (a) polyaniline (PANI) [71], (b) polypyttole (PPy) [69], and (c) PEDOT:PSS [72]., highlighting differences in material design strategies, interaction mechanisms, and limitations in electrical and mechanical performance.

2.3.1 PEDOT:PSS-Based Self-Healing Elastomer Blends

PEDOT:PSS is one of the most widely employed conductive materials in self-healing conductive polymer systems due to its facile processability, biocompatibility, high electrical conductivity, and compatibility with a broad range of polymer matrices. In addition, PEDOT:PSS possesses intrinsic structural features that allow the formation of hydrogen bonding and electrostatic interactions, enabling the simultaneous incorporation of electrical functionality and self-healing behavior when combined with elastomeric matrices. Over the past several years, the development of PEDOT:PSS-based self-healing composites has been actively explored through diverse material design strategies, with increasing sophistication in both structural control and targeted applications [53, 56].

One representative example (Figure 9a), in which PEDOT:PSS was combined with a polyurethane-based polymer matrix to fabricate an electrochromic film capable of self-healing at relatively low temperatures (~60 °C) [73]. The healing mechanism relied on a hydrogen-bonded polymer network, exhibiting adhesive behavior at room temperature and recovering cohesive strength upon heating. The restoration of both visual color contrast and electrochemical performance after damage demonstrated the retention of functional properties following healing. This system highlights the potential of PEDOT:PSS-based self-healing composites for applications such as flexible displays and electrochromic windows in environments where moderate thermal stimuli are acceptable.

In another study, PEDOT:PSS was blended with a poly(ionic liquid) (PIL) elastomer to simultaneously enhance electrical conductivity and self-healing capability (Figure 9b) [64]. The PIL matrix provided ionic interactions, high flexibility, and intrinsic adhesiveness, while its interaction with PEDOT:PSS facilitated charge transport and molecular rearrangement. The resulting composite maintained electrical conductivity under strains exceeding 150% and exhibited self-healing within one hour after damage. Importantly, sensor sensitivity was preserved after repeated damage–healing cycles, demonstrating suitability for wearable strain sensors and touch-sensing applications.

A third example is, which reported a PEDOT:PSS/polyurethane diol composite for dry, skin-attachable electrodes (Figure 9c) [74]. The material maintained adhesive and self-healing properties even under low-humidity conditions and recovered mechanical damage within 30

minutes at room temperature. After healing, the electrodes could be repeatedly reattached to skin with minimal change in electrical resistance, indicating strong potential for reusable wearable bioelectrodes. The compatibility of this system with printing and coating processes further supports its applicability to scalable fabrication of electrophysiological sensors, such as ECG and EMG electrodes.

Another notable study, which demonstrated a PEDOT:PSS-based composite integrated with a highly tough, water-responsive elastomer capable of autonomous self-healing in underwater environments (Figure 9d) [75]. In this system, water acted as a trigger for healing, enabling spontaneous recovery of cut samples within several hours under submerged conditions. The composite achieved both high mechanical toughness and extreme stretchability (>1000%), highlighting its applicability to underwater sensors and wearable electronics operating in harsh environments.

Collectively, these studies demonstrate that PEDOT:PSS serves not only as a conductive component but also as an effective platform for integrating self-healing functionality through interactions with diverse polymer matrices, including polyurethane, ionic elastomers, and water-responsive networks. The reported self-healing mechanisms encompass hydrogen bonding, ionic interactions, adhesive recovery, and moisture-assisted processes. Across these systems, key performance metrics commonly evaluated include healing time, recovery efficiency, electrical stability, and compatibility with fabrication techniques such as printing and coating.

Despite these advances, most PEDOT:PSS-based self-healing systems remain at the proof-of-concept stage, with limited consideration given to recyclability, long-term durability, and structural stability under repeated mechanical cycling. In contrast, this thesis extends beyond proof-of-concepts studies by demonstrating reproducible material performance, compatibility with solution processable, and stable operation under repeated mechanical stress. Furthermore, quantitative understanding of how interactions between PEDOT:PSS and polymer matrices influence the overall material properties remains limited. To address these limitations, increasing attention has been directed toward polyurethane-based composite systems that integrate self-healing capability, mechanical resilience, electrical conductivity, and reprocessability in a unified design framework. The following section therefore focuses on the design strategies and representative implementations of self-healing systems based on PEDOT:PSS and PU systems.

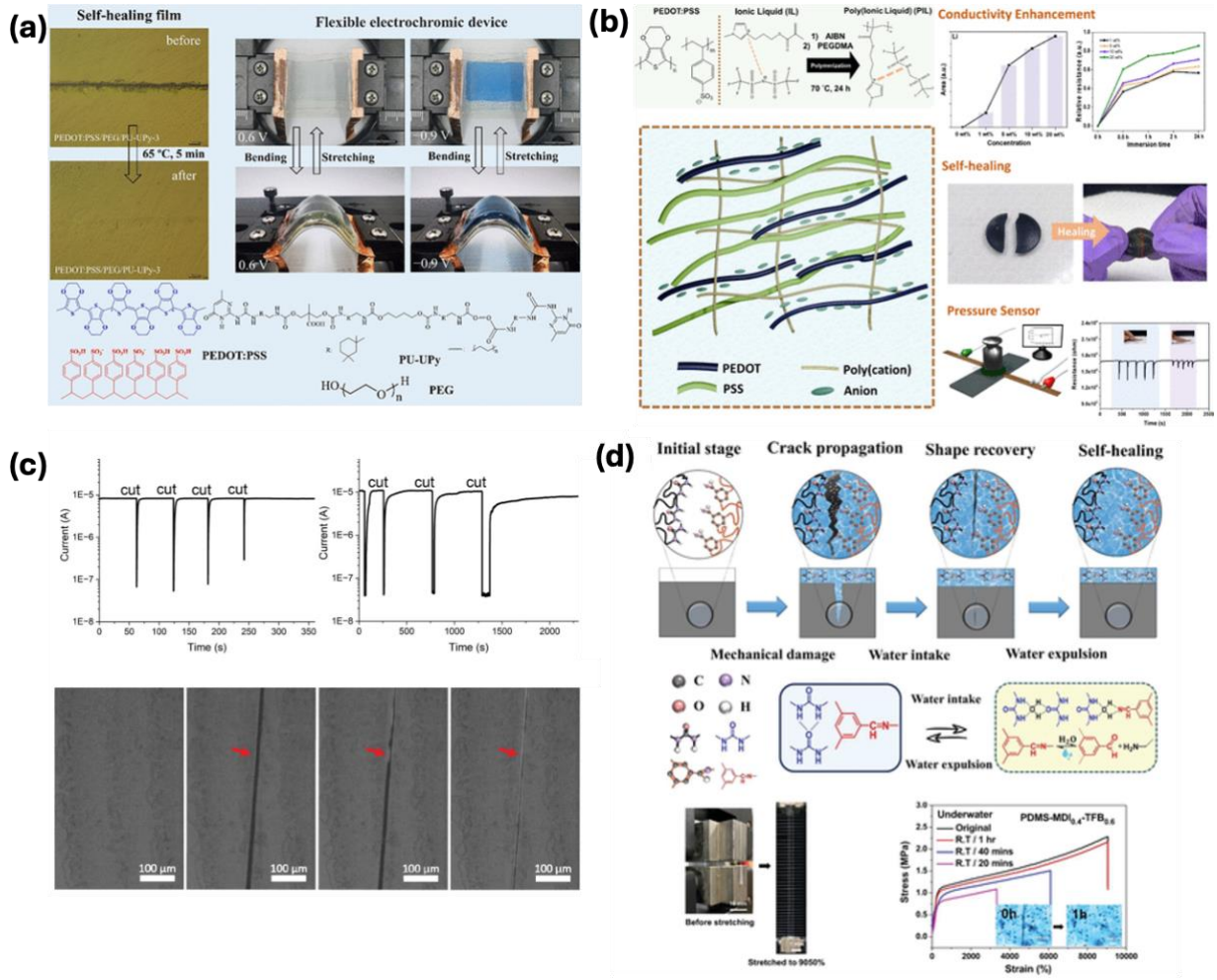

Figure 9. Representative PEDOT:PSS-based self-healing composite systems for flexible and wearable electronics. (a) Polyurethane/PEDOT:PSS electrochromic film exhibiting low-temperature healing enabled by hydrogen-bonded polymer networks [67]. (b) PEDOT:PSS blended with a poly(ionic liquid) elastomer providing enhanced conductivity, stretchability, and rapid self-repair for strain sensing [58]. (c) PEDOT:PSS/polyurethane diol composite used as reusable, skin-attachable dry electrodes with room-temperature healing and stable electrical performance [68]. (d) Water-responsive PEDOT:PSS elastomer composite demonstrating autonomous healing and extreme stretchability in underwater environments [69].

2.3.2 Recyclability of PEDOT:PSS and its Composites

Structurally, PEDOT:PSS consists of a micellar architecture composed of a conductive PEDOT-rich core surrounded by an insulating PSS-rich shell, while chemically the system is stabilized by electrostatic (Coulombic) interactions between the positively charged PEDOT chains and negatively charged PSS chains. Owing to this interaction-based assembly, PEDOT:PSS can be redispersed, redeposited, or reprocessed in response to solvent or water treatment, suggesting intrinsic potential for reuse and recycling.

A representative example is reported in conductive Cellulose/PEDOT:PSS films. In this study, PEDOT:PSS was integrated with a cellulose-based stretchable film and employed as a wearable sensor (Figure 10a). After device use, the conductive layer could be removed and reprocessed through a water-based washing and redeposition process, enabling recovery of electrical functionality (Figure 10b) [76]. The porous structure and water-permeable nature of the cellulose substrate facilitated repeated adsorption and desorption of PEDOT:PSS, demonstrating a solvent-assisted reprocessing strategy. Even after multiple recycling cycles, the electrical conductivity and sensing performance were largely preserved, and low hysteresis behavior was maintained after more than three reuse cycles (Figure 10c). This work provides experimental evidence that PEDOT:PSS can be recovered and reutilized as a water-processable electrode material.

Another notable example is presented, where a closed-loop recycling process was proposed for flexible organic electronic devices containing PEDOT:PSS (Figure 10d) [77]. In this approach, PEDOT:PSS layers were selectively separated from device substrates and redissolved using polar solvents such as dimethyl sulfoxide (DMSO) and ethylene glycol. The recovered PEDOT:PSS could then be purified, reformulated into ink form, and redeposited as conductive films, restoring electrical performance. This study extended the concept of recyclability beyond simple delamination and redeposition, demonstrating the feasibility of material recovery, re-inking, and film reformation within a circular processing framework. As a result, PEDOT:PSS was highlighted as a conductive polymer with potential applicability in closed-loop recycling systems rather than a single-use electrode material.

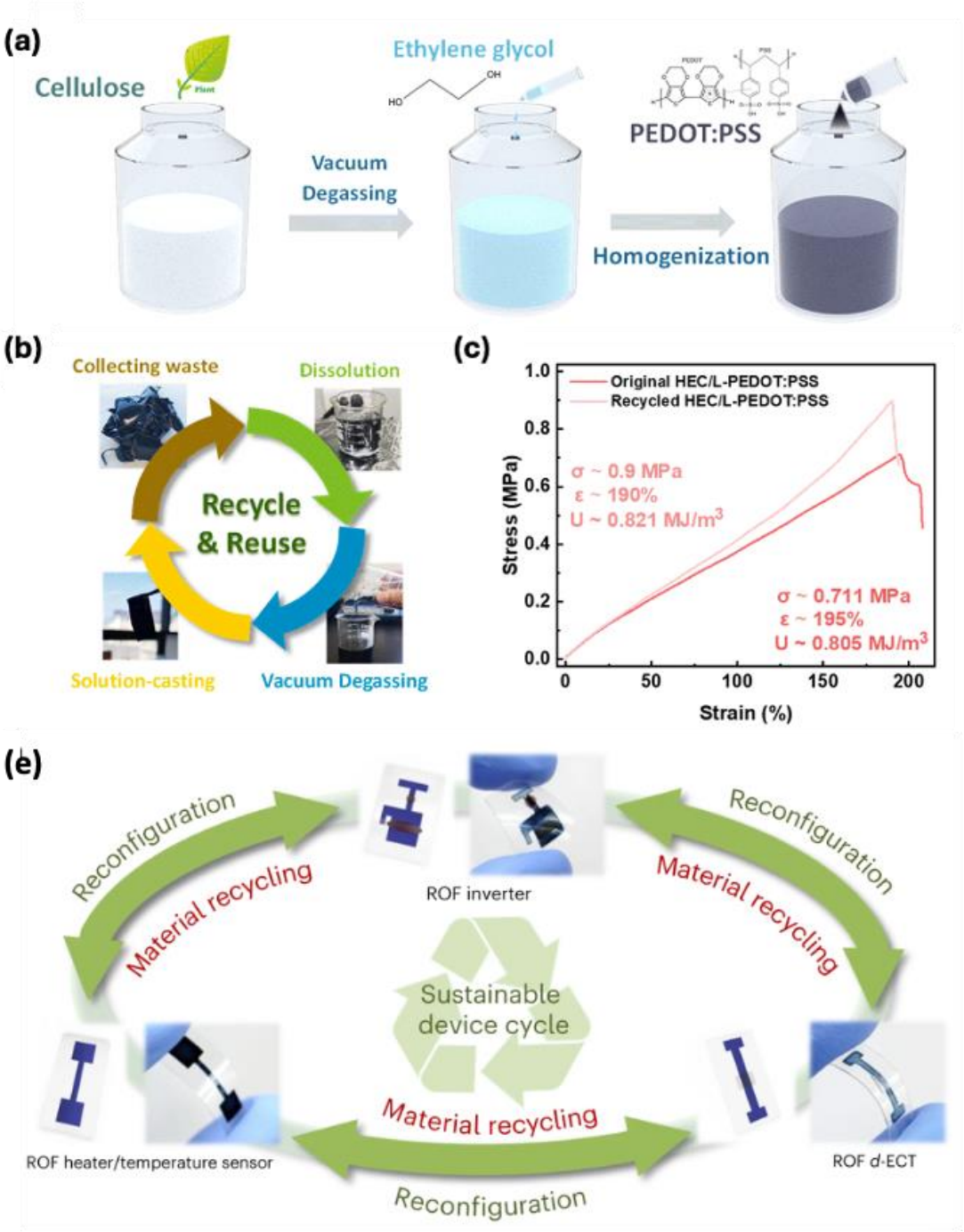

Figure 10. Recyclable PEDOT:PSS-based electronic systems. (a–c) Cellulose/PEDOT:PSS wearable sensors enabling water-assisted removal and redeposition of the conductive layer with preserved electrical performance [74]. (d) Closed-loop recycling of PEDOT:PSS films via solvent dissolution, purification, and re-inking for re-fabrication of flexible devices [75].

Collectively, these studies indicate that PEDOT:PSS exhibits solvent-assisted reprocessability through physical redispersion and redeposition mechanisms. However, because the phase-separated microstructure and electrical properties of PEDOT:PSS are highly sensitive to solvent conditions, the retention of performance after recycling strongly depends on interactions with the supporting substrate or polymer matrix, as well as on doping state and post-treatment conditions.

Despite these advances, most reported studies have focused on PEDOT:PSS as a single-component material or in relatively simple film architectures. Recyclable composite systems that simultaneously address mechanical robustness, electrical stability, and repeated reprocessing remain limited. In particular, recyclability in conductive polymer systems that also incorporate self-healing functionality has been scarcely explored. This gap provides a clear motivation for the present PhD thesis, which aims to develop PEDOT:PSS/PU-based composite systems capable of integrating self-healing behavior, electrical conductivity, and recyclability within a unified material platform.

2.4 PEDOT:PSS with Additives for Printable Self-Healing Electrodes

PEDOT:PSS is a widely used conductive polymer that simultaneously offers aqueous processability, electrical conductivity, mechanical flexibility, and biocompatibility, making it highly attractive for wearable and bioelectronic applications [78]. However, PEDOT:PSS as a single-component material is mechanically vulnerable under repeated deformation, exhibits rapid degradation of electrical performance upon damage, and lacks intrinsic self-healing capability [79]. To overcome these limitations, extensive efforts have been devoted to modifying PEDOT:PSS through blending or compositing with various polymeric or low-molecular-weight additives, with the aim of introducing damage tolerance and healing behavior while preserving electrical functionality and printability (Figure 11a) [80].

A representative approach involves the incorporation of polyethylene glycol (PEG) into PEDOT:PSS to induce hydrogen-bonding networks and impart physical self-healing behavior (Figure 11b) [3]. In this study, it was demonstrated that the molecular weight and concentration of PEG significantly influence interactions between PEDOT and PSS chains. These interactions enabled partial structural rearrangement after film damage, resulting in recovery of electrical conductivity. Notably, self-healing occurred under ambient conditions without external stimuli, and a certain level of electrical performance was retained even after repeated mechanical damage.

In a related approach, adhesive polymeric components were introduced into PEDOT:PSS to enhance adhesion to skin and flexible substrates while simultaneously enabling electro-mechanical self-healing (Figure 11c) [78]. The resulting composites exhibited recovery of conductive pathways under repeated stretching and damage, achieving a balance between mechanical resilience and functional stability. This strategy is particularly relevant for bioelectronic applications, where intimate and durable contact with soft biological tissues is required.

Other studies have explored the incorporation of citric acid and polyvinyl alcohol (PVA) were incorporated into PEDOT:PSS to simultaneously enhance electrical, mechanical, and self-healing performance (Figure 11d) [81]. Citric acid promoted improved alignment of PEDOT domains, leading to increased electrical conductivity, while PVA introduced hydrogel-like characteristics that enabled physical network recovery and moisture-assisted healing. The resulting composites exhibited self-adhesion and conductivity recovery under humid conditions, demonstrating suitability for wearable thermoelectric and electronic applications.

Overall, additive-based PEDOT:PSS composite systems represent an effective strategy for imparting self-healing behavior while simultaneously improving electrical and mechanical stability. Depending on the additive type, healing mechanisms may arise from physical interactions, domain structure reorganization, or hydrogel-assisted network recovery, leading to enhanced stretchability, adhesion, and durability. Nevertheless, most reported studies remain focused on film-level demonstrations of self-healing behavior. Comprehensive evaluations of electrode durability under repeated use, long-term stability, and compatibility with scalable fabrication processes are still limited. These limitations highlight the need for more structurally integrated material systems that can support practical, repeatable, and reliable self-healing electrode applications.

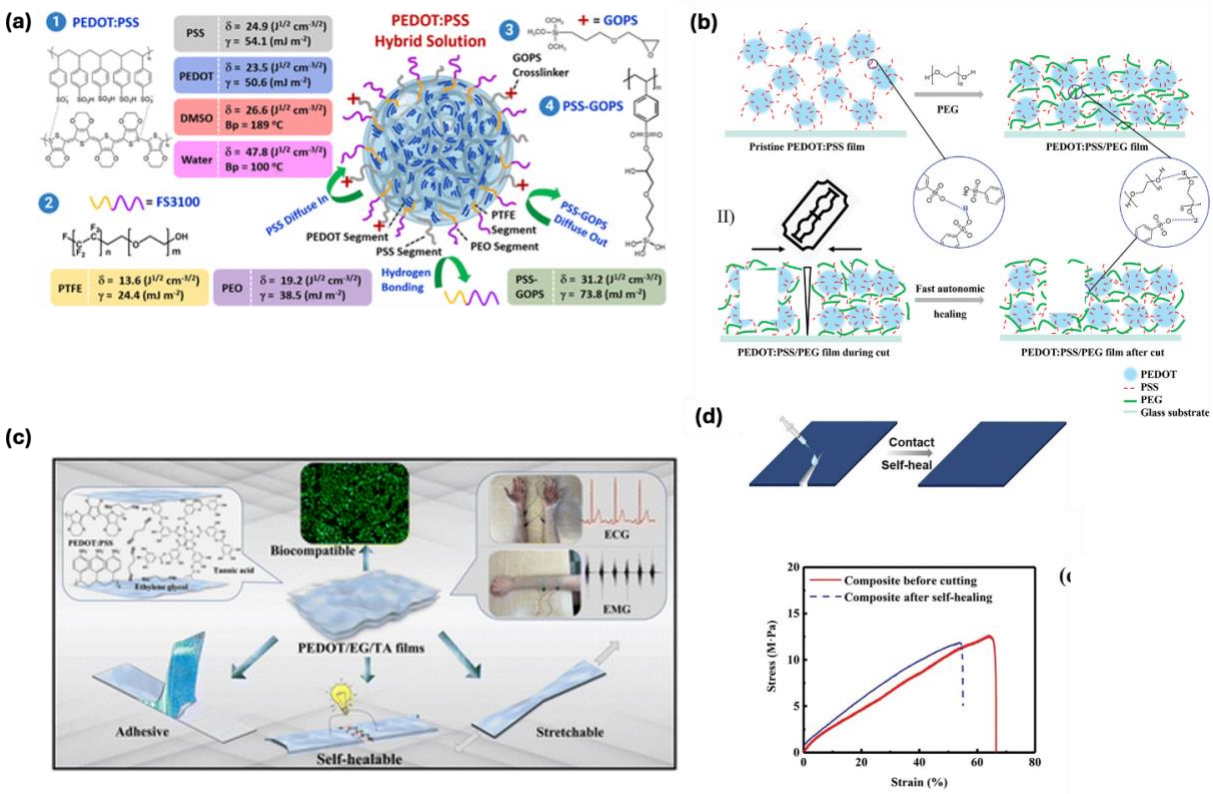

Figure 11. Strategies to enhance the self-healing performance of PEDOT:PSS through polymer blending and additive engineering. (a) Concept of composite modification to improve mechanical durability and damage tolerance [78]. (b) PEG incorporation enabling hydrogen-bond-mediated physical self-healing [79]. (c) Adhesive polymer blends providing electro-mechanical recovery for wearable bioelectronics [76]. (d) Citric acid/PVA additives improving conductivity and moisture-assisted healing behavior [80].

2.5 Applications of Self-Healing Conductive Polymers

Self-healing conductive polymers have emerged as key materials for next-generation electronic devices due to their ability to restore degraded electrical performance and reorganize damaged mechanical structures [60]. Conventional electronic devices are highly susceptible to physical damage such as fracture, cracking, and interlayer delamination. This vulnerability is particularly critical in applications involving repeated mechanical deformation, including wearable devices, flexible sensors, and e-skin, where long-term operational stability is difficult to maintain [82]. Consequently, self-healing conductive polymer systems that can autonomously repair damaged

regions or recover structure and functionality in response to external stimuli, such as heat or moisture, have been actively explored across a wide range of applications (Figure 12).

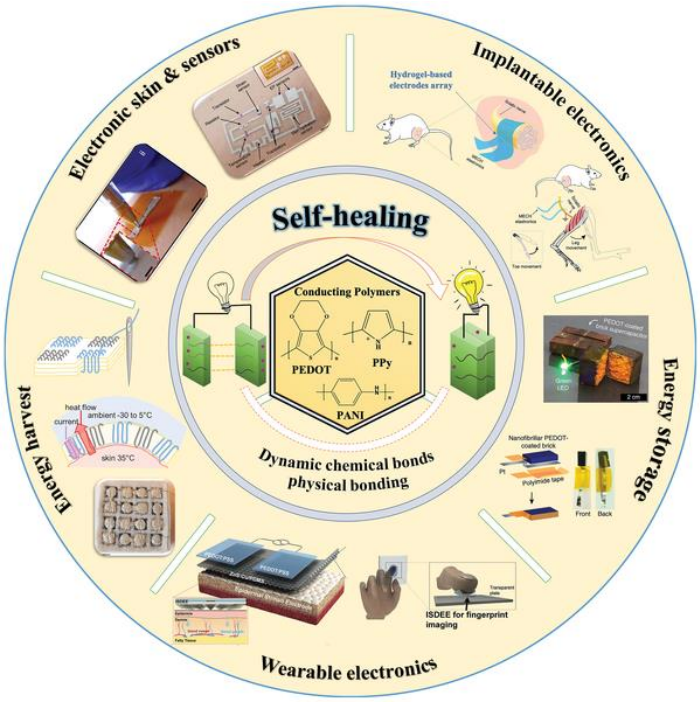

Figure 12. Schematic overview of representative applications of self-healing conductive polymers. By combining intrinsic conductivity with autonomous damage recovery, these materials support durable operation in electronic skin and sensors, implantable electronics, energy devices, and wearable systems [21].

Wearable sensors represent one of the most prominent application areas [83]. These devices enable real-time monitoring of physical and physiological signals, including human motion, biopotentials, pressure, and temperature, and are widely used in medical, sports, and healthcare applications. Wearable sensors are typically worn in direct contact with the skin for extended periods and are repeatedly exposed to stretching, bending, friction, and perspiration [84]. Under such conditions, maintaining both mechanical compliance and electrical stability is essential. Self-healing conductive polymers are well suited to meet these requirements, as they can preserve or recover conductive networks even after micro-scale damage. Indeed, numerous studies have reported

composite systems combining conductive materials such as PEDOT:PSS, polyaniline (PANI), or carbon nanotubes (CNTs) with self-healing elastomers including PU, poly(dimethylsiloxane) (PDMS), or poly(acrylic acid) (PAA), achieving elongation exceeding 50% and electrical conductivity recovery rates above 90% after repeated deformation [85].

Flexible and foldable displays, which are rapidly advancing toward commercialization, rely on thin and compliant structures that undergo repeated bending, folding, or rolling [20] to enable new forms of user interaction. However, functional layers such as electrodes, interconnects, and touch sensors are continuously subjected to mechanical strain, making them prone to microcrack formation and electrical failure [86]. Self-healing conductive polymers can be incorporated into transparent electrodes, sensing layers, or strain-buffer layers within display architectures, allowing microcracks or conductor disconnections to be repaired at the material level [7]. In particular, PEDOT:PSS-based materials have attracted attention as alternatives to indium tin oxide (ITO), offering high optical transparency, mechanical flexibility, solution processability, and compatibility with composite designs suitable for display manufacturing [87].

Self-healing conductive polymers also play an important role in bioelectronic applications that require biocompatibility and long-term functional stability, such as implantable electrodes, skin-mounted biosensors, and electrical stimulation devices [88, 89]. In both in vivo and on-skin environments, devices are exposed to combined effects of humidity, temperature fluctuations, body fluids, and subtle mechanical motion, which can lead to signal instability, device malfunction, or skin irritation [90]. Electrodes with self-healing capability can recover functionality without external power input, ensuring long-term reliability and improving user safety and comfort [91]. Healing mechanisms triggered by moisture or body temperature are particularly well matched to physiological conditions, making these materials attractive for wearable medical devices and disposable electrophysiological monitoring patches [91].

In the field of soft robotics, conductive polymers are used in flexible actuators and sensor components that enable complex and adaptive motion [92]. Repeated actuation often leads to material fatigue and damage, posing a major challenge to long-term reliability. Self-healing conductive polymers can autonomously repair damaged conductive networks, allowing circuits to remain operational and ensuring continuous sensing and control [17]. This capability directly

contributes to accurate position sensing, load distribution monitoring, and environmental interaction in soft robotic systems.

Beyond performance enhancement, self-healing conductive polymers also offer significant advantages for sustainable electronics by extending material lifetime and reducing E-waste [93]. Traditional electronic devices are often discarded due to localized damage, even when most components remain functional. By preventing irreversible performance loss from minor damage, self-healing materials increase reusability and reduce resource consumption. This contributes to energy and cost savings and supports environmentally responsible device design, while also enabling future concepts such as recyclable electrodes and recoverable organic electronic components.

Overall, self-healing conductive polymers provide a versatile strategy for overcoming the intrinsic limitations of conventional electrode materials across wearable sensors, flexible displays, bioelectronics, soft robotics, and sustainable electronic systems. By enabling enhanced functionality, reliability, and durability, these materials represent a critical platform for next-generation electronic devices. Future research will require more refined material designs that consider healing speed, repeatability, simplicity of healing conditions, and system-level integration to accelerate the practical implementation of self-healing electronic technologies.

2.5.1 Identified Gaps in the Literature

Despite the significant progress in self-healing conductive polymers and recyclable polymer systems, the simultaneous integration of self-healing capability and recyclability within PEDOT:PSS/PU composite systems has not yet been systematically demonstrated. As discussed in the previous sections, PEDOT:PSS-based composites have been extensively explored for self-healing electronic applications, primarily through hydrogen bonding, ionic interactions, or adhesive recovery mechanisms. Separately, recyclable PU systems have been actively developed using dynamic covalent chemistry or physically reversible network designs.

However, in most reported studies, these functionalities have been addressed independently. PEDOT:PSS-based self-healing systems typically focus on restoring electrical and mechanical performance after damage, without consideration of material recovery or reprocessing. Conversely, recyclable PU systems are often designed to maintain mechanical integrity and reprocessability, while electrical functionality and conductive network recovery are not considered. As a result,

composite systems that simultaneously satisfy self-healing behavior, electrical conductivity retention, mechanical robustness, and recyclability within a single PEDOT:PSS/PU platform remain largely unexplored.

In particular, the incorporation of dynamic healing mechanisms and recyclable network structures into PEDOT:PSS/PU composites introduces inherent material trade-offs, including the balance between polymer chain mobility, conductive pathway continuity, and structural stability during repeated healing and reprocessing cycles. Addressing these competing requirements within a unified material design framework remains a key challenge in the field.

This gap in the existing literature provides a clear motivation for the present study. By designing PEDOT:PSS/PU composite systems that integrate self-healing capability and recyclability without compromising electrical performance or mechanical durability, this work aims to establish a new material platform for sustainable and reliable soft electronic applications.

CHAPTER 3 METHODOLOGY

A comprehensive characterization was implemented to investigate the structural, thermal, mechanical, and electrical aspects of the developed polymer system. By combining multiple analytical techniques, both molecular-level features and macroscopic performance were systematically examined. This approach enables a coherent understanding of how material architecture governs overall functionality.

3.1 Fourier-transform Infrared (FTIR) Analysis

Fourier-transform infrared (FTIR) spectroscopy was employed to elucidate intermolecular interactions governing network formation in both liquid precursors and solid films. In supramolecular conductive polymer systems, macroscopic mechanical properties and functional recovery originate from reversible, non-covalent interactions rather than permanent covalent crosslinks. Therefore, spectroscopic identification of hydrogen bonding and dynamic bond rearrangement is essential to establish the molecular origin of network formation.

In the liquid state, FTIR analysis provides insight into interaction tendencies among individual components prior to film formation. Because supramolecular organization in the solid state evolves from molecular associations already present in solution, systematic evaluation of binary and ternary component combinations enables understanding of cooperative interaction effects and network development pathways. Monitoring vibrational modes associated with hydroxyl (–OH), carbonyl (C=O), sulfonate ($–SO_3^-$), and urethane groups allows detection of peak shifts and band broadening resulting from hydrogen-bond formation. Such spectral variations reflect changes in local bonding environments and reduced vibrational force constants, serving as molecular-level indicators of intermolecular interaction strength.

In the solid state, ATR-FTIR spectroscopy was used to examine dynamic bonding behavior under mechanical perturbation. Since self-healing behavior relies on reversible bond dissociation and reformation, tracking characteristic vibrational modes before damage, after disruption, and following recovery provides evidence of bond rearrangement processes. Variations in N–H, C=O, and related vibrational features indicate bond cleavage, reassociation, and structural reorganization within the polymer network.

By integrating liquid- and solid-state FTIR analyses, this approach establishes a direct connection between reversible intermolecular interactions and the macroscopic mechanical integrity and functional stability of the composite system.

3.2 Gel Permeation Chromatograph (GPC) Analysis

Gel permeation chromatography (GPC) was employed to evaluate the molecular weight distribution of the synthesized polyurethane (PU), as molecular weight fundamentally governs the mechanical behavior and network stability of elastomeric polymers. In segmented polyurethane systems, chain length and dispersity directly influence entanglement density, segmental mobility, and stress-transfer efficiency within the polymer matrix. Therefore, accurate determination of molecular weight parameters is essential to ensure that the observed mechanical and healing behaviors originate from controlled polymer architecture rather than unintended variations in chain growth. GPC separates polymer chains according to their hydrodynamic volume in solution, enabling estimation of number-average molecular weight (Mn), weight-average molecular weight (Mw), and dispersity (Đ). These parameters collectively describe chain length distribution, which determines the balance between elasticity and flow behavior. Higher molecular weight generally enhances entanglement-mediated elasticity, while broader dispersity can affect mechanical reproducibility and network uniformity. Because the polyurethane matrix serves as the mechanically supportive and dynamically interactive component in the composite system, establishing its molecular weight characteristics provides a necessary foundation for interpreting subsequent mechanical performance and supramolecular interaction behavior. Thus, GPC analysis ensures that network formation and functional properties are evaluated within a structurally defined polymer framework.

3.3 ^{1}H nuclear Magnetic Resonance (NMR) Analysis

^{1}H nuclear magnetic resonance (NMR) spectroscopy was employed to verify the chemical structure of the synthesized polyurethane (PU), as the macroscopic mechanical performance and network-forming capability of segmented polyurethanes are intrinsically determined by their molecular architecture. In these systems, the balance between soft segments and hard segments governs chain flexibility, phase separation behavior, and intermolecular interaction density. Therefore, confirmation of successful urethane bond formation and proper incorporation of segmental components is essential prior to evaluating composite performance. ^{1}H NMR provides

molecular-level structural information by probing the chemical environment of hydrogen atoms along the polymer backbone. The resonance positions and splitting patterns of characteristic protons allow identification of functional groups and verification of chain connectivity. In segmented PUs, signals associated with methylene units in the soft segment, urethane N–H protons, and aliphatic protons derived from diisocyanate and chain extender components collectively confirm successful polymerization and structural integration. Establishing the chemical integrity of the synthesized PU ensures that subsequent mechanical, electrical, and healing behaviors can be interpreted within a well-defined molecular framework. Thus, ^{1}H NMR analysis provides structural validation of the polymer matrix that underpins the composite system.

3.4 Thermal Analysis

Thermogravimetric analysis provides insight into the decomposition profile of the material by monitoring mass variation as a function of temperature. The absence of significant mass loss within the operational temperature window confirms that healing and recycling processes are governed by reversible intermolecular interactions rather than thermally induced chemical degradation. Additionally, negligible low-temperature mass variation indicates effective solvent removal during film fabrication, ensuring that observed mechanical and electrical behaviors arise from the polymer network itself rather than residual processing artifacts.

Differential scanning calorimetry (DSC) was employed to characterize thermomechanical transitions, particularly the glass transition temperature (T_g), which reflects segmental mobility within the polymer matrix. In elastomeric conductive composites, T_g is a critical parameter governing chain flexibility and the activation of dynamic bonding processes. Healing and reprocessing require sufficient molecular mobility to enable interfacial diffusion and bond rearrangement; therefore, T_g provides a fundamental reference point for interpreting temperature-dependent behavior.

3.5 Electrical Conductivity Test

Electrical transport characterization was conducted to evaluate the intrinsic conductivity of the PEDOT:PSS/PU composite films, as electrical performance directly reflects the continuity and stability of conductive pathways within the polymer matrix. In stretchable conductive composites, charge transport is governed by percolated networks formed by PEDOT-rich domains dispersed

within an insulating elastomeric framework. Therefore, accurate assessment of intrinsic resistivity is essential to determine how compositional variation and network architecture influence electrical functionality. To obtain reliable conductivity values, it is necessary to decouple bulk transport properties from extrinsic measurement artifacts such as electrode contact resistance. The four-point probe methodology provides this advantage by independently controlling current injection and voltage measurement, enabling precise determination of sheet resistance. Conversion of sheet resistance to bulk resistivity, and subsequently to conductivity, allows direct comparison between films of different thicknesses and compositions. Quantitative evaluation of electrical conductivity establishes whether mechanical reinforcement or dynamic interaction within the composite compromises percolation continuity. Thus, electrical transport analysis serves as a critical link between molecular design, network morphology, and functional performance in the conductive polymer system.

3.6 Mechanical and Electromechanical Characterization

Uniaxial tensile analysis was employed to investigate the deformation mechanics of the composite films, as the macroscopic mechanical response of stretchable conductive systems is governed by their underlying polymer network architecture. In elastomeric matrices containing conductive domains, stretchability, stiffness, and fracture resistance are determined by chain entanglement density, segmental mobility, and reversible intermolecular interactions. Quantitative stress–strain evaluation therefore provides direct insight into how compositional design influences load transfer and strain accommodation within the network.

The initial elastic region of the stress–strain curve reflects the effective network stiffness under small deformations, where polymer chains respond primarily through reversible stretching. At higher strains, nonlinear behavior captures chain alignment, interaction rearrangement, and progressive energy dissipation. The overall elongation at break indicates the network's ability to sustain large deformation without catastrophic failure. Toughness, defined as the total mechanical energy absorbed prior to fracture, serves as an integrated metric of elasticity and energy dissipation capacity within the network.

Fracture-related analysis based on pre-existing crack geometry enables evaluation of crack propagation resistance. In polymer networks, fracture behavior is governed by the competition between elastic energy release and energy dissipation mechanisms such as chain pull-out and

reversible bond rearrangement. Assessing fracture tolerance provides insight into the material's ability to redistribute stress and maintain structural integrity in the presence of defects.

Cyclic loading–unloading analysis further probes mechanical reversibility and hysteresis. The hysteresis area represents dissipated mechanical energy associated with internal friction and dynamic bond rearrangement.

Electromechanical characterization complements mechanical analysis by evaluating the stability of conductive percolation pathways under deformation. In conductive composites, electrical transport depends on nanoscale connectivity between PEDOT-rich domains embedded in a deformable matrix. Mechanical strain can alter inter-domain spacing and disrupt conductive continuity. Monitoring normalized resistance during deformation enables assessment of percolation robustness and the coupling between mechanical strain and electrical functionality.

Together, mechanical and electromechanical analyses establish the relationship between polymer network architecture, energy dissipation mechanisms, and strain-dependent electrical stability in the composite system.

3.7 Evaluating Self-healing Capability

3.7.1 Electrical Self-Healing Behavior

Electrical self-healing evaluation was conducted to assess the ability of the conductive network to restore charge transport continuity following mechanical damage. In stretchable conductive polymer composites. Mechanical disruption locally breaks these conductive pathways, resulting in abrupt changes in electrical resistance. Therefore, monitoring conductivity recovery provides a sensitive probe for evaluating dynamic structural reorganization within the composite. Unlike purely mechanical healing, electrical recovery requires re-establishment connectivity across damaged regions. This process involves interfacial polymer chain rearrangement, domain recontact, and restoration of percolation continuity. Because electrical transport is highly sensitive to small variations in inter-domain spacing, resistance recovery reflects not only macroscopic contact but also microscopic network reconstruction. By comparing the electrical response before damage and after recovery, the extent to which conductive pathways are reformed can be quantitatively assessed. Electrical self-healing analysis therefore serves as a functional validation

of dynamic network behavior, directly linking supramolecular interaction reversibility to restoration of electronic transport performance.

3.7.2 Mechanical Self-Healing Behavior

Mechanical self-healing behavior was examined to assess the ability of the polymer network to restore structural integrity after surface-level and through-thickness damage. In supramolecular elastomeric systems, healing arises from chain mobility, interfacial diffusion, and the reformation of reversible intermolecular interactions. Therefore, evaluating healing performance requires probing damage scenarios that impose different mechanical constraints and interfacial geometries.

Scratch-based healing provides insight into surface defect recovery, where deformation is primarily localized, and partial network continuity remains intact. In this regime, healing reflects short-range chain rearrangement and re-establishment of reversible bonding across shallow damage zones. Quantifying changes in defect depth before and after recovery allows assessment of surface-level structural restoration and the efficiency of local network reorganization.

Cut–stick experiments probe bulk healing across fully separated interfaces. Unlike surface scratches, complete fracture requires macromolecular interdiffusion and re-entanglement across the damaged interface to re-establish load transfer. The recovery of mechanical toughness following rejoining directly reflects the extent of network reconstruction and energy dissipation capability after healing. This method therefore evaluates whether the supramolecular network can restore mechanical functionality beyond simple surface closure.

Puncture healing introduces a more severe, through-thickness defect that combines localized fracture and out-of-plane deformation. In this case, healing requires cooperative chain mobility and interfacial reconstruction across a confined geometry. Autonomous closure of puncture damage demonstrates the material's capacity to redistribute stress and reorganize its network structure without external intervention. Because puncture represents a realistic mechanical failure mode for flexible membranes, its recovery provides practical validation of network resilience.

By integrating scratch, cut–stick, and puncture assessments, mechanical self-healing is evaluated across multiple damage scales, from superficial defects to complete structural separation. This multiscale framework establishes a direct relationship between reversible molecular interactions,

macromolecular mobility, and macroscopic restoration of mechanical performance in the composite system.

3.8 Recycling Evaluation

Recycling behavior was investigated to assess whether composite could undergo structural reconfiguration without significant loss of functionality. In dynamically interacting polymer networks, recyclability is governed by reversible intermolecular interactions and sufficient chain mobility that enable topological rearrangement under thermal activation. Therefore, evaluating recycling performance provides direct evidence of whether the network architecture is permanently capable of reprocessing.

Mechanical reprocessing was examined to determine whether fragmented materials could be reconsolidated into a continuous specimen through thermally activated interfacial reconnection. In this process, macromolecular interdiffusion and reformation of reversible bonding across fragment interfaces are required to restore load transfer pathways. Successful recovery of mechanical toughness and electrical conductivity after repeated reprocessing indicates that the supramolecular network can reorganize without irreversible degradation of its conductive percolation structure. Repeated cycling further probes structural stability and cumulative damage tolerance of the dynamic network.

In parallel, chemical recycling was evaluated to assess the feasibility of selectively separating and regenerating individual polymer components. This approach examines whether the composite can be deconstructed into its constituent phases and subsequently reassembled while retaining functional performance. Chemical recovery of the elastomeric matrix followed by re-blending with the conductive component tests the reversibility of phase organization and compatibility between regenerated components.

By integrating mechanical reprocessing and chemical recycling strategies, the recyclability assessment distinguishes between topology-preserving reshaping and component-level regeneration. This dual evaluation framework establishes whether the conductive composite platform supports circular material design through both physical reconfiguration and selective material recovery, thereby linking dynamic intermolecular interactions to sustainable functional reuse.

3.9 Bioelectronic Interface Validation

Pressure-sensing performance was evaluated to examine the piezoresistive response of the composite films under external mechanical stimuli. In conductive polymer composites, electrical resistance is highly sensitive to changes in microstructural connectivity within the percolated network. Applied pressure reduces inter-domain spacing and modifies contact resistance between conductive regions, resulting in measurable resistance variation. Therefore, monitoring normalized resistance changes under controlled loading provides quantitative insight into the coupling between mechanical deformation and electrical transport.

Sensitivity analysis establishes the relationship between applied stress and electrical response, reflecting how efficiently the conductive network translates mechanical perturbation into electronic signal modulation. This evaluation is essential for determining the feasibility of the material as a flexible pressure sensor, where stable baseline resistance and reproducible signal variation are critical.

To further assess processability and application versatility, the composite was reformulated into a printable conductive ink. In dynamically interacting polymer systems, solubility indicate that network formation is governed by reversible interactions rather than irreversible crosslinking. Successful ink formulation and patterning demonstrate that the material can be reconfigured into defined electrode geometries without loss of conductivity. This capability confirms compatibility with additive manufacturing approaches and scalable device fabrication.

Epidermal electrode configurations were investigated to evaluate skin conformity and bioelectronic interface stability. For wearable bioelectronics, intimate contact between electrode and skin is required to minimize impedance and motion artifacts. The ability to print, transfer, and mechanically reinforce ultrathin conductive films demonstrates structural adaptability and user comfort, both of which are critical for long-term epidermal applications.

Electrocardiogram (ECG) measurements were performed to validate functional bioelectronic performance. Because ECG signal acquisition requires stable low-impedance skin–electrode interfaces and consistent electrical conductivity under subtle body motion, successful signal detection confirms both mechanical compliance and electrical robustness of the composite. Comparative analysis with commercial electrodes further establishes the practical viability of the dynamic conductive polymer platform for wearable health monitoring.

Collectively, pressure sensing, printability, and bioelectronic evaluation extend the material validation beyond structural characterization, demonstrating that molecularly engineered dynamic networks can translate into functional, skin-compatible electronic systems.

CHAPTER 4 ARTICLE 1: PEDOT:PSS BASED SELF-HEALING MATERIALS

This article has been submitted in the journal “Flexible and Printed Electronics” on July 8th, 2025.

Jinsil Kim, Sadaf Khoomortezaei, and Fabio Cicoira

Department of Chemical Engineering, Polytechnique Montréal, Montréal, QC H3C 3A7, Canada

*Corresponding author. E-mail: fabio.cicoira@polymtl.ca

4.1 Status

In recent years, wearable and flexible electronics have attracted considerable attention owing to the increasing demand for technologies related to human health monitoring, wearable displays, soft sensors, and emerging energy harvesting and storage systems [19]. Unlike conventional rigid electronic devices, soft electronic systems—including wearable, implantable, stretchable devices, and soft robotics—can conform to complex geometries and integrate seamlessly with the human body. This mechanical compliance significantly expands their potential applications in healthcare monitoring, electronic skins, and human–machine interfaces. However, the intrinsic softness of these systems also renders them vulnerable to mechanical damage caused by external stress, repeated deformation, or long-term use. Addressing this vulnerability has motivated growing interest in self-healing materials, inspired by biological systems, as a strategy to restore functionality and improve device durability [94].

Self-healing materials have therefore emerged as a promising approach to extend the operational lifetime of soft electronic devices. Among various candidates, poly(3,4-ethylenedioxythiophene):poly(styrene sulfonate) (PEDOT:PSS) has been widely recognized as a benchmark conducting polymer due to its combined ionic–electronic conductivity, mechanical flexibility, biocompatibility, intrinsic self-healing capability, and compatibility with solution-based processing techniques [95]. In general, self-healing mechanisms can be classified into two categories: autonomic healing, which occurs spontaneously at room temperature without external stimuli, and non-autonomic healing, which requires external triggers such as heat, light, or

moisture. PEDOT:PSS is known to exhibit a rapid non-autonomic healing response in the presence of water (Figure 13a), where swelling of the PSS domains facilitates gap filling at damaged sites and enables near-complete recovery of mechanical and electrical properties [1].

Numerous strategies have been explored to exploit and enhance the self-healing behavior of PEDOT:PSS-based materials. While many studies have primarily focused on restoring electrical conductivity or improving charge transport performance, fewer approaches have addressed the recovery of mechanical integrity after damage [19]. This limitation becomes particularly critical as soft electronic devices increasingly transition from merely flexible to fully stretchable systems that must tolerate large strains during operation. Conventional flexible conductors often exhibit limited resistance to mechanical damage and show poor recovery after deformation, underscoring the need for materials that combine stretchability with effective mechanical self-healing.

In this context, there is a growing demand for PEDOT:PSS-based materials that not only recover electrical functionality but also withstand and heal from mechanical damage under realistic operating conditions. Current research efforts are therefore directed toward developing strategies that enhance stretchability, enable mechanical self-healability, and achieve autonomous healing without reliance on external stimuli. By overcoming these challenges—namely limited stretchability, insufficient mechanical self-healing, and dependence on non-autonomic healing mechanisms—it becomes possible to design more resilient and versatile conducting materials. Such advances are expected to play a critical role in enabling the next generation of organic and soft electronic devices with improved reliability and long-term performance.

4.2 Current and Future Challenges

Despite the attractive flexibility and intrinsic self-healing characteristics of PEDOT:PSS, several critical challenges remain that limit its reliability in soft and wearable electronic applications. In particular, PEDOT:PSS-based systems often exhibit insufficient mechanical durability under repeated deformation or severe mechanical damage, such as deep scratches, cuts, tears, or punctures [96]. While PEDOT:PSS can recover electrical conductivity after minor damage (typically up to ~20 μm), it generally fails to restore both electrical and mechanical integrity following more extensive damage. This limitation poses a significant obstacle for wearable, implantable, and soft electronic devices that are expected to operate reliably under continuous mechanical stress and prolonged real-world use.

Another major challenge arises from the degradation of electrical conductivity under repeated bending, stretching, or twisting. Continuous mechanical deformation can disrupt the conductive pathways within PEDOT:PSS films, leading to progressive performance deterioration and unstable electrical output. Such degradation is particularly problematic for applications that demand long-term signal fidelity, including health monitoring and bioelectronic interfaces.

From a practical perspective, effective self-healing materials for soft electronics must also exhibit room temperature healing, without reliance on external stimuli such as heat, light, or moisture. Autonomous healing is essential to ensure rapid recovery from damage under realistic operating conditions, where external intervention may not be feasible. However, PEDOT:PSS alone typically lacks this capability, as its healing response is often non-autonomic and strongly dependent on environmental humidity or water exposure. This dependence, combined with limited resistance to repeated mechanical stress, significantly constrains the applicability of pristine PEDOT:PSS in systems requiring long-term durability and reliability.

To overcome these limitations, various strategies have been explored based on blending PEDOT:PSS with functional additives or secondary polymers, including polyethylene glycol (PEG, Figure 13b), polyurethane diols (PUD), tannic acid (Figure 14a), and surfactants such as Triton X-100 [3]. These additives can enhance stretchability and, in some cases, introduce autonomous self-healing behavior. Nevertheless, while these approaches have demonstrated promising electrical and healing properties, systematic investigations into their mechanical durability remain limited. Achieving a balanced combination of high electrical conductivity, robust mechanical durability, and efficient self-healing continues to be a major challenge [78].

Looking forward, the development of advanced PEDOT:PSS-based composite systems incorporating novel polymers or multifunctional additives will be critical to addressing these challenges. Future materials must simultaneously achieve autonomous room-temperature healing, high stretchability, sustained electrical performance, and mechanical robustness under repeated deformation. Addressing these requirements will be essential for translating self-healing conducting polymers from laboratory demonstrations into reliable, long-lasting soft electronic technologies.

(a)

(b)

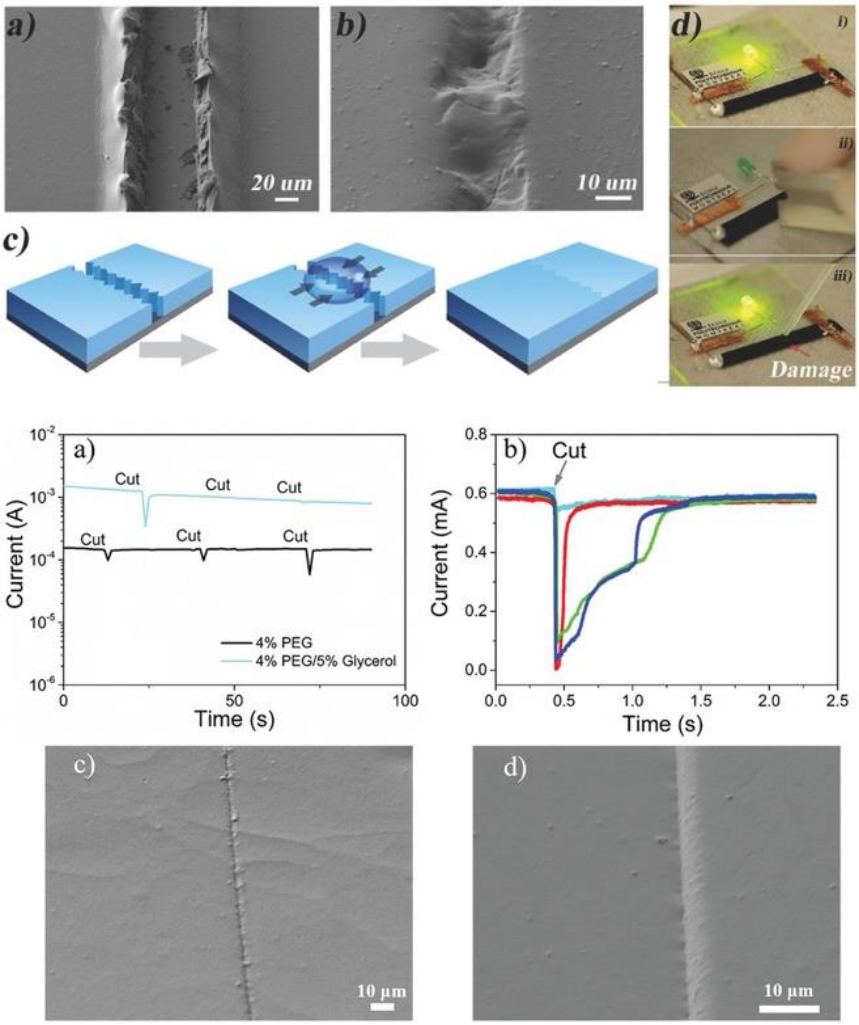

Figure 13. (a) SEM images of damaged and healed areas, schematic image of water-enabled healing of PEDOT:PSS film and electrical healing on PEDOT:PSS film connected with a LED bulb [1]. (b) Autonomous healing of PEDOT:PSS/PEG film and SEM images of the cut and healed region [3].

4.3 Advances in Science and Technology to Meet Current Challenges

Addressing the combined challenges of electrical conductivity, mechanical durability, and self-healing capability in PEDOT:PSS-based systems requires advances in materials design that go beyond simple formulation optimization. One of the most promising strategies reported to date involves integrating PEDOT:PSS with self-healing polymer matrices (Figure 14b) [4]. This

approach leverages the complementary properties of conducting polymers and mechanically resilient, self-healable elastomers to create multifunctional composite systems.

A wide range of stretchable polymers—including polydimethylsiloxane (PDMS), polyurethane (PU), polyacrylates (PA), and poly(vinyl alcohol) (PVA)—have been explored as self-healing matrices [2]. These polymers can exhibit self-healing behavior through either dynamic covalent interaction, such as disulfide exchange, imine formation, or Diels–Alder reactions, or through reversible non-covalent interactions, including hydrogen bonding and ionic interactions. When combined with PEDOT:PSS, such self-healing polymers can impart the ability to recover from mechanical damage while improving mechanical robustness and resistance to repeated deformation.

A critical factor governing the activation of self-healing interactions in these polymer systems is the glass transition temperature (T_g). Self-healing is typically enabled when polymer chain mobility is sufficient to allow bond rearrangement, which can be achieved by tuning T_g through molecular design. Strategies such as employing linear or flexible monomers, reducing crosslinking density, designing soft polymer backbones, or blending with plasticizing components have been shown to effectively lower T_g, thereby enabling autonomous healing at or near room temperature. This design principle is particularly important for wearable and implantable devices, where external heating or stimuli are impractical.

Despite these advantages, most self-healing polymers are intrinsically electrically insulating, which leads to a reduction in the overall conductivity of PEDOT:PSS-based composites. To compensate for this effect, various conductivity-enhancing additives—such as glycerol, polyethylene glycol (PEG), and ethylene glycol (EG)—have been incorporated to improve charge transport within PEDOT:PSS domains. These additives can promote PEDOT chain rearrangement, phase separation, or improved percolation pathways, partially mitigating conductivity losses introduced by the insulating polymer matrix.

Achieving an optimal balance among the self-healing polymer, conductivity-enhancing additives, and PEDOT:PSS remains a central challenge and requires careful consideration of both chemical and physical compatibility [97]. From a chemical perspective, functional groups present in the self-healing polymer (e.g., hydroxyl, carboxyl, or amine groups) can interact with PEDOT:PSS through dynamic bonding or supramolecular interactions, enabling efficient self-repair without

severely disrupting electrical pathways. From a physical standpoint, the mechanical properties of the polymer matrix and the conducting phase must be well matched to ensure structural integrity, shape recovery, and long-term durability under repeated mechanical stress.

Overall, the integration of self-healing polymers and functional additives with PEDOT:PSS represents a powerful strategy for addressing the intertwined challenges of conductivity, mechanical durability, and self-healing in soft electronic systems. Continued progress in this area is expected to enable the development of materials that are not only flexible and stretchable, but also autonomously self-repairing and electrically reliable. Such advances are essential for next-generation wearable, bioelectronic, implantable devices, and soft robotic systems that demand long-term operational stability.

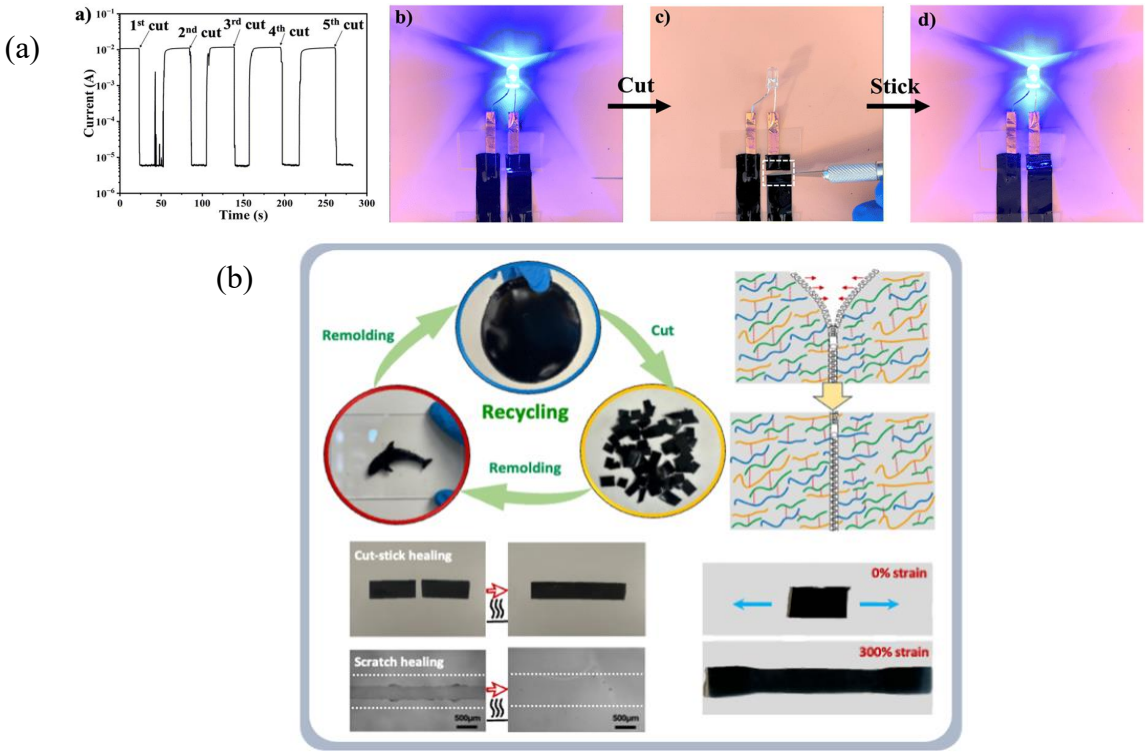

Figure 14. (a) Electrical cut-stick healing of PEDOT:PSS/EG/TA film with an LED indicator: original, cur and healed [2] (b) Schematic of self-healing and recyclable PEDOT:PSS/Polyurethane blends [4].

4.4 Concluding Remarks

PEDOT:PSS has emerged as one of the most promising conducting polymers for flexible, stretchable, and self-healing electronic devices. Nevertheless, significant challenges remain in maintaining mechanical durability and effective self-healing performance, particularly under repeated mechanical stress or severe damage such as scratches, cuts, and punctures—failure modes that are common in practical soft electronic applications. These limitations continue to hinder the long-term stability and reliability of PEDOT:PSS-based systems in demanding operating environments.

To address these challenges, substantial research efforts have focused on material design strategies that incorporate dynamic bonding mechanisms, supramolecular interactions, and conductivity-enhancing additives. Such approaches aim to simultaneously improve stretchability, enable autonomous healing under ambient conditions, and preserve high electrical performance. However, achieving an optimal balance among mechanical robustness, self-healing efficiency, and electrical conductivity remains a central challenge, as improvements in one aspect often come at the expense of another.

Looking forward, continued advances in polymer chemistry, composite design, and interfacial engineering—supported by interdisciplinary collaboration across materials science, electronics, and bioengineering—are expected to further expand the capabilities of PEDOT:PSS-based systems. With rational materials design and improved understanding of structure–property relationships, PEDOT:PSS holds strong potential to underpin the next generation of resilient, efficient, and sustainable electronic technologies. These developments will be particularly impactful for emerging applications such as wearable and implantable electronics, health monitoring systems, bioelectronics, soft robotics, and energy harvesting platforms.

CHAPTER 5 ARTICLE 2 : SELF-HEALING, STRETCHABLE AND RECYCLABLE POLYURETHANE-PEDOT:PSS CONDUCTIVE BLENDS

This article has been published in the journal “Material Horizons” on June 13th, 2024. The supporting information of this article is provided in Appendix A.

Jinsil Kim, Jiaxin Fan, Gayaneh Petrossian, Xin Zhou, Pierre Kateb, Noemy Gagnon-Lafrenais and Fabio Cicoira

Department of Chemical Engineering, Polytechnique Montréal, Montréal, QC H3C 3A7, Canada

*Corresponding author. E-mail: fabio.cicoira@polymtl.ca

Keywords: PEDOT:PSS, polyurethane, self-healing, recycling, stretchability

5.1 Abstract

Future electronic devices increasingly require materials that combine mechanical robustness with flexibility and stretchability. In addition, the incorporation of self-healing behavior and recyclability has become essential to address the growing environmental concerns associated with electronic waste. In this work, a stretchable, self-healing, and recyclable conductive material is developed based on a composite of poly(3,4-ethylenedioxythiophene):polystyrene sulfonate (PEDOT:PSS), a custom-designed polyurethane (PU), and polyethylene glycol (PEG). The resulting material exhibits large tensile deformability (~350% elongation at break), high toughness (~25 MJ m^{-3}), moderate electrical conductivity (~10 S cm^{-1}), and efficient recovery of both mechanical and electrical properties after damage. Furthermore, the composite demonstrates excellent recyclability, retaining its mechanical and electrical performance over up to 20 recycling cycles without noticeable degradation. To illustrate its applicability in sustainable electronic systems, the material is employed in electrocardiogram (ECG) electrodes and a pressure sensor, both of which maintain stable performance after repeated recycling. These results indicate that conductive polymer systems integrating self-healing and recyclability offer a promising pathway

toward sustainable electronic materials and provide a potential strategy for mitigating the e-waste problem.

5.2 Introduction

Blending conductive polymers with insulating polymer matrices provides an effective strategy for tailoring electrical and mechanical properties, enabling applications in bioelectronics, wearable electronics, and energy-storage devices [74, 98-100]. For emerging electronic systems, materials that simultaneously exhibit mechanical toughness, flexibility, stretchability, high electrical conductivity, self-healing capability, and recyclability are increasingly required [101-106]. Although soft electronic materials currently represent only a minor fraction of electronic waste, they hold significant potential for contributing to sustainable electronics by replacing critical materials in targeted applications such as sensing, bioelectronics, wearable electronics, and soft robotics. In this context, self-healing and recyclability represent complementary strategies, both aiming to extend material lifetime and reduce environmental impact. While self-healing materials can withstand repeated damage–healing cycles during operation, recycling remains essential for the recovery and reuse of materials at the end of their service life.

Among conducting polymers, poly(3,4-ethylenedioxythiophene) doped with polystyrene sulfonate (PEDOT:PSS) is the most extensively investigated system, owing to its high electrical conductivity, ease of processing in aqueous media, environmental stability, and biocompatibility [1, 106, 107]. In addition, PEDOT:PSS-based materials have demonstrated enhanced mechanical compliance and self-healing behavior when combined with secondary polymers or functional additives. For example, blending PEDOT:PSS with polyethylene glycol (PEG) [108], polyurethane diols [74],[4] tannic acid [78], or Triton X-100 [96] has been shown to improve flexibility, stretchability, and electrical self-healing performance. Improved mechanical self-healing has also been achieved by incorporating dynamic polymer networks, such as poly(vinyl alcohol)–borax [2] and poly(glutamic acid)–trimethoxysilane (GPTMS) systems [109]. Despite these advances, achieving PEDOT:PSS-based materials that simultaneously exhibit high stretchability, toughness, and robust self-healing capability remains challenging, motivating further investigation into rationally designed polymer blends [110].

Polyurethanes (PUs), with their highly tunable molecular architectures and well-established synthesis routes, are promising candidates for improving the mechanical robustness and self-

healing behavior of PEDOT:PSS-based systems [111, 112]. PUs are typically synthesized via addition polymerization of polyols, diisocyanates, and chain extenders [43]. In these materials, soft segments derived from polyols (e.g., polyether, polyester, or polycarbonate diols) provide elasticity and chain mobility, whereas hard segments formed by diisocyanates and chain extenders impart mechanical strength [113, 114]. By controlling the chemical composition and degree of crosslinking, PUs can be tailored to achieve a wide range of mechanical properties, from flexible thermoplastic elastomers to rigid thermosetting polymers [115-118]. To further enable self-healing and recyclability, dynamic covalent bonds, such as Diels–Alder adducts and disulfide bonds, as well as reversible noncovalent interactions including hydrogen bonding, host–guest interactions, and metal–ligand coordination, have been introduced into PU backbones [119, 120]. The reversibility of these interactions allows network reconstruction after damage, rendering PUs attractive platforms for recyclable and self-healing polymer systems [121-123].

In this study, we report a self-healing and recyclable conductive material with excellent mechanical properties, obtained by combining a custom-designed PU with PEDOT:PSS and PEG. The incorporation of PEG is expected to promote dynamic hydrogen-bonding interactions within the composite, enabling simultaneous mechanical and electrical healing. The resulting material exhibits high toughness, large stretchability, and efficient recovery of electrical and mechanical properties after damage. Furthermore, the material can be recycled multiple times without significant deterioration in performance. As a proof of principle for sustainable electronic devices, electrocardiogram (ECG) electrodes and a pressure sensor fabricated from this material demonstrate stable operation after repeated self-healing and recycling cycles.

5.3 Experimental Section

5.3.1 Materials

Poly(3,4-ethylenedioxythiophene) doped with polystyrene sulfonate (PEDOT:PSS) was used in the form of a screen-printing paste (Clevios™ SV3 STAB), which was supplied by Heraeus Precious Metals (Germany). The commercial paste formulation contained diethylene glycol (DEG) and propylene glycol (PG) as processing additives. Poly(caprolactone) diol with an average molecular weight of 2000 $g \cdot mol^{-1}$, polyethylene glycol (PEG, average molecular weight of 400 $g \cdot mol^{-1}$), glycerol, dimethylformamide (DMF), poly(4-styrenesulfonic acid) (PSS, Mw ≈ 75,000 $g \cdot mol^{-1}$, 18 wt% in water), and eutectic gallium–indium (EGaIn) were purchased from Millipore

Sigma (St. Louis, MO, USA). Isophorone diisocyanate (IPDI), 1,3-propanediol (PDO), dibutyltin dilaurate (DBTDL), and ethyl N-carbamate were obtained from Tokyo Chemical Industry (USA). Glass microscope slides were purchased from Corning (USA), and Teflon™ plates were obtained from McMaster-Carr. Dog-bone-shaped molds were fabricated using a stereolithography-based 3D printer (Form 3, Formlabs) with a high-temperature resin (Formlabs). Silver conductive ink (520 EI) was generously provided by Chimet S.p.A. Tegaderm™ adhesive films were purchased from 3M. Thermoplastic polyurethane (TPU) films on removable silicon paper (Elecrom Stretch White, thickness 80 μm) were supplied by Policrom Screens (Italy).

5.3.2 Synthesis of Self-healing PU

The PU was synthesized via a two-step polymerization process (Figure 15a) carried out at 70 °C in a three-neck round-bottom flask equipped with a rubber septum. In this system, isophorone diisocyanate (IPDI) and 1,3-propanediol (PDO) served as the hard-segment components, while poly(caprolactone) diol (PCL diol) constituted the soft segment. The molar ratio of IPDI to PCL diol was fixed at 2:1, and the overall stoichiometric ratio of PCL diol/IPDI/PDO was maintained at 1:2:1. In the first step, PCL diol (22.51 g, 10 mmol, 23.80 wt%) was dissolved in dimethylformamide (DMF, 66.20 g, 70 wt%) by magnetic stirring at room temperature for 10 min. The solution was subsequently heated to 70 °C in an oil bath and stirred for an additional 30 min to ensure complete dissolution. IPDI (5.0 g, 20 mmol, 5.30 wt%) and dibutyltin dilaurate (DBTDL, 0.09 g) were then introduced dropwise into the reaction flask. The reaction mixture was maintained at 70 °C for 4 h, allowing the hydroxyl groups of PCL diol to react with IPDI and form an isocyanate-terminated prepolymer. In the second step, the chain extender PDO (0.86 g, 10 mmol, 0.90 wt%) was added to the prepolymer solution, and the reaction was continued for an additional 2 h to complete polymer chain growth. After completion, the reaction mixture was cooled to room temperature, yielding a homogeneous PU solution with a solid content of approximately 30 wt% in DMF.

The number-average molecular weight of the synthesized PU was approximately 10,000 g mol^{-1}, as determined by gel permeation chromatography (GPC) (Figure S13a). The chemical structure of the PU was confirmed using Fourier-transform infrared spectroscopy (FTIR) and proton nuclear magnetic resonance (^{1}H NMR). The FTIR spectrum (Figure S13b) showed the disappearance of the characteristic isocyanate (–NCO) absorption band at 2270 cm^{-1}, indicating completion of the

polymerization reaction, while characteristic C=O and N–H stretching vibrations were observed at approximately 1700 cm^{-1} and 3200 cm^{-1}, respectively. The ^1H NMR spectrum (Figure S13c) exhibited proton signals corresponding to urethane N–H groups at approximately 7.0 ppm, further confirming successful PU formation.

5.3.3 Fabrication of PEDOT:PSS/PU-based Films

The PEDOT:PSS paste (Clevios™ S V3) was first homogenized using a centrifugal mixer (ARM-310, Thinky, USA) at 2000 rpm for 5 min. To improve compatibility with the polyurethane (PU) solution, the paste was subsequently diluted with dimethylformamide (DMF) at a 1:1 weight ratio and further mixed using a vortex mixer. Film-forming solutions with different compositions (Table 1) were prepared by blending the PEDOT:PSS dispersion with the PU solution at various ratios under vortex mixing. For formulations containing additives, polyethylene glycol (PEG) and/or glycerol were first incorporated into the PU solution, followed by the addition of PEDOT:PSS. The resulting mixtures were deposited by drop-casting onto glass substrates (5.0 × 7.0 cm^2) or Teflon plates and subjected to a stepwise thermal treatment on a hot plate: 50 °C for 16 h, 80 °C for 1 h, 120 °C for 1 h, 150 °C for 1 h, and finally 100 °C for 24 h (Figure 15b,c). This drying protocol produced uniform, bubble-free films that could be readily detached from the substrates after complete drying using a razor blade. This approach was employed to systematically investigate the effects of composition on the electrical and mechanical properties of PEDOT:PSS/PU films. Key factors, including PU content (8–30 wt%) and additive type and concentration (PEG and glycerol), were varied to evaluate their influence on film performance. Preliminary screening of different PEDOT:PSS/PU ratios was conducted by manually stretching the films to qualitatively evaluate their mechanical behavior. Films containing 8 wt% PU exhibited insufficient stretchability, whereas increasing the PU content to 25 wt% and 30 wt% resulted in a marked reduction in electrical conductivity (~1 $S \cdot cm^{-1}$) without a corresponding improvement in mechanical performance compared to films containing 16 wt% PU. In addition, PEG 400 content above 2 wt% led to phase separation, as indicated by oily residues on the film surface. Glycerol was therefore selected as a conductivity-enhancing additive. PEG 400 was chosen for further experiments, as no significant differences in mechanical properties were observed compared to PEG 200, consistent with previous studies.[108]. Thermogravimetric analysis (TGA) was performed using a TG Q500 instrument (TA Instruments, USA) to assess the thermal stability of

the materials under conditions relevant to self-healing and recycling, as well as to evaluate residual solvent content after processing. Approximately 15 mg of sample was placed in an open platinum pan and heated from 40 to 600 °C at a rate of 10 °C·min^{-1} under a nitrogen atmosphere (40 mL·min^{-1}). The weight loss profiles (Figure S4a) showed that all samples exhibited an onset decomposition temperature of approximately 300 °C, which is significantly higher than the temperatures employed for self-healing (50 °C) and recycling (100 °C), confirming the absence of thermal degradation during these processes. Moreover, no appreciable mass loss was observed in the temperature range corresponding to DMF evaporation, indicating negligible residual solvent content in the processed films. Differential scanning calorimetry (DSC, Q2000, TA Instruments, USA) was used to investigate the thermal transitions of the PEDOT:PSS/PU composite films and the neat PU. Samples (~5 mg) were sealed in standard aluminum pans and analyzed under a continuous nitrogen flow. To remove thermal history effects, the samples were first cooled to −30 °C and then heated to 250 °C at a rate of 10 °C·min^{-1}, followed by a second heating cycle under identical conditions. Data from the second heating cycle were used for analysis. No distinct glass transition temperature (T_g) or melting transition was observed for the PEDOT:PSS/PU composite films (Figure S4b), while the absence of a melting peak confirmed the thermosetting nature of the synthesized PU. To enhance sensitivity in T_g determination, modulated DSC (MDSC) measurements were additionally conducted. Approximately 15 mg of sample was analyzed in a sealed aluminum pan at a heating rate of 2 °C·min^{-1} with a modulation period of 60 s. The T_g values were determined using the analysis software provided by TA Instruments.

Table 1. Composition of the processing mixtures.

Samples	PEDOT:PSS solution (wt%)	PU (wt%)	PEG (wt%)	Glycerol (wt%)
PEDOT:PSS	100	-	-	-
PEDOT:PSS/PU	84	16	-	-
PEDOT:PSS/PU/PEG	82	16	2	-
PEDOT:PSS/PU/Glycerol	82	16	-	2
PEDOT:PSS/PU/PEG/Glycerol	80	16	2	2

5.3.4 Fourier-transform infrared (FTIR) spectroscopy

Fourier-transform infrared (FTIR) spectroscopy was employed to investigate intermolecular interactions in the liquid samples listed in Table 2. Measurements were carried out in absorption mode using a PerkinElmer Spectrum 65 spectrometer. Prior to data collection, a background spectrum was acquired under identical conditions. All spectra were recorded at room temperature over a wavenumber range of 4000–600 cm^{-1} with a spectral resolution of 4 cm^{-1}, averaging 16 scans per measurement. To ensure reproducibility, each sample was measured three times using the same acquisition parameters. Liquid samples for FTIR analysis were prepared from aqueous poly(4-styrenesulfonic acid) (PSS) solutions (18 wt% in H_2O), polyethylene glycol (PEG 400, >99%), and ethyl N-carbamate (urethane, U, >99%). A total of 14 distinct formulations were designed to systematically examine hydrogen-bonding interactions among different component combinations, including PSS/PEG, U/PEG, PSS/U, and ternary PSS/U/PEG systems. The detailed compositions of all samples are summarized in Table 2.

Table 2. Composition of solutions employed for FTIR analysis.

FTIR samples	PSS		PEG		U	
	(wt%)	(g)	(wt%)	(g)	(wt%)	(g)
Aqueous PSS	100	1	-	0	-	0
PSS/10wt% PEG	90	1	10	0.1	-	0
PSS/30wt% PEG	70	1	30	0.43	-	0
PSS/50wt% PEG	50	1	50	1	-	0
U	-	0	-	0	100	1
U/10wt% PEG	-	0	10	0.1	90	1
U/30wt% PEG	-	0	30	0.43	70	1
U/50wt% PEG	-	0	50	1	50	1
PSS/10wt% U	90	1	-	0	10	0.1
PSS/30wt% U	70	1	-	0	30	0.43
PSS/50wt% U	50	1	-	0	50	1
PSS/10wt% U/10wt% PEG	80	1	10	0.1	10	0.1
PSS/30wt% U/10wt% PEG	60	1	10	0.1	30	0.43
PSS/50wt% U/10wt% PEG	40	1	10	0.1	50	1

5.3.5 ^{1}H-nuclear Magnetic Resonance (NMR) Spectroscopy

^{1}H NMR spectroscopy was employed to confirm the chemical structure of the synthesized polyurethane (PU). The spectra were acquired using a Bruker AVANCE II 400 spectrometer operating at a resonance frequency of 400 MHz. All measurements were conducted at room

temperature, with PU dissolved at a concentration of 5 wt% in deuterated dimethyl sulfoxide (DMSO-d_6), which was used as the NMR solvent.

5.3.6 Gel Permeation Chromatography (GPC)

The molecular weight characteristics of the synthesized polyurethane (PU) were analyzed by gel permeation chromatography (GPC). For analysis, the original PU solution (30 wt% in DMF) was diluted with tetrahydrofuran (THF) to obtain a polymer concentration of 0.2 wt%. Prior to measurement, the diluted solution was passed through a 0.2 µm PTFE syringe filter to remove any particulate impurities. GPC analysis was performed using a 1260 Infinity system (Agilent Technologies) equipped with a Styragel HR 5E column (WAT044228, Waters). THF was used as the eluent at a constant flow rate of 1.0 mL min^{-1}, and the column temperature was maintained at 30 °C. Elution profiles were monitored using a refractive index detector. The system was calibrated with polystyrene standards prepared in THF, and the molecular weight values were calculated accordingly.

5.3.7 Electrical Measurements

The electrical properties of the PEDOT:PSS/PU composite films were evaluated by measuring their sheet resistance (R_s) using a standard four-point probe setup (Jandel Engineering) coupled to a source-measure unit (Agilent B2902A). Film thicknesses were independently determined with a surface profilometer (DEKTAK 150, Veeco). For each composition, five individual films were analyzed, and the average electrical resistivity (ρ) was calculated from the measured sheet resistance and film thickness according to the relation $\rho = R_s \cdot t$, where t represents the film thickness. The electrical conductivity (σ) was subsequently obtained as the reciprocal of the resistivity ($\sigma = 1/\rho$).

5.3.8 Mechanical and Electromechanical Characterization

Uniaxial tensile measurements were carried out using a Mach-1 V500csst MA009 mechanical testing system (Biomomentum Inc., Canada) at a constant crosshead speed corresponding to a strain rate of 10 mm/min. From the resulting stress–strain profiles, key mechanical parameters including elongation at break and Young's modulus were determined. The elastic modulus was obtained by linear fitting of the initial elastic region of the curve, defined here as strains up to 10%. Fracture-related tensile tests were additionally conducted according to the Rivlin–Thomas

methodology using notched specimens. The notches were introduced by manually cutting the films with a razor blade to a depth of 0.5 mm, corresponding to half of the film width. Cyclic mechanical loading–unloading experiments were performed by repeatedly stretching the films to a maximum strain of 200% at a rate of 10 mm/min, employing a 70 N load cell. The mechanical toughness of the films was quantified by integrating the area under the stress–strain curves using the built-in analysis functions of OriginLab software. For each film composition, measurements were conducted on three independent samples, and the data are reported as mean values with corresponding standard deviations. Electromechanical characterization was carried out on PEDOT:PSS/PU/PEG composite films under uniaxial tensile deformation up to 200% strain while simultaneously monitoring the electrical resistance. Resistance measurements were performed using an Agilent B2902A source-measure unit in combination with a custom-designed four-point probe configuration. To facilitate comparison between samples and deformation states, the resistance values were normalized to the initial resistance (R_0) measured at zero strain, and are reported as R/R_0.

5.3.9 Self-healing

Electrical self-healing behavior was evaluated using PEDOT:PSS/PU-based free-standing films with dimensions of 1.0 × 5.0 cm² and a thickness of approximately 25 μm. Electrical contacts were formed by placing two tungsten probes (miBot, Imina Technologies, Switzerland) into eutectic gallium–indium (EGaIn) droplets positioned on opposite sides of the film. A constant bias voltage of 0.2 V was applied, and the resulting current was continuously monitored using a source-measure unit (Agilent B2902A). To assess electrical healing performance, the films were deliberately damaged by manually introducing multiple cuts at different locations using a stainless-steel razor blade (Feather Hi Stainless Double Edge, Japan). The variation in current before damage, after cutting, and following healing was recorded. Electrical healing efficiency was quantified according to Equation (1):

$$\eta\,(\%) = 100 \times \frac{I_{\_healed}}{I_{\_pristine}}, \quad (1)$$

where η is the healing efficiency, $I_{\_pristine}$ corresponds the current measured prior to damage and $I_{\_healed}$ denotes the current after healing process.

Mechanical self-healing properties were investigated using free-standing PEDOT:PSS/PU-based films of identical dimensions through both scratching and cut-stick experiments (Figure S14). For scratch-based healing tests, controlled surface damage was introduced using a scratch pencil (Erichsen SmartPen, ISO 1518 test tip, 1.0 mm diameter) under applied loads of either 3 N or 5 N which were selected based in preliminary tests showing that 3N induces partial surface damage while 5N results in more pronounced or

deeper damage. Single-line scratches, grid patterns, and irregularly shaped defects were generated on the film surface. Additional grid-type scratches were manually created on PEDOT:PSS/PU/PEG films using a razor blade, while irregular damage patterns were produced using the scratch pencil. Following damage, the samples were placed on a hot plate and heated at 50 °C for 10 min to activate the healing process. The selected temperature and time were determined based on DSC results, where 50 °C was found to be sufficient to enhance polymer chain mobility and activate dynamic interactions without causing thermal degradation or structural damage. A healing duration of 10 min was chosen as it allowed reproducible recovery of electrical and mechanical properties within a practical timescale. These conditions represent a moderate thermal stimulus, making them relevant for potential applications where low-temperature and time-efficient healing are required. The depth of the scratched regions (single-line scratches produced with the pencil) was measured before and after healing using a profilometer (DEKTAK 150, Veeco). Surface morphology and healing behavior were further examined using an inverted optical microscope (Primovert, Carl Zeiss, Germany) and a digital microscope (Dino-Lite Edge 3.0 AM73915MT8, USA). The mechanical healing efficiency for scratch tests was calculated using Equation (2):

$$\eta\ (\%) = 100 \times \frac{d_{\_healed}}{d_{\_damaged}} \quad (2)$$

where $d_{\_damaged}$ is the scratch depth immediately after damage and $d_{\_healed}$ is the depth measured after healing. For comparison, the self-healing behavior of the synthesized pure PU was examined under similar conditions, except that the samples were heated at 60 °C for 50 min.

Cut-stick healing tests were conducted by cutting pristine films (1.0 × 5.0 cm², ~25 μm thick) into two separate pieces using a stainless-steel razor blade. The fractured ends were then brought into contact and placed on a hot plate at 50 °C for 10 min. A small manual pressure was applied to the joint region, as indicated in Figure S14b, to ensure intimate contact between the cut surfaces. Tensile tests were subsequently performed on both pristine and healed samples using a mechanical tester equipped with a 70 N load cell at a constant extension rate of 10 mm/min. The mechanical healing efficiency for cut-stick samples was determined based on the toughness values using Equation (3):

$$\eta\ (\%) = 100 \times \frac{U_{\_t,healed}}{U_{t,pristine}} \quad (3)$$

where $U_{\_t,pristine}$ represents the toughness of the original, undamaged film and $U_{\_t,healed}$ corresponds to the toughness after healing. The toughness was determined from the area under the stress–strain curve obtained during tensile testing. All measurements were performed until sample

failure at the center, and the healed samples were tested after a single cut–stick cycle by rejoining the damaged interface. Fracture typically occurred at or near the healed region, reflecting the effectiveness of interfacial reconnection.

5.3.10 Recycling Procedure

The PEDOT:PSS/PU/PEG blend was first cast into a standard dog-bone mold (ASTM D638 geometry, Figure S15) and subjected to a stepwise thermal treatment to obtain fully dried specimens. The temperature was sequentially increased following the program: 50 °C for 24 h, 80 °C for 3 h, 100 °C for 2 h, 120 °C for 2 h, and finally 150 °C for 2 h. This controlled heating protocol enabled complete solvent removal while preventing bubble formation within the samples. After cooling to room temperature, the specimens were demolded and used for tensile testing. Subsequently, the tested samples were cut into small fragments using scissors. These fragments were manually redistributed into a dog-bone mold and subjected to a remolding process using a hot press (Combo heat press machine). The mold was heated to 100 °C, and a pressure of approximately 3 GPa was applied for 20 min to consolidate the fragments into a single, continuous specimen. This temperature was selected to activate the material flow and interfacial reconnection required for effective recycling. After hot pressing, the mold was allowed to cool at ambient conditions for 2 h, after which the recycled samples were removed. This recycling protocol was repeated up to 20 cycles. Following each cycle, the mechanical and electrical properties of the remolded specimens were systematically characterized to evaluate the stability of material performance upon repeated recycling.

5.3.11 Fabrication of Electrodes and ECG Measurements

PEDOT:PSS/PU/PEG electrodes were prepared following the procedure illustrated in Figure S10a and b. First, PEDOT:PSS/PU/PEG films with dimensions of 5.0 × 7.0 cm² were patterned into circular disks with a diameter of 18 mm using a digital cutting system (Brother ScanNCut, model SDX225). The resulting disks were subsequently laminated onto thermoplastic polyurethane (TPU) substrates with a diameter of 20 mm. Electrical connections to the PEDOT:PSS/PU/PEG electrodes were established using silver (Ag) traces, which were connected to a commercial snap button (Ambu®). To ensure stable attachment to the skin during measurements, a transparent medical adhesive film (Tegaderm™, 3M) was applied to secure the electrodes in place. Skin–electrode impedance measurements and electrocardiogram (ECG) recordings were conducted

according to previously reported protocols [2, 74]. ECG signals were acquired using three different types of electrodes: commercial Ag/AgCl gel electrodes, pristine PEDOT:PSS/PU/PEG film electrodes, and PEDOT:PSS/PU/PEG electrodes prepared from healed and recycled films. Prior to measurement, the PEDOT:PSS/PU/PEG films underwent cut-stick self-healing and recycling treatments using the same procedures described earlier. All ECG data were collected from a single volunteer on the same day to minimize variability arising from physiological differences (Figure S10c and d).

5.3.12 PEDOT:PSS/PU/PEG film-based Pressure Sensor

PEDOT:PSS/PU/PEG films with dimensions of 1 × 2 cm² and an average thickness of approximately 25 μm were positioned onto interdigitated silver electrode patterns that were directly printed onto Tegaderm substrates using a direct-ink-writing printed circuit board system (Voltera V-One). To ensure reliable electrical contact, adhesive Tegaderm tape was applied to firmly fix the PEDOT:PSS/PU/PEG films onto the printed silver electrodes. Electrical connections to the measurement system were established using two alligator clips connected to a source-measure unit (Agilent B2902A). During the pressure-sensing experiments, a constant bias voltage of 0.2 V was applied, and the corresponding resistance changes of the films were continuously monitored under externally applied pressure. A series of discrete loads (1, 5, 10, 50, 100, and 500 g), as well as finger touch, were sequentially applied to the film surface to evaluate the pressure response. The pressure sensitivity was assessed by calculating the relative resistance change induced by each applied load. Sensitivity (S) was determined from the slope of the plot of normalized resistance change as a function of applied pressure and was calculated using the following equation:

$$S = \frac{\Delta(\Delta R/R_0)}{\Delta Pressure} \quad (4)$$

where R_0 denotes the initial resistance of the film in the absence of applied pressure, and ΔR corresponds to the resistance variation induced by the applied pressure.

5.4 Results and Discussion

5.4.1 Synthesis of PU and Preparation of PEDOT:PSS/PU-based Films

The PU employed in this work (Figure 15a) was synthesized using poly(ε-caprolactone) diol (PCL diol), isophorone diisocyanate (IPDI), and 1,3-propanediol (PDO) as the chain extender. The linear PCL diol functions as a soft segment, providing enhanced chain flexibility and mobility. This structural feature facilitates dynamic intermolecular interactions within the polymer network, which is essential for enabling efficient self-healing behavior and recyclability [104, 124-126]. In contrast, IPDI and PDO form the hard segments of the PU, imparting mechanical robustness and structural stability to the material. For the fabrication of conductive, stretchable, and self-healable films (Figure 15c), the synthesized PU was blended with PEDOT:PSS, polyethylene glycol (PEG), and glycerol, as illustrated by their chemical structures in Figure 15b. Based on preliminary electrical and mechanical characterizations, a PU content of 16 wt% was selected as the most suitable composition, representing a balance between conductivity and self-healing performance rather than a results of formal optimization. PEG with an average molecular weight of 400 was incorporated to promote autonomous self-healing of PEDOT:PSS, consistent with previous reports. Glycerol was introduced as a conductivity-enhancing additive, as it is known to improve electrical transport in PEDOT:PSS by inducing a more ordered arrangement of PEDOT chains [127, 128]. At the molecular level, the hydroxyl and ether functionalities present in PEG are expected to form hydrogen bonds with both PU and PEDOT:PSS. These interactions reduce interchain packing density and increase free volume within the composite, thereby enhancing polymer chain mobility [129]. Such increased molecular mobility contributes to improved toughness by allowing the material to undergo greater plastic deformation and dissipate mechanical energy prior to fracture [104, 130-132]

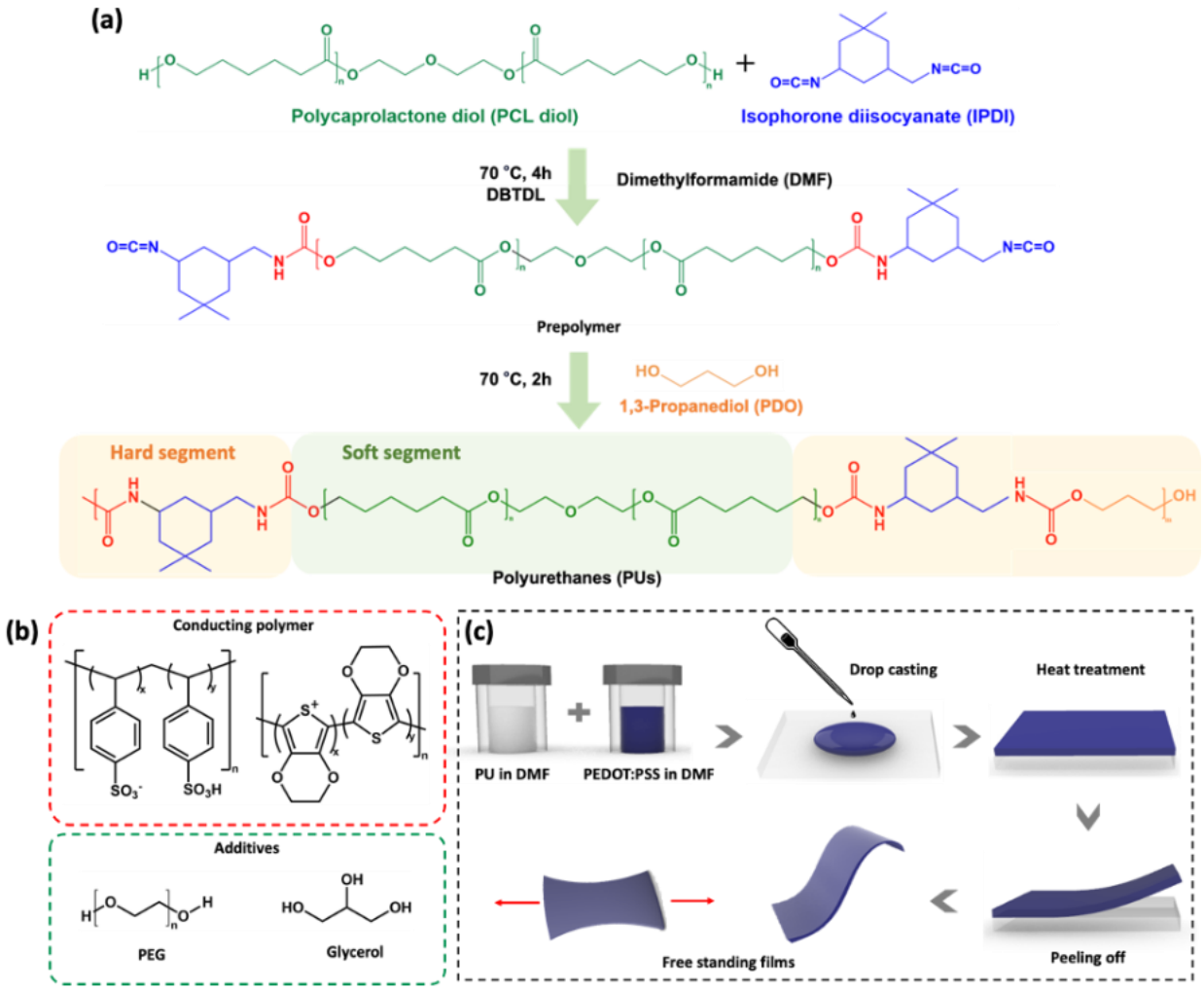

Figure 15. (a) Schematic of the synthesis of polyurethane (PU) used in this thesis. (b) Chemical structures of PEDOT:PSS, PEG, and glycerol. (c) Film preparation process.

5.4.2 Mechanical and Electrical Properties

The electrical conductivity of the PEDOT:PSS/PU-based composite films was found to lie in the range of approximately 5–15 S·cm^{-1}, depending on composition (Table 3). Although these values are lower than that of pristine PEDOT:PSS screen-printing formulations (~60 S·cm^{-1}), they fall within the typical conductivity range required for soft and wearable electronic devices (approximately 1–20 S·cm^{-1}). This range is generally sufficient to ensure stable electrical

performance in applications such as strain sensors, electronic skin, and epidermal electrodes, where mechanical compliance and durability are often prioritized over maximum conductivity [133].

Materials intended for soft bioelectronics, particularly wearable systems designed to interface with biological tissues, must satisfy competing mechanical requirements. Such materials should exhibit high stretchability and toughness to accommodate repetitive and complex deformations, while maintaining a sufficiently high Young's modulus to preserve structural integrity. Stress–strain measurements performed on films with different compositions (Figure 16a) revealed a linear elastic response up to approximately 30% strain. Beyond this regime, samples containing PEG exhibited pronounced plastic deformation.

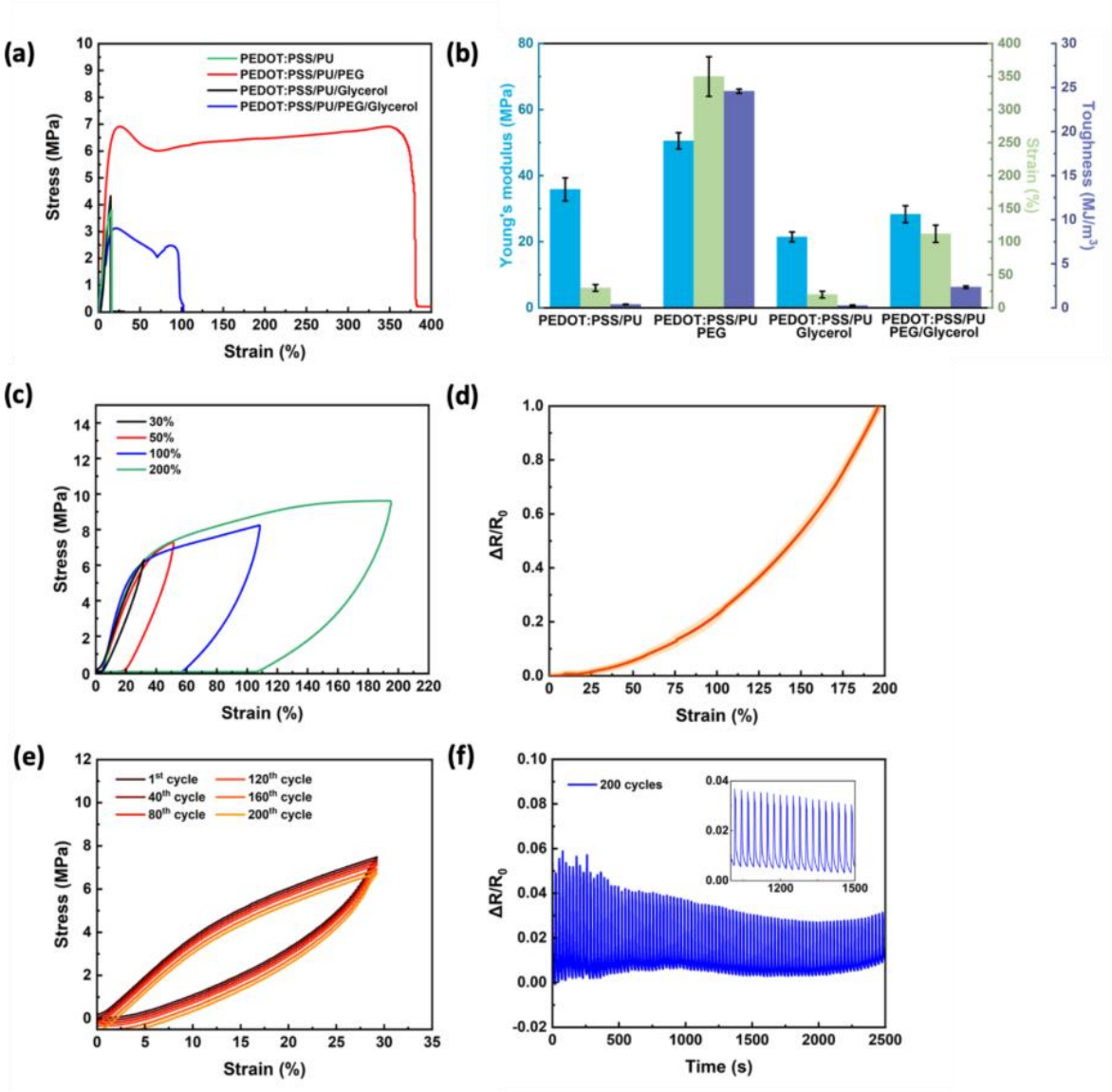

Figure 16. Mechanical properties of PEDOT:PSS/PU-based films. (a) Tensile stress-strain curves. (b) Young's moduli (0–10% strain), elongation at break, and toughness. Value (n = 3) are presented as mean ± standard deviation. (c) Cyclic stress-strain hysteresis curves of PEDOT:PSS/PU/PEG at different strain ranges (30, 50, 100, and 200%). (d) Normalized resistance change ($\Delta R/R_0$) as a function of strain for PEDOT:PSS/PU/PEG films (n = 3) as mean ± standard deviation. (e) Representative loading-unloading curves at selected cycles within a 0–30% strain range. (f) Normalized resistance change ($\Delta R/R_0$) vs. time during 200 cyclic strains between 0 and 30%. The Inset shows a magnified view of the signal response.

Among the investigated formulations, the PEDOT:PSS/PU/PEG films demonstrated the most favorable mechanical performance (Table 3, Figure 16b, and Figure S1a).

These films showed an exceptionally high elongation at break of approximately 350%, combined with a high toughness of ~24.6 MJ·m^{-3} and a relatively high Young's modulus of ~50 MPa. Notably, the incorporation of 2 wt% PEG resulted in a tenfold increase in elongation at break and a 65-fold enhancement in toughness compared to PEG-free samples. While the addition of glycerol slightly improved electrical conductivity, it led to a deterioration of the mechanical properties. This behavior is likely associated with the disruption of hydrogen-bonding interactions between polymer chains, which reduces effective load transfer and mechanical strength. When toughness was calculated using the Rivlin–Thomas method (Figure S1b) [133], a reduction of approximately 30% was observed (16.54 ± 1.24 MJ·m^{-3}, Figure S1c,d), consistent with the method-dependent sensitivity of fracture-based toughness evaluation. Owing to its superior mechanical performance, the PEDOT:PSS/PU/PEG composition was selected for subsequent durability and electromechanical studies.

Table 3. Summary of thickness, Young's modulus (0–10% strain range), elongation at break, toughness, and electrical conductivity of the films. Values (n = 3) are given as mean ± standard deviation.

Samples	**Thickness (µm)**	**Young's modulus (MPa)**	**Elongation at break (%)**	**Toughness (MJ/m^3)**	**Conductivity (S·cm^{-1})**
PEDOT:PSS/PU	24 ± 2	35.8 ± 3.5	30 ± 5	0.37 ± 0.03	5.2 ± 0.3
PEDOT:PSS/PU/PEG	25 ± 3	50.5 ± 2.5	350 ± 30	24.60 ± 0.23	9.4 ± 0.5
PEDOT:PSS/PU/Glycerol	22 ± 2	21.5 ± 1.5	20 ± 4	0.26 ± 0.05	15.4 ± 1.2
PEDOT:PSS/PU/PEG/Glycerol	25 ± 1	28.3 ± 2.6	112 ± 13	2.35 ± 0.14	11.5 ± 0.7

The mechanical stability of the PEDOT:PSS/PU/PEG films was further evaluated using tensile loading–unloading experiments at different maximum strains (Figure 16c). The films exhibited nearly ideal elastic behavior up to 30% strain, with negligible energy dissipation as indicated by the small hysteresis loop area. At higher applied strains, energy dissipation increased substantially—from 0.24 $MJ \cdot m^{-3}$ at 30% strain to 6.32 $MJ \cdot m^{-3}$ at 200% strain—accompanied by irreversible plastic deformation.

The electromechanical response of the films was investigated by monitoring resistance changes under uniaxial stretching up to 200% strain (Figure 16d). Minimal resistance variation (~4%) was observed within the elastic regime (≤30% strain). In contrast, a pronounced increase in resistance occurred between 30% and 200% strain, with the resistance nearly doubling at 200% strain. This behavior is attributed to strain-induced rearrangement and partial disruption of the conductive polymer network at high deformation levels.

Cyclic loading–unloading tests conducted within the elastic region (0–30% strain, Figure 16e) demonstrated excellent mechanical durability. After 200 cycles, only a minor increase in dissipated energy was observed, from 0.21 ± 0.02 $MJ \cdot m^{-3}$ in the first cycle to 0.27 ± 0.04 $MJ \cdot m^{-3}$ in the 200th cycle. Electrical stability during cyclic deformation was evaluated by recording resistance changes during repeated stretching cycles (0–30% strain, Figure 16f). A small resistance increase of approximately 6% was observed during the initial 40 cycles, after which the resistance stabilized at around 3%, as shown in the inset of Figure 16f. This stabilization suggests that the polymer stacking network reaches a mechanically stable configuration, resisting further conformational rearrangements, microstructural damage, or network breakdown during repeated deformation [134].

Overall, the PEDOT:PSS/PU/PEG films exhibited outstanding mechanical and electrical stability under repeated elastic deformation up to 30% strain. These results highlight the effectiveness of PEG incorporation in enhancing the mechanical robustness of PEDOT:PSS/PU-based systems, thereby enabling their use in durable, wearable, and flexible electronic applications [135-137].

Hydrogen bonding plays a key role in governing the intermolecular interactions among PEG, PEDOT:PSS, and PU, ultimately determining the mechanical properties of the composite films. To clarify the specific hydrogen-bonding interactions involved, Fourier transform infrared (FTIR) spectroscopy was performed on a simplified model system designed to mimic the relevant

functional groups present in the composite. This model system consisted of liquid mixtures of poly(4-styrenesulfonic acid) (PSS), ethyl N-carbamate (urethane, U), and PEG, with compositions summarized in Table 2. A schematic illustration of the possible intermolecular interactions is shown in Figure 17a.

Based on the chemical functionalities of these components, five distinct hydrogen-bonding interactions are possible (Figure 17b, i–v), each expected to induce characteristic red-shifts in the FTIR absorption peaks. Systematic shifts were observed for the characteristic S=O and SO_3–H peaks of PSS (Figure 17c and Figure S2a), as well as for the C=O and C–O–C vibrations associated with the urethane groups (Figure 17d and Figure S2b), with increasing PEG content (Table S1). These shifts can be attributed to hydrogen bonding between the hydroxyl and ether groups of PEG and both PSS and urethane moieties.

In contrast, the N–H stretching vibration of urethane and the O–H stretching of PEG overlap significantly, making it difficult to directly resolve hydrogen bonding involving these groups. Importantly, no appreciable peak shifts were observed when varying the ratio of PSS to urethane in the absence of PEG (Figure S2c,d), indicating negligible hydrogen-bonding interactions between PSS and urethane. Upon the addition of PEG to the PSS–U mixtures, the peak shifts of both PSS (Figure S2e) and urethane (Figure S2f) followed trends similar to those observed in the corresponding binary mixtures with PEG. These results confirm that PEG selectively introduces additional hydrogen-bonding interactions without promoting direct PSS–urethane bonding.

Taken together, the formation of PEG-mediated hydrogen-bonding networks provides a mechanistic explanation for the observed simultaneous enhancement in Young's modulus, stretchability, and toughness of the PEDOT:PSS/PU/PEG films.

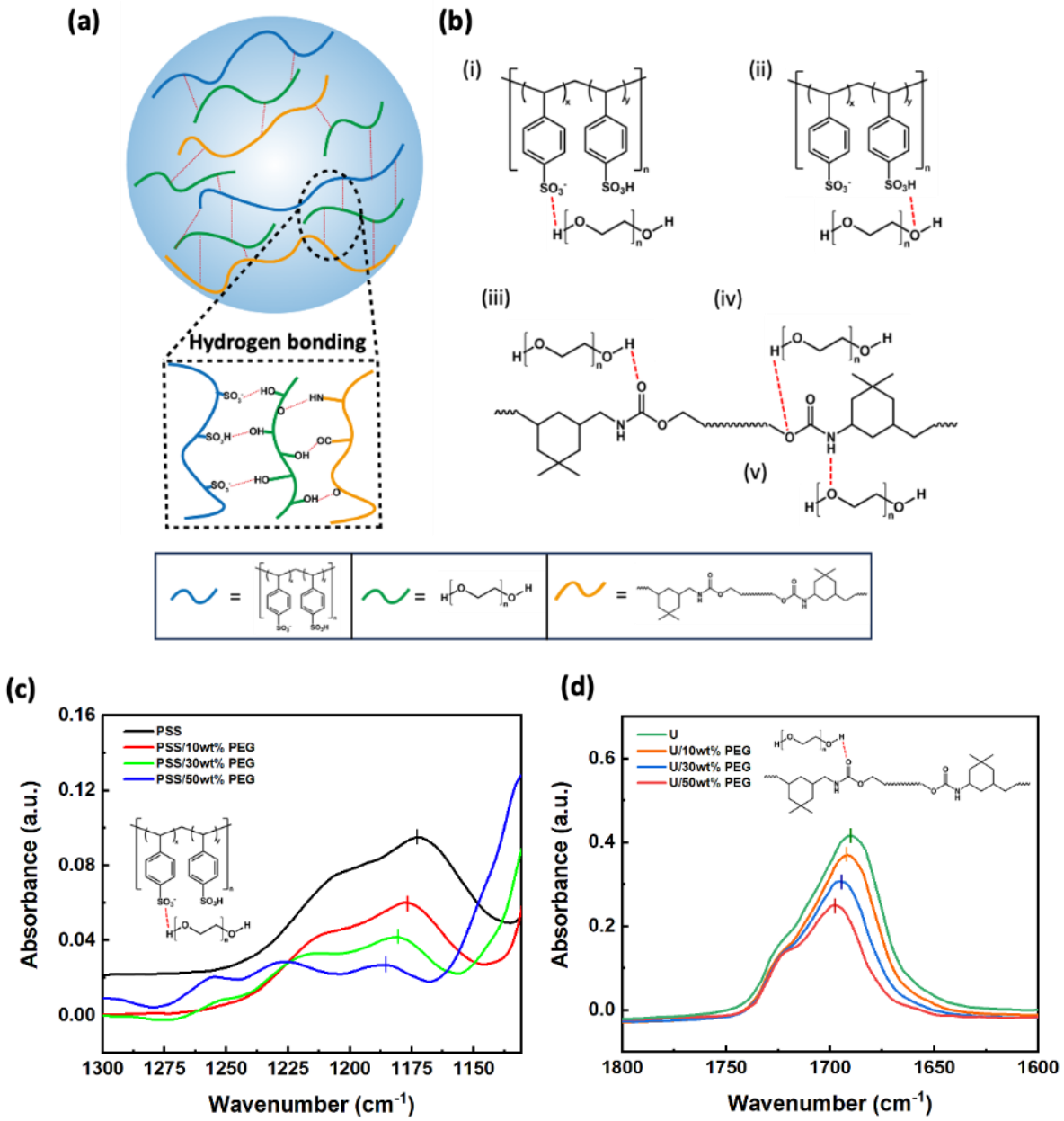

Figure 17. (a) Scheme illustration of hydrogen bonding interactions among PEG, PSS, and U. (b) Representative hydrogen bonding configurations within PEG, PSS, and U: (i) O-H (PEG), and O=S (PSS), (ii) SO_3-H and O-H (iii) O-H and O=C (urethane), (iv) -O- (urethane) and O-H and (v) N-H (urethane) and ether -O- groups. (c) FTIR spectra of pristine PSS and PSS/PEG mixture with varying compositions (10%, 30%, 50%). (d) FTIR spectra of pristine urethane (U) and U/PEG mixtures with varying compositions (10%, 30%, 50%).

5.4.3 Electrical and Mechanical Self-healing

All PEDOT:PSS/PU-based composite films exhibited autonomous electrical self-healing upon repeated cutting with a razor blade, producing an average gap width of approximately 20 μm. In contrast, pristine PEDOT:PSS films showed no electrical recovery under identical conditions (Figure S3a). Among the composites, PEDOT:PSS/PU/PEG and PEDOT:PSS/PU displayed an exceptionally rapid electrical self-healing response, restoring their electrical conductivity within approximately 0.1 s after damage (Figure 18a and Figure S3b).

Optical microscopy observations of the PEDOT:PSS/PU/PEG films during the cut–healing process revealed that the gap generated by the blade (~20 μm) was fully closed after healing (Figure 18b,c). Although a visible scar remained at the healed site, electrical continuity was completely restored. In comparison, films containing glycerol exhibited noticeably slower recovery kinetics. The PEDOT:PSS/PU/glycerol films required approximately 5 s to recover, while PEDOT:PSS/PU/PEG/glycerol films showed an intermediate recovery time of around 0.5 s (Figure S3c,d).

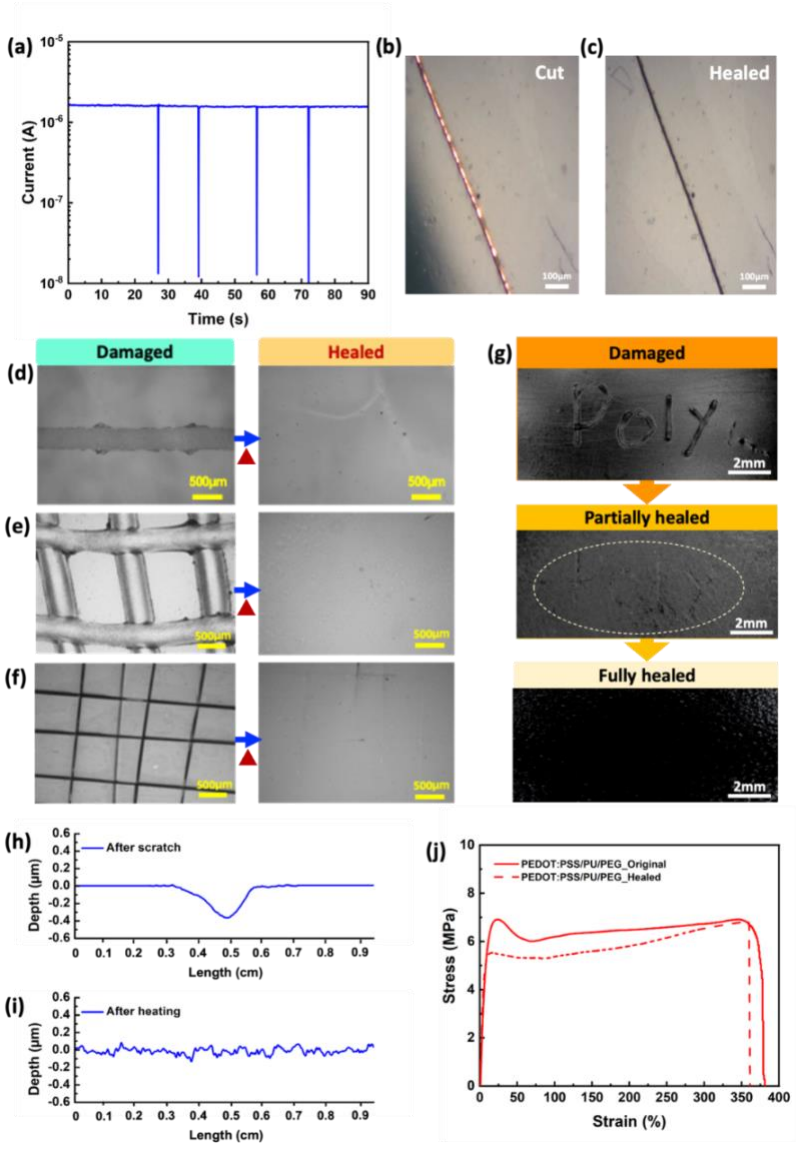

Figure 18. (a) Current–time response during repeated cut/healing cycles under an applied bias of 0.2 V; abrupt current drops correspond to sequential cuts. (b,c) Optical images of the film after cutting and after healing (~40 s), respectively. (d,e) Optical images after pencil-induced surface scratching (single-line and grid patterns) and subsequent healing. (f) Optical images after blade-induced surface scratching and healing. (g) Digital images showing the healing process after irregular damage induced by a pencil. (h,i) Depth profiles of the film after surface scratching and after healing, respectively. (j) Tensile stress–strain curves of the as-prepared film (solid line) and after cut–stick self-healing at 50 °C (dashed line).

Mechanical self-healing behavior was investigated by introducing controlled surface damage through scratching and cutting (Figure 18d–j). Since no significant healing was observed at room temperature even after three days, thermal activation was employed. Healing experiments were conducted at 50 °C, a temperature close to the glass transition temperature (T_g) of PU (Figure S4c). Near T_g , the PU matrix undergoes a transition from a glassy to a rubbery state, leading to increased polymer chain mobility. This enhanced mobility facilitates the reorganization and reformation of dynamic intermolecular interactions, particularly hydrogen bonds, which are critical for the self-healing process [138].

Optical microscopy images demonstrated complete healing of single surface scratches on PEDOT:PSS/PU/PEG and PEDOT:PSS/PU films after heating at 50 °C for 10 min (Figure 18d,e and Figure S5b). In contrast, no appreciable recovery was observed for pure PEDOT:PSS films under the same conditions (Figure S5a). To further assess the robustness of the healing capability, two distinct scratch patterns were applied, including single lines and grid structures. Both PEDOT:PSS/PU/PEG and PEDOT:PSS/PU films fully recovered from pencil-induced single-line and grid-shaped scratches following thermal treatment (Figure 18e and Figure S5f).

More severe surface damage was also examined. PEDOT:PSS/PU/PEG films subjected to grid-pattern cuts created using a blade exhibited complete healing after heating (Figure 18f). For irregular surface damage generated with a pencil, partial healing was observed after 2 min of heating, while full recovery was achieved after 10 min (Figure 18g). Quantitative analysis indicated healing efficiencies of 100% for both PEDOT:PSS/PU/PEG and PEDOT:PSS/PU films, as calculated using Equation (2) (Figure 18h,i and Figure S6a), whereas pristine PEDOT:PSS films showed negligible healing (Figure S6c).

The intrinsic self-healing capability of the PU component was also evaluated independently. Pure PU films demonstrated effective healing of surface scratches (Figure S7); however, the process required a longer healing time (~50 min) and a slightly higher temperature (60 °C). In contrast, films containing glycerol exhibited reduced healing efficiency (Figure S5c–e, Figure S5g,h, and Figure S6b, S8), suggesting that glycerol interferes with the dynamic intermolecular interactions responsible for healing.

In addition to surface healing, free-standing PEDOT:PSS/PU-based films exhibited cut-and-stick mechanical self-healing behavior, as demonstrated in Movie S1. Tensile stress–strain

measurements performed on intact and healed PEDOT:PSS/PU/PEG samples revealed a mechanical healing efficiency of approximately 90%, as calculated using Equation (3) (Figure 18j), indicating that the healed films retained most of their original toughness after cut–stick healing process.

The recovery of electrical functionality after cut–stick healing was further verified using a simple electrical circuit connected to a light-emitting diode (LED) (Figure S9). Upon cutting the film, the LED immediately turned off, indicating electrical failure. After rejoining the cut pieces and heating at 50 °C, the LED switched back on instantly, confirming effective restoration of electrical conductivity.

Overall, the combined electrical and mechanical self-healing behaviors of the PEDOT:PSS/PU/PEG films can be attributed to a healing mechanism governed by dynamic non-covalent interactions. These interactions, primarily hydrogen bonding, enable rapid reconnection of conductive pathways and efficient mechanical recovery, consistent with the FTIR analysis discussed earlier.

5.4.4 Recyclability of PEDOT:PSS/PU/PEG

The recyclability and reusability of electronic materials without degradation of electrical and mechanical performance are essential requirements for reducing electronic waste. Accordingly, this study aims to develop conductive polymer systems capable of undergoing repeated recycling processes while retaining their functional properties. Among the investigated compositions, PEDOT:PSS/PU/PEG was selected for recyclability evaluation owing to its outstanding mechanical performance and self-healing capability.

For recycling tests, PEDOT:PSS/PU/PEG films were cut into small fragments and subsequently remolded at 100 °C (Figure 19a). This temperature was chosen to enhance material fluidity and enable rapid reshaping. As demonstrated in Movie S3, the fragmented films could be readily remolded by simple hand pressing immediately after removal from the hot plate, indicating excellent thermoplastic-like processability.

Mechanical properties of pristine and recycled dogbone-shaped samples were assessed using tensile stress–strain measurements. After the first recycling cycle, the material retained approximately 85% of its original toughness, and this value remained nearly constant over

subsequent recycling cycles (Figure 19b). The initial decrease is attributed to incomplete reconstruction of the polymer network during reprocessing, including partial disruption of intermolecular interactions and microstructural rearrangement, which can lead to slight loss of mechanical integrity. In parallel, electrical characterization revealed no significant degradation in conductivity even after 20 remolding cycles (Figure 19c), highlighting the exceptional electrical stability of the recycled material.

The preservation of both mechanical and electrical performance upon repeated reprocessing can be attributed to enhanced polymer chain mobility when the material is heated above the glass transition temperature (T_g) of PU. At elevated temperatures, increased chain mobility facilitates the reversible dissociation and reformation of hydrogen bonds among PEG, PEDOT:PSS, and PU. These dynamic non-covalent interactions enable efficient structural rearrangement during reprocessing, ensuring consistent performance across multiple recycling cycles.

Overall, the ability of PEDOT:PSS/PU/PEG to maintain stable electrical conductivity and mechanical robustness after extensive reprocessing underscores its strong potential for use in sustainable and recyclable electronic devices. As summarized in Table S2, the PEDOT:PSS/PU/PEG films combine multiple advantageous properties, including high stretchability, exceptional toughness, autonomous electrical and mechanical self-healing, and excellent recyclability. While prior studies have individually reported higher electrical conductivity, enhanced stretchability, or self-healing behavior, the present work provides a comprehensive demonstration of a multifunctional material platform that simultaneously achieves recyclability, high toughness, and concurrent recovery of both electrical and mechanical properties [1, 2, 74, 106, 108].

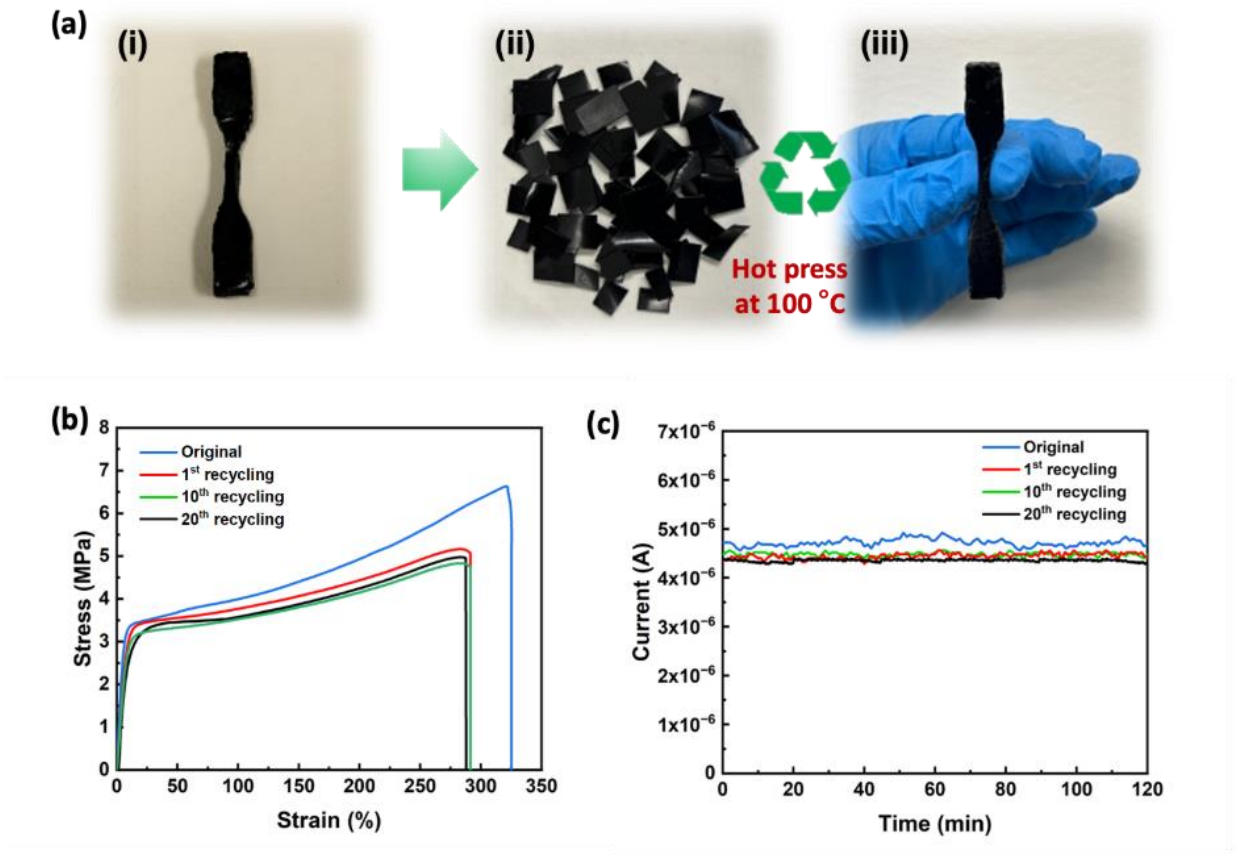

Figure 19. Recycling of PEDOT:PSS/PU/PEG via hot pressing at 100 °C. (a) Photographs of the original sample, after cutting into small fragments, and after reprocessing by hot pressing. (b) Comparison of tensile stress–strain curves for the original film and after the 1st, 10th, and 20th recycling cycles. (c) Current–time responses of the original film and after the 1st, 10th, and 20th recycling cycles under an applied bias of 0.2 V.

5.4.5 Self-healable and Recyclable Skin-electrode Impedance, ECG Signal Monitoring and Pressure Sensor

To demonstrate the practical applicability of the PEDOT:PSS/PU/PEG blend, we fabricated two representative soft electronic devices: an epidermal electrode and a resistive pressure sensor. When applied to human skin, the epidermal electrodes exhibited an impedance in the range of 10^3–10^6 Ω, comparable to that of commercial gel-based electrodes (Figure 20a). Importantly, the electrode impedance remained stable after both electrical self-healing and multiple recycling processes,

indicating the robustness of the material under repeated damage and reprocessing conditions (Figure 20a).

The electrophysiological performance of the PEDOT:PSS/PU/PEG electrodes was evaluated through ECG recordings. The obtained ECG signals closely matched those recorded using commercial electrodes (Figure 20b and Figure S11), with clearly distinguishable P waves, QRS complexes, and T waves (Figure 20c). These results confirm that the PEDOT:PSS/PU/PEG electrodes provide reliable skin–electrode contact and stable signal acquisition, even after undergoing self-healing and recycling treatments.

In addition to epidermal electrodes, a flexible resistive pressure sensor was fabricated by integrating the PEDOT:PSS/PU/PEG film with printed interdigitated silver electrodes on a compliant substrate (Figure S12a). Sensor performance was evaluated by applying controlled weights to the active sensing region and monitoring the resulting resistance changes. For repeated applications of the same load, the sensor exhibited consistent and reproducible resistance decreases. Notably, this signal stability was preserved after both mechanical self-healing and recycling of the PEDOT:PSS/PU/PEG layer (Figure S12b–g).

The sensor also demonstrated clear differentiation between applied pressures, showing distinct resistance responses to different weights in the pristine state as well as after healing and recycling (Figure S12b–g). From these measurements, the relative resistance change as a function of applied pressure was calculated to determine the sensor sensitivity (S) (Figure S12h). The pristine sensor exhibited two characteristic sensitivity regimes: a high-sensitivity region of approximately 1.25 kPa^{-1} in the low-pressure range (0.002–0.2 kPa), followed by a lower sensitivity of approximately 0.06 kPa^{-1} in the higher-pressure range (0.2–1.2 kPa). Crucially, these sensitivity profiles remained nearly unchanged after mechanical self-healing and recycling, indicating minimal degradation of sensing performance.

Taken together, these application demonstrations highlight the functional reliability of the PEDOT:PSS/PU/PEG films in realistic device configurations. The preservation of electrical, mechanical, and sensing performance after damage and reprocessing underscores the strong potential of this material system for use in sustainable, self-healable, and recyclable soft electronic devices.

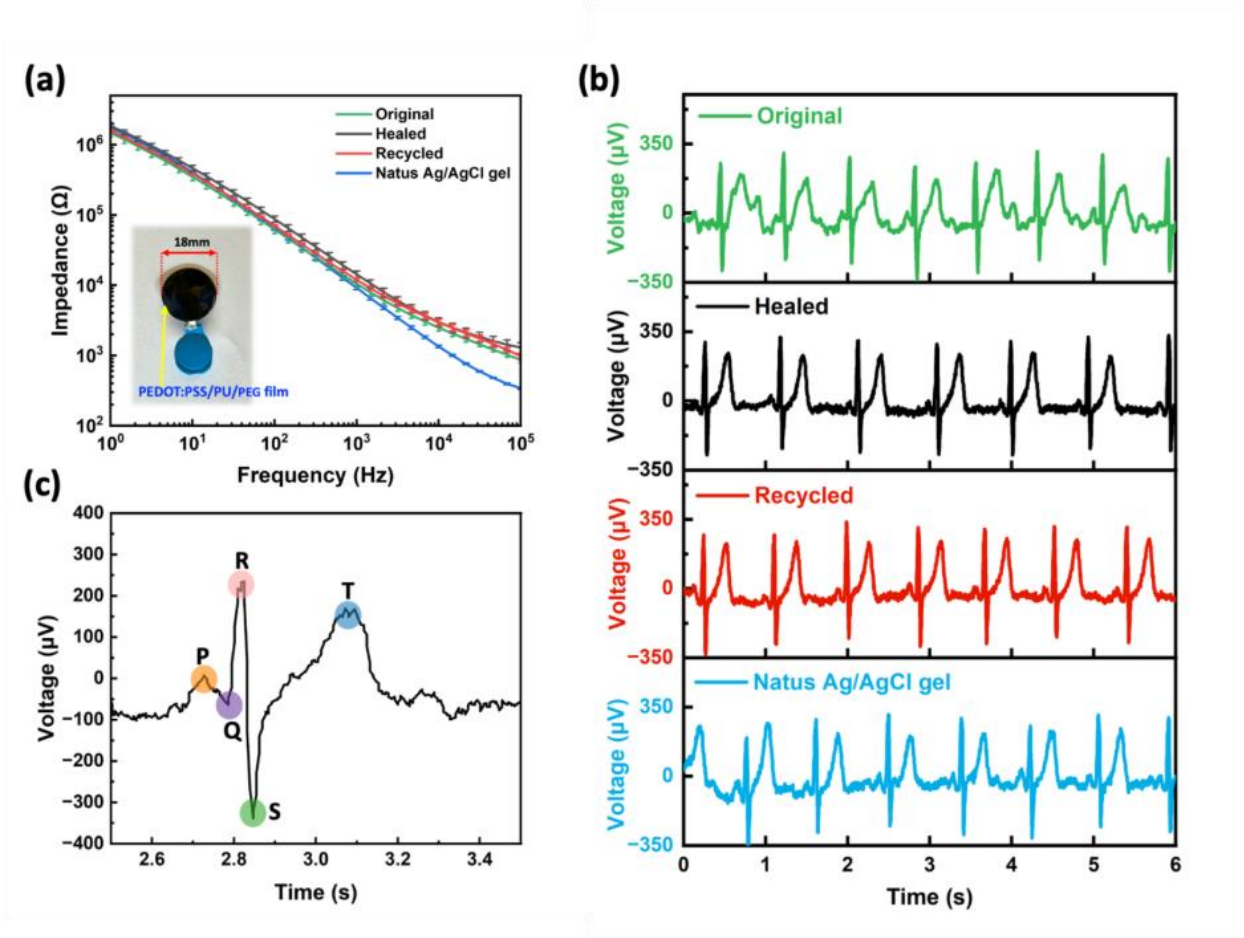

Figure 20. Skin–electrode impedance and ECG signal performance of PEDOT:PSS/PU/PEG film electrodes. (a) Skin–electrode impedance as a function of frequency for commercial Natus® Ag/AgCl gel electrodes and PEDOT:PSS/PU/PEG film electrodes (original, healed, and recycled). The inset shows a representative electrode. (b) ECG signals recorded using PEDOT:PSS/PU/PEG film electrodes before healing (green), after self-healing (black), after recycling (red), and commercial Natus® Ag/AgCl gel electrodes (blue). (c) Enlarged ECG waveform obtained from the original PEDOT:PSS/PU/PEG electrode, highlighting the P wave (atrial depolarization), QRS complex (ventricular depolarization), and T wave (ventricular repolarization).

5.5 Conclusions

In conclusion, the PEDOT:PSS/PU/PEG composite developed in this study demonstrated robust mechanical and electrical self-healing behavior, along with excellent recyclability enabled by

moderate thermal and mechanical treatment. The incorporation of PEG played a critical role in enhancing the mechanical performance of the material through hydrogen-bonding interactions with both PEDOT:PSS and PU. As a result, the composite exhibited a markedly improved toughness of approximately 24.6 $MJ \cdot m^{-3}$ and a high elongation at break of around 350%.

The material further showed outstanding mechanical durability, maintaining stable mechanical and electrical performance under repeated elastic deformation of up to 30% strain for at least 200 loading–unloading cycles. These properties highlight the ability of the PEDOT:PSS/PU/PEG system to withstand repetitive mechanical stresses commonly encountered in wearable and flexible electronic applications. As a proof of concept, the PEDOT:PSS/PU/PEG films were successfully implemented as epidermal ECG electrodes and as the active layer in a resistive pressure sensor. In both device configurations, the electrical response and sensing sensitivity were preserved after undergoing self-healing and recycling processes, demonstrating the functional reliability of the material in realistic device environments. 70Overall, this work establishes PEDOT:PSS/PU/PEG as a multifunctional conductive polymer platform that combines stretchability, toughness, self-healing, and recyclability within a single material system. By addressing both performance and sustainability requirements, this study contributes to the development of next-generation wearable electronics and provides a viable materials-based approach toward mitigating electronic waste through durable and recyclable device design.

5.6 Acknowledgments

This work was supported by the Natural Sciences and Engineering Research Council of Canada (NSERC) through a Discovery Grant awarded to FC, as well as by National Defence Canada under the IDEas program (Project CFPMN1-008, awarded to FC). The equipment and research infrastructure utilized in this study were funded and maintained by the Canada Foundation for Innovation.

JK gratefully acknowledges financial support from the Trottier Energy Institute through a doctoral scholarship. XZ acknowledges the China Scholarship Council for financial support during doctoral studies. PK acknowledges funding support from the Pierre Arbour Foundation and NSERC through a Master's scholarship. JF acknowledges support from an NSERC Postdoctoral Fellowship. GP acknowledges funding from the NSERC Vanier Canada Graduate Scholarship.

CHAPTER 6 ARTICLE 3 : PRINTABLE, SELF-HEALING AND RECYCLABLE PEDOT:PSS/POLYURETHANE COMPOSITES FOR DURABLE BIOELECTRONICS

This article has been submitted in the journal "Material Horizons" on Jan. 29th, 2026. The supporting information of this article is provided in Appendix B.

Jinsil Kim[1] and Fabio Cicoira[*]

[1]Department of Chemical Engineering, Polytechnique Montréal, Montréal, QC H3C 3A7, Canada

*Corresponding author. E-mail: fabio.cicoira@polymtl.ca

6.1 Abstract

The realization of self-healing conductive materials that are simultaneously printable, recyclable, and tolerant to severe mechanical damage remains a significant challenge in the field of soft and bioelectronics. In this work, we present a multifunctional conductive composite based on poly(3,4-ethylenedioxythiophene):polystyrene sulfonate (PEDOT:PSS) blended with a custom-engineered polyurethane (PU) featuring dynamic disulfide linkages and hydrogen-bonding functionalities. This molecular design enables autonomous self-healing at room temperature, allowing the material to recover from scratches, cuts, and puncture damage without the need for external stimuli, while maintaining both mechanical robustness and electrical continuity. The composite is processable from environmentally benign solvents and is compatible with spin-coating and printing techniques, yielding uniform, transparent, and highly stretchable thin films, as well as free-standing membranes that can be transferred onto a variety of substrates. PEDOT:PSS/PU/glycerol formulations exhibit moderate electrical conductivity (~15 $S \cdot cm^{-1}$), exceptional stretchability exceeding 650%, strong self-adhesion, and stable electromechanical performance under repeated deformation. Beyond self-healing, the material demonstrates excellent sustainability, supporting both mechanical reuse and chemical recycling for at least 15 cycles while retaining over 90% of its mechanical strength and fully restoring electrical conductivity. Mechanistic studies indicate that rapid network reorganization driven by reversible disulfide exchange and dynamic hydrogen-bond

reformation underpins the efficient self-repair behavior. As a proof of concept, printed electronic tattoos and free-standing electrodes fabricated from this composite were demonstrated as soft bioelectronic interfaces, delivering low-impedance contact and high-fidelity electrocardiogram (ECG) signal acquisition. Collectively, these results establish a versatile and sustainable materials platform that extends self-healing conductors beyond superficial damage, offering a practical pathway toward durable, recyclable, and manufacturable soft bioelectronic devices.

6.2 Introduction

Self-healing electronic materials play a pivotal role in the advancement of soft, wearable, and biointegrated devices, as they enable the autonomous recovery of electrical and mechanical functionality after damage, thereby prolonging device lifetime and mitigating electronic waste [139, 140]. In applications such as wearable health monitoring, soft robotics, energy storage, and implantable bioelectronics, devices are routinely subjected to mechanical deformation, accidental damage, and cyclic loading. Under these conditions, rapid and reliable self-repair is essential for maintaining long-term functionality and user safety [141, 142]. Despite substantial progress in this field, the realization of a single material platform that simultaneously offers high electrical conductivity, mechanical compliance, autonomous room-temperature (RT) healing, and recyclability remains a formidable challenge [116, 143, 144].

To date, most self-healing conductors have been developed as polymer composites or hydrogel-based systems capable of restoring electrical pathways after scratches or cuts [145, 146]. However, these materials are commonly fabricated via drop-casting, resulting in thick and poorly controlled films that hinder integration into complex device architectures and limit compatibility with scalable microfabrication processes [145]. In contrast, only a limited number of self-healing conductors are compatible with spin-coating or printing, despite the fact that thin-film processability is critical for achieving optical transparency, high pattern resolution, and compatibility with established manufacturing workflows [147]. Moreover, free-standing and transferable films—highly desirable for epidermal electrodes and soft electronic interfaces—are rarely accessible within existing material systems [147, 148].

Another major limitation of current self-healing conductors is the frequent reliance on external stimuli, such as heat, pressure, or chemical triggers, to activate repair mechanisms [149]. For practical wearable and implantable applications, autonomous healing under ambient conditions is

highly desirable, as it enables immediate functional recovery without external intervention, minimizes energy consumption, and ensures compatibility with biological environments [150]. Furthermore, while healing from surface scratches and cuts has been widely reported, puncture damage—one of the most severe and realistic mechanical failure modes encountered in soft electronics—has received remarkably little attention [1]. Achieving puncture healing in a fully solid-state conductive material would therefore represent a significant step forward in improving the durability and reliability of soft electronic systems.

Poly(3,4-ethylenedioxythiophene) doped with polystyrene sulfonate (PEDOT:PSS) is among the most widely used conducting polymers due to its high electrical conductivity, intrinsic softness, aqueous processability, and humidity-assisted self-repair capability [1, 107]. To enhance its mechanical compliance and stretchability, PEDOT:PSS has frequently been blended with flexible or functional additives, including poly(ethylene glycol) (PEG) [108], polyurethane diol (PUD) [74], tannic acid (TA) [78], Triton X-100 [96], and poly(vinyl alcohol) (PVA) [2]. While these strategies can improve stretchability and, in some cases, self-healing behavior, no PEDOT:PSS-based system reported to date has simultaneously achieved thin-film printability or spin-coating compatibility, autonomous RT self-healing—including puncture recovery—and recyclability within a single material framework.

Recyclability remains a particularly underexplored aspect of soft electronic materials. Most self-healing conductors are difficult to reprocess, and their disposal contributes to the rapidly growing issue of electronic waste. Enabling either chemical or mechanical recycling without compromising electrical or mechanical performance would substantially enhance the sustainability of soft electronic technologies [151]. Polyurethanes (PUs) are especially attractive candidates in this context due to their segmented architectures and the ability to incorporate dynamic covalent or supramolecular interactions, which allow tunable mechanical properties, reversible bond exchange, and reprocessability. The chemistry of PUs can be precisely tailored through the selection of polyols, which govern elasticity, and diisocyanates and chain extenders, which regulate strength and flexibility [4]. Incorporating long-chain polyols can further reduce the glass transition temperature (T_g), thereby enhancing chain mobility, healing efficiency, and solubility in environmentally benign solvents—features that are advantageous for both recyclability and solution-based processing such as spin-coating and printing [152, 153].

In this work, we address these unmet challenges by designing a polyurethane incorporating dynamic disulfide bonds and hydrogen-bonding soft segments, which is subsequently blended with PEDOT:PSS to form a multifunctional, processable, and recyclable conductive composite. The resulting material can be spin-coated or printed into uniform, transparent thin films as well as free-standing membranes, enabling precise thickness control and facile patterning. The composites combine moderate electrical conductivity (~15 $S \cdot cm^{-1}$), exceptional stretchability exceeding 650%, strong self-adhesion, and rapid autonomous RT healing from scratches, cuts, and punctures. In addition, the films support both chemical and mechanical recycling over multiple cycles with minimal degradation in performance, advancing the concept of circular soft electronics.

Beyond demonstrating multifunctional performance, we provide molecular-level insight into the autonomous healing mechanism through solid-state FTIR analysis, revealing that reversible disulfide exchange and hydrogen-bond reformation govern efficient network reorganization and damage recovery. As a proof of concept, printed electronic-tattoo electrodes fabricated from this composite exhibit stable, low-impedance electrocardiogram (ECG) recordings and enable facile water-assisted detachment and reuse. Rather than optimizing a single performance metric, this study demonstrates how thin-film processability, autonomous RT self-healing—including solid-state puncture recovery—and true recyclability can be integrated within a single PEDOT:PSS-based conducting polymer platform. Collectively, these results establish a unified materials strategy for the development of durable, sustainable, and manufacturable soft bioelectronic systems.

6.3 Experimental Section

6.3.1 Materials

Clevios™ SV3 STAB, a commercially available screen-printing formulation of poly(3,4-ethylenedioxythiophene) doped with polystyrene sulfonate (PEDOT:PSS) containing diethylene glycol and propylene glycol, was purchased from Heraeus Precious Metals (Germany). Poly(ε-caprolactone) diol (PCL diol, number-average molecular weight = 2000 $g \cdot mol^{-1}$), polyethylene glycol (PEG, average molecular weight = 2000 $g \cdot mol^{-1}$), trimethylolpropane (TMP, >98%), dimethylformamide (DMF, >99.5%), anisole (>99%), and acetonitrile (>99%) were obtained from Millipore Sigma (St. Louis, MO, USA) and used without further purification. Isophorone diisocyanate (IPDI, >99%), aminophenyl disulfide (APDS, >98%), and dibutyltin dilaurate

(DBTDL, >95%) were purchased from Tokyo Chemical Industry (USA). Ethanol (EtOH, >95%), acetone (>95%), and isopropanol (IPA, >95%) were also obtained from Millipore Sigma and used as received. Glass substrates were supplied by Corning (USA). Polytetrafluoroethylene (PTFE, Teflon™) molds were purchased from McMaster-Carr. Polyethylene terephthalate (PET, XF-122, thickness 25 μm) sheets were obtained from Polyonics. Temporary tattoo paper was purchased from Sunnyscopa.

6.3.2 Synthesis of PU

The synthesis of PU, schematically shown in Figure 21a, was performed under ambient laboratory conditions using a three-necked round-bottom flask. Prior to each reaction, the flask was purged with nitrogen for 15 min to eliminate residual oxygen and moisture. Poly(ε-caprolactone) diol (PCL diol, 3 g, 1.5 mmol), polyethylene glycol (PEG, 8 g, 4 mmol), isophorone diisocyanate (IPDI, 2.45 g, 11 mmol), and aminophenyl disulfide (APDS, 1.18 g, 5.5 mmol) were used according to a molar ratio of 1.5:4:11:5.5. In this formulation, IPDI and APDS constituted the hard segments, while PCL diol and PEG served as the soft segments; trimethylolpropane (TMP) was employed as a crosslinking agent.

PCL diol and PEG were first dissolved in dimethylformamide (DMF, 10 g) and heated to 80 °C under continuous stirring. Subsequently, IPDI was added dropwise along with dibutyltin dilaurate (DBTDL, 0.09 g) as the catalyst. The reaction mixture was maintained at this temperature for 2.5 h to generate an isocyanate-terminated prepolymer.

In a separate step, APDS and TMP (0.1 g, 0.5 mmol) were dissolved in DMF (10 g) and introduced into the prepolymer solution. The resulting mixture was allowed to react at 55 °C for an additional 2 h to complete chain extension and crosslinking. Finally, the reaction product was cast into a polytetrafluoroethylene (PTFE) mold and dried at 120 °C for 24 h, yielding a solid PU material.

6.3.3 Preparation of PEDOT:PSS/PU Composite Films

The PEDOT:PSS paste was first homogenized using a centrifugal mixer (ARM-310, Thinky, USA) at 2000 rpm for 5 min, followed by dilution with dimethylformamide (DMF) at a weight ratio of 50:50. Solid PU was separately redissolved in DMF at a concentration of 30 wt% and stirred until a homogeneous solution was obtained using a vortex mixer (VWR). When required, glycerol was incorporated into the PU solution as a plasticizer and conductivity-enhancing

additive. Final PEDOT:PSS/PU-based formulations were prepared by blending the PEDOT:PSS and PU solutions at the desired ratios (as listed in Table 4), followed by additional homogenization using a vortex mixer.

Thin films were fabricated using multiple deposition techniques, including drop-casting onto glass substrates (5.0 × 7.0 cm²) and PTFE molds, spin-coating onto glass slides (2.0 × 2.0 cm²) or polyethylene terephthalate (PET) substrates, and printing onto glass slides and tattoo paper, as detailed in Section 2.9. Drop-cast films were dried via sequential thermal treatment on a hot plate at 50 °C for 16 h, followed by annealing at 100 °C for 1 h, 120 °C for 1 h, and 150 °C for 1 h.

Spin-coated films were deposited at rotational speeds of 500, 1000, and 1500 rpm for 10 s, resulting in film thicknesses of approximately 2.5, 1.8, and 1.4 μm, respectively. These films were subsequently baked at 50 °C for 3 h and at 150 °C for 1 h. Both fabrication methods yielded uniform and bubble-free films.

Optical transmittance of the resulting films was measured using UV–Vis spectroscopy (AS SEC2022, Bio-Logic). In addition to DMF, the PEDOT:PSS/PU-based films were also found to be soluble in environmentally benign solvents, including anisole and ethanol.

6.3.4 Thermal Analysis

Thermogravimetric analysis (TGA) was carried out using a Q500 instrument (TA Instruments) under a nitrogen atmosphere with a flow rate of 40 mL·min^{-1}. Measurements were conducted from 30 °C to 800 °C at a heating rate of 10 °C·min^{-1}. Film samples with a mass of approximately 15 mg were placed in open platinum crucibles. All samples exhibited an onset of thermal decomposition at temperatures close to 300 °C, which is significantly higher than the temperatures used for self-healing (25 °C) and recycling (55 °C). In addition, no noticeable mass loss associated with residual dimethylformamide (DMF) evaporation was detected, indicating effective solvent removal during film processing.

Differential scanning calorimetry (DSC) measurements were performed using a Q2000 calorimeter (TA Instruments). Approximately 5 mg of each film sample was sealed in aluminum pans and analyzed under a nitrogen atmosphere. To eliminate prior thermal history, samples were first cooled to −25 °C and then heated to 150 °C at a rate of 10 °C·min^{-1} for two consecutive cycles.

The glass transition temperature (T_g) was determined from the second heating cycle using the analysis software provided by the instrument manufacturer.

6.3.5 Attenuated Total Reflectance Fourier-transform Infrared Spectroscopy (ATR-FTIR)

Attenuated total reflectance Fourier-transform infrared (ATR-FTIR) spectroscopy was employed to investigate dynamic bonding interactions in the solid state. Spectra were acquired using a Spectrum 65 FTIR spectrometer (PerkinElmer) operated in ATR mode, with a spectral resolution of 4 cm^{-1} and 32 accumulated scans over the range of 4000–550 cm^{-1}.

Measurements were conducted on pristine samples as well as after scratching and subsequent healing. Particular attention was paid to characteristic vibrational modes associated with N–H, C=O, and S–S bonds in order to track bond dissociation and reformation processes during the self-healing behavior of the materials.

6.3.6 Electrical Characterization

The sheet resistance (R_s) of the films (1 × 1 cm^2) was measured using a standard four-point probe setup (Jandel Engineering) connected to a source-measure unit (B2902A, Keysight). Film thickness (t) was determined using a three-dimensional optical profilometer (Photomap, Fogale Nanotech).

The electrical resistivity (ρ) was calculated according to $\rho = R_s \times t$, where R_s is the measured sheet resistance and t is the film thickness. Electrical conductivity (σ) was subsequently obtained as $\sigma = 1/\rho$. All resistivity and conductivity values were averaged over five independent samples.

6.3.7 Mechanical and Electromechanical Tests

Uniaxial tensile and adhesion measurements were conducted using a Mach-1 V500csst MA009 mechanical tester (Biomomentum). Stress–strain behavior was evaluated on film specimens with dimensions of 5 × 1 cm^2 at a constant crosshead speed of 500 $mm \cdot min^{-1}$. Adhesion strength was assessed by laminating free-standing films (6 × 1 cm^2, thickness ≈ 25 μm) either to themselves or to glass substrates, followed by 90° peel tests performed over a peel length of 3 cm at a rate of 50 $mm \cdot min^{-1}$, in accordance with ASTM D6862.

Cyclic tensile testing was carried out for 500 loading–unloading cycles at a maximum strain of 50% and a deformation rate of 10 mm·min^{-1} to evaluate mechanical durability. Electromechanical stability was investigated using a custom-built uniaxial translational manipulator integrated with a source-measure unit (B2902A, Keysight). During cyclic deformation, the electrical resistance of the films was continuously recorded under a constant bias voltage of 0.2 V. Additional electromechanical tests were performed by stretching the films up to 400% strain at the same deformation rate and applied voltage.

Resistance variations were expressed as normalized resistance (R/R_0), where R corresponds to the instantaneous resistance and R_0 represents the initial resistance prior to deformation. Unless otherwise specified, all mechanical and electrical measurements were conducted on three independently prepared samples (n = 3). For clarity, representative curves are presented in the main text, while corresponding replicate datasets are provided in the Supporting Information to confirm reproducibility.

6.3.8 Electrical and Mechanical Self-healing

Electrical self-healing behavior was evaluated under ambient conditions using drop-cast films (1.0 × 5.0 cm², thickness ≈ 2.5 μm) and spin-coated films (thicknesses of 1.8 and 1.4 μm). Electrical measurements were conducted with a source-measure unit (B2902A, Keysight) connected to two tungsten probes (miBots, Imina Technologies), positioned at both ends of the films. A constant bias voltage of 0.2 V was applied, and the current was monitored in real time. Mechanical damage was introduced by manually cutting the films at multiple locations using a stainless-steel razor blade (Feather Hi-Stainless, Japan), producing cut widths of approximately 20 μm. The resulting current variations were recorded to assess the electrical self-healing response. Each cut–healing experiment was repeated at least three times. The electrical healing efficiency (η) was defined as:

$$\eta_{\,eletrical\ healing}\ (\%) = 100 \times \frac{I_{\_healed}}{I_{\_original}} \quad (1)$$

Where $I_{\_original}$ is the initial current prior to cutting and $I_{\_healed}$ is the recovered current after healing. Mechanical self-healing was investigated using free-standing membranes (1.0 × 5.0 cm², thickness ≈ 25 μm) under scratching, cut–stick, and puncture damage modes. For scratch healing tests, surface damage was introduced by applying a normal load of 3 N using a scratch pen (SmartPen, Erichsen) equipped with a test tip conforming to ISO 1518 (tip diameter = 1.0 mm).

Following scratching, the films were placed on a hot plate at 25 °C for 1 h to allow autonomous healing. Scratch depths before and after healing were quantified using a three-dimensional optical profilometer (Photomap, Fogale Nanotech), and surface images were captured with the integrated optical microscope. Each experiment was performed on three independent samples. The scratch healing efficiency (η) was calculated as:

$$\eta_{scratch\ healing}(\%) = 100 \times \frac{d\_damaged - d\_healed}{d\_damaged} \quad (2)$$

Where $d_{\_damaged}$ and $d_{\_healed}$ denote the scratch depth after damage and after healing, respectively. For cut–stick self-healing tests, free-standing films (1.0 × 5.0 cm², thickness ≈ 25 μm) were severed into two pieces using a stainless-steel double-edge razor blade. The fractured edges were brought into contact and placed on a hot plate at 25 °C for 20 min, with gentle manual pressure applied initially to ensure intimate contact. Tensile tests were conducted on pristine and healed samples using a mechanical tester equipped with a 70 N load cell at a constant strain rate of 10 mm·min⁻¹. Three samples were tested. The cut–stick healing efficiency (η) was defined as:

$$\eta_{cut-stick\ healing}(\%) = 100 \times \frac{E\_healed}{E_{pristine}} \quad (3)$$

Where $E_{\_healed}$ and $E_{\_pristine}$ represent the elongation at break after healing and that of the pristine film, respectively.

Puncture healing tests were carried out using a stainless-steel sewing needle with a diameter of 0.5 mm mounted on a mechanical tester (Biomomentum). Free-standing membranes (1.0 × 5.0 cm², thickness ≈ 25 μm) were fixed on a square rubber frame with an open center to allow full penetration of the needle (Figure S36). The needle was driven downward and upward at a speed of 10 mm·s⁻¹, generating a puncture force of approximately 3 N. After puncturing, the films were placed on a hot plate at 25 °C for 1 h to enable autonomous healing. Optical images were acquired using an inverted optical microscope (Primovert, Carl Zeiss). Each puncture experiment was repeated three times. In this study, puncture healing is defined as the autonomous closure of through-thickness damage accompanied by restoration of surface continuity, rather than complete recovery of the original microstructure.

6.3.9 Printed E-tattoos and Freestanding Electrodes for ECG Signal Monitoring

A printable conductive ink was prepared by dissolving drop-cast PEDOT:PSS/PU-18/Gly-2.2 films in ethanol (EtOH). The resulting low-viscosity ink was used to print circular electrode patterns with a diameter of approximately 17 mm onto tattoo paper and glass substrates using a direct ink writing printer (Voltera Nova, Voltera). Printing was performed with a stainless-steel dispensing nozzle (Nordson EFD, nozzle diameter ≈ 150 µm) mounted on a 3 cc syringe. A dispensing pressure of 500 and a printing speed of 2000 mm·min^{-1} were employed.

Ethanol was selected as a green solvent due to its ability to dissolve both the polyurethane and PEDOT:PSS components more effectively than anisole, acetonitrile, or isopropanol (Figure S37). Although a larger solvent volume was required compared to N,N-dimethylformamide (DMF), ethanol was fully compatible with the printer nozzle membrane, whereas DMF was not. Electrode layouts were designed using DipTrace software. Following printing, the samples were dried at 60 °C for 2 h to remove residual solvent.

For epidermal tattoo electrodes, disc-shaped electrodes were first printed directly onto tattoo paper. A transparent adhesive film with a central circular opening (diameter = 10 mm) was subsequently laminated over the printed layer to ensure direct electrical contact between the electrode and the skin while providing mechanical reinforcement. The tattoo electrodes were transferred onto the skin by wetting the backing paper with water for approximately 10 s and gently peeling it off, leaving the printed electrode adhered to the skin. A commercial snap-button connector (Ambu) was attached to the exposed electrode surface and secured using Tegaderm™ adhesive film to ensure stable electrical contact.

Freestanding electrodes were fabricated by printing the conductive ink onto glass substrates. To release the electrodes, a small amount of water was applied to the printed films for approximately 5 s, enabling facile detachment from the glass surface. The released electrodes were then transferred directly onto the skin, and electrical connections were established using the same procedure as for the tattoo-based electrodes. This strategy highlights the compatibility of the material with multiple transfer approaches and improves user comfort during electrode removal.

ECG measurements were performed using both commercial Ag/AgCl gel electrodes and the printed PEDOT:PSS/PU-18/Gly-2.2 electrodes. All measurements were collected from the same volunteer on the same day following previously reported protocols. ECG signals were acquired using a Cyton biosensing board (OpenBCI) at a sampling rate of 250 Hz, with a band-pass filter of 0.5–40 Hz and a 60 Hz notch filter applied. All ECG experiments were conducted in accordance with the approved protocol CER-2021-04-D.

6.3.10. Reuse and Recycling Procedures

PEDOT:PSS/PU-18/Gly-2.2 films were subjected to both chemical recycling and mechanical recycling to evaluate their suitability for circular reprocessing.

Chemical recycling was performed to selectively recover and reprocess the individual polymer components of the composite. PEDOT:PSS/PU films were first immersed in ethanol (10 mL) for 10 min, during which the PU phase was preferentially dissolved. The resulting suspension was centrifuged at 1500 rpm for 15 min, enabling separation of the PU-rich supernatant from the PEDOT:PSS-rich precipitate. The recovered PU solution was drop-cast onto glass substrates and dried at 50 °C for 1 h to remove the solvent, yielding solid PU. The isolated PU was then redissolved in ethanol to prepare a 30 wt% solution. To regenerate the composite material, this PU solution was blended with freshly prepared PEDOT:PSS diluted in ethanol at a 50:50 (w/w) ratio. The resulting mixture was drop-cast onto glass substrates and dried sequentially at 50 °C for 1 h followed by 80 °C for 1 h, allowing efficient solvent removal while minimizing bubble formation. The electrical and mechanical properties of the chemically recycled films were subsequently characterized to assess performance retention after recycling.

Mechanical reuse was achieved by reshaping the composite material without altering its chemical composition. Drop-cast films were initially prepared in a circular PTFE mold following the procedure described in Section 2.3. After cooling to room temperature, the films were cut into small fragments and transferred into a rectangular mold. Gentle pressure was applied to ensure intimate contact between adjacent pieces. The mold was then heated at 55 °C for 30 min to promote healing and remolding of the fragments, followed by cooling to ambient temperature for 5 min prior to demolding. The remolded samples were subsequently subjected to mechanical and electrical characterization to evaluate the preservation of material performance after mechanical reuse.

6.4 Results and Discussion

6.4.1 Synthesis of PU

A self-healing, stretchable, and recyclable PU was designed by combining poly(ε-caprolactone) diol (PCL diol) and PEG as soft segments with IPDI as the hard segment, APDS as a dynamic chain extender, and TMP as a crosslinking agent (Figure 21a). In this molecular architecture, the PCL diol and PEG segments enhance chain mobility and solubility, while IPDI provides mechanical strength. The incorporation of APDS introduces dynamic disulfide bonds, and TMP enables controlled crosslinking within the polymer network. In our previous work, we reported a PU system composed of PCL diol, IPDI, and 1,3-propanediol (PDO), which exhibited self-healing and mechanical reprocessability at moderate temperatures (~50 °C) when blended with PEG and PEDOT [4]. In that system, the flexibility of the PCL soft segments played a key role in enabling dynamic rearrangement of the polymer chains. Building on this concept, the present work aims to achieve autonomous healing and reprocessing at room temperature while simultaneously improving solution-based processability. To this end, PEG and dynamic disulfide bonds were deliberately integrated into the PU backbone. PEG effectively lowers the glass transition temperature (T_g) of the polymer network and increases chain mobility, whereas disulfide bonds—widely employed to enhance durability and sustainability in polymeric materials [154, 155]—enable reversible bond exchange above T_g, thereby promoting autonomous healing and reprocessability. The PU was synthesized via a two-step polymerization process. In the first step, hydroxyl-terminated PCL diol and PEG reacted with the isocyanate groups of IPDI to form an –NCO-terminated prepolymer. In the second step, APDS and TMP were introduced to extend the polymer chains while simultaneously incorporating disulfide bonds and crosslinking points. Fourier-transform infrared (FTIR) spectroscopy provided clear evidence of successful PU formation. The presence of a characteristic absorption band at 2270 cm^{-1} in the prepolymer spectrum (Figure S16) confirmed the existence of terminal isocyanate groups, while the disappearance of this band in the final PU indicated complete consumption of the isocyanates. In addition, the emergence of characteristic C=O stretching vibrations at approximately 1700 cm^{-1} and N–H stretching bands near 3200 cm^{-1} confirmed the formation of urethane linkages. Mechanical characterization further demonstrated that the synthesized PU possessed high stretchability and mechanical robustness. The material could withstand severe deformations,

including twisting and knotting, without mechanical failure (Figure S17), confirming that the designed molecular architecture successfully combines elasticity, toughness, and structural integrity.

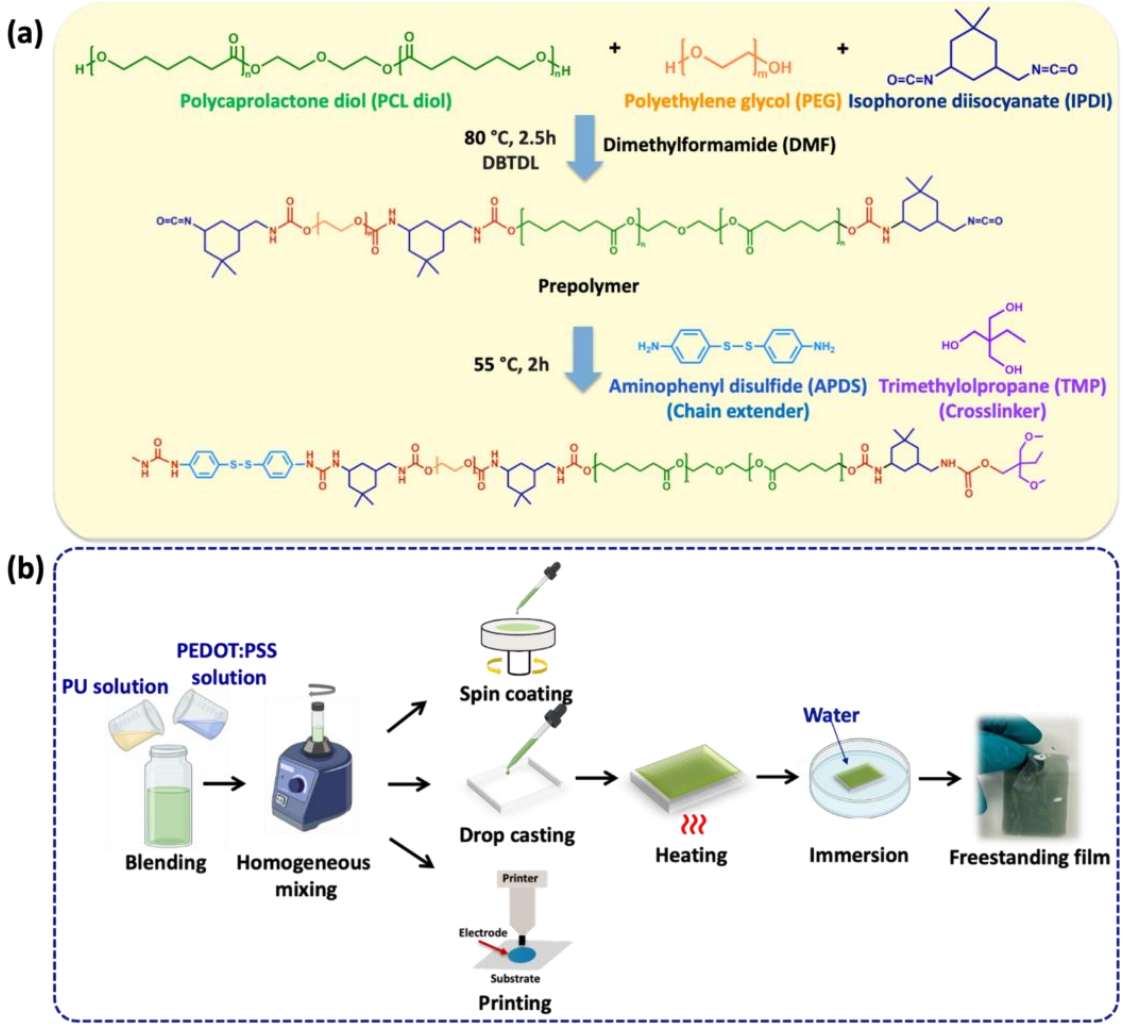

Figure 21. Synthesis and fabrication of PEDOT:PSS/PU composites. (a) Schematic illustration of the synthetic route for the self-healing, stretchable, and recyclable polyurethane (PU). (b) Fabrication process of PEDOT:PSS/PU composites, including solution preparation, film deposition (spin-coating, printing, and drop-casting), thermal curing, and water-assisted release to obtain freestanding films.

6.4.2 Formulation and Processing Versatility of Conductive Composites

Stretchable, self-healing, and recyclable conductive composites were prepared by blending the synthesized polyurethane (PU) with PEDOT:PSS, followed by drop casting to form free-standing films (Figure 21b). As anticipated, increasing the PU content led to a gradual reduction in electrical conductivity relative to the pristine PEDOT:PSS printing formulation (~50 $S \cdot cm^{-1}$). Specifically, varying the PU concentration from 3.5 wt% to 18 wt% resulted in conductivities spanning from approximately 20 $S \cdot cm^{-1}$ down to ~0.1 $S \cdot cm^{-1}$ (Table 4). The incorporation of glycerol, which is known to promote PEDOT chain alignment and enhance charge transport [150], significantly mitigated this conductivity loss, increasing the conductivity of composites with high PU content to approximately 15 $S \cdot cm^{-1}$.

A major advantage of the polyurethane developed in this work lies in its exceptional processing versatility. The incorporation of PEG soft segments effectively lowers the glass transition temperature of the polymer network and markedly improves solubility in polar, environmentally benign solvents such as ethanol and anisole (Supplementary Table 1). As a result, uniform conductive films can be fabricated using a range of solution-based techniques, including drop casting, spin coating, and printing. This level of processability represents a clear improvement over our previously reported polyurethane systems, as well as many other self-healing conductive materials reported in the literature (Supplementary Table 2), and directly facilitates scalable manufacturing and integration into soft electronic platforms.

Importantly, the solvent compatibility of the composite enables the formulation of printable, ethanol-based inks, allowing high-resolution patterning of stretchable and self-healing conducting features. When printed onto glass substrates, the patterned films can be readily released by simple water-assisted detachment and transferred onto alternative substrates or directly onto skin. This transferability provides a straightforward and low-cost route toward conformal wearable electronic devices, highlighting the practical relevance of the materials design.

6.4.3 Mechanical and Electromechanical Properties

The mechanical and electromechanical performance of the drop-cast conductive composites was systematically investigated to assess their stretchability, durability, and suitability for soft electronic applications, including electronic tattoos and freestanding electrodes. Key mechanical

parameters—elongation at break, Young's modulus, and adhesion strength—are summarized in Table 4 and reveal a clear dependence on PU and glycerol content, reflecting the tunability of mechanical compliance through formulation.

6.4.4 Tensile Properties

Uniaxial stress–strain measurements (Figure 22a and Figure S18) showed that increasing the PU fraction led to a pronounced reduction in Young's modulus accompanied by a significant increase in elongation at break (Table 4). Lower modulus values are desirable for minimizing mechanical mismatch with human skin (≈0.01–0.1 MPa), while high elongation at break enables the films to accommodate large deformations without mechanical failure [78, 141]. Compared to our previously reported system, the stress–strain curves displayed smooth, continuous profiles without a distinct yield point. This behavior is consistent with the presence of dynamic disulfide bonds, which facilitate chain rearrangement and energy dissipation through reversible bond exchange [156, 157].

The addition of glycerol further enhanced mechanical compliance, resulting in a substantial decrease in modulus and a marked increase in stretchability [135]. This improvement is attributed to the plasticizing effect of glycerol, which increases chain mobility and reinforces interfacial interactions between PEDOT:PSS and the PU matrix.[35] Among all tested formulations, PEDOT:PSS/PU-18/Gly-2.2 exhibited the most balanced mechanical performance, combining a high elongation at break of approximately 630% with a low Young's modulus of ~0.02 MPa. This stretchability is comparable to that of state-of-the-art stretchable conductive polymers and represents an approximately 1.5-fold improvement over our previously reported material (Supplementary Table 2).

6.4.5 Cyclic Durability

To evaluate long-term mechanical stability under conditions relevant to skin deformation, cyclic loading–unloading tests were conducted over 500 cycles at strains ranging from 0 to 50%. Representative hysteresis curves (Figure S19a,b) show large energy input and dissipation during the initial cycle, followed by progressively increased energy recovery with repeated cycling. The energy recovery stabilized after approximately 100 cycles (Figure S20), indicating gradual rearrangement of the dynamic polymer network into a mechanically stable configuration. Among

all compositions, PEDOT:PSS/PU-18/Gly-2.2 exhibited the highest energy recovery, reaching approximately 75%. The dissipated energy decreased from about 145 to 110 kJ·m^{-3} and remained stable over subsequent cycles. Importantly, the material retained its mechanical integrity after 500 cycles, demonstrating excellent fatigue resistance. This stabilization behavior is characteristic of networks containing dynamic covalent bonds and reflects progressive chain rearrangement and network reorganization under repeated mechanical stress.

6.4.6 Electromechanical Stability

Electromechanical performance was evaluated by monitoring the normalized resistance (R/R_0) under a constant bias voltage of 0.2 V during uniaxial stretching from 50% up to 400% strain (Figure S19c). PEDOT:PSS/PU-18/Gly-2.2 consistently exhibited the smallest resistance variation among all formulations (Figure 22b), confirming superior electromechanical stability. During cyclic deformation at 50% strain, resistance fluctuations remained within approximately 10% over 500 cycles (Figure 22c), substantially lower than those observed for other compositions (Figure S21). These results highlight the strong coupling between mechanical deformation and electrical transport, as well as the excellent fatigue resistance of the optimized composite.

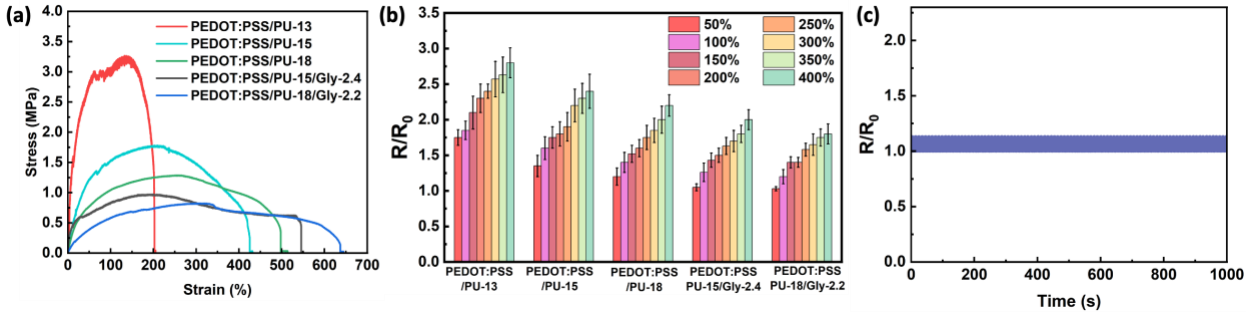

Figure 22. Electromechanical performance of PEDOT:PSS/PU-based films. (a) Tensile stress–strain curves. (b) Normalized resistance (R/R_0) under a constant bias of 0.2 V during uniaxial stretching at different strain levels (50–400%). Values (n = 3) are presented as mean ± standard deviation. (c) Normalized resistance (R/R_0) during 500 cyclic strains between 0% and 50%. The inset shows a magnified view highlighting resistance variation during cyclic loading.

6.4.7 Adhesion Performance

Adhesion measurements revealed strong self-adhesion, which is critical for maintaining conformal contact with skin (Figure S22). PEDOT:PSS/PU-18/Gly-2.2 exhibited the highest adhesion

strength, reaching 1.35 $N \cdot cm^{-1}$ on glass substrates (Figure S19d) and 2.85 $N \cdot cm^{-1}$ in self-adhesion tests (Table 4 and Figure S19e). The enhanced adhesion is attributed to the high PU content and the presence of glycerol, which likely promote reversible disulfide-mediated bond exchange at the interface. In contrast, adhesion to glass is governed primarily by weaker physical interactions, resulting in comparatively lower values. Taken together, these results identify PEDOT:PSS/PU-18/Gly-2.2 as a versatile and durable material platform that integrates high stretchability, mechanical robustness, electromechanical stability, strong self-adhesion, and relatively high electrical conductivity (13 ± 2 $S \cdot cm^{-1}$). These attributes are essential for next-generation electronic tattoos and wearable bioelectronic devices designed to operate reliably under continuous mechanical deformation. Complementary experiments further indicated that a minimum PU content of approximately 15 wt% is required to achieve autonomous room-temperature self-healing; therefore, subsequent analyses focused on formulations meeting or exceeding this threshold.

Table 4. Electrical conductivity, elongation at break, Young's modulus (0–10% strain range), and adhesion of PEDOT:PSS/PU-based drop-cast films with varying compositions. Values (n = 3) are presented as mean ± standard deviation.

Samples	PEDOT:PSS solution (wt%)	PU solution (wt%)	Glycerol (wt%)	Conductivity (S cm^{-1})	Elongation at break (%)	Young's modulus (MPa)	Adhesion	
							Glass	Itself
PEDOT:PSS/PU-3.5	96.5	3.5		22 ± 2				
PEDOT:PSS/PU-6	94.0	6.0		20 ± 2				
PEDOT:PSS/PU-10	90.0	10.0		2.4 ± 0.1				
PEDOT:PSS/PU-13	87.0	13.0		0.50 ± 0.02	202±10	0.14±0.04	0.16±0.05	0.48±0.16
PEDOT:PSS/PU-15	85.0	15.0		0.10 ± 0.03	432±12	0.13±0.02	0.31±0.10	1.02±0.37
PEDOT:PSS/PU-18	82.0	18.0		0.10 ± 0.01	500±15	0.09±0.03	0.59±0.12	1.71±0.42
PEDOT:PSS/PU-15/Gly-2.4	83.0	14.6	2.4	15 ± 2	545±12	0.040±0.01	0.97±0.14	2.25±0.50
PEDOT:PSS/PU-18/Gly-2.2	80.3	17.5	2.2	13 ± 2	630±19	0.020±0.002	1.35±0.33	2.85±0.71

6.4.8 Electrical and Mechanical Self-healing

The dynamic disulfide chemistry that underpins the strong adhesion and cyclic durability of the composites also plays a central role in their self-healing behavior. Reversible S–S bond exchange within the PU network enables rapid reorganization of the polymer chains after mechanical damage, allowing simultaneous recovery of mechanical integrity and electrical pathways. Building on the outstanding mechanical and electromechanical performance of PEDOT:PSS/PU-18/Gly-2.2, we investigated its ability to autonomously restore both electrical conductivity and mechanical properties after damage, a key requirement for long-term operation of wearable and stretchable electronic devices.

6.4.9 Electrical Self-healing

Electrical self-healing experiments were conducted at 25 °C, slightly above the glass transition temperature of the composite (T_g = 21 °C, Figure S23a). At this temperature, sufficient chain mobility is available to promote reformation of reversible hydrogen bonds and dynamic disulfide linkages. All drop-cast PEDOT:PSS/PU composites fully recovered their electrical conductivity after repeated cutting with a razor blade (Figure S24). Among the tested formulations, PEDOT:PSS/PU-18/Gly-2.2 exhibited particularly rapid recovery, restoring electrical conductivity within approximately 0.1 s and achieving a healing efficiency of 99.7 ± 0.3%. Notably, this high healing efficiency was preserved in transparent spin-coated films with thicknesses ranging from 1.4 to 2.5 μm (Figure 23a), a regime in which complete electrical reconnection is often challenging. This behavior is attributed to the highly uniform microstructure obtained by spin coating, in contrast to many previously reported self-healing conductors (Supplementary Table 2), which are typically demonstrated using thicker, drop-cast films where electrical reconnection is inherently less demanding. Across all investigated thicknesses, the films recovered their conductivity within approximately 0.3 s and maintained healing efficiencies close to 100% over multiple cut–heal cycles. The minimum film thickness required to achieve full electrical recovery was determined to be 1.4 μm. Spin-coated films deposited on glass and polyethylene terephthalate (PET) substrates also exhibited high optical transmittance (95.2 ± 0.7%, Figure S25a,b), underscoring their suitability for self-healing electrochromic and optoelectronic applications. In addition to optical transparency, spin coating provides precise control over film thickness and uniformity, which is critical for optimizing device performance.

6.4.10 Mechanical Self-healing

Mechanical self-healing was evaluated using cut–stick, scratch, and puncture damage modes. In cut–stick experiments, PEDOT:PSS/PU-18/Gly-2.2 exhibited near-complete recovery of elongation at break (98 ± 0.2%) after healing at room temperature (Figure S26), consistent with its strong intrinsic self-adhesion. Scratch-healing experiments further demonstrated excellent mechanical recovery. Surface scratches were completely eliminated within 1 h at 25 °C, as confirmed by optical microscopy and three-dimensional profilometry (Figure 23b–d and Figure S26–27), corresponding to a healing efficiency of 99.7 ± 0.1%. Achieving full scratch healing under ambient conditions represents a significant advance compared to most reported self-healing conductors, which typically require elevated temperatures or external stimuli. Beyond scratches and cuts, the composites displayed a rare and highly desirable ability to recover from puncture damage. Puncture-induced defects, which introduce localized through-thickness damage, represent one of the most severe and realistic failure modes in soft electronics and have been scarcely explored in solid-state conductive polymers. Holes were introduced using a stainless-steel needle, and the healing process was monitored by optical microscopy (Figure S29a). Free-standing PEDOT:PSS/PU-18/Gly-2.2 membranes exhibited near-complete closure of the punctured region within 1 h at room temperature, with only minimal residual traces (Figure S29b). These traces primarily arise from slight differences in optical reflectivity rather than incomplete structural recovery (Figure 23e). Because electrical current in continuous thin films can readily bypass localized through-thickness defects, local conductivity measurements are not directly correlated with puncture closure. Similarly, global tensile measurements before and after puncture are not representative, as the small puncture size has a negligible influence on the overall stress–strain response. Consequently, puncture healing is assessed qualitatively based on the autonomous closure of the damaged region and restoration of surface continuity. In contrast to previously reported puncture-healing systems based on liquid metal composites [11, 158], the present results demonstrate that a fully solid-state conducting polymer can autonomously recover from severe mechanical damage. This solid-state puncture-healing capability is particularly relevant for ensuring the long-term durability and reliability of soft electronic systems, including electronic tattoos and wearable health-monitoring devices, which are routinely exposed to accidental impact, puncture, and mechanical deformation during daily use. Collectively, these findings highlight the versatility of the PEDOT:PSS/PU-18/Gly-2.2 composite, which rapidly restores both electrical

conductivity and mechanical integrity at room temperature after damage. Notably, the ability of a fully solid-state conducting polymer to autonomously recover from puncture damage—a severe and rarely addressed failure mode—underscores its strong potential for reliable, long-term operation in soft and stretchable electronic devices.

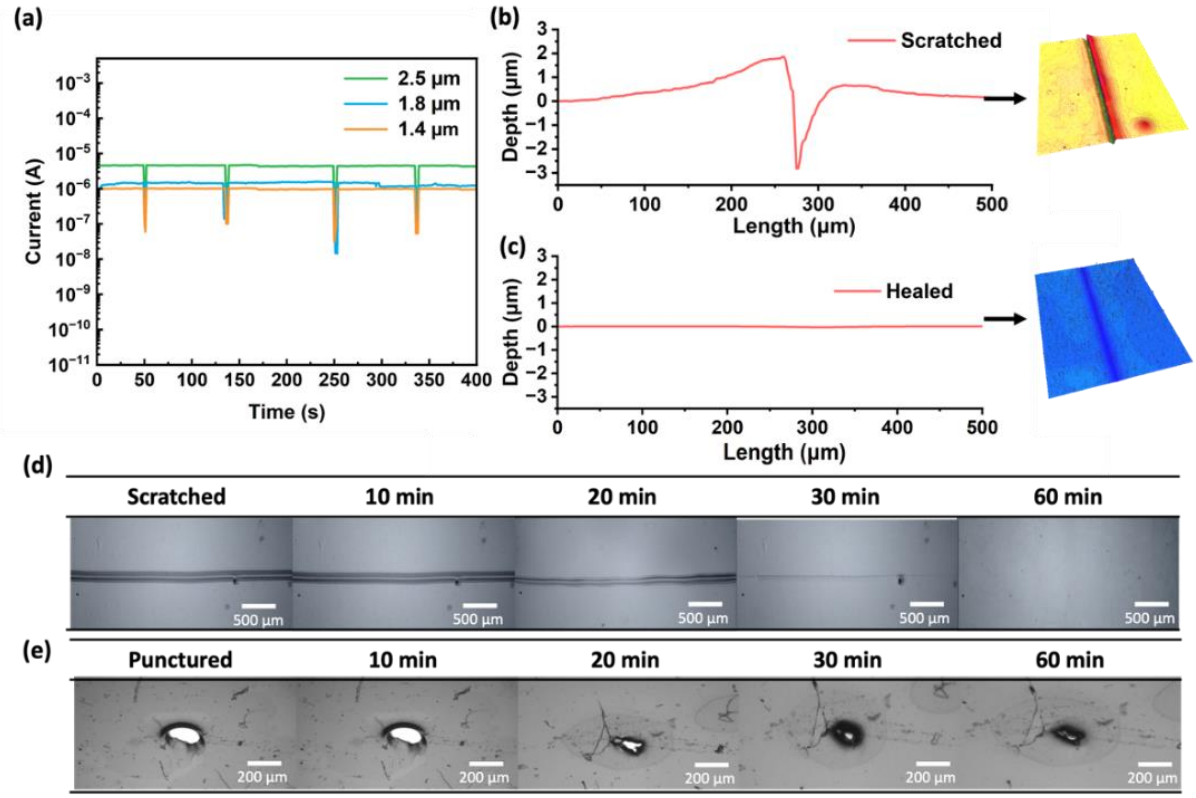

Figure 23. Electrical and mechanical self-healing behavior of PEDOT:PSS/PU-18/Gly-2.2 films. (a) Current–time responses of spin-coated films with different thicknesses (2.5, 1.8, and 1.4 μm) during repeated cut–healing cycles under a constant 0.2 V bias. (b,c) Depth profiles and three-dimensional optical profilometry maps of the films after surface scratching (3 N pencil) and after healing at 25 °C, respectively. The color scale indicates surface height variation. (d) Optical microscopy images of the film surface before and after healing of pencil-induced scratches. (e) Optical images showing puncture damage and subsequent recovery of a free-standing membrane after healing at room temperature. All experiments were performed in triplicate (n = 3).

6.4.11 Proposed Mechanism For Self-healing

To elucidate the molecular origin of the self-healing behavior, solid-state FTIR spectroscopy was employed to investigate the reversible interactions responsible for damage repair in the PEDOT:PSS/PU system. The analysis focused on vibrational modes associated with S–S, C=O, and N–H groups, which correspond to dynamic disulfide bonds and hydrogen-bonding motifs intentionally incorporated into the polyurethane backbone to enable autonomous network reorganization. Spectra were collected from pristine, scratched, and subsequently healed samples, allowing direct tracking of chemical changes within the damaged region rather than relying solely on comparisons between pristine and healed states. Across all examined samples, no discernible peak shifts were detected for the S–S, C=O, or N–H vibrational bands, indicating that the overall chemical structure of the constituent polymers remained unchanged during both damage and recovery. This result confirms that the self-healing process does not involve irreversible chemical reactions or bond scission, but instead proceeds through reversible interactions within the polymer network. Notably, the characteristic S–S stretching band centered at approximately 600 cm^{-1} exhibited a clear decrease in intensity following scratching, reflecting disruption of disulfide linkages within the PU matrix (Figure 24a). Upon healing at room temperature, the intensity of this band recovered nearly to its original level, consistent with reformation of disulfide bonds through reversible exchange. A similar trend was observed for hydrogen-bond-related vibrations. The C=O stretching band at approximately 1720 cm^{-1} (Figure 24b) and the N–H stretching band near 3350 cm^{-1} (Figure 24c) both weakened after mechanical damage and subsequently regained intensity following healing. These reversible intensity changes indicate temporary disruption and restoration of hydrogen-bonding interactions during the damage–healing cycle. The evolution of these spectral features is quantitatively summarized in Figure 24d using normalized peak intensities referenced to the pristine state, clearly illustrating the reversible nature of both disulfide and hydrogen-bond interactions. Collectively, these observations support a self-healing mechanism governed by dynamic disulfide exchange coupled with reversible hydrogen bonding (Figure 24e). This combination enables enhanced chain mobility and efficient network reorganization at damaged sites without permanent chemical modification of the material. Importantly, comparable FTIR behavior was observed for other PEDOT:PSS/PU formulations (Figure S30), indicating that this healing mechanism is intrinsic to the material platform rather than specific to a single composition. Overall, the solid-state FTIR analysis provides direct

molecular-level evidence for autonomous room-temperature self-healing in PEDOT:PSS/PU composites. The synergistic interplay between dynamic covalent disulfide bonds and reversible hydrogen-bonding interactions offers an efficient pathway for network repair, providing mechanistic insight that can guide the rational design of next-generation solid-state self-healing conductive polymers.

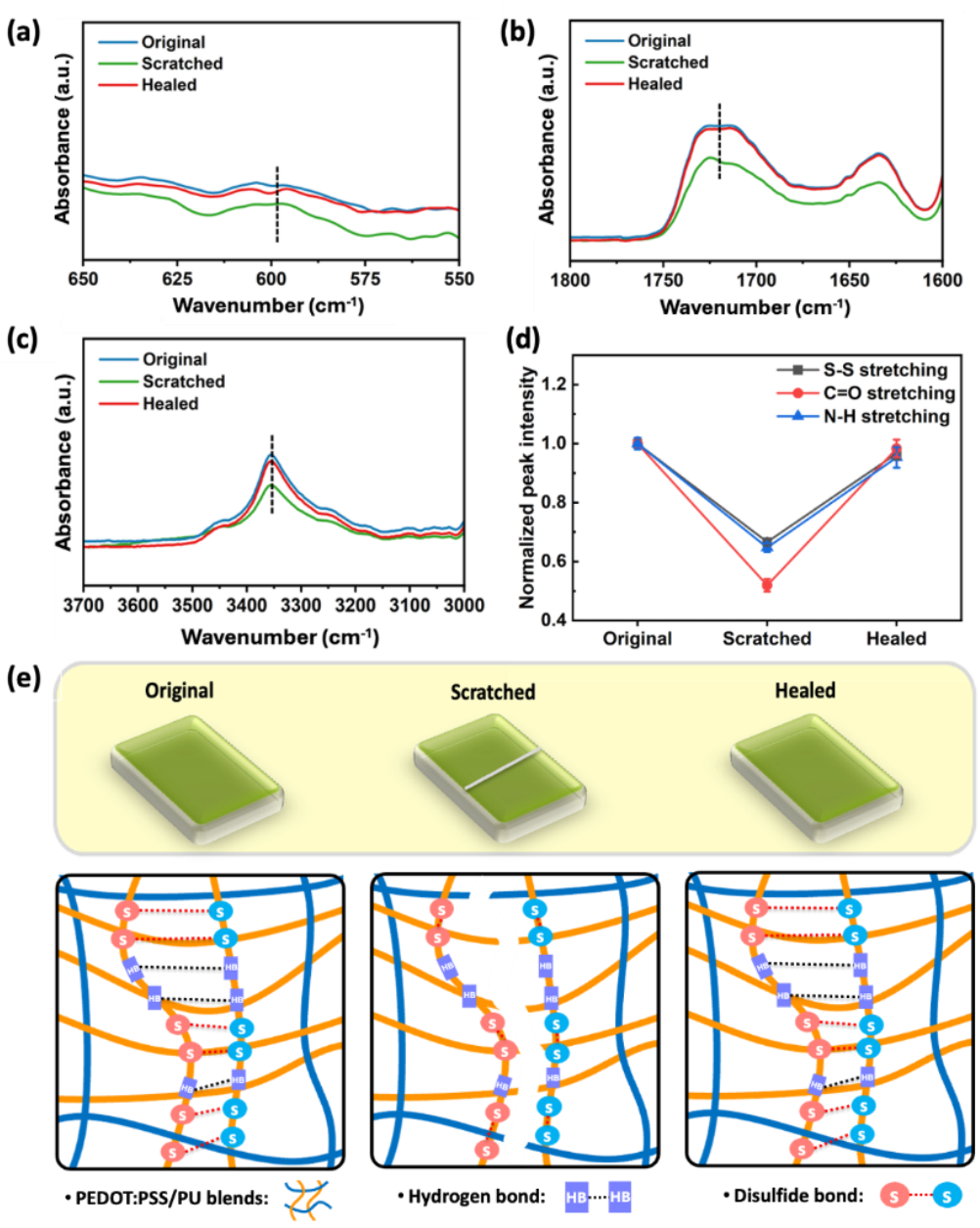

Figure 24. FTIR analysis and proposed self-healing mechanism of PEDOT:PSS/PU-18/Gly-2.2. (a–c) FTIR spectra obtained in the pristine, scratched, and healed states, highlighting regions corresponding to (a) S–S stretching, (b) C=O stretching, and (c) N–H stretching vibrations. (d) Normalized peak intensities referenced to the pristine state (n = 3). (e) Schematic illustration of reversible disulfide exchange and hydrogen-bonding interactions within the network under pristine, damaged, and healed conditions.

6.4.12 Demonstration of Reliable ECG Monitoring with Printed PEDOT:PSS/PU-based E-Tattoo Electrodes

Taking advantage of their high stretchability, strong self-adhesion, rapid self-healing capability, electromechanical stability, and printability, PEDOT:PSS/PU-18/Gly-2.2 films were implemented as skin-conformal electrodes (Figure 25a). Two device formats were explored: disposable tattoo electrodes and reusable freestanding electrodes. Tattoo electrodes are designed for single-use attachment via tattoo paper, whereas printed freestanding films can be released from the substrate, transferred onto skin, and subsequently removed using water for repeated reuse or recycling, as illustrated in Figure S31. This dual-format strategy highlights the versatility of the materials platform for wearable bioelectronic applications. PEDOT-based tattoo electrodes have been extensively studied for skin-conformal electrophysiological monitoring owing to their low skin–electrode impedance and enhanced wearer comfort compared with conventional Ag/AgCl gel electrodes [137, 159]. Printed PEDOT:PSS tattoo electrodes have previously been demonstrated for electrocardiogram (ECG) acquisition, and stretchable, self-adhesive PEDOT:PSS/polyurethane systems have been reported for biopotential monitoring. Together with related PEDOT:PSS-based approaches, these studies have established a strong foundation for soft, skin-compatible bioelectronic interfaces. Building on this prior work, the electrodes presented here introduce intrinsic self-healing, robust adhesion, and combined reuse–recycling capability without compromising electrical performance, representing an important advance toward more durable and sustainable electronic tattoos for continuous health monitoring.[43,44] Both electrode configurations enabled high-quality ECG recordings with stable and well-defined waveform features comparable to those obtained using commercial Ag/AgCl gel electrodes (Figure 25b). In addition, the PEDOT:PSS/PU-18/Gly-2.2 electrodes exhibited lower skin–electrode impedance over the measured frequency range (Figure 25c). In practical use, the electrodes conform closely to the skin surface and maintain reliable contact under compression, stretching, and twisting (Figure 25d and Figure S32). The films also showed excellent water stability, exhibiting negligible swelling after 24 h of immersion and only a minor reduction in elongation at break (Figure S33). Importantly, freestanding electrodes preserved clear and stable ECG signals after multiple attachment–removal cycles (Figure S34), underscoring their mechanical robustness and functional reliability. Together, these results demonstrate that PEDOT:PSS/PU-18/Gly-2.2 electrodes provide a durable, reusable, and skin-compatible interface suitable for long-term wearable bioelectronic applications.

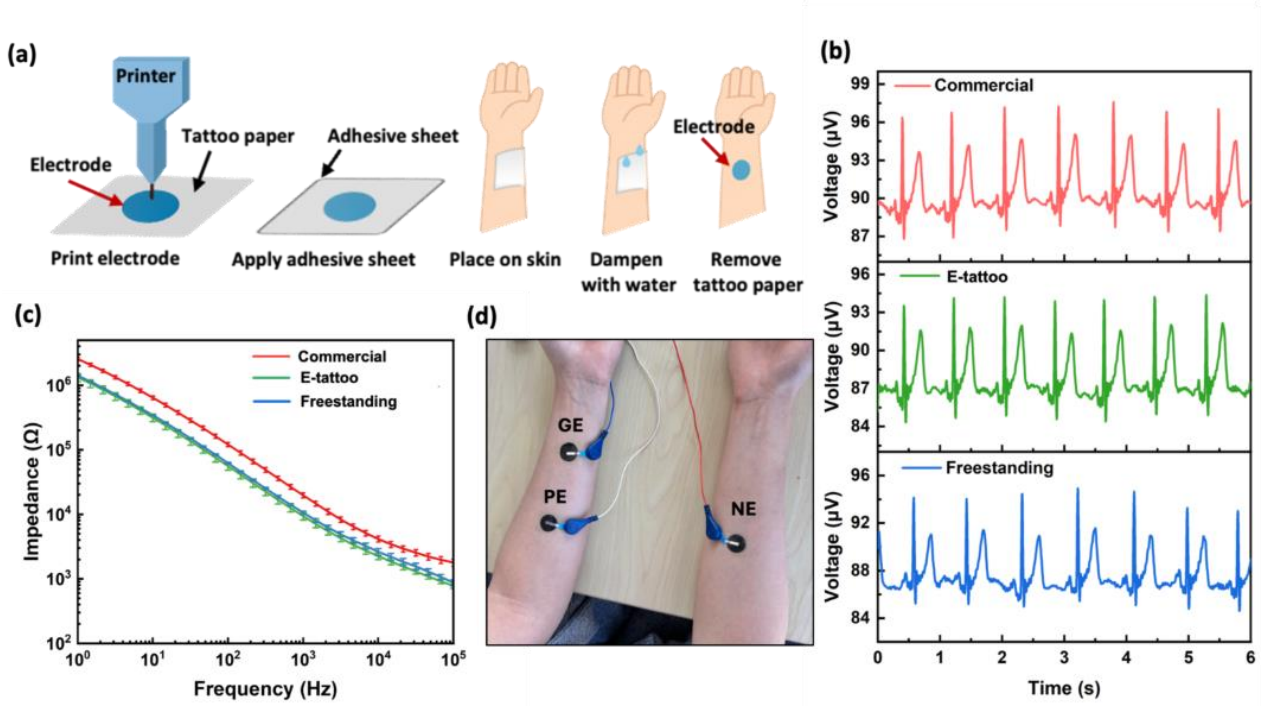

Figure 25. Printed bioelectronic electrodes and ECG performance. (a) Schematic illustration of the fabrication process for electrodes printed on tattoo paper. (b) Representative electrocardiogram (ECG) recordings obtained using commercial Natus® Ag/AgCl gel electrodes, electronic tattoos (e-tattoos), and freestanding electrodes (n = 3 for each type). (c) Comparison of skin–electrode impedance for commercial electrodes, e-tattoos, and freestanding electrodes (n = 3). (d) Photograph of the ECG measurement setup, showing placement of the positive (PE) and ground (GE) electrodes on the left forearm and the negative (NE) electrode on the right forearm.

6.4.13 Chemical and Mechanical Recycling

Growing concerns regarding electronic waste underscore the importance of recycling strategies that preserve both the functionality and value of soft electronic materials. To evaluate the circular potential of the PEDOT:PSS/PU composite, we investigated chemical recycling and mechanical reuse as complementary pathways enabling either component-level recovery or low-energy reprocessing. In contrast to many reported self-healing conductors that rely on permanently crosslinked networks or sacrificial additives, the present system uniquely supports both chemical recycling and mechanical remolding while maintaining functional performance.

6.4.14 Chemical Recycling

Chemical recycling was achieved using ethanol (EtOH) as a green solvent compatible with both PEDOT:PSS and PU (Figure 26a). This approach enabled reprocessing of the composite without inducing polymer degradation and allowed repeated recycling cycles with minimal loss of mechanical and electrical properties. After immersion in ethanol for 10 min, centrifugation separated a PU-rich supernatant from the PEDOT:PSS phase. The recovered PU fraction was readily redissolved, blended with fresh PEDOT:PSS and glycerol, and re-cast into new composite films. Although the isolated PEDOT:PSS could not be fully redispersed, it nevertheless formed conductive films upon drying (red arrow, Figure 26a). This process was reproducible over multiple cycles, demonstrating an effective closed-loop recycling route for the composite.

6.4.15 Mechanical Recycling

Mechanical reuse was assessed by cutting the composite films into small fragments and remolding them under light pressure at 55 °C (Figure 26b). Under these mild conditions, the fragments rapidly fused into continuous films, confirming that dynamic disulfide bonds and reversible hydrogen bonding enable efficient reprocessability. After 15 mechanical reuse cycles, the films retained 95 ± 4% of their original elongation at break (Figure 24c and Figure S35a–c) and 98 ± 1% of their initial electrical conductivity (Figure 26d and Figure S35d–f), indicating negligible degradation in performance. Importantly, thermal degradation of the composite occurs only above approximately 280 °C (Figure S25b); therefore, the low processing temperature of 55 °C avoids polymer degradation and represents a significant reduction in energy input compared to the ~100 °C required in our previously reported system. This reduction further enhances the sustainability of the reprocessing strategy.

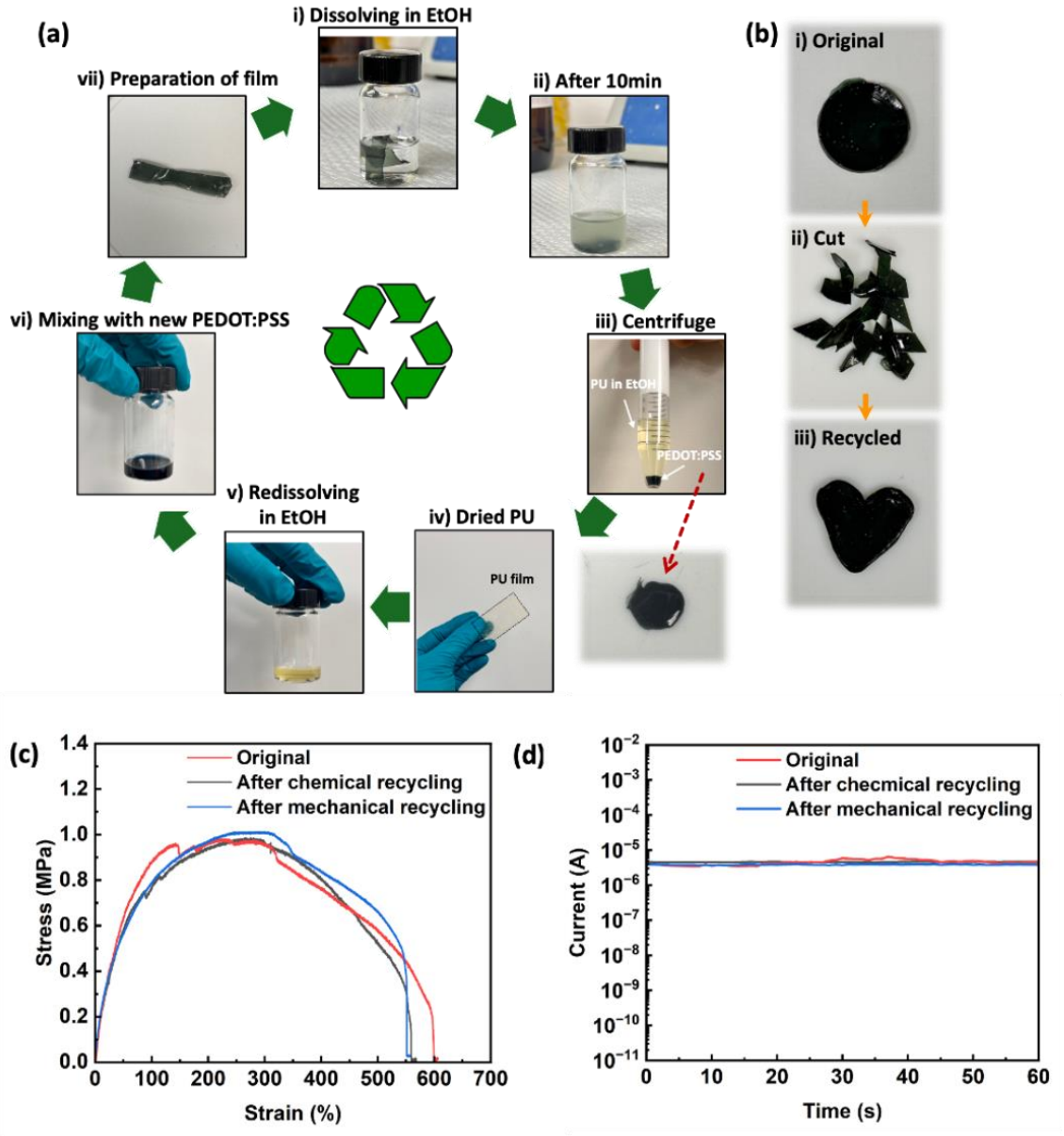

Figure 26. Chemical and mechanical recycling of PEDOT:PSS/PU-18/Gly-2.2 composites. (a) Schematic illustration of the chemical recycling process (i–vii). (b) Mechanical reuse process involving fragmentation followed by thermally assisted remolding to form continuous films (i–iii). (c) Tensile stress–strain curves and (d) current–time responses of the original and recycled films, demonstrating recovery of mechanical and electrical performance after repeated recycling cycles (n = 3). Electrical and mechanical measurements were conducted over 15 recycling cycles to evaluate performance stability and reproducibility.

6.4.16 Comparison with Reported Systems

Comparison with previously reported self-healing conductors (Table S2, Supporting Information) highlights that the present composite integrates a combination of properties that is rarely achieved simultaneously within a single conducting polymer platform. Specifically, the material exhibits autonomous room-temperature electrical self-healing with rapid recovery after cutting (≈0.1–0.3 s), effective healing of puncture damage on the hour timescale, high stretchability (~630%), and near-unity healing efficiency across multiple damage modes, including cuts, scratches, and punctures. Notably, autonomous electrical self-healing is demonstrated in continuous films as thin as 1.4 μm, whereas many prior reports focus on substantially thicker, drop-cast films in which electrical reconnection is inherently less challenging. In addition, while recyclability is often limited or entirely absent in many self-healing conductive systems, the PEDOT:PSS/PU composite presented here supports both mechanical reuse and chemical recycling over multiple cycles with minimal loss of electrical and mechanical performance. Collectively, these attributes position this material among the highest-performing self-healing conducting polymer systems currently reported, as many existing approaches emphasize only selected aspects such as stretchability, conductivity, or single-mode healing [160-164].

6.5 Conclusions

In this study, we developed a multifunctional PEDOT:PSS/PU composite that unifies autonomous room-temperature self-healing, recyclability, printability, and mechanical compliance within a single materials platform. The rationally engineered polyurethane matrix, incorporating dynamic disulfide linkages and hydrogen-bonding motifs, enables spontaneous recovery from scratches, cuts, and puncture damage without the need for external stimuli, while maintaining high electrical conductivity, strong interfacial adhesion, and exceptional stretchability. In addition, the use of environmentally benign solvents allows the fabrication of uniform, transparent, and transferable films through spin coating or printing, supporting seamless integration into soft and stretchable electronic systems. Solid-state FTIR spectroscopy provides direct molecular-level evidence that the self-healing behavior is governed by reversible intermolecular interactions—specifically disulfide bond exchange and hydrogen-bond reformation—rather than irreversible chemical transformations. These dynamic interactions facilitate efficient network reorganization, enabling restoration of both mechanical integrity and electrical continuity after damage. Beyond self-

healing, the composite demonstrates robust sustainability through its ability to undergo repeated mechanical reuse and chemical recycling with minimal degradation in electrical or mechanical performance. This dual reprocessing capability highlights the potential of the material as a circular electronic platform. As a proof of concept, printed electronic-tattoo electrodes fabricated from the composite deliver stable, low-impedance electrocardiogram (ECG) signals and allow straightforward detachment and reuse, confirming their suitability for wearable bioelectronic interfaces. Collectively, these results demonstrate that self-healing conductors can progress beyond superficial damage recovery to tolerate severe mechanical deformation while preserving functionality. By integrating printability, autonomous room-temperature self-healing, and recyclability within a single PEDOT:PSS-based composite, this work offers a practical and scalable materials strategy for enhancing the durability, sustainability, and manufacturability of next-generation soft electronic and bioelectronic devices.

6.6 Acknowledgments

The authors thank G. Petrossian, S. Khoomortezaei, and C. Kim for insightful discussions. This research was supported by the Natural Sciences and Engineering Research Council of Canada (NSERC) through a Discovery Grant awarded to FC. JK gratefully acknowledges financial support from the Fonds de recherche du Québec – Nature et technologies (FRQNT) and the Trottier Energy Institute through doctoral scholarships. The equipment and research infrastructure used in this work were funded and maintained by the Canada Foundation for Innovation. All experiments involving human participants were conducted in accordance with the protocol approved by the Ethics Committee of Polytechnique Montréal (certificate CER-2021-04-D). The authors also acknowledge CMC Microsystems, manager of the FABrIC project funded by the Government of Canada, for providing products and services that supported this research.

CHAPTER 7 CONCLUSION AND RECOMMENDATIONS

7.1 Conclusion

This thesis set out to address fundamental limitations in PEDOT:PSS-based conducting polymers that hinder their long-term use in soft and wearable electronic applications. In particular, challenges related to mechanical fragility, limited self-healing capability, and lack of sustainability have restricted the practical deployment of these materials under realistic operating conditions. Through systematic material design and experimental validation, this work demonstrates that these challenges can be addressed in an integrated manner by combining rational polymer engineering with dynamic bonding strategies.

Across Chapters 4 and 5, two generations of PEDOT:PSS/polyurethane composites were developed to progressively enhance mechanical durability, self-healing behavior, and recyclability. Chapter 4 established a foundational strategy in which hydrogen-bonding interactions and polymer plasticization significantly improved stretchability, toughness, and mechanical self-healing while maintaining electrical functionality. Importantly, this chapter highlighted that electrical recovery alone is insufficient for reliable soft electronics, and that restoration of mechanical integrity is equally critical for preventing cumulative damage during repeated deformation.

Building on this foundation, Chapter 5 advanced the material design to achieve autonomous self-healing at room temperature through the incorporation of dynamic disulfide bonds in conjunction with hydrogen bonding. This next-generation system demonstrated rapid electrical and mechanical recovery without external stimuli and, notably, exhibited the rare ability to self-heal after puncture damage in a fully solid-state conducting polymer. The demonstration of electrical self-healing in continuous films as thin as ~1.4 μm, together with printability, strong self-adhesion, and stable electromechanical performance, underscores the relevance of this platform for practical wearable and bioelectronic devices.

Beyond healing performance, this thesis emphasizes sustainability as a core design criterion. The materials developed herein support both mechanical reuse and chemical recycling over multiple cycles with minimal degradation of electrical or mechanical properties. These results demonstrate that dynamic molecular interactions can simultaneously enable self-healing, durability, and

circular reprocessing, challenging the conventional view that performance and sustainability are inherently conflicting objectives in electronic materials.

Chapter 6 contextualized these experimental findings within the broader landscape of soft electronics, identifying persistent trade-offs that have limited prior PEDOT:PSS-based systems. By linking material behavior to molecular design principles—such as low glass-transition polymer networks and reversible covalent and supramolecular interactions—this thesis provides a coherent framework for understanding how autonomous healing, mechanical robustness, and processability can be jointly achieved.

Overall, this work demonstrates that PEDOT:PSS-based conductors can evolve from humidity-dependent, damage-sensitive materials into robust, multifunctional, and sustainable platforms suitable for soft and wearable electronics. The insights gained here contribute not only to the fundamental understanding of self-healing conductive polymers but also to the practical design of next-generation bioelectronic, wearable, and soft robotic systems.

7.2 Recommendations

While this thesis establishes a robust platform for self-healing and recyclable PEDOT:PSS-based conductors, several practical research directions can be pursued to further strengthen the reliability and applicability of these materials.

First, future work should focus on evaluating the long-term stability of the self-healing behavior under realistic operating conditions. Although autonomous healing was demonstrated at room temperature, systematic studies under repeated mechanical fatigue (e.g., thousands of stretching cycles) and prolonged environmental exposure, such as moderate humidity and body-temperature conditions, would provide critical insight into performance retention over device lifetimes. Second, the quantification of severe-damage healing, particularly puncture recovery, represents an important next step. While puncture healing was qualitatively demonstrated in this work, practical methods such as localized resistance mapping, optical image analysis, or thickness profiling could be developed to quantitatively assess the extent and reproducibility of puncture closure. These measurements would help establish standardized evaluation protocols for severe damage tolerance in solid-state self-healing conductors. Third, further processing and formulation could improve device reproducibility. Investigating the influence of film thickness, printing parameters, and solvent composition on healing efficiency and electrical stability would be valuable for

transitioning from laboratory-scale fabrication to more consistent device manufacturing. In particular, improving uniformity in large-area printed films would enhance compatibility with wearable electronics. In terms of device integration, future studies could extend the current proof-of-concept demonstrations by incorporating these materials into simple multilayer structures, such as encapsulated electrodes or sensor stacks. This would allow assessment of interfacial stability, adhesion between layers, and healing behavior in more realistic device architectures. Finally, continued efforts toward sustainable processing and safer polymer chemistries are recommended. In addition to optimizing solvent recovery, minimizing processing temperatures, and evaluating material reuse over extended recycling cycles, future studies may explore the development of non-isocyanate polyurethane (NIPU) systems as alternative matrices. Since conventional PU synthesis relies on isocyanate chemistry, which poses environmental and health concerns, the adoption of NIPU approaches could further enhance the sustainability profile of self-healing conductive composites while maintaining dynamic bonding functionality. Overall, these recommendations aim to translate the material concepts demonstrated in this thesis into more reliable, reproducible, and application-ready systems, bridging the gap between fundamental materials development and practical soft electronic devices.

REFERENCES

[1] S. Zhang and F. Cicoira, "Water-Enabled Healing of Conducting Polymer Films," *Advanced Materials,* vol. 29, no. 40, p. 1703098, 2017.

[2] X. Zhou *et al.*, "Self-healing, stretchable, and highly adhesive hydrogels for epidermal patch electrodes," (in English), *Acta Biomater,* vol. 139, pp. 296-306, Feb 2022, doi: 10.1016/j.actbio.2021.07.069.

[3] Y. Li *et al.*, "Autonomic Self-Healing of PEDOT:PSS Achieved Via Polyethylene Glycol Addition," (in English), *Advanced Functional Materials,* vol. 30, no. 30, Jul 2020, doi: ARTN 2002853 10.1002/adfm.202002853.

[4] J. Kim *et al.*, "Self-healing, stretchable and recyclable polyurethane-PEDOT:PSS conductive blends," (in English), *Mater Horiz,* vol. 11, no. 15, Jul 29 2024, doi: 10.1039/d4mh00203b.

[5] R. P. Wool, "Self-healing materials: a review," (in English), *Soft Matter,* vol. 4, no. 3, pp. 400-418, 2008, doi: 10.1039/b711716g.

[6] W. H. Li *et al.*, "Biomimetic Hybrid Networks with Excellent Toughness and Self-Healing Ability in the Glassy State," (in English), *Chem Mater,* vol. 35, no. 2, pp. 682-691, Jan 5 2023, doi: 10.1021/acs.chemmater.2c03266.

[7] K. S. Toohey, N. R. Sottos, J. A. Lewis, J. S. Moore, and S. R. White, "Self-healing materials with microvascular networks," (in English), *Nat Mater,* vol. 6, no. 8, pp. 581-585, Aug 2007, doi: 10.1038/nmat1934.

[8] P. Cordier, F. Tournilhac, C. Soulié-Ziakovic, and L. Leibler, "Self-healing and thermoreversible rubber from supramolecular assembly," (in English), *Nature,* vol. 451, no. 7181, pp. 977-980, Feb 21 2008, doi: 10.1038/nature06669.

[9] M. Burnworth *et al.*, "Optically healable supramolecular polymers," (in English), *Nature,* vol. 472, no. 7343, pp. 334-U230, Apr 21 2011, doi: 10.1038/nature09963.

[10] J. Kang, J. B.-H. Tok, and Z. Bao, "Self-healing soft electronics," *Nature Electronics,* vol. 2, no. 4, pp. 144-150, 2019.

[11] E. J. Markvicka, M. D. Bartlett, X. N. Huang, and C. Majidi, "An autonomously electrically self-healing liquid metal-elastomer composite for robust soft-matter robotics and electronics," (in English), *Nat Mater,* vol. 17, no. 7, pp. 618-+, Jul 2018, doi: 10.1038/s41563-018-0084-7.

[12] T. Someya, T. Sekitani, S. Iba, Y. Kato, H. Kawaguchi, and T. Sakurai, "A large-area, flexible pressure sensor matrix with organic field-effect transistors for artificial skin applications," (in English), *P Natl Acad Sci USA,* vol. 101, no. 27, pp. 9966-9970, Jul 6 2004, doi: 10.1073/pnas.0401918101.

[13] S. R. Forrest, "The path to ubiquitous and low-cost organic electronic appliances on plastic," (in English), *Nature,* vol. 428, no. 6986, pp. 911-918, Apr 29 2004, doi: 10.1038/nature02498.

[14] Y. Peng, S. Y. Gu, Q. Wu, Z. T. Xie, and J. R. Wu, "High-Performance Self-Healing Polymers," (in English), *Accounts Mater Res,* vol. 4, no. 4, pp. 323-333, Apr 28 2023, doi: 10.1021/accountsmr.2c00174.

[15] M. Irimia-Vladu, ""Green" electronics: biodegradable and biocompatible materials and devices for sustainable future (vol 43, pg 588, 2014)," (in English), *Chem Soc Rev,* vol. 43, no. 17, pp. 6470-6470, 2014. [Online]. Available: <Go to ISI>://WOS:000340705900013.

[16] K. Ragaert, L. Delva, and K. Van Geem, "Mechanical and chemical recycling of solid plastic waste," (in English), *Waste Manage,* vol. 69, pp. 24-58, Nov 2017, doi: 10.1016/j.wasman.2017.07.044.

[17] M. D. Hager, P. Greil, C. Leyens, S. van der Zwaag, and U. S. Schubert, "Self-Healing Materials," (in English), *Advanced Materials,* vol. 22, no. 47, pp. 5424-5430, Dec 14 2010, doi: 10.1002/adma.201003036.

[18] R. Kappera *et al.*, "Phase-engineered low-resistance contacts for ultrathin MoS transistors (vol 13, pg 1128, 2014)," (in English), *Nat Mater,* vol. 13, no. 12, Dec 2014. [Online]. Available: <Go to ISI>://WOS:000345432200016.

[19] Y. Yang, H. Deng, and Q. Fu, "Recent progress on PEDOT:PSS based polymer blends and composites for flexible electronics and thermoelectric devices," (in English), *Materials Chemistry Frontiers,* vol. 4, no. 11, pp. 3130-3152, Nov 1 2020, doi: 10.1039/d0qm00308e.

[20] T. Someya, Z. N. Bao, and G. G. Malliaras, "The rise of plastic bioelectronics," (in English), *Nature,* vol. 540, no. 7633, pp. 379-385, Dec 15 2016, doi: 10.1038/nature21004.

[21] Y. Li, X. Zhou, B. Sarkar, N. Gagnon-Lafrenais, and F. Cicoira, "Recent Progress on Self-Healable Conducting Polymers," (in English), *Advanced Materials,* vol. 34, no. 24, Jun 2022, doi: ARTN 2108932 10.1002/adma.202108932.

[22] A. M. Nardes *et al.*, "Microscopic understanding of the anisotropic conductivity of PEDOT:PSS thin films," (in English), *Advanced Materials,* vol. 19, no. 9, pp. 1196-+, May 7 2007, doi: 10.1002/adma.200602575.

[23] R. Kroon *et al.*, "Thermoelectric plastics: from design to synthesis, processing and structure-property relationships," (in English), *Chem Soc Rev,* vol. 45, no. 22, pp. 6147-6164, Nov 21 2016, doi: 10.1039/c6cs00149a.

[24] J. Ouyang, Q. F. Xu, C. W. Chu, Y. Yang, G. Li, and J. Shinar, "On the mechanism of conductivity enhancement in poly (3,4-ethylenedioxythiophene): poly(styrene sulfonate) film through solvent treatment," (in English), *Polymer,* vol. 45, no. 25, pp. 8443-8450, Nov 25 2004, doi: 10.1016/j.polymer.2004.10.001.

[25] X. Crispin *et al.*, "The origin of the high conductivity of poly(3,4-ethylenedioxythiophene)-poly(styrenesulfonate) (PEDOT- PSS) plastic electrodes," (in English), *Chem Mater,* vol. 18, no. 18, pp. 4354-4360, Sep 5 2006, doi: 10.1021/cm061032+.

[26] M. Kaltenbrunner *et al.*, "Ultrathin and lightweight organic solar cells with high flexibility," (in English), *Nat Commun,* vol. 3, Apr 2012, doi: ARTN 770 10.1038/ncomms1772.

[27] M. W. Urban, D. Davydovich, Y. Yang, T. Demir, Y. Z. Zhang, and L. Casabianca, "Key-and-lock commodity self-healing copolymers," (in English), *Science,* vol. 362, no. 6411, pp. 220-+, Oct 12 2018, doi: 10.1126/science.aat2975.

[28] T. P. Huynh, P. Sonar, and H. Haick, "Advanced Materials for Use in Soft Self-Healing Devices," (in English), *Advanced Materials,* vol. 29, no. 19, May 17 2017, doi: ARTN 1604973 10.1002/adma.201604973.

[29] J. T. Wang, J. Tang, D. D. Chen, S. L. Xing, X. Y. Liu, and J. Y. Hao, "Intrinsic and extrinsic self-healing fiber-reinforced polymer composites: A review," (in English), *Polym Composite,* vol. 44, no. 10, pp. 6304-6323, Oct 2023, doi: 10.1002/pc.27623.

[30] W. T. Ma *et al.*, "Exploration and Application of Self-Healing Strategies in Lithium Batteries," (in English), *Advanced Functional Materials,* vol. 33, no. 15, Apr 2023, doi: 10.1002/adfm.202212821.

[31] H. Xu, Z. J. Fan, H. Z. Li, X. D. Zhang, C. Q. Deng, and X. D. Guo, "Intrinsic Self-Healing Polymers: Research Progress, Application Direction, and Prospects," (in English), *Polym-Plast Tech Mat,* vol. 64, no. 17, pp. 2637-2669, Nov 22 2025, doi: 10.1080/25740881.2025.2562430.

[32] D. H. Turkenburg and H. R. Fischer, "Diels-Alder based, thermo-reversible cross-linked epoxies for use in self-healing composites," (in English), *Polymer,* vol. 79, pp. 187-194, Nov 19 2015, doi: 10.1016/j.polymer.2015.10.031.

[33] J. Dahlke, S. Zechel, M. D. Hager, and U. S. Schubert, "How to Design a Self-Healing Polymer: General Concepts of Dynamic Covalent Bonds and Their Application for Intrinsic Healable Materials," (in English), *Adv Mater Interfaces,* vol. 5, no. 17, Sep 7 2018, doi: ARTN 1800051 10.1002/admi.201800051.

[34] W. T. Hao *et al.*, "Multi-Stimulus Responsive Nonconventional Fluorescent Supramolecular Polymeric Material," (in English), *Macromol Chem Phys,* vol. 226, no. 8, Apr 2025, doi: 10.1002/macp.202400484.

[35] Y. Yang and M. W. Urban, "Self-Healing of Polymers via Supramolecular Chemistry," (in English), *Adv Mater Interfaces,* vol. 5, no. 17, Sep 7 2018, doi: ARTN 1800384 10.1002/admi.201800384.

[36] W. R. Zhang *et al.*, "Recent achievements in self-healing materials based on ionic liquids: a review," (in English), *J Mater Sci,* vol. 55, no. 28, pp. 13543-13558, Oct 2020, doi: 10.1007/s10853-020-04981-0.

[37] J. H. Jin, L. L. Cai, Y. G. Jia, S. Liu, Y. H. Chen, and L. Ren, "Progress in self-healing hydrogels assembled by host-guest interactions: preparation and biomedical applications," (in English), *J Mater Chem B,* vol. 7, no. 10, pp. 1637-1651, Mar 14 2019, doi: 10.1039/c8tb02547a.

[38] S. Utrera-Barrios, R. Verdejo, M. A. López-Manchado, and M. H. Santana, "Evolution of self-healing elastomers, from extrinsic to combined intrinsic mechanisms: a review," (in English), *Mater Horiz,* vol. 7, no. 11, pp. 2882-2902, Nov 1 2020, doi: 10.1039/d0mh00535e.

[39] J. D. Rule, N. R. Sottos, and S. R. White, "Effect of microcapsule size on the performance of self-healing polymers," (in English), *Polymer,* vol. 48, no. 12, pp. 3520-3529, Jun 4 2007, doi: 10.1016/j.polymer.2007.04.008.

[40] J. F. Patrick, N. R. Sottos, and S. R. White, "Microvascular based self-healing polymeric foam," (in English), *Polymer,* vol. 53, no. 19, pp. 4231-4240, Aug 31 2012, doi: 10.1016/j.polymer.2012.07.021.

[41] H. W. Engels *et al.*, "Polyurethanes: Versatile Materials and Sustainable Problem Solvers for Today's Challenges," (in English), *Angew Chem Int Edit,* vol. 52, no. 36, pp. 9422-9441, Sep 2 2013, doi: 10.1002/anie.201302766.

[42] M. F. Sonnenschein, "POLYURETHANES Science, Technology, Markets, and Trends INTRODUCTION," (in English), *Wiley Ser Polym Eng,* pp. 1-9, 2015. [Online]. Available: <Go to ISI>://WOS:000358670500001.

[43] J. O. Akindoyo, M. D. H. Beg, S. Ghazali, M. R. Islam, N. Jeyaratnam, and A. R. Yuvaraj, "Polyurethane types, synthesis and applications - a review," (in English), *Rsc Advances,* vol. 6, no. 115, pp. 114453-114482, 2016, doi: 10.1039/c6ra14525f.

[44] M. A. Hood, B. B. Wang, J. M. Sands, J. J. La Scala, F. L. Beyer, and C. Y. Li, "Morphology control of segmented polyurethanes by crystallization of hard and soft segments," (in English), *Polymer,* vol. 51, no. 10, pp. 2191-2198, May 4 2010, doi: 10.1016/j.polymer.2010.03.027.

[45] X. P. Li *et al.*, "Self-Healing Polyurethane Elastomers Based on a Disulfide Bond by Digital Light Processing 3D Printing," (in English), *Acs Macro Lett,* vol. 8, no. 11, pp. 1511-1516, Nov 2019, doi: 10.1021/acsmacrolett.9b00766.

[46] J. Hu, R. B. Mo, X. Jiang, X. X. Sheng, and X. Y. Zhang, "Towards mechanical robust yet self-healing polyurethane elastomers via combination of dynamic main chain and dangling quadruple," (in English), *Polymer,* vol. 183, Nov 21 2019, doi: ARTN 121912 10.1016/j.polymer.2019.121912.

[47] B. Willocq, F. Khelif, J. Brancart, G. Van Assche, P. Dubois, and J. M. Raquez, "One-component Diels-Alder based polyurethanes: a unique way to self-heal," (in English), *Rsc Advances,* vol. 7, no. 76, pp. 48047-48053, 2017, doi: 10.1039/c7ra09898g.

[48] G. Rossignolo, G. Malucelli, and A. Lorenzetti, "Recycling of polyurethanes: where we are and where we are going," (in English), *Green Chem,* vol. 26, no. 3, pp. 1132-1152, Feb 5 2024, doi: 10.1039/d3gc02091f.

[49] X. Y. Li, B. Yu, J. Bai, B. C. Guo, M. Tian, and F. Chen, "Recycling Polyurethane with Properties Maintained in Multiple Reprocessing Realized via Dynamic Polysulfide Bond," (in English), *Macromolecules,* vol. 58, no. 13, pp. 6607-6616, Jun 23 2025, doi: 10.1021/acs.macromol.5c00670.

[50] Y. Gao, J. W. Hu, G. H. Hang, L. Li, and S. X. Zheng, "Reprocessing and shape recovery of polyurethane networks enabled with introduction of transcarbamoylation," (in English), *Polymer,* vol. 295, Mar 1 2024, doi: ARTN 126760 10.1016/j.polymer.2024.126760.

[51] X. L. Gao *et al.*, "Self-reinforced thermoplastic polyurethane composite with excellent mechanical properties, heat resistance and sustainable recycling," (in English), *Compos*

Part B-Eng, vol. 297, May 15 2025, doi: ARTN 112342 10.1016/j.compositesb.2025.112342.

[52] K. X. Hou and C. H. Li, "Self-healing materials for wearable electronics," (in English), *Wear Electron,* vol. 2, pp. 270-290, Dec 2025, doi: 10.1016/j.wees.2025.08.001.

[53] B. H. Zhao *et al.*, "Recent progress in the biomedical application of PEDOT:PSS hydrogels," (in English), *Chinese Chem Lett,* vol. 35, no. 10, Oct 2024, doi: ARTN 109810 10.1016/j.cclet.2024.109810.

[54] J. Li *et al.*, "PEDOT:PSS-based bioelectronics for brain monitoring and modulation," (in English), *Microsyst Nanoeng,* vol. 11, no. 1, May 13 2025, doi: ARTN 87 10.1038/s41378-025-00948-w.

[55] X. H. Tan *et al.*, "Recent advances in self-healing hydrogel composites for flexible wearable electronic devices," (in English), *Nano Res Energy,* vol. 3, no. 3, Sep 2024, doi: ARTN e9120123 10.26599/NRE.2024.9120123.

[56] A. Prameswati *et al.*, "Self-Healable Conductive Hydrogels with High Stretchability and Ultralow Hysteresis for Soft Electronics," (in English), *Acs Applied Materials & Interfaces,* vol. 15, no. 20, pp. 24648-24657, May 11 2023, doi: 10.1021/acsami.3c02407.

[57] V. P. Vu, H. M. So, A. Kim, J. Y. Lee, M. Oh, and S. Hyun, "Self-healing polymer binders: next-generation battery applications," (in English), *J Mater Chem A,* vol. 13, no. 45, Nov 18 2025, doi: 10.1039/d5ta04403k.

[58] Z. G. Quan, X. Y. Xiu, M. Li, L. Song, X. T. Jin, and Z. Zhou, "Recent progress and challenges of self-healing batteries," (in English), *Energy Mater Devices,* vol. 3, no. 1, Mar 25 2025, doi: Artn 9370058 10.26599/Emd.2025.9370058.

[59] Y. H. Geng, W. Zhong, S. Zhou, B. W. Yao, and J. J. Fu, "Electrically Functional Self-Healing Polymers: Design, Assessment, and Progress," (in English), *Macromol Mater Eng,* vol. 308, no. 9, Sep 2023, doi: 10.1002/mame.202300058.

[60] Y. Zhou, L. Li, Z. B. Han, Q. Li, J. L. He, and Q. Wang, "Self-Healing Polymers for Electronics and Energy Devices," (in English), *Chem Rev,* vol. 123, no. 2, pp. 558-612, Jan 25 2023, doi: 10.1021/acs.chemrev.2c00231.

[61] D. Zhao *et al.*, "Flexible Sensors Based on Conductive Polymer Composites," (in English), *Sensors-Basel,* vol. 24, no. 14, Jul 2024, doi: ARTN 4664 10.3390/s24144664.

[62] K. Zhao, Y. B. Zhao, J. Xu, R. Qian, Z. M. Yu, and C. Q. Ye, "Stretchable, adhesive and self-healing conductive hydrogels based on PEDOT:PSS-stabilized liquid metals for human motion detection," (in English), *Chem Eng J,* vol. 494, Aug 15 2024, doi: ARTN 152971 10.1016/j.cej.2024.152971.

[63] T. M. Jang *et al.*, "Stretchable and biodegradable self-healing conductors for multifunctional electronics," (in English), *Sci Adv,* vol. 10, no. 36, Sep 6 2024, doi: ARTN eadp9818 10.1126/sciadv.adp9818.

[64] H. W. Lin, C. T. Wu, C. W. Chang, T. Y. Lo, H. R. Chen, and J. T. Chen, "Enhancing Conductivity and Self-Healing in PEDOT:PSS/Poly(ionic liquid) Elastomers for Sensor Applications," (in English), *Acs Appl Polym Mater,* vol. 6, no. 23, pp. 14740-14748, Nov 21 2024, doi: 10.1021/acsapm.4c02949.

[65] J. H. Qiu *et al.*, "Highly conductive polymer with vertical phase separation for enhanced bioelectronic interfaces," (in English), *Npj Flex Electron,* vol. 9, no. 1, Jul 15 2025, doi: ARTN 69 10.1038/s41528-025-00441-4.

[66] G. Molnár, S. Rat, L. Salmon, W. Nicolazzi, and A. Bousseksou, "Spin Crossover Nanomaterials: From Fundamental Concepts to Devices," (in English), *Advanced Materials,* vol. 30, no. 5, Feb 1 2018, doi: ARTN 17003862 10.1002/adma.201703862.

[67] J. Y. Oh *et al.*, "Intrinsically stretchable and healable semiconducting polymer for organic transistors," (in English), *Nature,* vol. 539, no. 7629, pp. 411-415, Nov 17 2016, doi: 10.1038/nature20102.

[68] K. M. Zhu *et al.*, "Self-healing waterborne polyurethane originated from waste PET and their composites with polypyrrole for stretchable strain sensor," (in English), *Chem Eng J,* vol. 510, Apr 15 2025, doi: ARTN 161515 10.1016/j.cej.2025.161515.

[69] S. Yan *et al.*, "A self-healing polypyrrole/oxidized natural rubber conductive composite as a building block for highly sensitive strain sensors," (in English), *Colloid Surface A,* vol. 683, Feb 20 2024, doi: ARTN 133043 10.1016/j.colsurfa.2023.133043.

[70] J. Rivnay, S. Inal, A. Salleo, R. M. Owens, M. Berggren, and G. G. Malliaras, "Organic electrochemical transistors," *Nature Reviews Materials,* vol. 3, no. 2, pp. 1-14, 2018.

[71] C. Duprey *et al.*, "A recyclable PANI/PAAMPSA nanocomposite with repeatable, rapid, autonomous self-healing, and unprecedented electro-mechanical properties," (in English), *Adv Compos Hybrid Ma,* vol. 8, no. 5, Sep 5 2025, doi: ARTN 349 10.1007/s42114-025-01361-7.

[72] Y. Z. Meng *et al.*, "Self-healing electrochromic energy storage devices based on PEDOT:PSS," (in English), *Journal of Materials Chemistry C,* vol. 11, no. 40, pp. 13752-13762, Oct 19 2023, doi: 10.1039/d3tc02458j.

[73] M. Zhou *et al.*, "Low-Heat-Driven Self-Healing Flexible Electrochromic Film Relying on a PEDOT:PSS-Based All-Organic Composite," (in English), *Acs Appl Polym Mater,* vol. 6, no. 14, pp. 8598-8607, Jul 13 2024, doi: 10.1021/acsapm.4c01575.

[74] P. Kateb, J. Fan, J. Kim, X. Zhou, G. A. Lodygensky, and F. Cicoira, "Printable, adhesive, and self-healing dry epidermal electrodes based on PEDOT: PSS and polyurethane diol," *Flex Print Electron,* 2023.

[75] C. L. He *et al.*, "Super Tough and Spontaneous Water-Assisted Autonomous Self-Healing Elastomer for Underwater Wearable Electronics," (in English), *Adv Sci,* vol. 8, no. 21, Nov 2021, doi: ARTN 2102275 10.1002/advs.202102275.

[76] A. F. Wibowo *et al.*, "Recyclable, ultralow-hysteresis, multifunctional wearable sensors based on water-permeable, stretchable, and conductive cellulose/PEDOT:PSS hybrid films," (in English), *J Mater Chem A,* vol. 12, no. 30, pp. 19403-19413, Jul 30 2024, doi: 10.1039/d4ta02875a.

[77] H. Park *et al.*, "Organic flexible electronics with closed-loop recycling for sustainable wearable technology," (in English), *Nature Electronics,* vol. 7, no. 1, pp. 39-50, Jan 2024, doi: 10.1038/s41928-023-01078-9.

[78] X. Zhou *et al.*, "Conducting polymer films and bioelectrodes combining high adhesion and electro-mechanical self-healing," (in English), *Journal of Materials Chemistry C,* Dec 13 2023. [Online]. Available: <Go to ISI>://WOS:001127735600001.

[79] J. Xu *et al.*, "Highly stretchable polymer semiconductor films through the nanoconfinement effect," (in English), *Science,* vol. 355, no. 6320, pp. 59-+, Jan 6 2017, doi: 10.1126/science.aah4496.

[80] H. S. Tseng, Y. L. Chen, P. Y. Zhang, and Y. S. Hsiao, "Additive Blending Effects on PEDOT:PSS Composite Films for Wearable Organic Electrochemical Transistors," (in English), *Acs Applied Materials & Interfaces,* vol. 16, no. 11, pp. 13384-13398, Mar 8 2024, doi: 10.1021/acsami.3c14961.

[81] L. J. Lu *et al.*, "Citric Acid and Polyvinyl Alcohol Induced PEDOT: PSS with Enhanced Electrical Conductivity and Stretchability for Eco-Friendly, Self-Healable, Wearable Organic Thermoelectrics," (in English), *Macromol Rapid Comm,* vol. 45, no. 20, Oct 2024, doi: ARTN 2400394 10.1002/marc.202400394.

[82] S. Q. Zhao, D. P. Liu, and F. Yan, "Wearable Resistive-Type Stretchable Strain Sensors: Materials and Applications," (in English), *Advanced Materials,* vol. 37, no. 5, Feb 2025, doi: 10.1002/adma.202413929.

[83] H. C. Ates *et al.*, "End-to-end design of wearable sensors," (in English), *Nature Reviews Materials,* vol. 7, no. 11, pp. 887-907, Nov 2022, doi: 10.1038/s41578-022-00460-x.

[84] C. Liu, S. O. Kelley, and Z. J. Wang, "Self-Healing Materials for Bioelectronic Devices," (in English), *Advanced Materials,* vol. 36, no. 35, Aug 2024, doi: 10.1002/adma.202401219.

[85] H. Yuk, T. Zhang, G. A. Parada, X. Y. Liu, and X. H. Zhao, "Skin-inspired hydrogel-elastomer hybrids with robust interfaces and functional microstructures," (in English), *Nat Commun,* vol. 7, Jun 27 2016, doi: ARTN 12028 10.1038/ncomms12028.

[86] Y. Wang, S. S. Jia, and Z. T. Zhang, "PEDOT and PEDOT:PSS thin-film electrodes: patterning, modification and application in stretchable organic optoelectronic devices," (in English), *Journal of Materials Chemistry C,* vol. 11, no. 31, pp. 10435-10454, Aug 10 2023, doi: 10.1039/d3tc01579c.

[87] B. Y. Ouyang, C. W. Chi, F. C. Chen, Q. F. Xi, and Y. Yang, "High-conductivity poly (3,4-ethylenedioxythiophene):poly(styrene sulfonate) film and its application in polymer optoelectronic devices," (in English), *Advanced Functional Materials,* vol. 15, no. 2, pp. 203-208, Feb 2005, doi: 10.1002/adfm.200400016.

[88] Z. K. Li *et al.*, "Self-Healing Hydrogel Bioelectronics," (in English), *Advanced Materials,* vol. 36, no. 21, May 2024, doi: 10.1002/adma.202306350.

[89] K. Sagdic, E. Fernández-Lavado, M. Mariello, O. Akouissi, and S. P. Lacour, "Hydrogels and conductive hydrogels for implantable bioelectronics," (in English), *Mrs Bull,* vol. 48, no. 5, pp. 495-505, May 2023, doi: 10.1557/s43577-023-00536-1.

[90] X. L. Li *et al.*, "Body temperature-triggered adhesive ionic conductive hydrogels for bioelectrical signal monitoring," (in English), *Chem Eng J,* vol. 498, Oct 15 2024, doi: ARTN 155195 10.1016/j.cej.2024.155195.

[91] M. Yang *et al.*, "Highly-stable, injectable, conductive hydrogel for chronic neuromodulation," (in English), *Nat Commun,* vol. 15, no. 1, Sep 12 2024, doi: ARTN 7993 10.1038/s41467-024-52418-y.

[92] G. Z. Yang *et al.*, "The grand challenges of," (in English), *Sci Robot,* vol. 3, no. 14, Jan 24 2018, doi: ARTN eaar7650 10.1126/scirobotics.aar7650.

[93] M. Irimia-Vladu, E. D. Glowacki, G. Voss, S. Bauer, and N. S. Sariciftci, "Green and biodegradable electronics," (in English), *Mater Today,* vol. 15, no. 7-8, pp. 340-346, Jul-Aug 2012, doi: Doi 10.1016/S1369-7021(12)70139-6.

[94] H. S. Guo, Y. Han, W. Q. Zhao, J. Yang, and L. Zhang, "Universally autonomous self-healing elastomer with high stretchability," (in English), *Nat Commun,* vol. 11, no. 1, Apr 27 2020, doi: ARTN 2037 10.1038/s41467-020-15949-8.

[95] Y. Wang *et al.*, "A highly stretchable, transparent, and conductive polymer," (in English), *Sci Adv,* vol. 3, no. 3, Mar 2017, doi: ARTN e1602076 10.1126/sciadv.1602076.

[96] J. Y. Oh, S. Kim, H. K. Baik, and U. Jeong, "Conducting polymer dough for deformable electronics," *Advanced Materials,* vol. 28, no. 22, pp. 4455-4461, 2016.

[97] T. Zhou *et al.*, "3D printable high-performance conducting polymer hydrogel for all-hydrogel bioelectronic interfaces," (in English), *Nat Mater,* vol. 22, no. 7, pp. 895-+, Jul 2023, doi: 10.1038/s41563-023-01569-2.

[98] N. A. M. Radzuan, A. B. Sulong, and J. Sahari, "A review of electrical conductivity models for conductive polymer composite," *International Journal of Hydrogen Energy,* vol. 42, no. 14, pp. 9262-9273, 2017.

[99] T. K. Das and S. Prusty, "Review on conducting polymers and their applications," *Polymer-plastics technology and engineering,* vol. 51, no. 14, pp. 1487-1500, 2012.

[100] M. H. Naveen, N. G. Gurudatt, and Y.-B. Shim, "Applications of conducting polymer composites to electrochemical sensors: A review," *Applied materials today,* vol. 9, pp. 419-433, 2017.

[101] S. J. Benight, C. Wang, J. B. Tok, and Z. Bao, "Stretchable and self-healing polymers and devices for electronic skin," *Progress in Polymer Science,* vol. 38, no. 12, pp. 1961-1977, 2013.

[102] Y. Cao *et al.*, "Self-healing electronic skins for aquatic environments," *Nature Electronics,* vol. 2, no. 2, pp. 75-82, 2019.

[103] X. M. An *et al.*, "A robust and self-healing elastomer achieved by a thio-β-diketone-Cu(ii) coordination and H-bonding dual crosslinked system," (in English), *Materials Chemistry Frontiers,* vol. 6, no. 13, pp. 1779-1787, Jun 27 2022, doi: 10.1039/d2qm00259k.

[104] B. Q. Wan *et al.*, "Dynamic Sustainable Polyimide Film Combining Hardness with Softness via a "

-Like" Bionic Strategy," (in English), *Advanced Materials,* vol. 35, no. 2, p. 2304175, Jan 12 2023, doi: 10.1002/adma.202207451.

[105] T. Wang *et al.*, "A Self-Healable, Highly Stretchable, and Solution Processable Conductive Polymer Composite for Ultrasensitive Strain and Pressure Sensing," (in English),

Advanced Functional Materials, vol. 28, no. 7, Feb 14 2018, doi: ARTN 1705551 10.1002/adfm.201705551.

[106] Y. Li *et al.*, "Tailoring the Self-Healing Properties of Conducting Polymer Films," (in English), *Macromol Biosci,* vol. 20, no. 11, p. 2000146, Nov 2020, doi: ARTN 2000146 10.1002/mabi.202000146.

[107] Y. Li, X. Zhou, B. Sarkar, N. Gagnon-Lafrenais, and F. Cicoira, "Recent Progress on Self-Healable Conducting Polymers," *Advanced Materials,* vol. 34, no. 24, p. 2108932, 2022.

[108] Y. Li *et al.*, "Autonomic self-healing of PEDOT: PSS achieved via polyethylene glycol addition," *Advanced Functional Materials,* vol. 30, no. 30, p. 2002853, 2020.

[109] C. Y. Zhang *et al.*, "Highly adhesive and self-healing γ-PGA/PEDOT:PSS conductive hydrogels enabled by multiple hydrogen bonding for wearable electronics," (in English), *Nano Energy,* vol. 95, p. 106991, May 2022, doi: ARTN 106991 10.1016/j.nanoen.2022.106991.

[110] H. G. Liao, S. L. Liao, X. L. Tao, C. Liu, and Y. P. Wang, "Intrinsically recyclable and self-healable conductive supramolecular polymers for customizable electronic sensors," (in English), *Journal of Materials Chemistry C,* vol. 6, no. 47, pp. 12992-12999, Dec 21 2018, doi: 10.1039/c8tc04699a.

[111] P. J. Taroni *et al.*, "Toward Stretchable Self-Powered Sensors Based on the Thermoelectric Response of PEDOT:PSS/Polyurethane Blends," (in English), *Advanced Functional Materials,* vol. 28, no. 15, p. 1704285, Apr 11 2018, doi: ARTN 1704285 10.1002/adfm.201704285.

[112] M. Z. Seyedin, J. M. Razal, P. C. Innis, and G. G. Wallace, "Strain-Responsive Polyurethane/PEDOT:PSS Elastomeric Composite Fibers with High Electrical Conductivity," (in English), *Advanced Functional Materials,* vol. 24, no. 20, pp. 2957-2966, May 2014, doi: 10.1002/adfm.201303905.

[113] Y. Li, Y. Jin, W. Fan, and R. Zhou, "A review on room-temperature self-healing polyurethane: synthesis, self-healing mechanism and application," *Journal of Leather Science and Engineering,* vol. 4, no. 1, p. 24, 2022.

[114] F. W. Xie, T. L. Zhang, P. Bryant, V. Kurusingal, J. M. Colwell, and B. Laycock, "Degradation and stabilization of polyurethane elastomers," (in English), *Progress in Polymer Science,* vol. 90, pp. 211-268, Mar 2019, doi: 10.1016/j.progpolymsci.2018.12.003.

[115] Y. Yao, M. Xiao, and W. G. Liu, "A Short Review on Self-Healing Thermoplastic Polyurethanes," (in English), *Macromol Chem Phys,* vol. 222, no. 8, p. 2100002, Apr 2021, doi: ARTN 2100002 10.1002/macp.202100002.

[116] X. H. Chen *et al.*, "A Multiple Remotely Controlled Platform from Recyclable Polyurethane Composite Network with Shape-Memory Effect and Self-Healing Ability," (in English), *Small,* vol. 18, no. 50, p. 2205286, Dec 15 2022, doi: 10.1002/smll.202205286.

[117] S. W. Yang, S. Wang, X. S. Du, Z. L. Du, X. Cheng, and H. B. Wang, "Mechanically robust self-healing and recyclable flame-retarded polyurethane elastomer based on

thermoreversible crosslinking network and multiple hydrogen bonds," (in English), *Chem Eng J,* vol. 391, p. 123544, Jul 1 2020, doi: ARTN 123544 10.1016/j.cej.2019.123544.

[118] Z. Q. Zhou *et al.*, "Room temperature self-healing crosslinked elastomer constructed by dynamic urea bond and hydrogen bond," (in English), *Progress in Organic Coatings,* vol. 154, p. 106213, May 2021, doi: ARTN 106213 10.1016/j.porgcoat.2021.106213.

[119] S. H. Lee, S. R. Shin, and D. S. Lee, "Self-healing of cross-linked PU via dual-dynamic covalent bonds of a Schiff base from cystine and vanillin," (in English), *Mater Design,* vol. 172, p. 107774, Jun 15 2019, doi: ARTN 107774 10.1016/j.matdes.2019.107774.

[120] N. Zheng, Y. Xu, Q. Zhao, and T. Xie, "Dynamic Covalent Polymer Networks: A Molecular Platform for Designing Functions beyond Chemical Recycling and Self-Healing," (in English), *Chem Rev,* vol. 121, no. 3, pp. 1716-1745, Feb 10 2021, doi: 10.1021/acs.chemrev.0c00938.

[121] B. Willocq, J. Odent, P. Dubois, and J. M. Raquez, "Advances in intrinsic self-healing polyurethanes and related composites," (in English), *Rsc Advances,* vol. 10, no. 23, pp. 13766-13782, Apr 3 2020, doi: 10.1039/d0ra01394c.

[122] R. H. Aguirresarobe *et al.*, "Healable and self-healing polyurethanes using dynamic chemistry," (in English), *Progress in Polymer Science,* vol. 114, p. 101362, Mar 2021, doi: ARTN 101362 10.1016/j.progpolymsci.2021.101362.

[123] Z. W. An *et al.*, "Recent advances in self-healing polyurethane based on dynamic covalent bonds combined with other self-healing methods," (in English), *Nanoscale,* vol. 15, no. 14, pp. 6505-6520, Apr 6 2023, doi: 10.1039/d2nr07110j.

[124] Z. X. Fei, C. X. Yin, J. R. Sun, L. Yuan, and L. Y. Shi, "Healable and recyclable multiblock polyurethanes with mechanical performance Tailorability based on hierarchical phase separation and dynamic bond interaction," (in English), *Polymer,* vol. 289, p. 126467, Dec 15 2023, doi: ARTN 126467 10.1016/j.polymer.2023.126467.

[125] S. Yu, R. C. Zhang, Q. Wu, T. H. Chen, and P. C. Sun, "Bio-Inspired High-Performance and Recyclable Cross-Linked Polymers," (in English), *Advanced Materials,* vol. 25, no. 35, pp. 4912-4917, Sep 20 2013, doi: 10.1002/adma.201301513.

[126] F. T. Sai *et al.*, "Multifunctional waterborne polyurethane films: Amine-response, thermal-driven self-healing and recyclability," (in English), *Appl Surf Sci,* vol. 573, Jan 30 2022, doi: ARTN 151526 10.1016/j.apsusc.2021.151526.

[127] H. Shi, C. C. Liu, Q. L. Jiang, and J. K. Xu, "Effective Approaches to Improve the Electrical Conductivity of PEDOT:PSS: A Review," (in English), *Adv Electron Mater,* vol. 1, no. 4, p. 1500017, Apr 2015, doi: ARTN 1500017 10.1002/aelm.201500017.

[128] S. L. Lai, M. Y. Chan, M. K. Fung, C. S. Lee, and S. T. Lee, "Concentration effect of glycerol on the conductivity of PEDOT film and the device performance," (in English), *Mat Sci Eng B-Solid,* vol. 104, no. 1-2, pp. 26-30, Nov 15 2003, doi: 10.1016/S0921-5107(03)00262-9.

[129] E. Mehrbakhsh, M. Rezaei, R. Lotfi Mayan Sofla, and A. Babaie, "Physical and thermo-mechanical properties of PCL/PEG based shape memory polyurethane for orthodontic

ligature application," *International Journal of Polymeric Materials and Polymeric Biomaterials,* vol. 73, pp. 239-249, 2024.

[130] A. X. Chen, A. T. Kleinschmidt, K. Choudhary, and D. J. Lipomi, "Beyond Stretchability: Strength, Toughness, and Elastic Range in Semiconducting Polymers," (in English), *Chem Mater,* vol. 32, no. 18, pp. 7582-7601, Sep 22 2020, doi: 10.1021/acs.chemmater.0c03019.

[131] X. L. Niu, L. X. Huo, C. T. Cai, J. S. Guo, and H. Zhou, "Rod-Like Attapulgite Modified by Bifunctional Acrylic Resin As Reinforcement for Epoxy Composites," (in English), *Ind Eng Chem Res,* vol. 53, no. 42, pp. 16359-16365, Oct 22 2014, doi: 10.1021/ie502869c.

[132] J. W. Chen, J. Dai, J. H. Yang, N. Zhang, T. Huang, and Y. Wang, "Enhancing chain segments mobility to improve the fracture toughness of polypropylene," (in English), *Chinese J Polym Sci,* vol. 31, no. 2, pp. 232-241, Feb 2013, doi: 10.1007/s10118-013-1221-z.

[133] C. Kim *et al.*, "Flexible and stretchable printed conducting polymer devices for electrodermal activity measurements," *Flex Print Electron,* vol. 7, no. 1, p. 014008, 2022.

[134] M. Uchida, K. Kamimura, T. Yoshida, and Y. Kaneko, "Viscoelastic-viscoplastic modeling of epoxy based on transient network theory," (in English), *Int J Plasticity,* vol. 153, Jun 2022, doi: ARTN 103262 10.1016/j.ijplas.2022.103262.

[135] Y. R. Jeong, G. Lee, H. Park, and J. S. Ha, "Stretchable, Skin-Attachable Electronics with Integrated Energy Storage Devices for Biosignal Monitoring," (in English), *Accounts Chem Res,* vol. 52, no. 1, pp. 91-99, Jan 2019, doi: 10.1021/acs.accounts.8b00508.

[136] X. H. Ma, Z. F. Jiang, and Y. J. Lin, "Flexible energy storage devices for wearable bioelectronics," (in English), *J Semicond,* vol. 42, no. 10, p. 101602, Oct 2021, doi: Artn 101602 10.1088/1674-4926/42/10/101602.

[137] H. W. Sheng *et al.*, "Recent Advances of Energy Solutions for Implantable Bioelectronics," (in English), *Adv Healthc Mater,* vol. 10, no. 17, p. 2100199, Sep 2021, doi: ARTN 2100199 10.1002/adhm.202100199.

[138] J. H. Xu, J. Y. Chen, Y. N. Zhang, T. Liu, and J. J. Fu, "A Fast Room-Temperature Self-Healing Glassy Polyurethane," (in English), *Angew Chem Int Edit,* vol. 60, no. 14, pp. 7947-7955, Mar 29 2021, doi: 10.1002/anie.202017303.

[139] J. Xue *et al.*, "New Carbon Materials for Multifunctional Soft Electronics," (in English), *Advanced Materials,* vol. 37, no. 2, Jan 2025, doi: 10.1002/adma.202312596.

[140] Y. C. Ren, F. Zhang, Z. Yan, and P. Y. Chen, "Wearable bioelectronics based on emerging nanomaterials for telehealth applications," (in English), *Device,* vol. 3, no. 1, Jan 17 2025, doi: ARTN 100676 10.1016/j.device.2024.100676.

[141] H. B. Li *et al.*, "E-Tattoos: Toward Functional but Imperceptible Interfacing with Human Skin," (in English), *Chem Rev,* vol. 124, no. 6, pp. 3220-3283, Mar 11 2024, doi: 10.1021/acs.chemrev.3c00626.

[142] H. U. Chung *et al.*, "Skin-interfaced biosensors for advanced wireless physiological monitoring in neonatal and pediatric intensive-care units," (in English), *Nat Med,* vol. 26, no. 3, pp. 418-+, Mar 2020, doi: 10.1038/s41591-020-0792-9.

[143] L. H. Jia, Y. H. Li, A. B. Ren, T. Xiang, and S. B. Zhou, "Degradable and Recyclable Hydrogels for Sustainable Bioelectronics," (in English), *Acs Applied Materials & Interfaces,* vol. 16, no. 26, pp. 32887-32905, Jun 21 2024, doi: 10.1021/acsami.4c05663.

[144] M. Qi *et al.*, "Bioinspired Self-healing Soft Electronics," (in English), *Advanced Functional Materials,* vol. 33, no. 17, Apr 2023, doi: 10.1002/adfm.202214479.

[145] Y. F. Guo *et al.*, "Degradable and Fully Recyclable Dynamic Thermoset Elastomer for 3D-Printed Wearable Electronics," (in English), *Advanced Functional Materials,* vol. 31, no. 9, Feb 2021, doi: ARTN 2009799 10.1002/adfm.202009799.

[146] J. Jung *et al.*, "Self-healing electronic skin with high fracture strength and toughness," (in English), *Nat Commun,* vol. 15, no. 1, Nov 11 2024, doi: ARTN 9763 10.1038/s41467-024-53957-0.

[147] R. A. Lehane *et al.*, "Electrosynthesis of Biocompatible Free-Standing PEDOT Thin Filmsat a Polarized Liquid|Liquid Interface," (in English), *Journal of the American Chemical Society,* vol. 144, no. 11, pp. 4853-4862, Mar 23 2022, doi: 10.1021/jacs.1c12373.

[148] R. Singh, J. Tharion, S. Murugan, and A. Kumar, "ITO-Free Solution-Processed Flexible Electrochromic Devices Based on PEDOT:PSS as Transparent Conducting Electrode," (in English), *Acs Applied Materials & Interfaces,* vol. 9, no. 23, pp. 19427-19435, Jun 14 2017, doi: 10.1021/acsami.6b09476.

[149] X. L. Hu, M. Xia, M. H. Zhang, W. Yang, F. Z. Yang, and Y. J. Luo, "Technologies for room-temperature self-healing polymer materials and their applications in energetic materials," (in English), *Energ Mater Front,* vol. 5, no. 2, pp. 158-174, Jun 2024, doi: 10.1016/j.enmf.2024.06.001.

[150] L. Yang *et al.*, "Mechanically Robust and Room Temperature Self-Healing Ionogel Based on Ionic Liquid Inhibited Reversible Reaction of Disulfide Bonds," (in English), *Adv Sci,* vol. 10, no. 20, Jul 2023, doi: 10.1002/advs.202207527.

[151] F. Dong *et al.*, "Self-healing polyurethane with high strength and toughness based on a dynamic chemical strategy," *J Mater Chem A,* vol. 10, no. 18, pp. 10139-10149, 2022.

[152] D. K. Chattopadhyay and D. C. Webster, "Thermal stability and flame retardancy of polyurethanes," (in English), *Progress in Polymer Science,* vol. 34, no. 10, pp. 1068-1133, Oct 2009, doi: 10.1016/j.progpolymsci.2009.06.002.

[153] T. K. Chen, J. Y. Chui, and T. S. Shieh, "Glass transition behaviors of a polyurethane hard segment based on 4,4'-diisocyanatodiphenylmethane and 1,4-butanediol and the calculation of microdomain composition," (in English), *Macromolecules,* vol. 30, no. 17, pp. 5068-5074, Aug 25 1997, doi: DOI 10.1021/ma9618639.

[154] H. Zhang *et al.*, "Dynamic Bond-Enhanced, Recyclable Polyurethane Elastomer with High Strength and Self-Healing Properties for Advanced 3D Printing," *Composites Part B: Engineering,* p. 112500, 2025.

[155] Y. Chen, Z. H. Tang, Y. J. Liu, S. W. Wu, and B. C. Guo, "Mechanically Robust, Self-Healable, and Reprocessable Elastomers Enabled by Dynamic Dual Cross-Links," (in

English), *Macromolecules,* vol. 52, no. 10, pp. 3805-3812, May 28 2019, doi: 10.1021/acs.macromol.9b00419.

[156] Q. Liu, Y. B. Liu, H. Zheng, C. M. Li, Y. Zhang, and Q. Y. Zhang, "Design and development of self-repairable and recyclable crosslinked poly(thiourethane-urethane) via enhanced aliphatic disulfide chemistry," (in English), *J Polym Sci,* vol. 58, no. 8, pp. 1092-1104, Apr 15 2020, doi: 10.1002/pol.20190186.

[157] X. X. Jian, Y. W. Hu, W. L. Zhou, and L. Q. Xiao, "Self-healing polyurethane based on disulfide bond and hydrogen bond," (in English), *Polym Advan Technol,* vol. 29, no. 1, pp. 463-469, Jan 2018, doi: 10.1002/pat.4135.

[158] R. Tutika, A. B. M. T. Haque, and M. D. Bartlett, "Self-healing liquid metal composite for reconfigurable and recyclable soft electronics," (in English), *Commun Mater,* vol. 2, no. 1, Jun 14 2021, doi: ARTN 64 10.1038/s43246-021-00169-4.

[159] M. Namkoong *et al.*, "Moldable and transferrable conductive nanocomposites for epidermal electronics," (in English), *Npj Flex Electron,* vol. 6, no. 1, Jun 7 2022, doi: ARTN 41 10.1038/s41528-022-00170-y.

[160] C. X. Zheng, Y. Y. Yue, L. Gan, X. W. Xu, C. T. Mei, and J. Q. Han, "Highly Stretchable and Self-Healing Strain Sensors Based on Nanocellulose-Supported Graphene Dispersed in Electro-Conductive Hydrogels," (in English), *Nanomaterials-Basel,* vol. 9, no. 7, Jul 2019, doi: ARTN 937 10.3390/nano9070937.

[161] D. H. Kim, Z. A. Akbar, Y. T. Malik, J. W. Jeon, and S. Y. Jang, "Self-healable polymer complex with a giant ionic thermoelectric effect," (in English), *Nat Commun,* vol. 14, no. 1, Jun 5 2023, doi: ARTN 3246 10.1038/s41467-023-38830-w.

[162] Y. Wang, B. S. Park, V. P. Vu, and S. H. Lee, "Self-healing conducting composite electrodes derived from chemical recycling of PET plastic wastes for flexible supercapacitors," (in English), *Polym Eng Sci,* vol. 65, no. 4, pp. 1854-1867, Apr 2025, doi: 10.1002/pen.27117.

[163] J. C. Zou, Z. X. Yang, J. Y. Liang, Y. F. Xie, M. M. Fan, and X. Zhang, "Recyclable, high strength and electrical-mechanical self-healing wearable ionic hydrogel sensor," (in English), *Polymer,* vol. 315, Dec 17 2024, doi: ARTN 127826 10.1016/j.polymer.2024.127826.

[164] H. Y. Mao, Y. Y. Zhang, L. X. Zhao, H. Li, H. L. Wu, and L. Lin, "Self-Healing and Recyclable Fabric Coatings Based on Boroxine-Polyurethane," (in English), *Acs Appl Polym Mater,* vol. 7, no. 1, pp. 164-174, Dec 18 2024, doi: 10.1021/acsapm.4c02845.

[165] L. V. Kayser *et al.*, "RAFT Polymerization of an Intrinsically Stretchable Water-Soluble Block Copolymer Scaffold for PEDOT," (in English), *Chem Mater,* vol. 30, no. 13, pp. 4459-4468, Jul 10 2018, doi: 10.1021/acs.chemmater.8b02040.

[166] X. Q. Su *et al.*, "A Highly Conducting Polymer for Self-Healable, Printable, and Stretchable Organic Electrochemical Transistor Arrays and Near Hysteresis-Free Soft Tactile Sensors," (in English), *Advanced Materials,* vol. 34, no. 19, p. 2200682, May 2022, doi: ARTN 2200682 10.1002/adma.202200682.

[167] Y. Lu *et al.*, "Ultrastretchable Conductive Polymer Complex as a Strain Sensor with a Repeatable Autonomous Self-Healing Ability," (in English), *Acs Applied Materials & Interfaces,* vol. 11, no. 22, pp. 20453-20464, Jun 5 2019, doi: 10.1021/acsami.9b05464.

[168] F. Y. Sun *et al.*, "Self-Healable, Highly Stretchable, Ionic Conducting Polymers as Efficient Protecting Layers for Stable Lithium-Metal Electrodes," (in English), *Acs Applied Materials & Interfaces,* vol. 14, no. 22, pp. 26014-26023, Jun 8 2022, doi: 10.1021/acsami.2c04166.

[169] R. Li, T. Fan, G. X. Chen, H. J. Xie, B. Su, and M. H. He, "Highly transparent, self-healing conductive elastomers enabled by synergistic hydrogen bonding interactions," (in English), *Chem Eng J,* vol. 393, Aug 1 2020, doi: ARTN 124685 10.1016/j.cej.2020.124685.

APPENDIX A SUPPLEMENTARY INFORMATION FOR ARTICLE 2 : SELF-HEALING, STRETCHABLE AND RECYCLABLE POLYURETHANE-PEDOT:PSS CONDUCTIVE BLENDS

Jinsil Kim, Jiaxin Fan, Gayaneh Petrossian, Xin Zhou, Pierre Kateb, Noemy Gagnon-Lafrenais and Fabio Cicoira

Department of Chemical Engineering, Polytechnique Montréal, Montréal, QC H3C 3A7, Canada

*Corresponding author. E-mail: fabio.cicoira@polymtl.ca

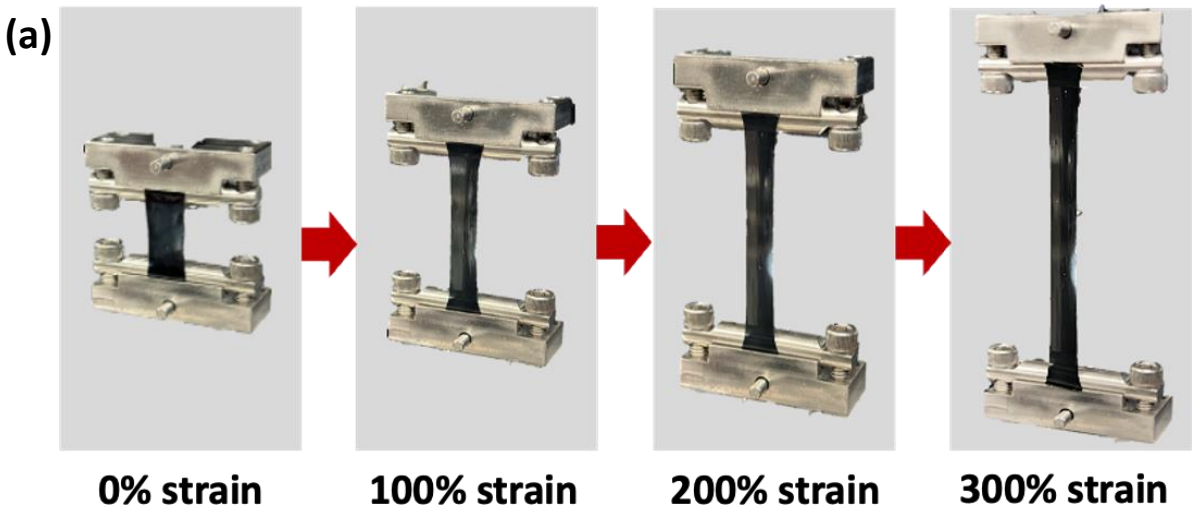

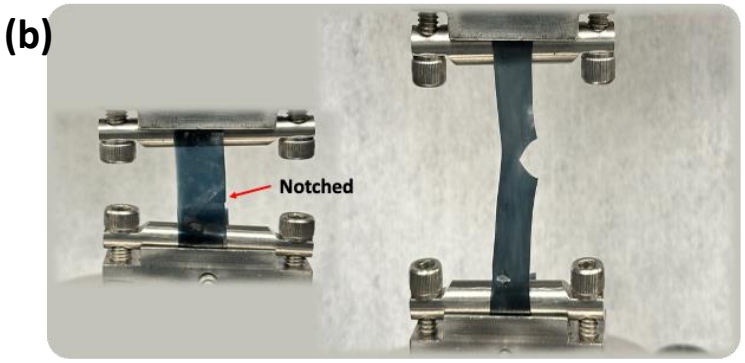

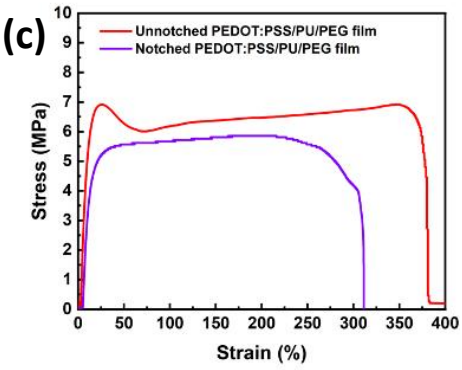

(d)

Samples	Toughness (MJ/m³)
Unnotched PEDOT:PSS/PU/PEG film	24.60 ± 0.23
Notched PEDOT:PSS/PU/PEG film	16.54 ± 1.24

Figure S1. Fracture behavior of PEDOT:PSS/PU/PEG films. (a) Photograph of a pristine film. (b) Notched film under uniaxial strain. (c) Tensile stress–strain curves of unnotched and notched films. (d) Toughness comparison between unnotched and notched films. Values (n = 3) are presented as mean ± standard deviation.

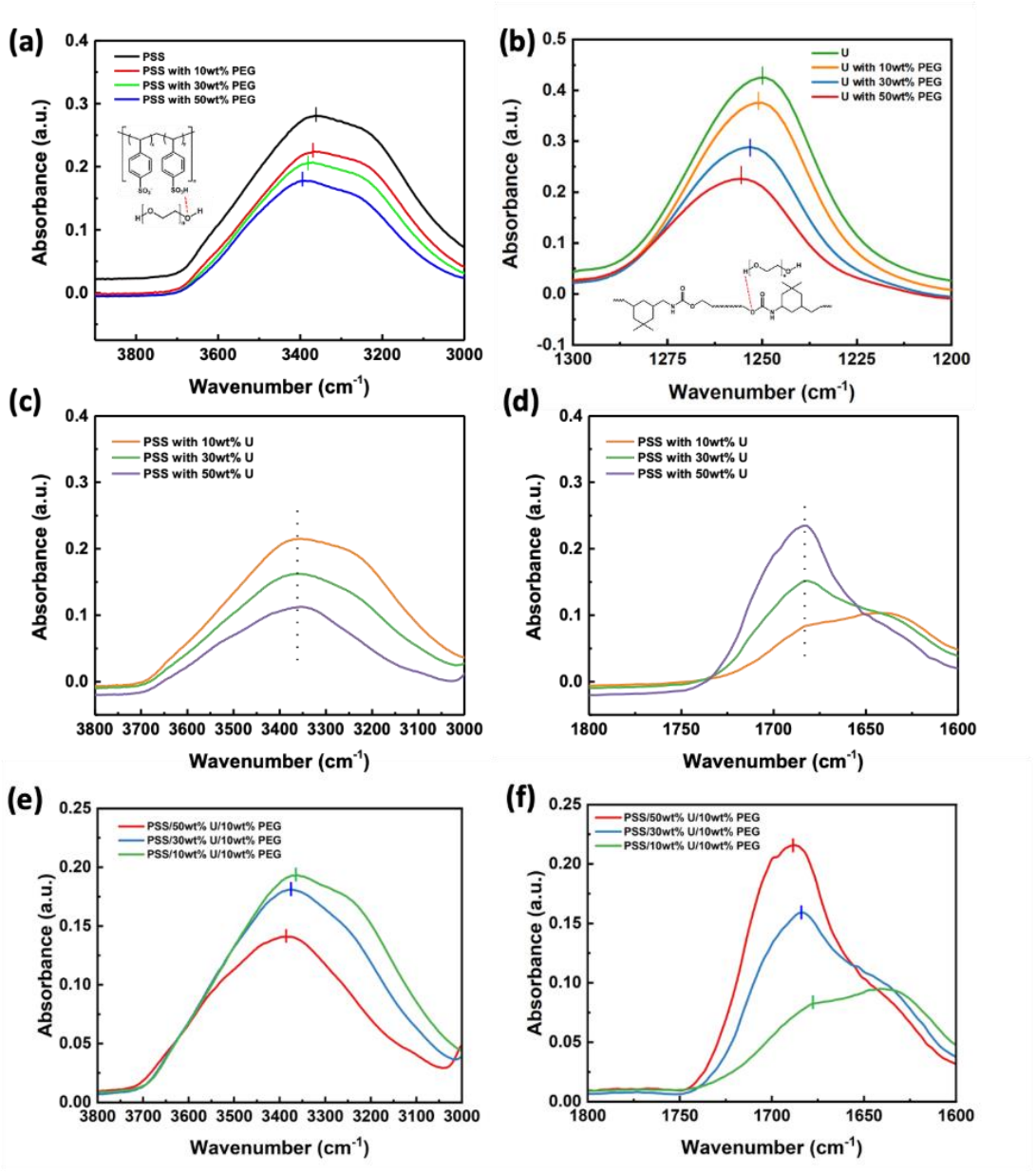

Figure S2. FTIR spectra of precursor mixtures with varying compositions. (a) Pristine PSS and PSS/PEG mixtures (10%, 30%, and 50%). (b) Pristine urethane (U) and U/PEG mixtures (10%, 30%, and 50%). (c,d) PSS/U mixtures with varying compositions (10%, 30%, and 50%). (e,f) PSS/U/PEG mixtures with varying U contents (10%, 30%, and 50%) and a fixed PEG content of 10%.

Table S1. FTIR peak assignments of SO_3–H and S=O bands in PSS and C–O–C and C=O bands in urethane (U).

Samples	SO_3-H in PSS (cm^{-1})	S=O in PSS (cm^{-1})	C-O-C in U (cm^{-1})	C=O in U (cm^{-1})
PSS	3360.1	1172.8	-	-
PSS/10wt% PEG	3369.4	1176.8	-	-
PSS/30wt% PEG	3381.1	1180.4	-	-
PSS/50wt% PEG	3394.6	1186.0	-	-
U	-	-	1250.1	1690.0
U/10wt% PEG	-	-	1251.3	1692.1
U/30wt% PEG	-	-	1253.2	1695.0
U/50wt% PEG	-	-	1255.8	1697.6
PSS/10wt% U				
PSS/30wt% U	3362.6	-	-	1683.3
PSS/50wt% U				
PSS/10wt% U/10wt% PEG	3366.6	-	-	1678.3
PSS/30wt% U/10wt% PEG	3376.8	-	-	1683.9
PSS/50wt% U/10wt% PEG	3381.4	-	-	1688.0

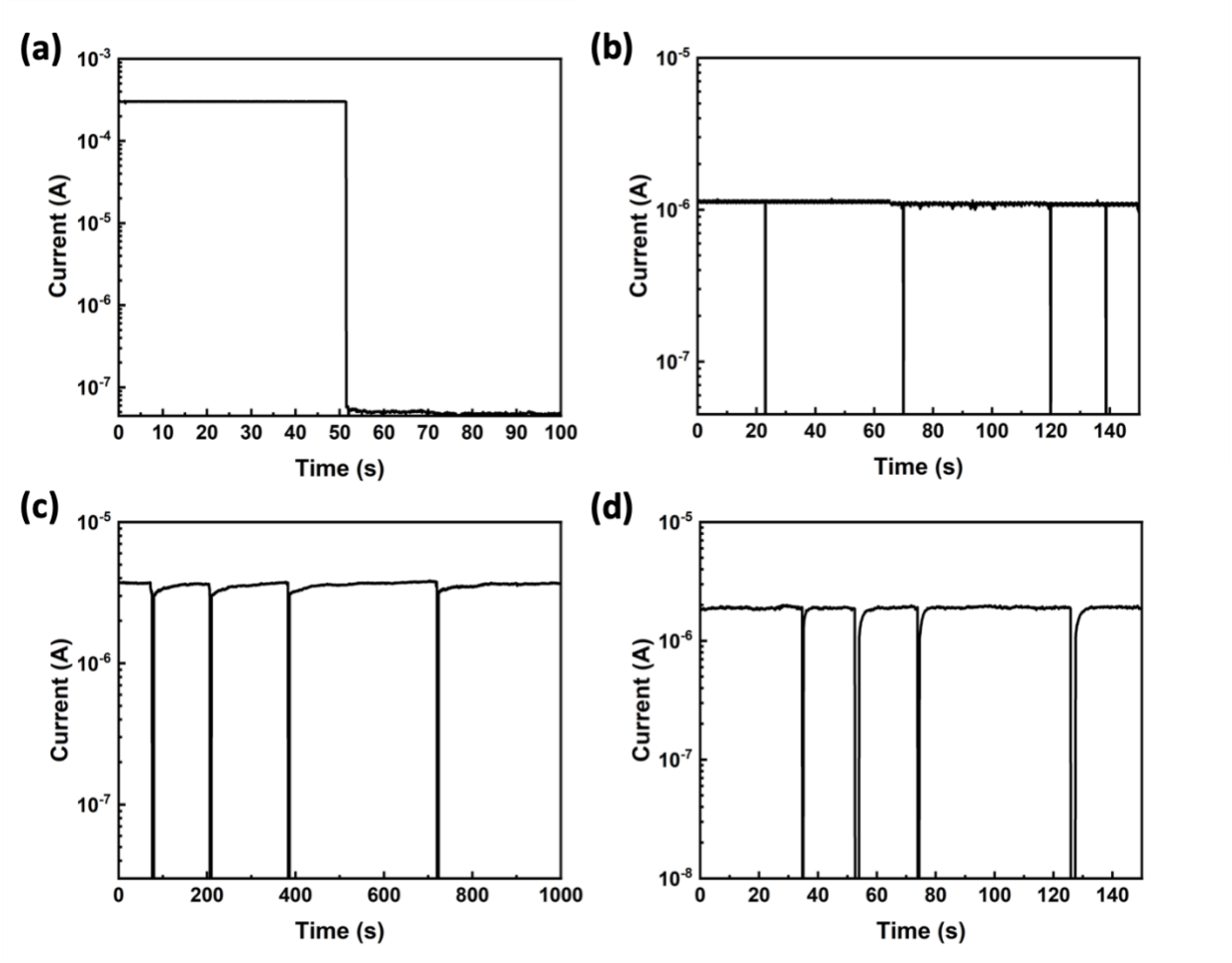

Figure S3. Current–time responses of (a) PEDOT:PSS, (b) PEDOT:PSS/PU, (c) PEDOT:PSS/PU/Glycerol, and (d) PEDOT:PSS/PEG/Glycerol films during repeated cut–healing cycles.

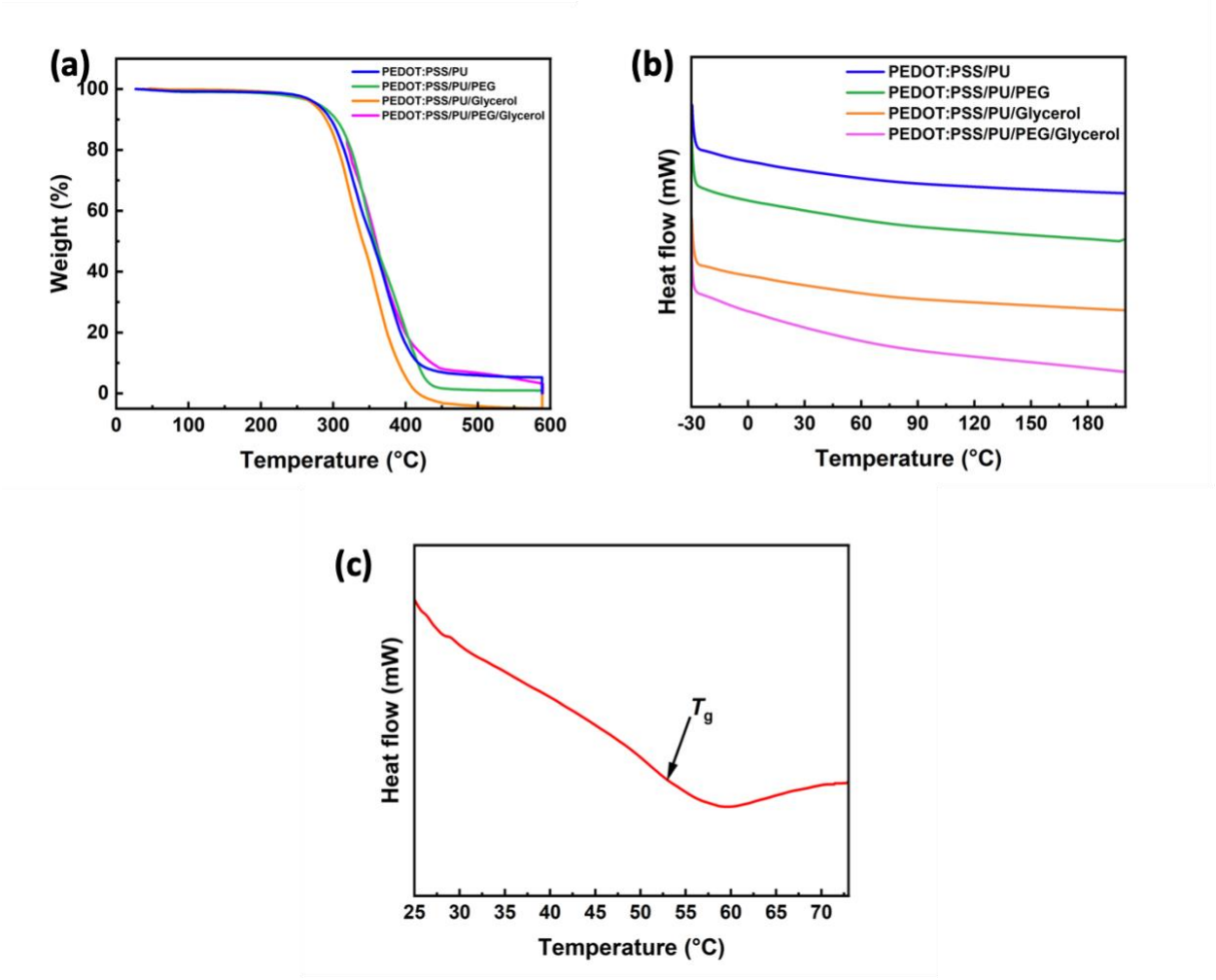

Figure S4. Thermal analysis of PEDOT:PSS/PU-based films. (a) TGA thermograms and (b) DSC thermograms of PEDOT:PSS/PU (blue), PEDOT:PSS/PU/PEG (green), PEDOT:PSS/PU/Glycerol (orange), and PEDOT:PSS/PU/PEG/Glycerol (magenta) films. (c) Modulated DSC thermogram of PU, indicating a glass transition temperature (T_g) of approximately 53 °C.

We investigated the mechanical self-healing properties of PEDOT:PSS/PU/Glycerol and PEDOT:PSS/PU/PEG/Glycerol. Notably, the PEDOT:PSS/PU/PEG/Glycerol film exhibited partial scratch recovery (Figure S5d), while the PEDOT:PSS/PU/Glycerol film ruptured under a 5N applied force (Figure S5c) and showed no recovery under a 3N force scratch (Figure S5e). A healing efficiency of 55% was obtained for PEDOT:PSS/PU/PEG/Glycerol films (Figure S6b). The branched molecular structure of glycerol is identified as a potential cause for the observed decline in both the self-healing and mechanical properties, acting as a plasticizer and disrupting hydrogen bonding in the linearly structured PEG, PU, and PEDOT:PSS in the polymeric blends.

For the cut-stick self-healing tests, tensile stress-strain curves obtained from intact and healed PEDOT:PSS/PU/PEG/Glycerol demonstrated similar recovery in stretchability (Figure S8a) and slightly reduced healing efficiency (Figure S8b).

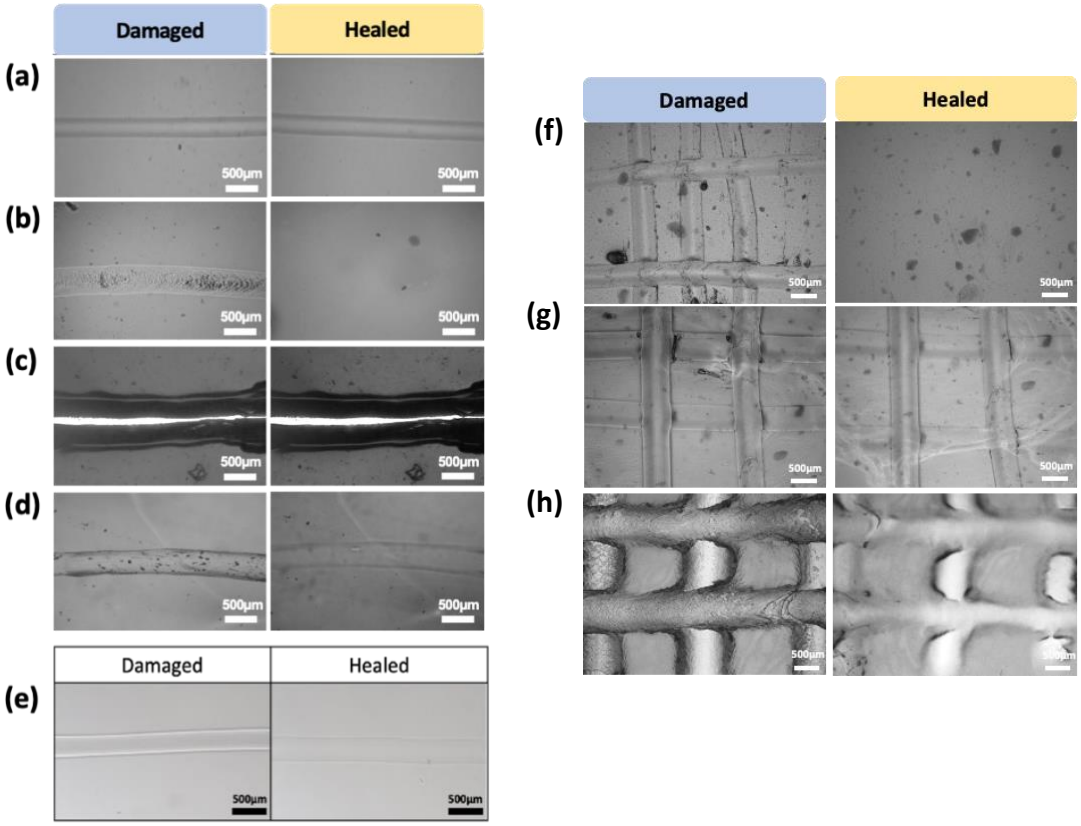

Figure S5. Optical microscopy images of PEDOT:PSS-based films after surface damage and healing. (a–d) PEDOT:PSS, PEDOT:PSS/PU, PEDOT:PSS/PU/Glycerol, and PEDOT:PSS/PU/PEG/Glycerol films after single-line scratching (5 N) and subsequent healing at 50 °C for 10 min. (e) PEDOT:PSS/PU/PEG/Glycerol film after surface scratching (3 N) and healing. (f–h) PEDOT:PSS/PU, PEDOT:PSS/PU/Glycerol, and PEDOT:PSS/PU/PEG/Glycerol films after grid-pattern scratching and healing.

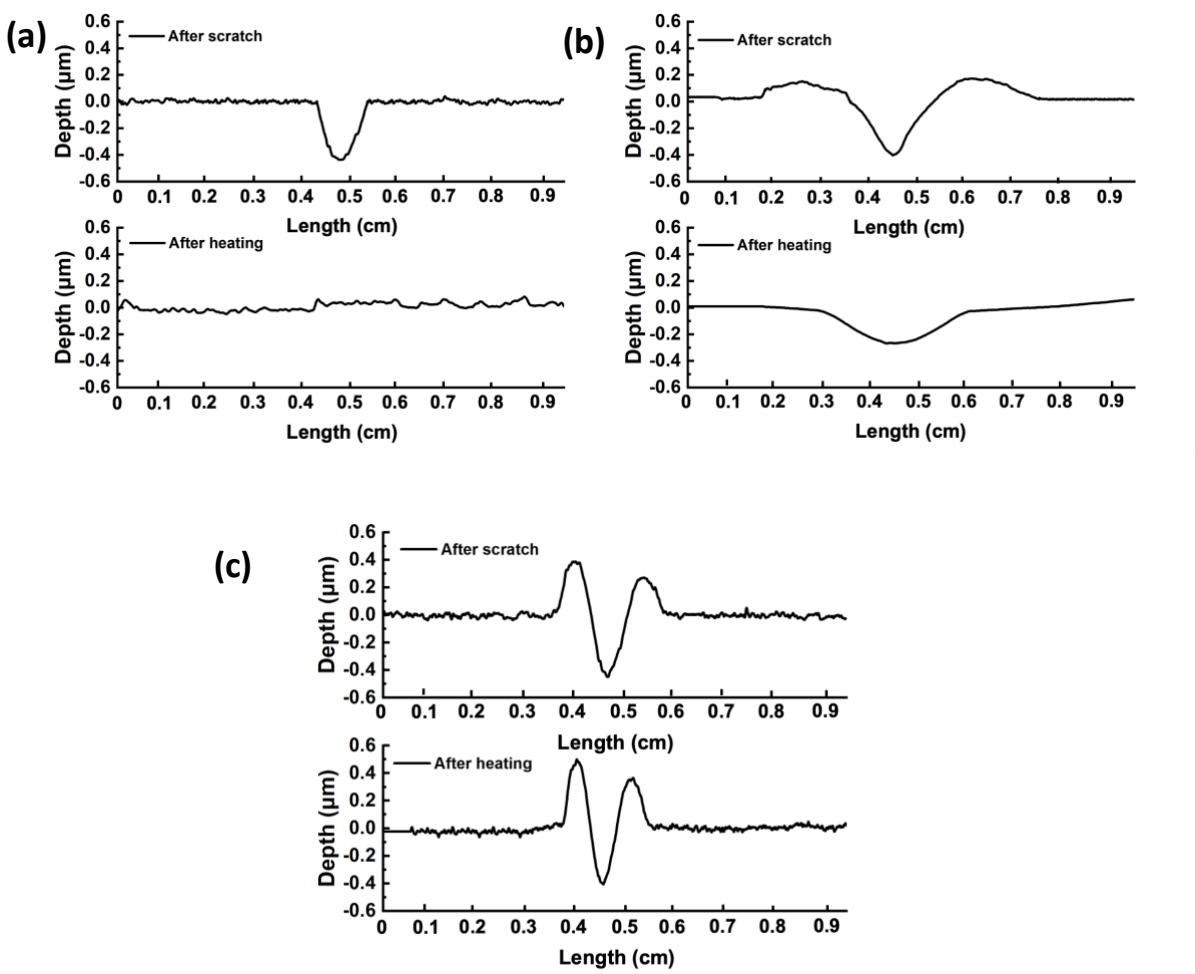

Figure S6. Depth profiles of PEDOT:PSS-based films after surface scratching and healing. (a) PEDOT:PSS/PU, (b) PEDOT:PSS/PU/PEG/Glycerol, and (c) PEDOT:PSS films scratched under a 5 N load and subsequently healed at 50 °C for 10 min.

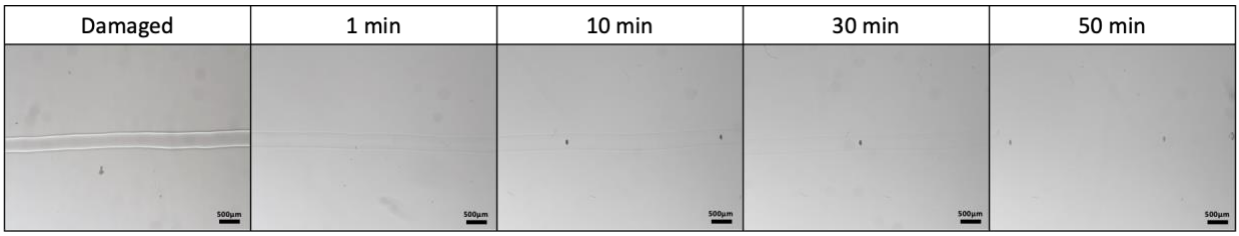

Figure S7. Optical microscopy images of self-healing PU after surface scratching (5 N) and subsequent healing at 60 °C for 50 min. The average film thickness was approximately 21 µm.

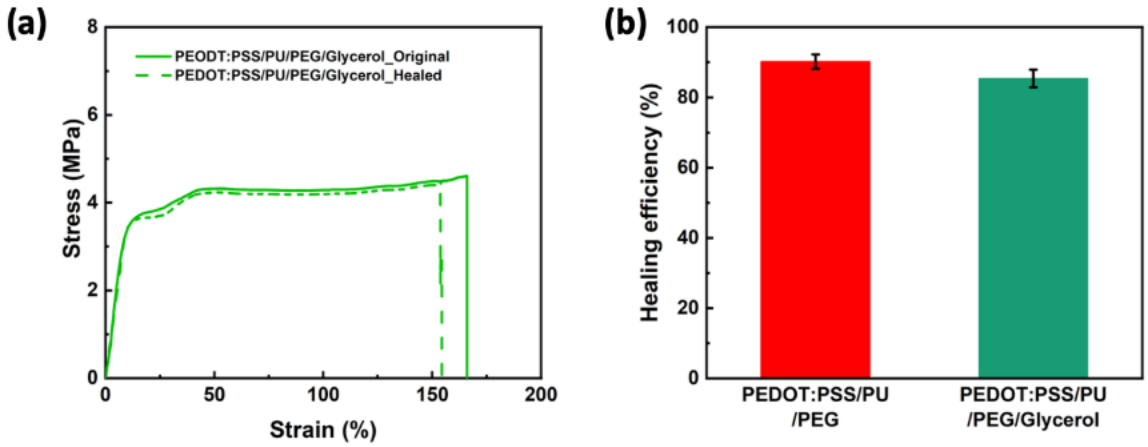

Figure S8. Mechanical healing performance of PEDOT:PSS/PU-based films. (a) Tensile stress–strain curves of original and healed PEDOT:PSS/PU/PEG/Glycerol films. (b) Average healing efficiencies of PEDOT:PSS/PU/PEG and PEDOT:PSS/PU/PEG/Glycerol films derived from stress–strain analysis. Values (n = 3) are presented as mean ± standard deviation.

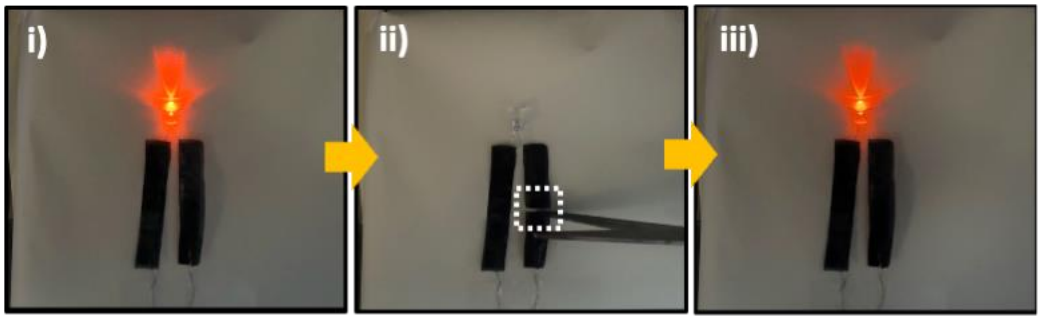

Figure S9. Demonstration of cut-induced damage and healing in a PEDOT:PSS/PU/PEG film integrated into an LED circuit. (i) Original state, (ii) after cutting, and (iii) after thermal healing at 50 °C. The film was operated under a constant bias of 0.2 V.

Materials	**Recyclable**	**Healing behavior**	**Maximum elongation at break (%)**	**Toughness (MJ/m^3)**	**Mechanical healing efficiency (%)**	**Conductivity (S/cm)**	**Electrical healing efficiency (%)**	**Healing response time**	**Ref.**
PEDOT:PSS/PEG	No	Autonomous	6.5	-	-	201	≈ 100	≈ 50–800ms	[108]
PEDOT:PSS/Triton X-100	No	Autonomous	57	-	-	78	≈ 70-100	≈ 1s	[96]
PEDOT:PSS/Glycerol	No	Water-enabled	12	-	-	500	≈ 100	≈150ms	[1]
PEDOT:PSS-*b*-PPEGMEA	No	Water-enabled	128	3.4	-	0.05	≈ 50	≈ 1s	[165]
PEDOT:PSS/PAAMPAS/IL	No	Autonomous	600	-	≈ 85	320	≈ 100	≈ 19ms	[166]
		Cut-stick						≈ 24h	
PANI/PAA	No	Cut-stick	470	-	≈ 99	0.1	≈ 99	≈ 24h	[105]
PEDOT:Tos	No	Water-enabled	-	-	-	1600	≈ 95	0.3s	[106]
PAAMPSA/PANI/PA	No	Autonomous	2000	-	≈ 50	200	≈ 98.6	3h	[167]
		Cut-stick (Pressure)							

BCOE/PEGMMA@Li/LFP	No	Cut-stick	600	-	-	1.9 x10^{-4}	≈ 100	1h	[168]
Poly(PDES)-PA	No	Cut-stick	1300	-	≈ 91.5	7.8x10^{-4}	≈ 100	48h	[169]
PEDOT:PSS/PU/PEG	Yes	Autonomous	350	24.6	≈ 90	15.4	≈ 100	≈ 0.1s	This work
		Cut-stick (heated at 50 °C)						≈ 5min	

Table S2. Summary of PEDOT:PSS-based films exhibiting recyclability and self-healing behavior, including maximum elongation at break, toughness, mechanical healing efficiency, electrical conductivity, and electrical healing efficiency.

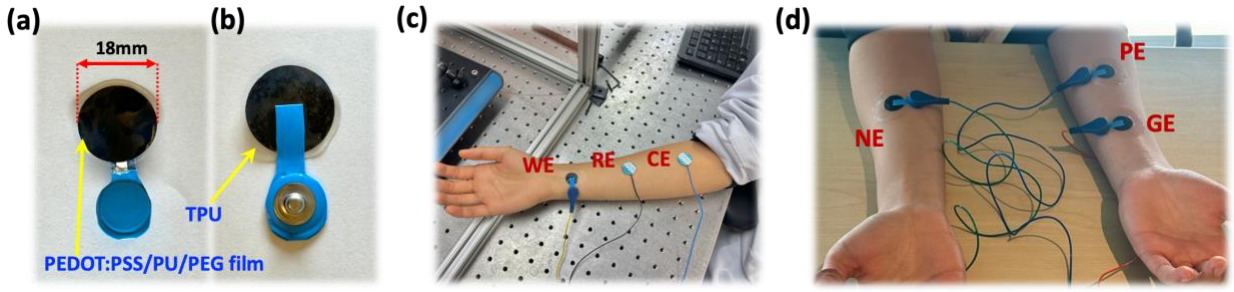

Figure S10. Electrode configuration and measurement setup.(a,b) Front and back views of the electrodes. (c) Photograph of the skin–electrode impedance and ECG measurement configuration. The PEDOT:PSS/PU/PEG film served as the working electrode (WE), while commercial Ag/AgCl gel electrodes (Natus®) were used as the reference (RE) and counter (CE) electrodes. Measurements were conducted on the same volunteer and at the same location. Skin–electrode impedance data are presented as mean ± standard deviation (n = 3). (d) ECG measurement configuration on a volunteer, showing the positive (PE) and ground (GE) electrodes positioned on the left forearm and the negative electrode (NE) on the right forearm.

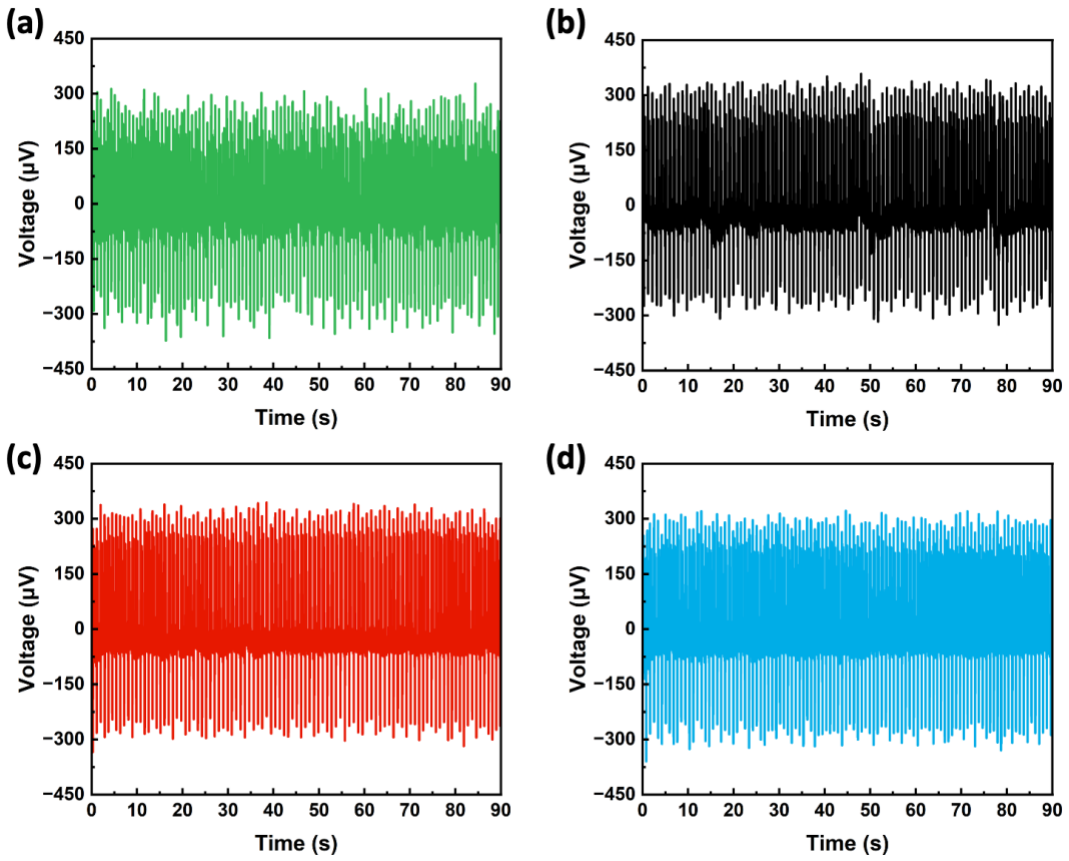

Figure S11. ECG signal recordings over 90 s using (a) PEDOT:PSS/PU/PEG film electrodes before healing (green), (b) after self-healing (black), (c) after recycling (red), and (d) commercial Natus® Ag/AgCl gel electrodes (blue).

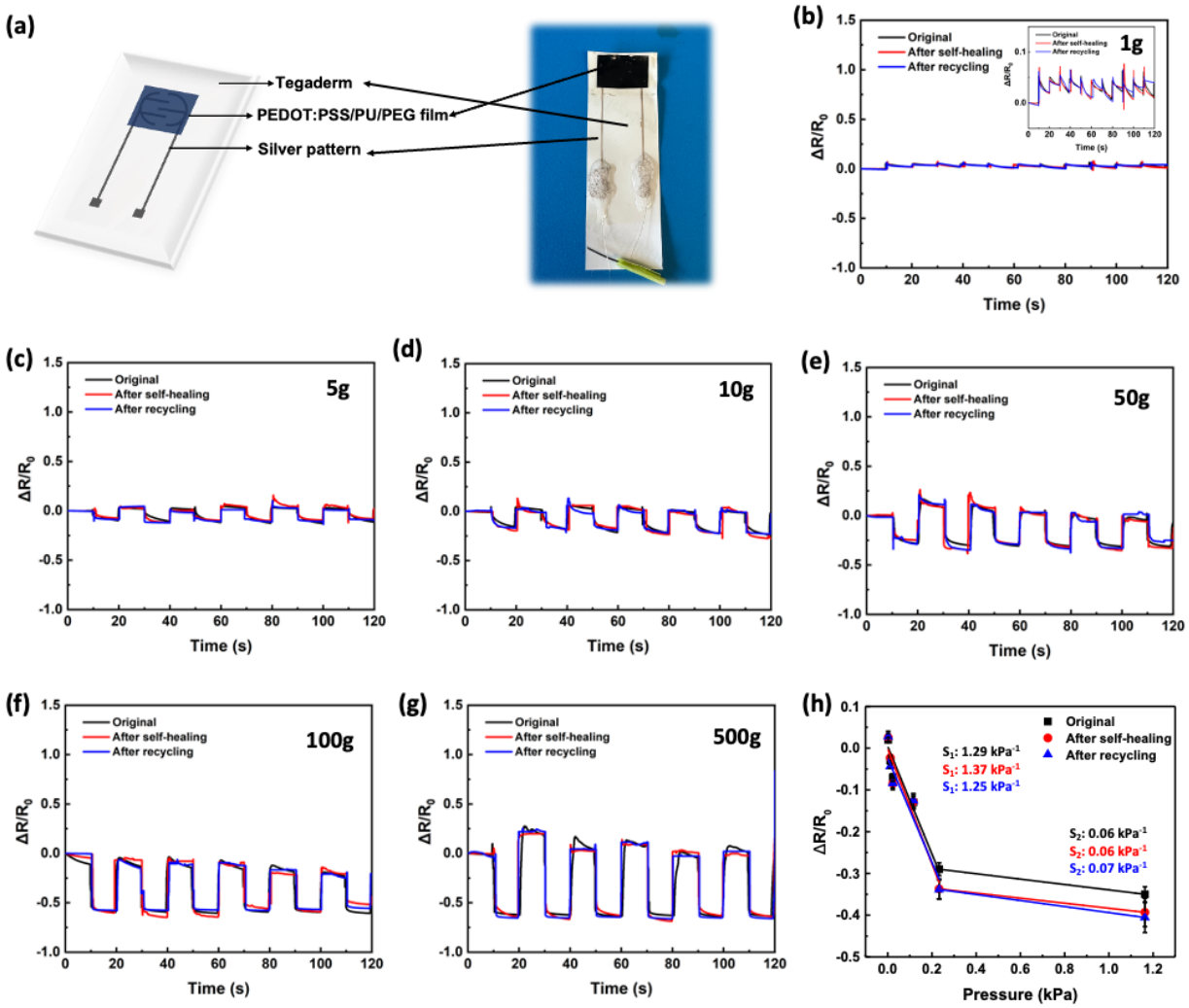

Figure S12. Resistive pressure sensing performance of PEDOT:PSS/PU/PEG films. (a) Schematic illustration and photograph of the multilayer pressure sensor composed of a PEDOT:PSS/PU/PEG film (top layer), a printed Ag contact pattern, and a Tegaderm substrate. (b–g) Real-time normalized resistance change (ΔR/R₀) under repeated application of different loads (1, 5, 10, 50, 100, and 500 g) for the original (black), self-healed (red), and recycled (blue) films. The same film was used for all measurements. (h) Extracted sensitivity curves of the original sensor before and after self-healing and recycling.

The working principle of our pressure sensor is based on the change of contact resistance at the Ag/PEDOT:PSS/PU/PEG interface upon applying pressure. We observed two pressure sensitivity ranges. For an applied pressure up to 0.2 kPa, two mechanisms contribute to the steep contact

resistance reduction: i) new electrical connections formed between Ag and PEDOT:PSS/PU/PEG, and ii) the increased contact area for the existing electrical contacts. For the higher-pressure range, the lower sensitivity suggests that the change of resistance predominantly depends on the increased contact area.

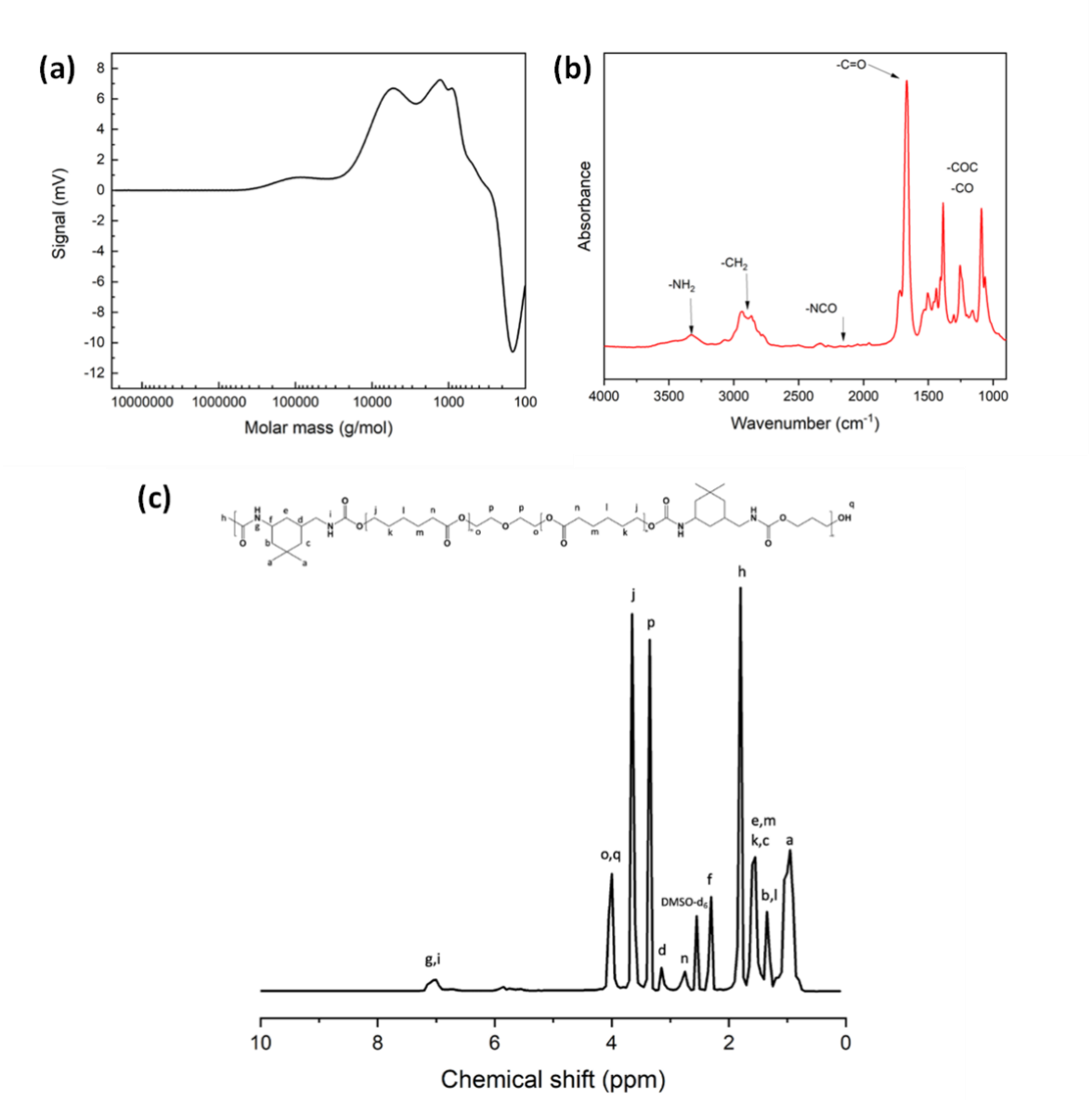

Figure S13. Characterization of the synthesized self-healing polyurethane. (a) GPC chromatogram, (b) FTIR spectrum, and (c) ^{1}H NMR spectrum.

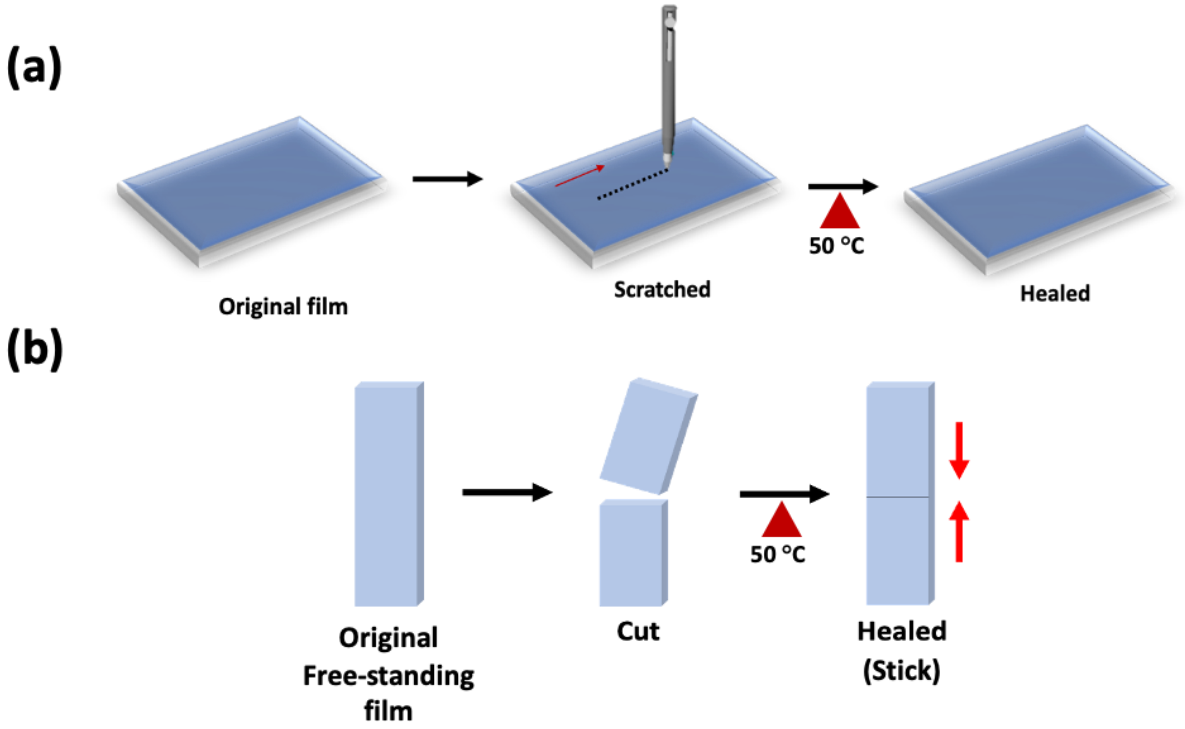

Figure S14. Schematic illustration of the mechanical self-healing tests employed in this study: (a) scratch test and (b) cut–stick test.

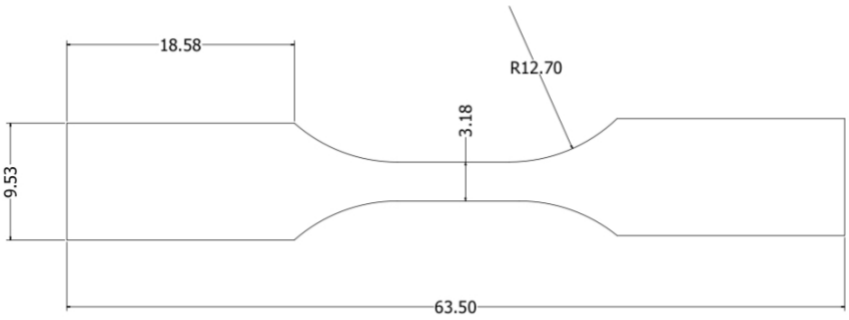

Figure S15. Dog-bone mold conforming to ASTM D638 Type V geometry.

APPENDIX B SUPPLEMENTARY INFORMATION FOR ARTICLE 3 : PRINTABLE, FLEXIBLE, SELF-HEALING, AND RECYCLABLE PEDOT:PSS/POLYURETHANE COMPOSITES FOR DURABLE BIOELECTRONICS

Jinsil Kim and Fabio Cicoira

Department of Chemical Engineering, Polytechnique Montréal, Montréal, QC H3C 3A7, Canada

*Corresponding author. E-mail: fabio.cicoira@polymtl.ca

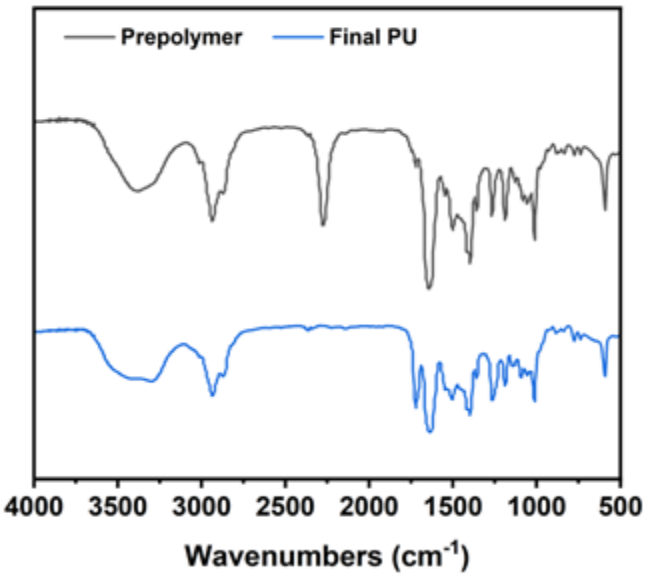

Figure S16. FTIR spectra of the prepolymer and the synthesized polyurethane.

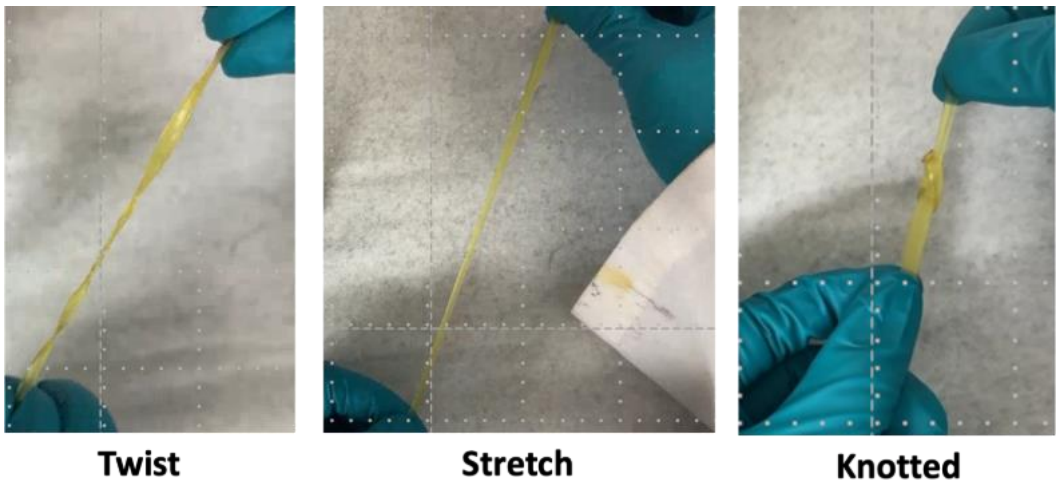

Figure S17. Photographs demonstrating the twisting, stretching, and knotting behavior of the synthesized polyurethane (PU).

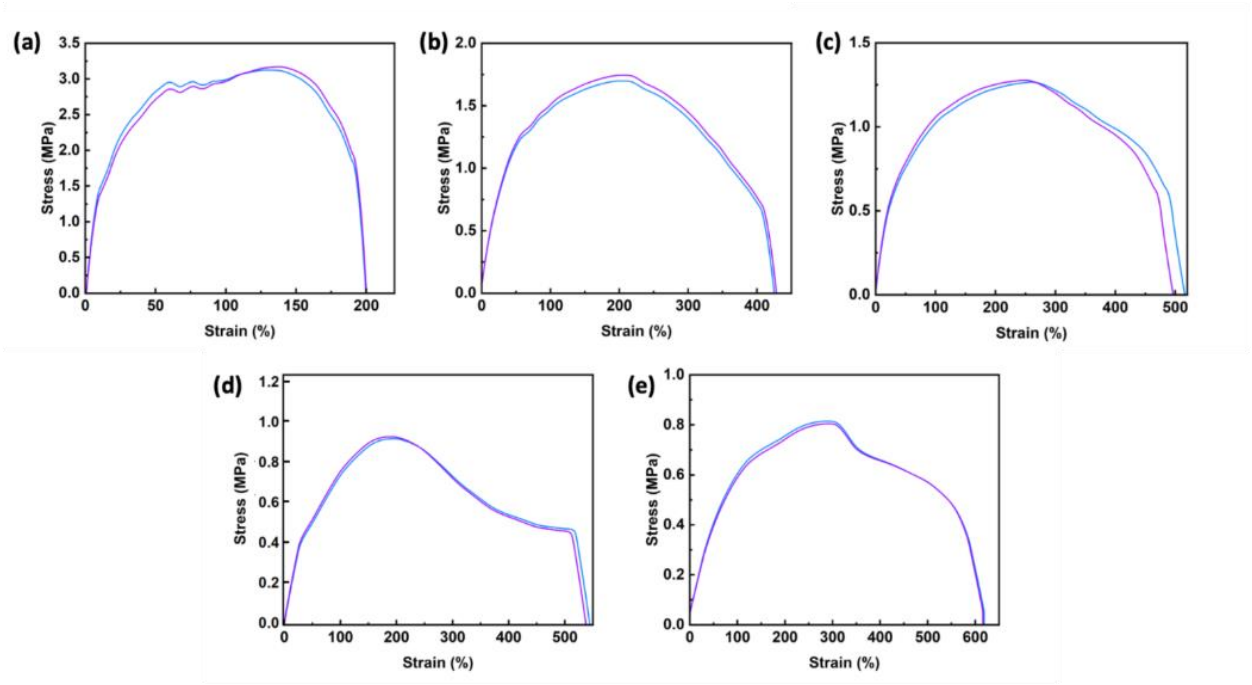

Figure S18. Tensile stress–strain curves of PEDOT:PSS/PU-based films: (a) PEDOT:PSS/PU-13, (b) PEDOT:PSS/PU-15, (c) PEDOT:PSS/PU-18, (d) PEDOT:PSS/PU-15/Gly-2.4, and (e) PEDOT:PSS/PU-18/Gly-2.2. Two independent measurements are shown for each composition.

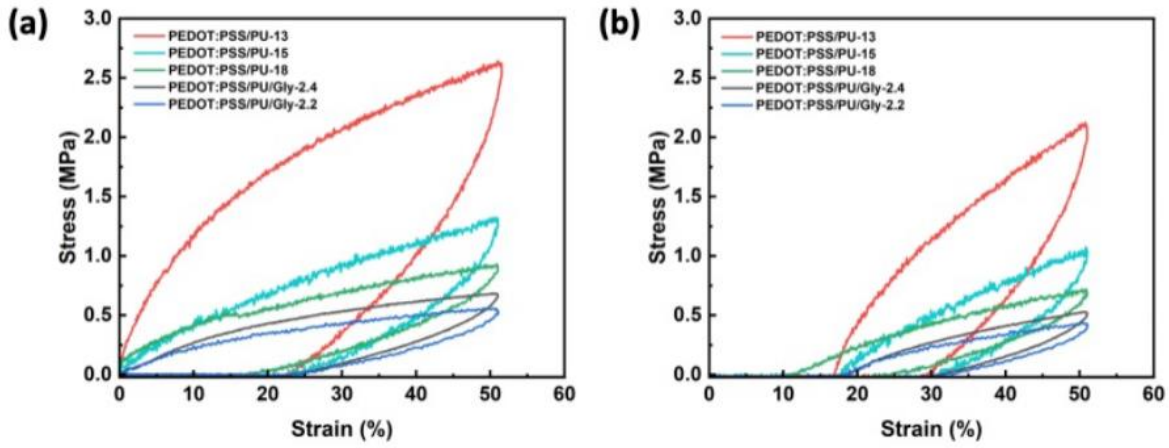

Figure S19. Tensile loading–unloading curves of PEDOT:PSS/PU-based films recorded during (a) the first cycle and (b) the 500th cycle within a 0–50% strain range.

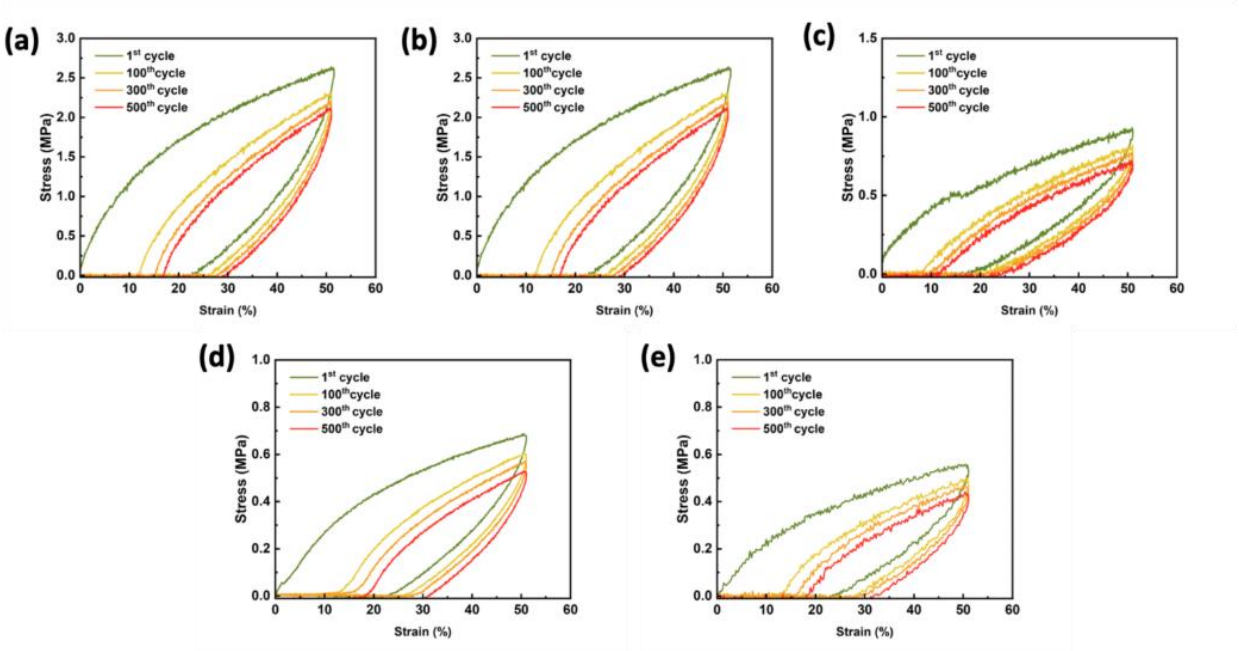

Figure S20. Tensile loading–unloading curves of PEDOT:PSS/PU-based films: (a) PEDOT:PSS/PU-13, (b) PEDOT:PSS/PU-15, (c) PEDOT:PSS/PU-18, (d) PEDOT:PSS/PU-15/Gly-2.4, and (e) PEDOT:PSS/PU-18/Gly-2.2. Curves were recorded during the first, 100th, 300th, and 500th tensile cycles within a 0–50% strain range.

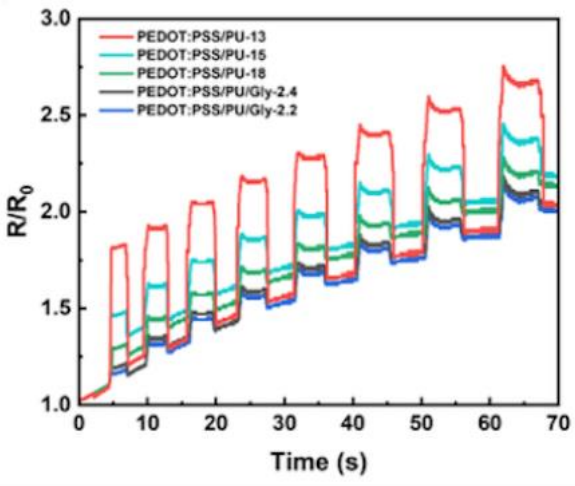

Figure S21. Normalized resistance (R/R_0) as a function of tensile strain under a constant 0.2 V bias. The strain was incrementally increased from 50% to 400% in 50% steps.

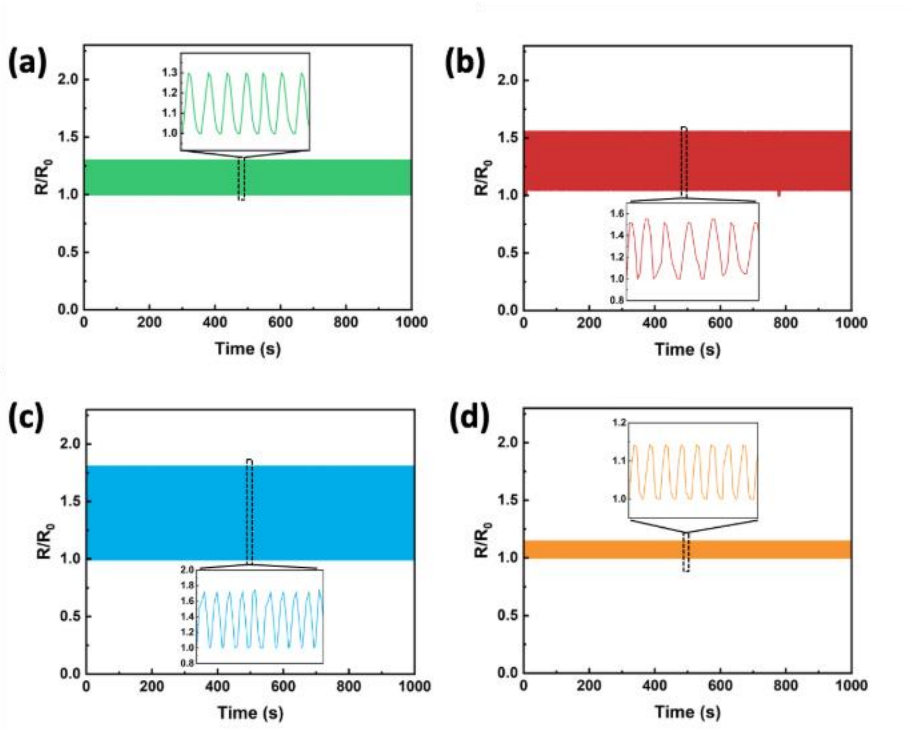

Figure S22. Normalized resistance (R/R_0) as a function of time during 500 cyclic tensile strains (0–50%) for (a) PEDOT:PSS/PU-13, (b) PEDOT:PSS/PU-15, (c) PEDOT:PSS/PU-18, and (d) PEDOT:PSS/PU/Gly-2.4 films. Insets show magnified views of cycles 500–530, highlighting resistance variations during cyclic deformation.

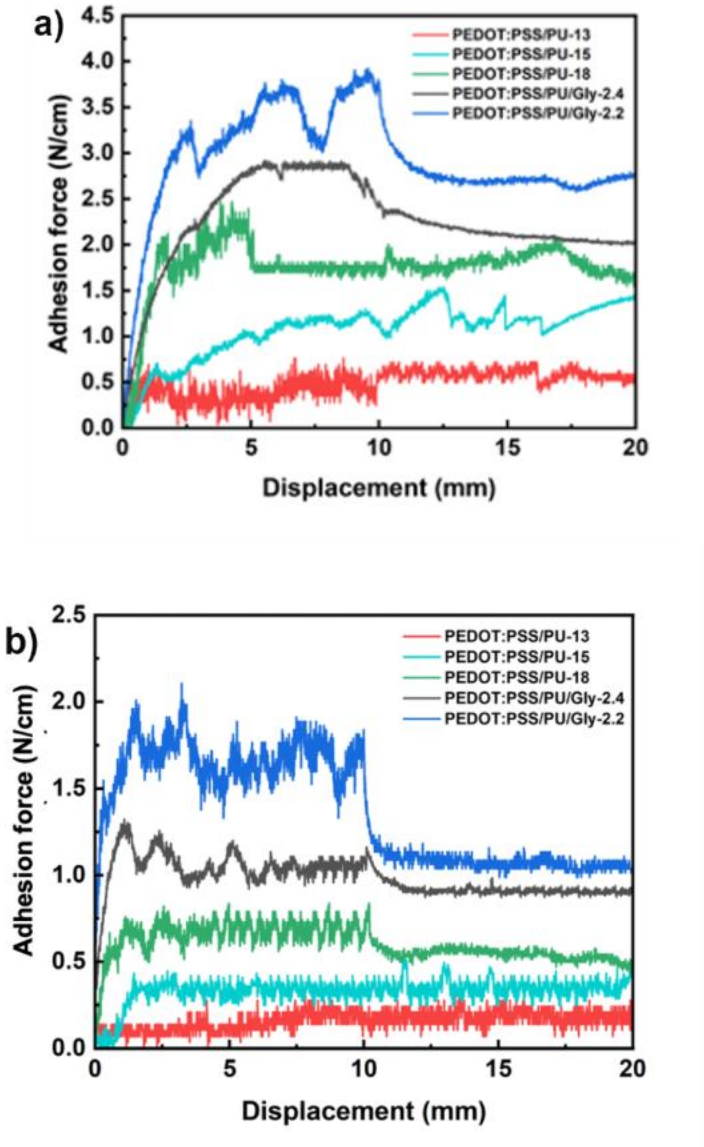

Figure S23. Adhesion strength of PEDOT:PSS/PU-based films measured on (a) film-to-film self-adhesion interfaces and (b) glass substrates.

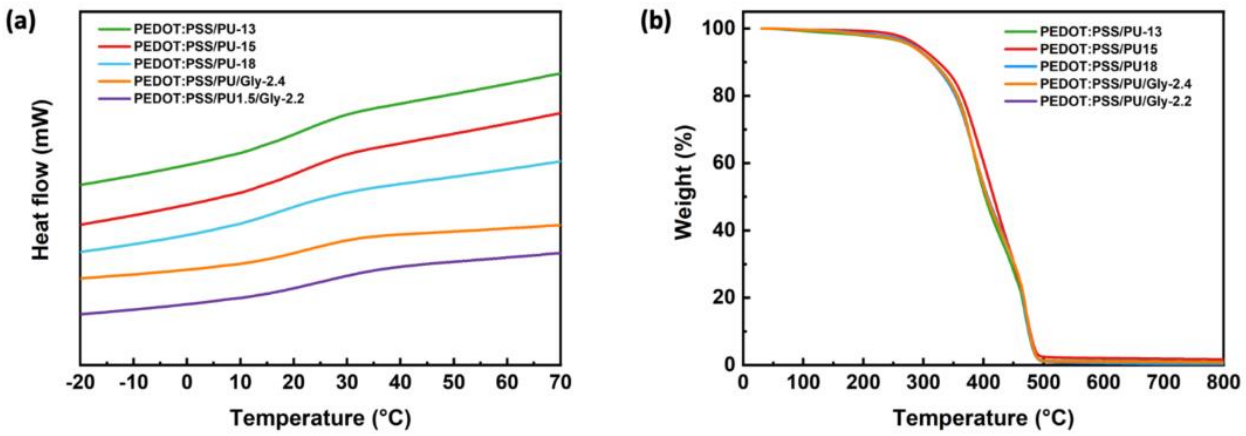

Figure S24. Thermal analysis of PEDOT:PSS/PU-based films: (a) DSC thermograms and (b) TGA thermograms.

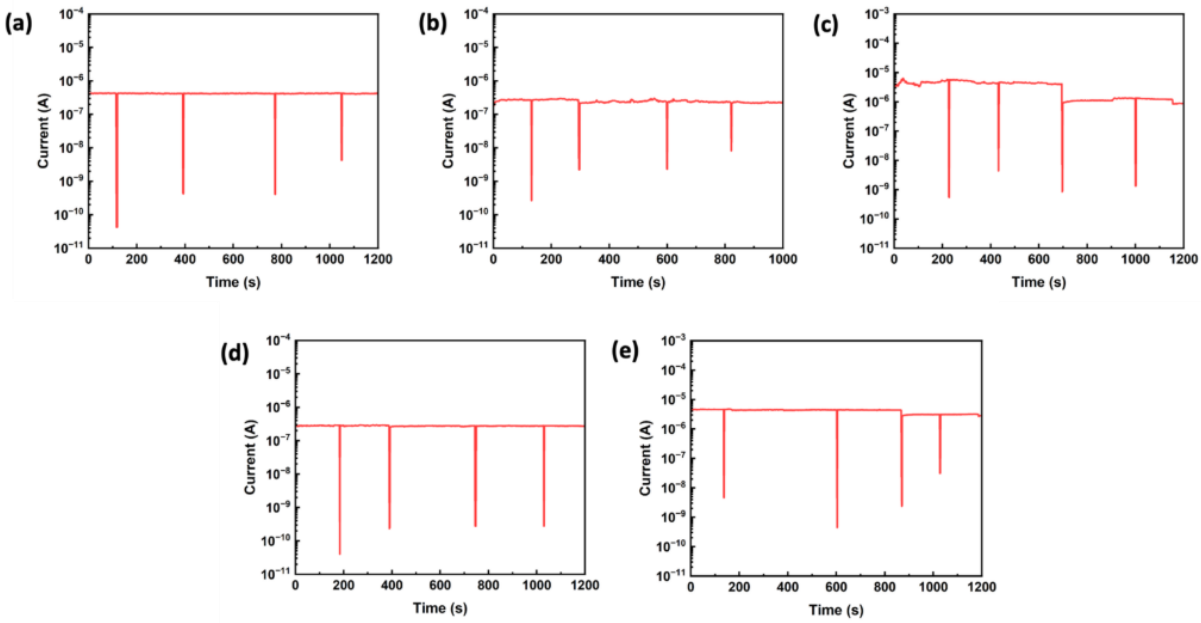

Figure S25. Current–time responses of drop-cast PEDOT:PSS/PU-based films during repeated cut–heal cycles under a constant 0.2 V bias: (a) PEDOT:PSS/PU-13, (b) PEDOT:PSS/PU-15, (c) PEDOT:PSS/PU-18, (d) PEDOT:PSS/PU-15/Gly-2.4, and (e) PEDOT:PSS/PU-18/Gly-2.2.

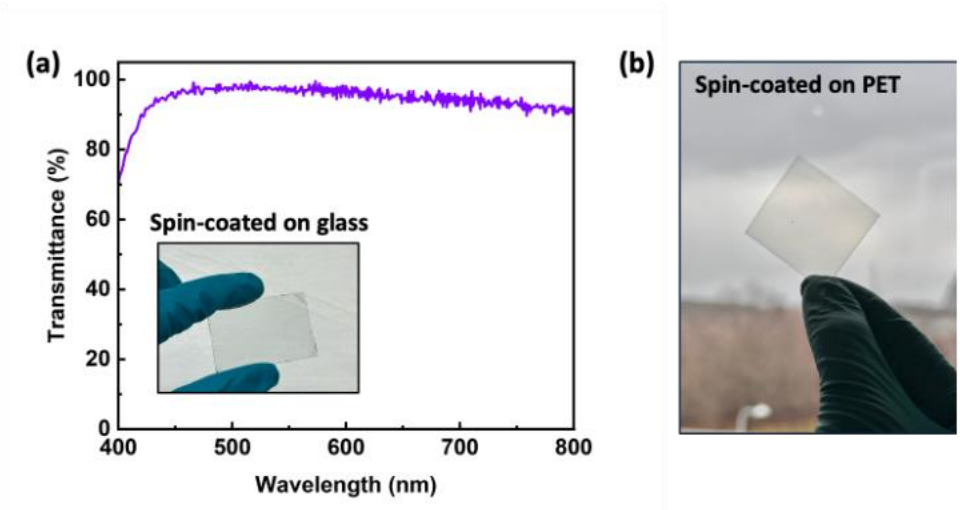

Figure S26. Optical transparency of PEDOT:PSS/PU-18/Gly-2.2 films. (a) UV–Vis transmittance spectrum of a spin-coated film on glass (400–900 nm), with the corresponding photograph. (b) Photograph of a spin-coated film on a PET substrate.

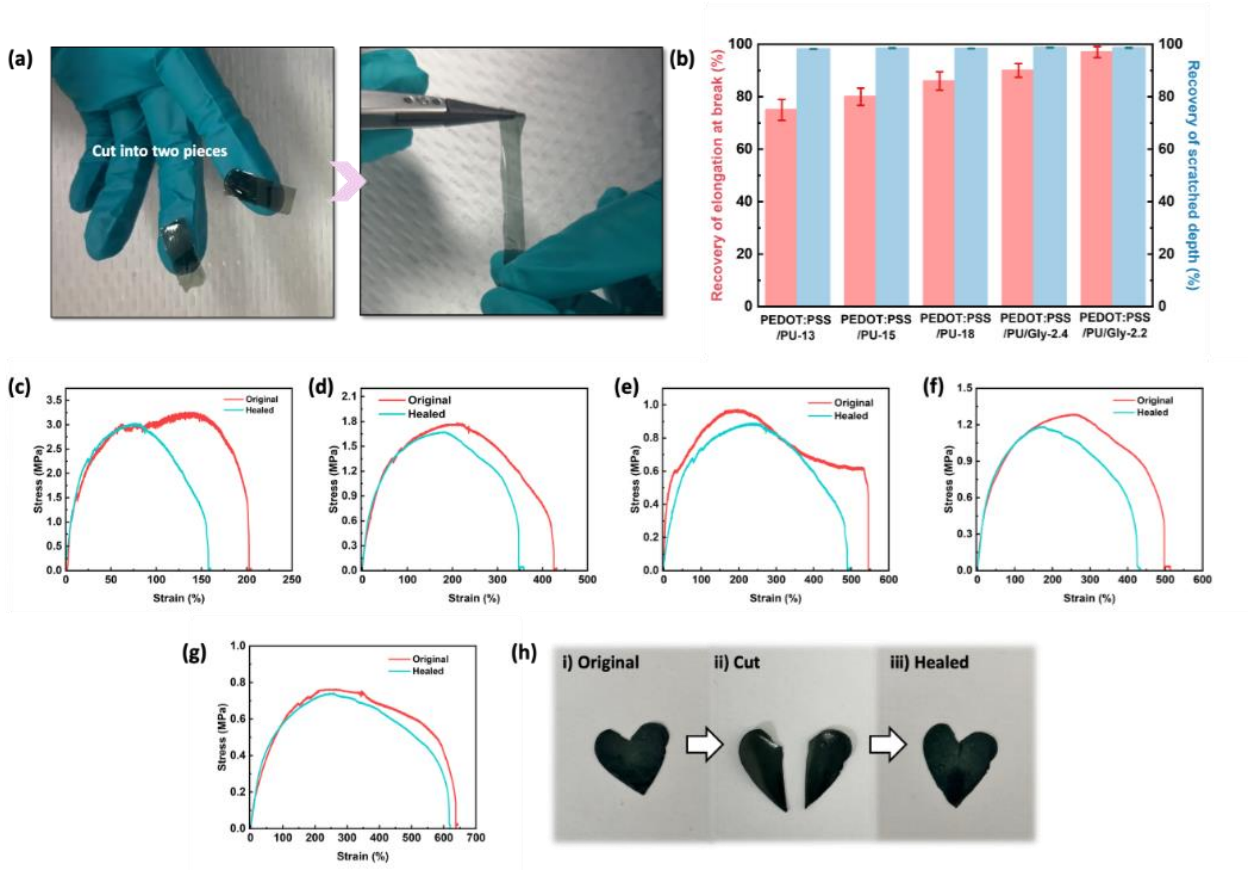

Figure S27. (a) Photographs illustrating the cut–stick self-healing procedure. (b) Average healing efficiencies derived from recovery of elongation at break and scratch depth. (c–g) Tensile stress–strain curves of PEDOT:PSS/PU-13, PEDOT:PSS/PU-15, PEDOT:PSS/PU-18, PEDOT:PSS/PU-15/Gly-2.4, and PEDOT:PSS/PU-18/Gly-2.2 films in their original (red) and healed (blue) states after cut–stick healing at room temperature. (h) Representative images of PEDOT:PSS/PU-18/Gly-2.2 films in the original, cut, and healed states.

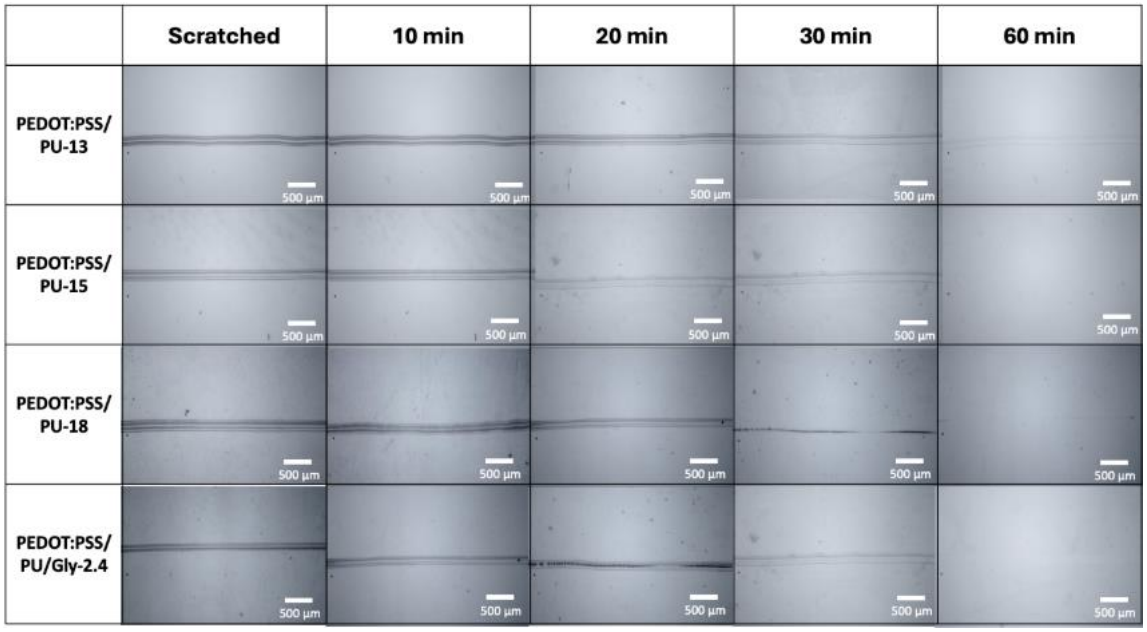

Figure S28. Optical microscopy images showing induced damage and subsequent healing of PEDOT:PSS/PU composite films.

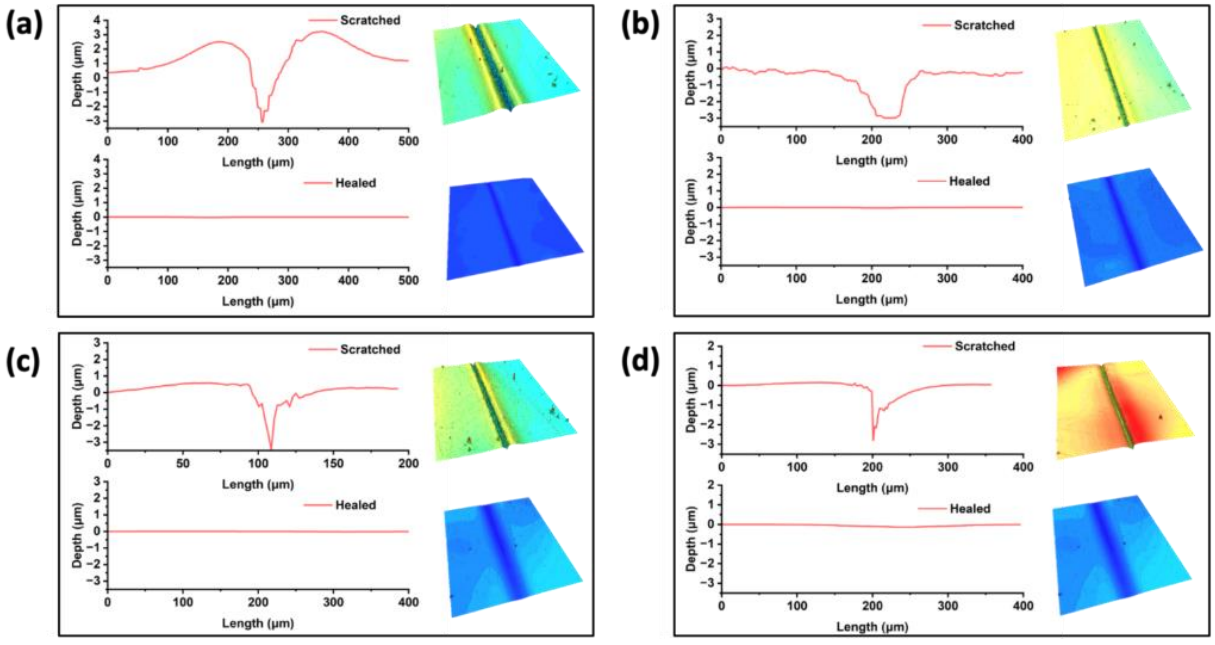

Figure S29. Surface depth profiles and three-dimensional optical profilometry images of PEDOT:PSS/PU-based films after pencil-induced surface scratching and subsequent healing at

room temperature: (a) PEDOT:PSS/PU-13, (b) PEDOT:PSS/PU-15, (c) PEDOT:PSS/PU-18, and (d) PEDOT:PSS/PU-15/Gly-2.4.

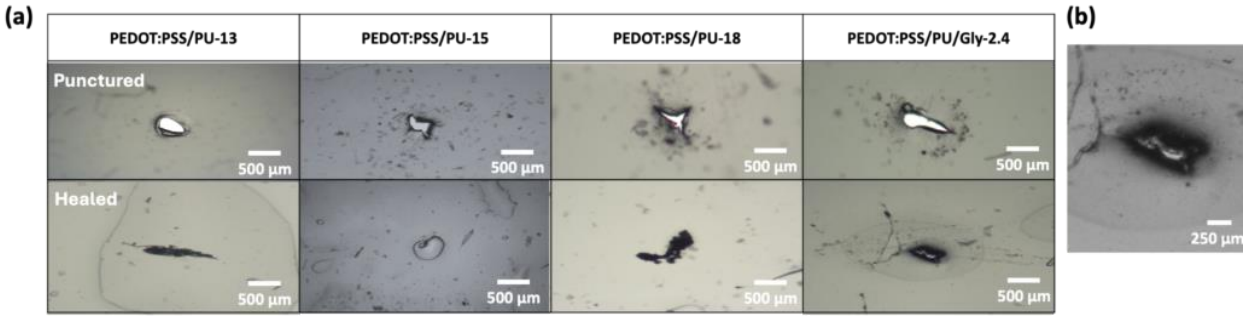

Figure S30. Optical microscopy images of PEDOT:PSS/PU-based films after puncture and subsequent healing at room temperature: (a) Representative images of the damaged and healed states, and (b) magnified view of the healed region in a PEDOT:PSS/PU/Gly-2.2 film.

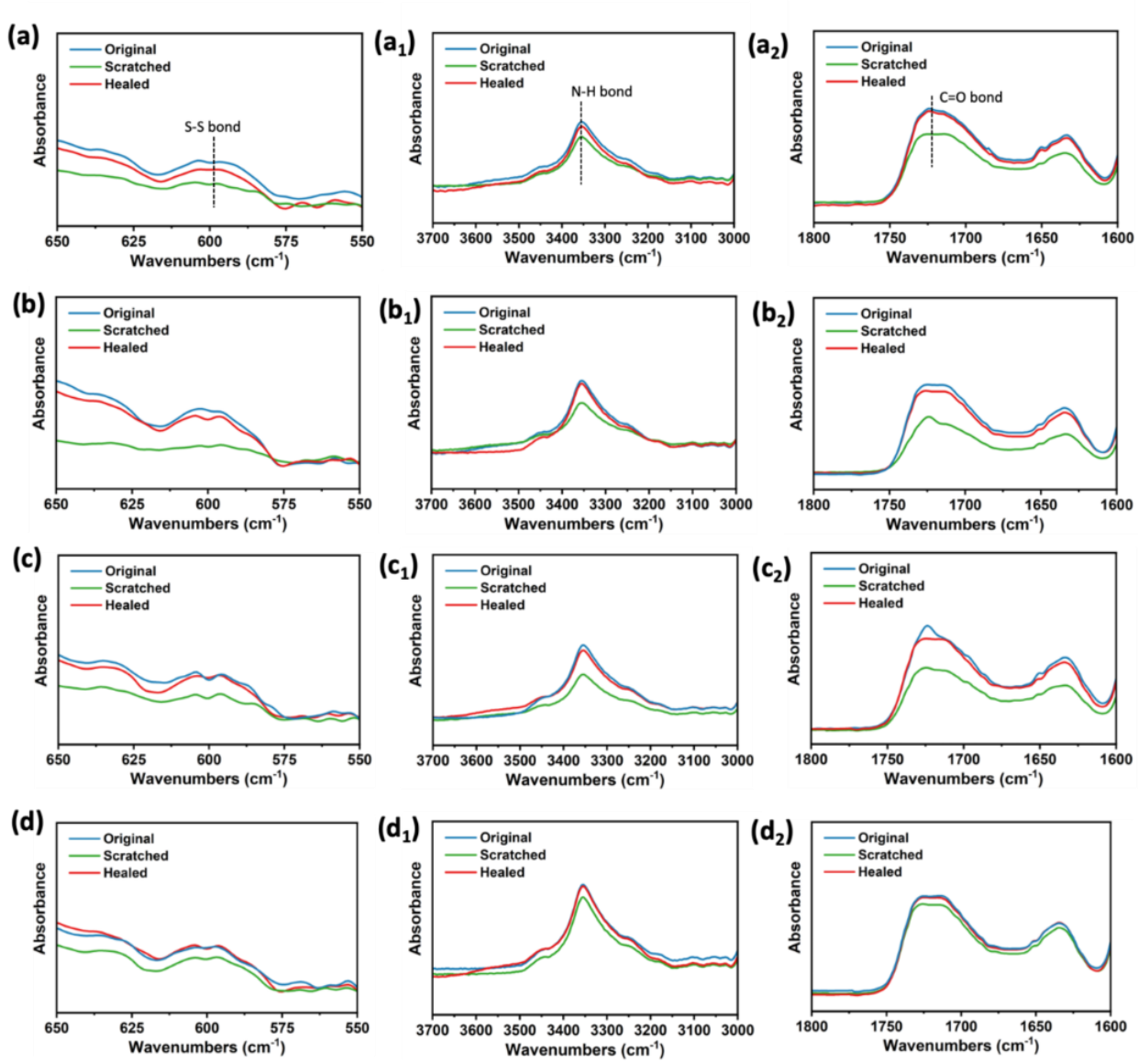

Figure S31. Solid-state FTIR spectra of PEDOT:PSS/PU-based films recorded in the original, scratched, and healed states. (a_1-a_3) PEDOT:PSS/PU-13, (b_1-b_3) PEDOT:PSS/PU-15, (c_1-c_3) PEDOT:PSS/PU-18, and (d_1-d_3) PEDOT:PSS/PU-15/Gly-2.4. Highlighted regions correspond to characteristic vibrational bands of S–S stretching, C=O stretching, and N–H stretching.

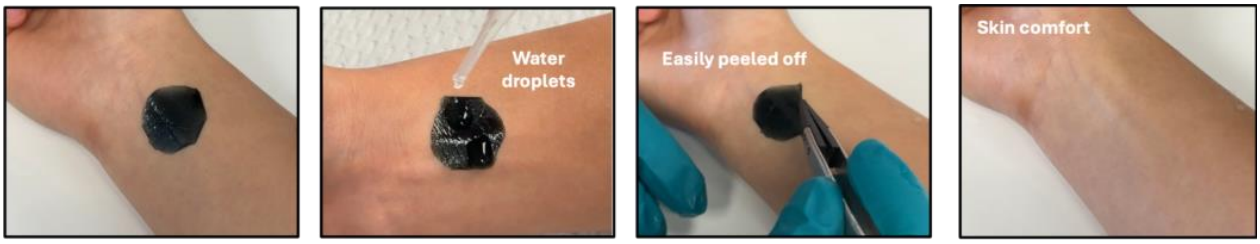

Figure S32. Direct transfer of a freestanding electrode onto skin and its gentle removal using water without causing skin or electrode damage.

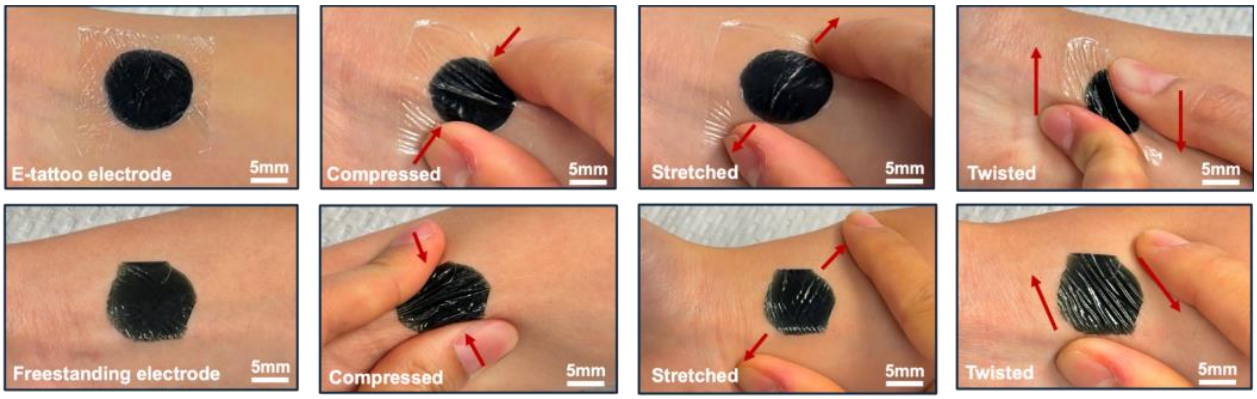

Figure S33. Demonstration of the conformability of e-tattoo and freestanding electrodes on human skin under various mechanical deformations, including compression, stretching, and twisting.

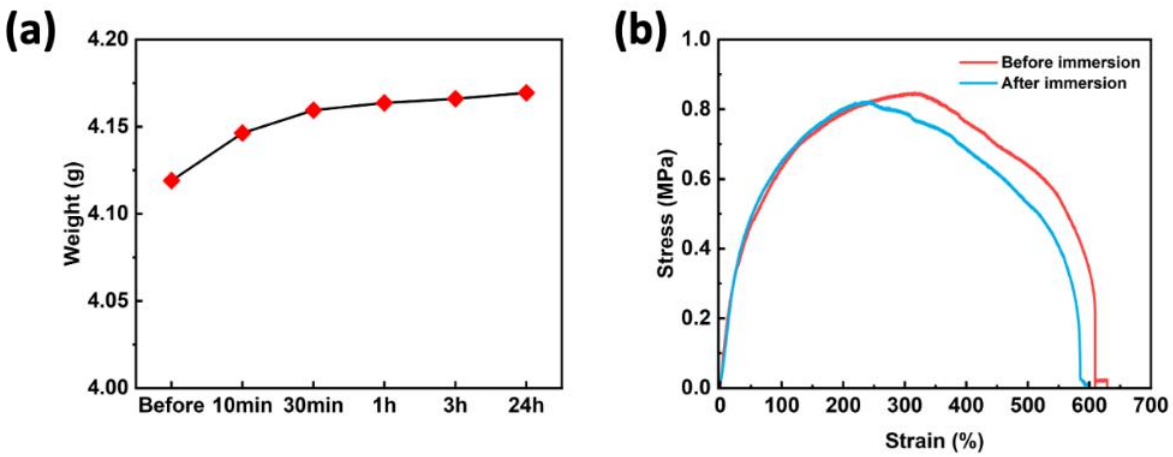

Figure S34. Water stability of PEDOT:PSS/PU-15/Gly-2.2 films. (a) Relative weight increase after immersion in water for 24 h. (b) Tensile stress–strain curves measured before and after water immersion.

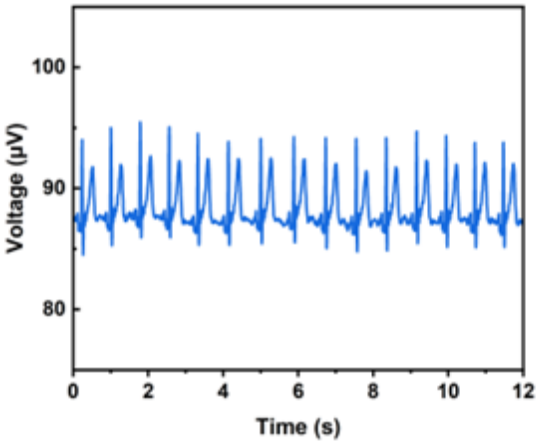

Figure S35. Representative ECG signal recorded using freestanding PEDOT:PSS/PU-18/Gly-2.2 electrodes after mechanical reuse.

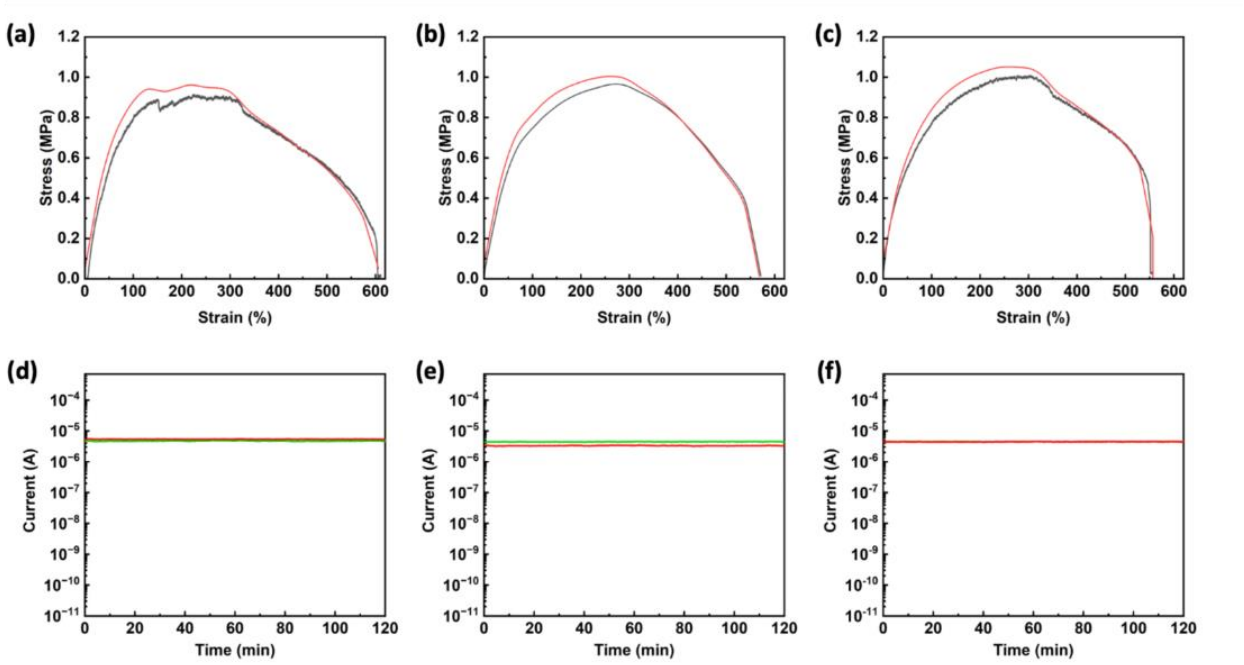

Figure S36. Electrical and mechanical performance over 15 recycling cycles. (a,d) Original samples, (b,e) after chemical recycling, and (c,f) after mechanical recycling. Measurements were conducted on independently prepared samples at each cycle to confirm reproducibility.

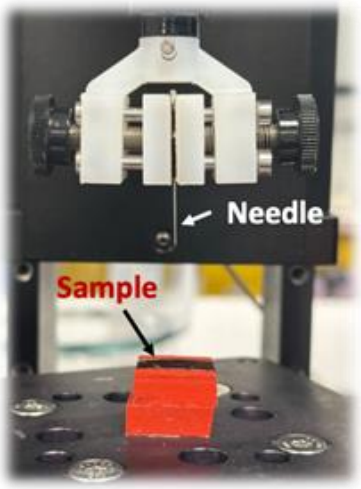

Figure S37. Schematic illustration of the puncture healing experimental setup.

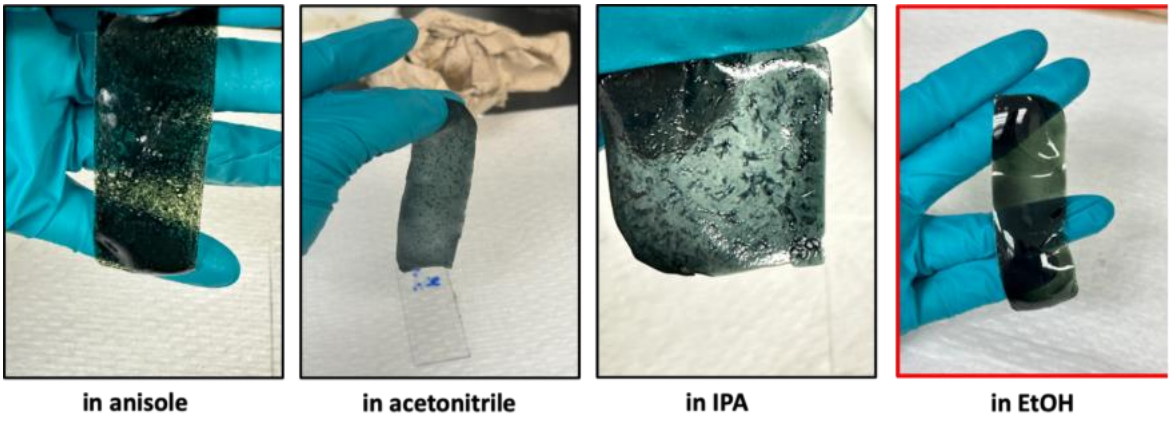

Figure S38. Photographs of PEDOT:PSS/PU-18/Gly-2.2 drop-cast films prepared using different solvents.

Solvents	Solubility of PU	Solubility of PEDOT:PSS (SV3)
Acetonitrile	O	△
IPA	O	△
EtOH	O	O
Anisole	O	X

Table S3. Solubility test of PU and PEDOT:PSS (SV3) in different solvents. The symbols represent the dissolution behavior of the samples: O indicates complete dissolution, △ indicates partial dissolution, and X indicates no dissolution.

Table S4. Comparison of the electromechanical properties, self-healing behavior, and recyclability of the PEDOT:PSS/PU composite developed in this work with recently reported self-healing conductive materials.

Category	This work	Ref 1 (Graphene/ CNF)	Ref 2 (PEDOT:PAAMPSA:PA)	Ref 3 (CB/CNT/ PU)	Ref 4 (PAA/Al/ PQ hydrogel)	Ref 5 (Boroxine/ PU)	Ref 6 (WPU/PPy)	Ref 7 (PEDOT:PSS/ PU/PEG)
Elongation at break	630%	1000%	1050%	245%	1400%	500%	597%	350%
Mechanical Healing efficiency	98%	-	92%	87%	50%	94%	83%	90%
Healing time	1 h	24 h	2 h	7 min	24 h	1 h	1 h	10 min
Type of healed damage	Cut, Scratch, Puncture	Cut, Scratch	Cut	Cut	Cut	Cut, Scratch	Cut	Cut, Scratch
Healing Temp.	r.t	r.t	r.t	70 °C	r.t	r.t	60 °C	50 °C
Recyclability	Yes (Chemical & Mechanical)	Yes (Mechanical)	No	Yes (Chemical)	Yes (Mechanical)	Yes (Mechanical)	Yes (Mechanical)	Yes (Mechanical)
Processing	Drop-cast Spin-coating Printing	Spin-coating	Drop-cast Spin-coating	Hot pressing	Drop-cast	Drop-cast	Drop-cast	Drop-cast
Conductivity	14 S/cm	0.309 S/cm	0.309 S/cm	8.20 S/cm	0.006 S/cm	-	-	10 S/cm

1. C. Zheng, Y. Yue, L. Gan, C. Mei and J. Han, Nanomaterials, 2019, 9(7), 937.
2. D. Kim, Z. A. Akbar, Y. T. Malik, J. Jeon and S. Jang, Nature Communications, 2023, 14, 3246.
3. Y. Wang, B. Park, V. Vu, and S. Lee, Polymer Engineering & Science, 2025, 65(4), 1854-1867.
4. J. Zou, Z. Yang, J. Liang, Y. XIe, M. Fan and X. Zhang, Polymer, 2024, 315, 127826.
5. H. Mao, Y. Zhang, L. Zhao, H. Li, H. Wu and L. Lin, ACS Applied Polymer Materials, 2024, 7(1), 164-1745.
6. K. Zhu, L. Yang, X. Zhou, X. Zhang, Y. Hao, F. Li, W. Lei, Q. Wang and G. Wang, Chemical Engineering Journal, 2025, 510, 161515.
7. J. Kim, J. X. Fan, G. Petrossian, X. Zhou, P. Kateb, N. Gagnon-Lafrenais and F. Cicoira, Mater Horiz, 2024, 11.

APPENDIX C LIST OF PUBLICATIONS AT POLYTECHNIQUE MONTREAL NOT INCLUDED IN THE THESIS

1. Chi-hyeong Kim, **Jinsil Kim**, Jiaxin Fan, Meijing Wang, Fabio Cicoira, “Recyclable Printed Liquid Metal Composite for Underwater Stretchable Electronics”, Small Science, vol. 5, Issue 5, 2400553, 2025, doi: 1002/smsc.202400553.
2. Meijing Wang, **Jinsil Kim**, Floriane Miquet-Westphal, Xin Zhou, Pierre Kateb, Jiaxin Fan, Fabio Cicoira, “Self-healable PEDOT-based film, hydrogel, and OECT devices for bioelectronics”, Material Matters, vol. 19, issue 1, 2024.
3. Xin Zhou, Pierre Kateb, Jiaxin Fan, **Jinsil Kim**, Gregory A. Lodygensky b, Bénédicte Amilhon bc, Damiano Pasini and Fabio Cicoira, “Conducting polymer films and bioelectrodes combining high adhesion and electro-mechanical self-healing”, J. Mater. Chem. C, vol. 12, 5708-5717, 2024, doi: 10.1039/D3TC04230H
4. Pierre Kateb, Jiaxin Fan, **Jinsil Kim**, Xin Zhou, Gregory A Lodygensky and Fabio Cicoira, “Printable, adhesive, and self-healing dry epidermal electrodes based on PEDOT:PSS and polyurethane diol”, Flexible and Printed Electronics, vol. 8, issue 4, 045006 2023, doi: 10.1088/2058-8585/ad05d6